

**IN THE UNITED STATES DISTRICT COURT
FOR THE WESTERN DISTRICT OF PENNSYLVANIA**

HAYNES INTERNATIONAL, INC.,)	
a Delaware corporation,)	
)	
Plaintiff,)	Civil Action No. 04-197(E)
)	
v.)	JURY TRIAL DEMANDED
)	
ELECTRALLOY, a Division of G.O.)	
CARLSON, INC.,)	Judge Cohill
a Pennsylvania corporation,)	
)	
Defendant.)	

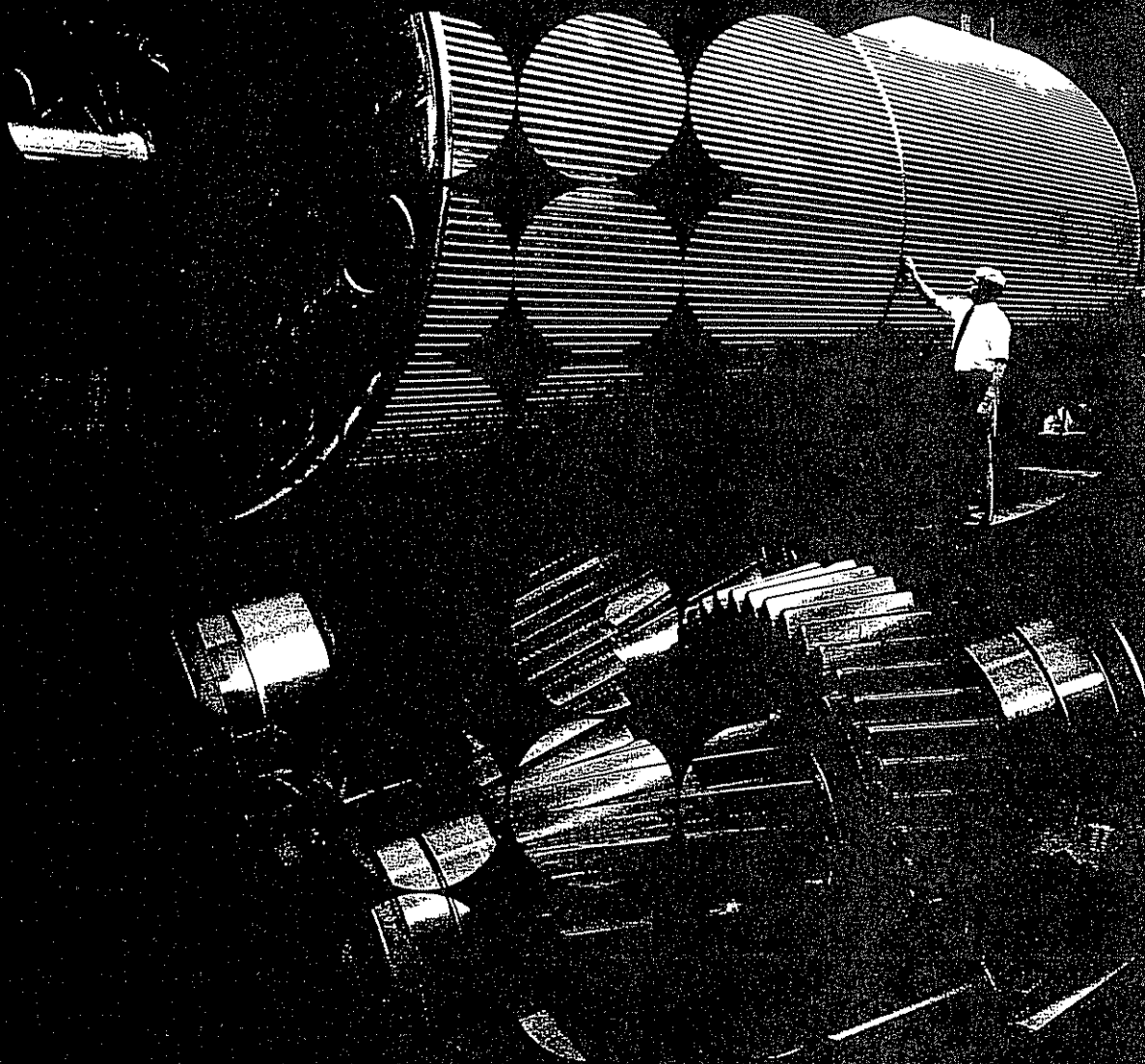
**DOCUMENTS REFERENCED IN PLAINTIFF'S OPPOSITION TO DEFENDANT'S
MOTION TO STRIKE THE THIRD DECLARATION OF PAUL MANNING**

EXHIBIT 1

MOLYBDENUM Mosaic

The Journal of Molybdenum Technology

Volume 10, Number 1, 1987



Continued		Information Data		Steels for Carbonizing Steels						
				Weight Percent						
Alloy Type		S	Mn	P	S	Cr	Ni	Mo	B	Hardness
PS (EX)		0.17	0.79	0.015	0.019	0.56	0.86	0.47		I-255
PS (EX)		0.17	0.79	0.80	0.022	0.54	0.85	0.51		I-49
PS 31 + ca		0.18	0.27	0.82	0.023	0.40	0.84	0.54		I-260
PS (EX) 55		0.17	0.24	0.85	0.015	0.007	0.59	1.75	0.73	I-256
PS (EX) 55		0.17	0.28	0.87	0.015	0.023	0.49	1.84	0.74	I-254
PS 55 1/2		0.17	0.28	0.87	0.023	0.49	1.84	0.74		I-254
325		0.17	0.28	0.87	0.023	0.49	1.84	0.74		I-254
		0.17	0.28	0.87	0.023	0.49	1.84	0.74		I-254
		0.17	0.28	0.87	0.023	0.49	1.84	0.74		I-254
		0.17	0.28	0.87	0.023	0.49	1.84	0.74		I-254
		0.17	0.28	0.87	0.023	0.49	1.84	0.74		I-254
		0.17	0.28	0.87	0.023	0.49	1.84	0.74		I-254
		0.17	0.28	0.87	0.023	0.49	1.84	0.74		I-254
		0.17	0.28	0.87	0.023	0.49	1.84	0.74		I-254
		0.17	0.28	0.87	0.023	0.49	1.84	0.74		I-254
		0.17	0.28	0.87	0.023	0.49	1.84	0.74		I-254
		0.17	0.28	0.87	0.023	0.49	1.84	0.74		I-254
		0.17	0.28	0.87	0.023	0.49	1.84	0.74		I-254
		0.17	0.28	0.87	0.023	0.49	1.84	0.74		I-254
		0.17	0.28	0.87	0.023	0.49	1.84	0.74		I-254
		0.17	0.28	0.87	0.023	0.49	1.84	0.74		I-254
		0.17	0.28	0.87	0.023	0.49	1.84	0.74		I-254
		0.17	0.28	0.87	0.023	0.49	1.84	0.74		I-254
		0.17	0.28	0.87	0.023	0.49	1.84	0.74		I-254
		0.17	0.28	0.87	0.023	0.49	1.84	0.74		I-254
		0.17	0.28	0.87	0.023	0.49	1.84	0.74		I-254
		0.17	0.28	0.87	0.023	0.49	1.84	0.74		I-254
		0.17	0.28	0.87	0.023	0.49	1.84	0.74		I-254
		0.17	0.28	0.87	0.023	0.49	1.84	0.74		I-254
		0.17	0.28	0.87	0.023	0.49	1.84	0.74		I-254
		0.17	0.28	0.87	0.023	0.49	1.84	0.74		I-254
		0.17	0.28	0.87	0.023	0.49	1.84	0.74		I-254
		0.17	0.28	0.87	0.023	0.49	1.84	0.74		I-254
		0.17	0.28	0.87	0.023	0.49	1.84	0.74		I-254
		0.17	0.28	0.87	0.023	0.49	1.84	0.74		I-254
		0.17	0.28	0.87	0.023	0.49	1.84	0.74		I-254
		0.17	0.28	0.87	0.023	0.49	1.84	0.74		I-254
		0.17	0.28	0.87	0.023	0.49	1.84	0.74		I-254
		0.17	0.28	0.87	0.023	0.49	1.84	0.74		I-254
		0.17	0.28	0.87	0.023	0.49	1.84	0.74		I-254
		0.17	0.28	0.87	0.023	0.49	1.84	0.74		I-254
		0.17	0.28	0.87	0.023	0.49	1.84	0.74		I-254
		0.17	0.28	0.87	0.023	0.49	1.84	0.74		I-254
		0.17	0.28	0.87	0.023	0.49	1.84	0.74		I-254
		0.17	0.28	0.87	0.023	0.49	1.84	0.74		I-254
		0.17	0.28	0.87	0.023	0.49	1.84	0.74		I-254
		0.17	0.28	0.87	0.023	0.49	1.84	0.74		I-254
		0.17	0.28	0.87	0.023	0.49	1.84	0.74		I-254
		0.17	0.28	0.87	0.023	0.49	1.84	0.74		I-254
		0.17	0.28	0.87	0.023	0.49	1.84	0.74		I-254
		0.17	0.28	0.87	0.023	0.49	1.84	0.74		I-254
		0.17	0.28	0.87	0.023	0.49	1.84	0.74		I-254
		0.17	0.28	0.87	0.023	0.49	1.84	0.74		I-254
		0.17	0.28	0.87	0.023	0.49	1.84	0.74		I-254
		0.17	0.28	0.87	0.023	0.49	1.84	0.74		I-254
		0.17	0.28	0.87	0.023	0.49	1.84	0.74		I-254
		0.17	0.28	0.87	0.023	0.49	1.84	0.74		I-254
		0.17	0.28	0.87	0.023	0.49	1.84	0.74		I-254
		0.17	0.28	0.87	0.023	0.49	1.84	0.74		I-254
		0.17	0.28	0.87	0.023	0.49	1.84	0.74		I-254
		0.17	0.28	0.87	0.023	0.49	1.84	0.74		I-254
		0.17	0.28	0.87	0.023	0.49	1.84	0.74		I-254
		0.17	0.28	0.87	0.023	0.49	1.84	0.74		I-254
		0.17	0.28	0.87	0.023	0.49	1.84	0.74		I-254
		0.17	0.28	0.87	0.023	0.49	1.84	0.74		I-254
		0.17	0.28	0.87	0.023	0.49	1.84	0.74		I-254
		0.17	0.28	0.87	0.023	0.49	1.84	0.74		I-254
		0.17	0.28	0.87	0.023	0.49	1.84	0.74		I-254
		0.17	0.28	0.87	0.023	0.49	1.84	0.74		I-254
		0.17	0.28	0.87	0.023	0.49	1.84	0.74		I-254
		0.17	0.28	0.87	0.023	0.49	1.84	0.74		I-254
		0.17	0.28	0.87	0.023	0.49	1.84	0.74		I-254
		0.17	0.28	0.87	0.023	0.49	1.84	0.74		I-254
		0.17	0.28	0.87	0.023	0.49	1.84	0.74		I-254
		0.17	0.28	0.87	0.023	0.49	1.84	0.74		I-254
		0.17	0.28	0.87	0.023	0.49	1.84	0.74		I-254
		0.17	0.28	0.87	0.023	0.49	1.84	0.74		I-254
		0.17	0.28	0.87	0.023	0.49	1.84	0.74		I-254
		0.17	0.28	0.87	0.023	0.49	1.84	0.74		I-254
		0.17	0.28	0.87	0.023	0.49	1.84	0.74		I-254
		0.17	0.28	0.87	0.023	0.49	1.84	0.74		I-254
		0.17	0.28	0.87	0.023	0.49	1.84	0.74		I-254
		0.17	0.28	0.87	0.023	0.49	1.84	0.74		I-254
		0.17	0.28	0.87	0.023	0.49				

Contents

- Page 1**
New Advances in
Molybdenum-containing
Corrosion Resistant Alloys
- Page 6**
Molybdenum Carburizing Steel
Provides Performance Edge
- Page 11**
New CCT Diagrams for Carburizing
Steels
- Page 13**
New Literature

Molybdenum Mosaic is published by AMAX Metal Products, 1370 Washington Pike, Bridgeville, Pennsylvania 15017, U.S.A.

Permission is granted to reprint material appearing in this publication provided appropriate credit is given to *Molybdenum Mosaic* and AMAX Metal Products. Where material not originally written by AMAX Metal Products is involved, permission to reprint or use must be requested from the appropriate writer, editor or publication.

Molybdenum Mosaic is presented as a public service. While every effort is made to avoid error, AMAX Metal Products does not verify all of the data presented and disclaims any liability and responsibility for the information contained herein.

The editor of *Molybdenum Mosaic* welcomes letters from readers pertaining to material appearing in *Molybdenum Mosaic* or other subjects of interest.

Editor's Note:

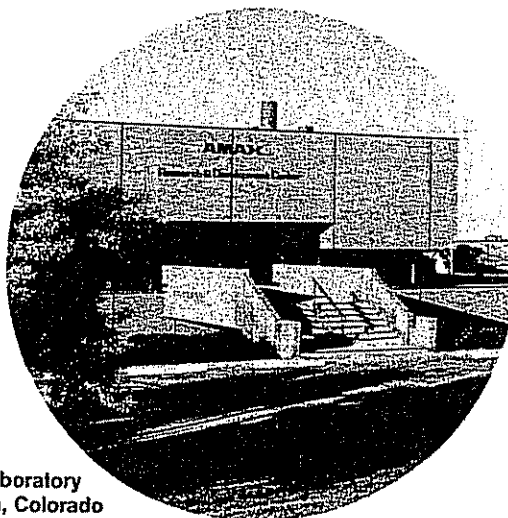
Many of our readers have inquired about the number of issues per volume. Here is the information:

- Volume 1, Numbers 1, 2, 3 and 4
- Volume 2, Numbers 1, 2, 3 and 4
- Volume 3, Numbers 1, 2 and 3
- Volume 4, Numbers 1, 2 and 3
- Volume 5, Numbers 1, 2, 3 and 4
- Volume 6, Numbers 1, 2 and 3
- Volume 7, Numbers 1, 2 and 3
- Volume 8, Numbers 1 and 2
- Volume 9, Number 1

AMAX Consolidates Laboratory Facilities; Opens New Office in Michigan

It has been called the end of an era by some, but AMAX prefers to think of it as a move to make better and more efficient use of its research facilities. As of June 30, 1987, the AMAX Materials Research Center in Ann Arbor, Michigan was shut down and a significant portion of its staff will have transferred to the company's other laboratory site in Golden, Colorado. The address for the Golden laboratory is:

AMAX R&D Center
 5950 McIntyre Street
 Golden, Colorado 80403
 Telephone (303) 279-7636



AMAX Laboratory
 in Golden, Colorado

At the same time, the company has established a new business unit in Ann Arbor, Michigan. This new unit, known as AMAX Specialty Businesses, has been established to develop a wide range of specialty chemical markets ranging from polymer additives to electronic materials. The address of this new AMAX unit is:

AMAX Specialty Businesses
 Atrium Office Center, Suite 320
 900 Victors Way
 Ann Arbor, Michigan 48108
 Telephone (313) 665-0100

HE 00002

tungsten, i.e. chromium is ineffective in reducing acids and beneficial in oxidizing acids. In view of these concepts, a logical basis for comparison of corrosion resistance of the various compositions is the atomic percent factor (APF) which reflects the opposing role of chromium to that of molybdenum and tungsten. The APF is defined as the ratio of four times the chromium weight percent over the sum of twice the molybdenum weight percent and one times the tungsten weight percent.

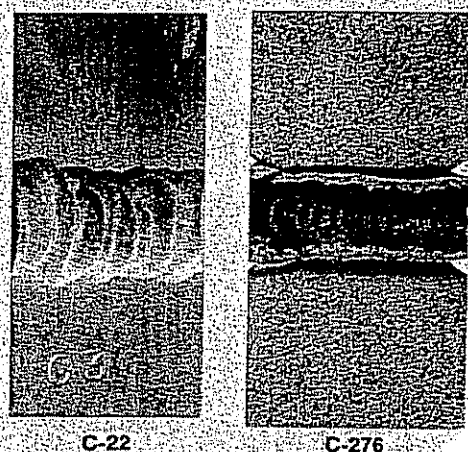
$$\text{APF} = 4\text{Cr} / (2\text{Mo} + 1\text{W})$$

In oxidizing environments, such as nitric acid and sulfuric acid plus ferric sulfate (ASTM G 28), the higher the chromium content (i.e. the higher the APF), the lower the corrosion rates (Figure 1). On the other hand, in reducing environments, such as boiling hydrochloric acid and dilute sulfuric acid, the higher the molybdenum and tungsten contents (i.e. the lower the APF), the lower are the corrosion rates (Figure 2).

The ultimate versatility providing the best resistance to both oxidizing and

reducing environments is achieved by careful adjustment of alloying elements to yield an APF in the range of 2.5 to 3.3 (Figure 3). HASTELLOY alloy C-22 with 22% Cr, 13% Mo and 3% W lies within the range identified for the lowest corrosion rates in oxidizing and reducing environments. In addition, the composition of 22Cr-13Mo-3W in Ni-base alloys shows much improved thermal stability over that of 16Cr-16Mo-4W in alloy C-276. The corrosion resistance of as-welded alloy C-22 is enhanced over that of alloy C-276 (Figure 4). Also, resistance to pitting (Figure 5) and to crevice corrosion attack is the highest of presently available nickel-base alloys.⁵

Figure 5—Corrosion behavior of welded samples showing the improved performance of alloy C-22 over that of alloy C-276.

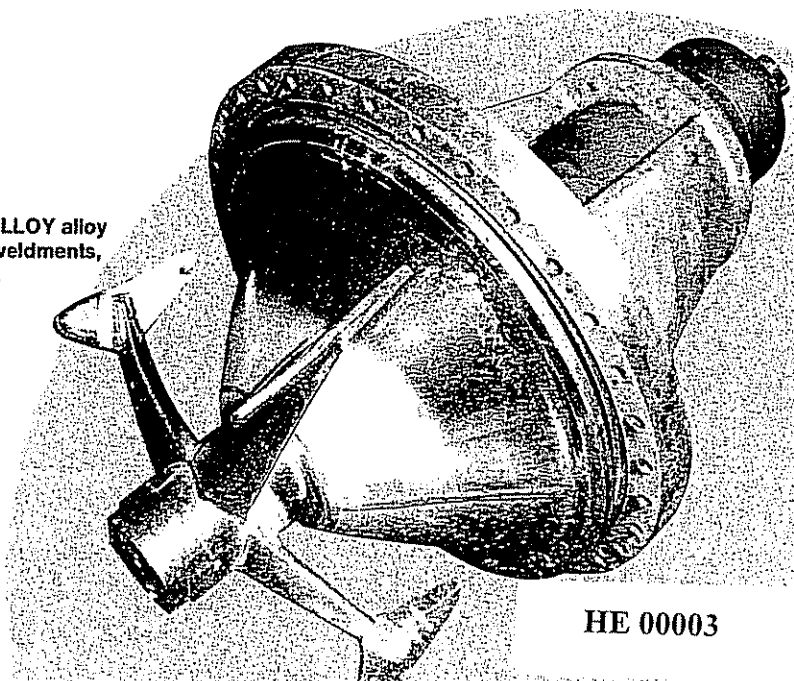


A Wide Range of Industrial Applications

Because of its vastly improved corrosion resistance, HASTELLOY alloy C-22 has very rapidly demonstrated its ability to solve difficult industrial corrosion problems where other corrosion resistant alloys have failed. Details of a few of these applications follow.

- **Pulp and Paper**—HASTELLOY alloy C-22 is being used in a number of applications in pulp bleaching systems in perhaps the most severe environ-

Figure 6—Weld overlays of HASTELLOY alloy C-22, used to protect alloy C-276 weldments, can be seen on bleach plant mixer.



HE 00003

ments where pulp, water and chlorine exist. This superior performance is clearly evident in the bleach plant mixer at the Crown Zellerbach plant in Camas, Washington (Figure 6). The trouble spot was a mixer for a 685 ADMI/D unit installed in early 1984. The C-276 weldments had experienced corrosion problems. In order to improve service life, the builder, Kamy, Inc., ground off 3 mm (0.11 in.) of the welds of alloy C-276 and overlaid them with HASTELLOY alloy C-22. At last inspection, the alloy C-22 weld overlay unit which has been operating for over a year and a half had experienced no problems. At this time, six similar chlorine mixers, made entirely

from HASTELLOY alloy C-22, have been put in service and continue to perform well.

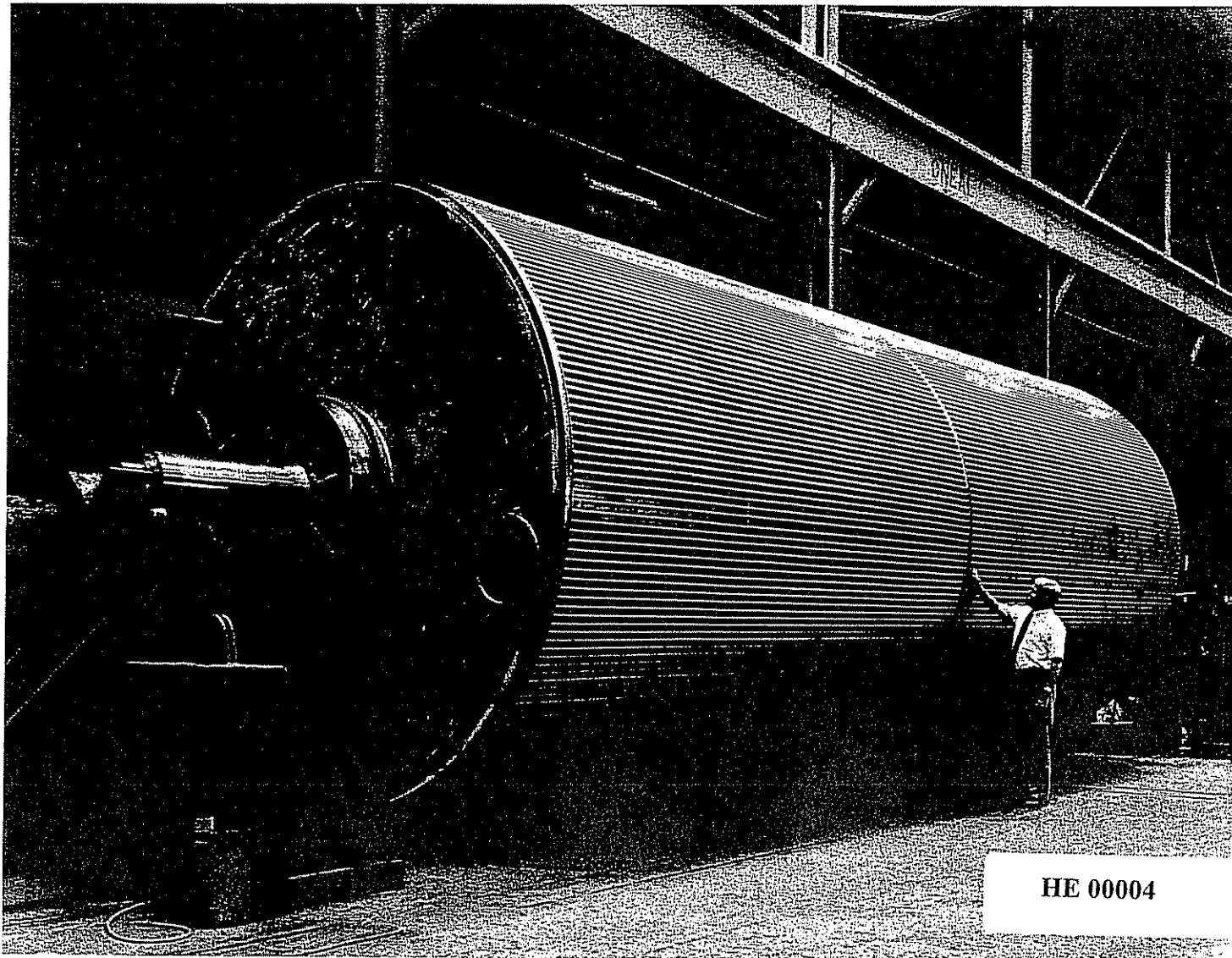
Another application is the large "C" stage bleach washer drum being constructed out of HASTELLOY alloy C-22 at Goslin-Birmingham for a paper mill in the Southeast (Figure 7). The new alloy was selected over titanium because of its excellent corrosion resistance in the residual chlorine, high temperature environment in the bleach washer drum along with its ease of fabrication and repairability.

- **Galvanizing Bath**—Fans used to ventilate zinc galvanizing effluents from a scrubber system were once a source of constant problems at a leading steel company. The effluent [consisting of aluminum, ammonium and zinc chlo-

rides + hydrochloric acid at 26 to 52 C (80 to 125 F)] was eating up 316L stainless steel fans every three to four months. Recently, a fan made of HASTELLOY alloy C-22 was inspected after completing 21 months service (Figure 8) and only slight attack was evident in the form of abrasion/corrosion. Because of the good service provided by the alloy C-22, parts of the housing and shaft that were badly corroded were also replaced with alloy C-22.

Another application involves using HASTELLOY alloy C-22 for electrogalvanizing rolls at several steel mills. Alloy C-276 and C-4 have proven inadequate for this service because of preferential weld and/or HAZ attack.

Figure 7—This bleach washer, made entirely of HASTELLOY alloy C-22 is being constructed at Goslin-Birmingham for a large papermill in the southeast. Alloy C-22 was selected as the prime construction material after extensive corrosion testing.



HE 00004

See how HASTELLOY alloy C-22 outperforms C-276. And it doesn't cost a penny more.

When it comes to corrosion resistance, HASTELLOY alloy C-22 has been proven superior to alloy C-276 in tests after test and application after application. Pick any aggressive environment, especially mixed acids, such as sulfuric plus hydrochloric or nitric plus hydrochloric. Alloy C-22 is consistently better at fighting corrosion.

And that added protection doesn't cost anything extra.

Different alloys — the same technological leader

Who better to invent the successor to HASTELLOY alloy C-276 than the same group that invented the HASTELLOY alloy family (C, C-4 and C-276)? Our researchers carefully balanced the chromium, molybdenum, tungsten and iron content of the new alloy to make a product with unique versatility in resisting corrosion in oxidizing and reducing acids.

For more than a year now, HASTELLOY alloy C-22 has been used with outstanding results in pulp and paper bleaching, chlorine line duty, nuclear waste treatment, pickling, electrogalvanizing, and herbicide manufacture.

Excellent thermal stability and corrosion resistance of weldments

HASTELLOY alloy C-22 has not only the best anti-corrosion resistance but also outstanding thermal stability. And we can prove it. Alloy C-22 has been used to solve corrosion problems of alloy C-276 weldments.

One brochure gives you all the information you'll need to make a comparison. Find out how HASTELLOY alloy C-22 performs in ferric and cupric chlorides, hot contaminated corrosive media, formic and acetic acids, seawater, and brines.

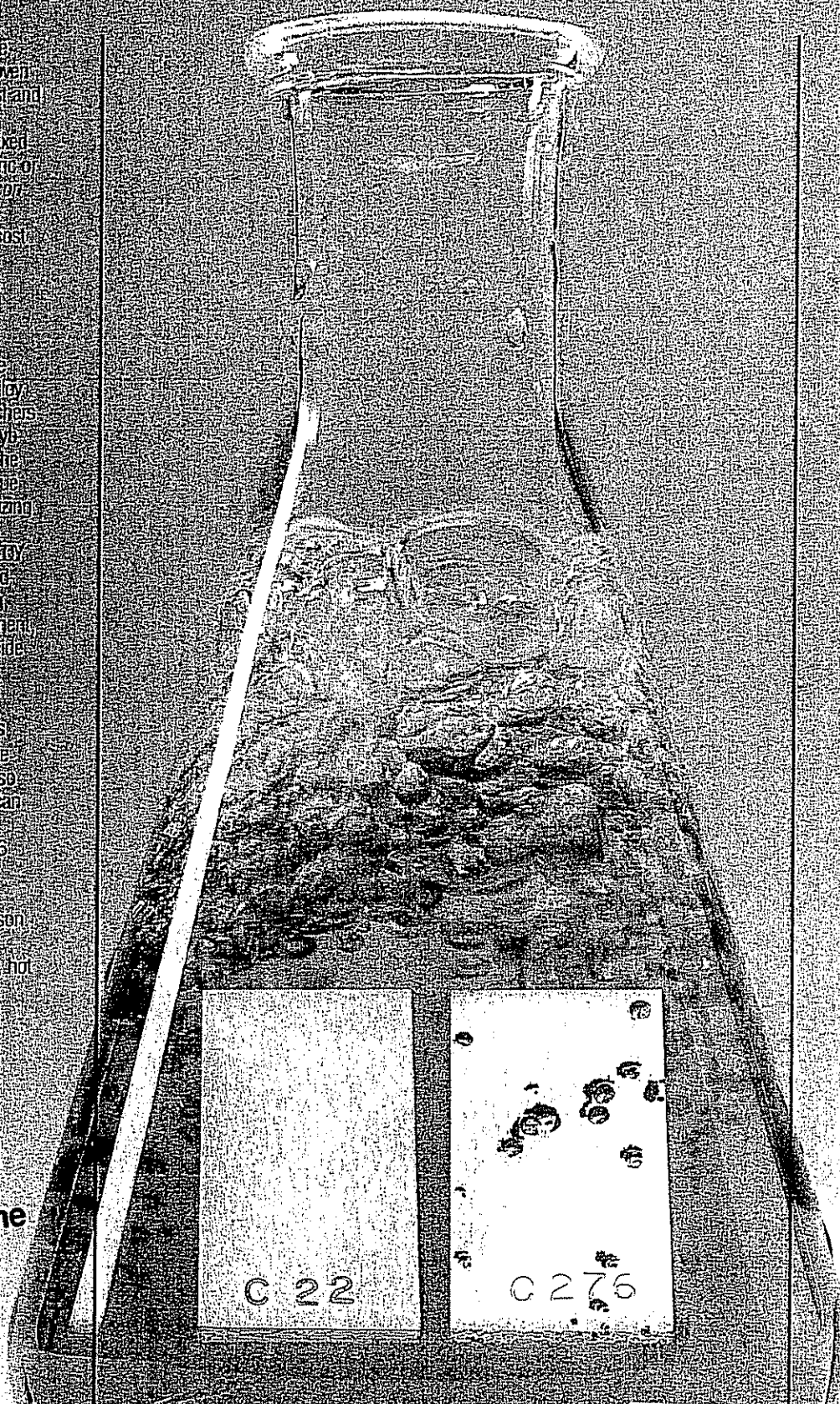
For your free copy of this brochure, simply circle the reader service number below. Or give us a call. You can see for yourself how alloy C-22 performs against alloy C-276, alloy 625 and others.

We changed our name
from Cabot to:

HAYNES

International

In state	Toll-free
Anaheim, CA 714-978-1775	1-800-531-0285
Houston, TX 713-462-2177	1-800-231-4548
Kokomo, IN 317-456-6612	1-800-354-0606
Windsor, CT 203-688-7771	1-800-426-1963



HE 00105

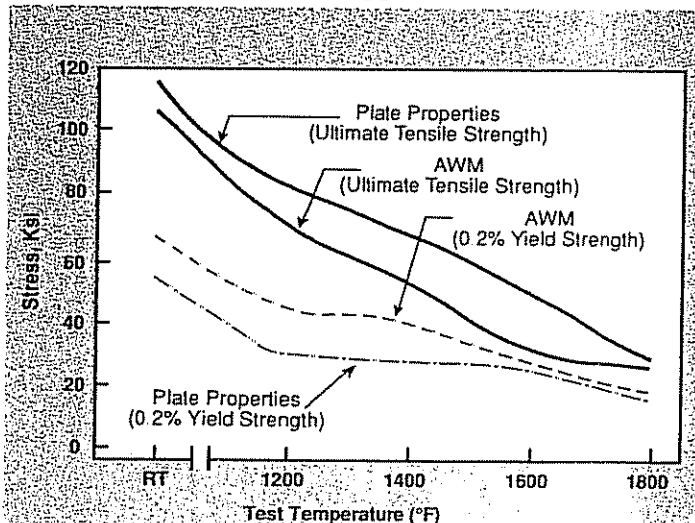
Here are two of the best "universal" weld filler metals for your worst corrosive and high- temperature environments

These two versatile filler metals are the only alloys you need for welding materials used in severely corrosive and high-temperature environments. They've been proved in our laboratory, and we've put them to work in the real world, too. And both alloys are easy to weld.

HAYNES® alloy 556 offers outstanding high-temperature all-weld-metal strength

HAYNES alloy 556 displays excellent welding characteristics and outstanding all-weld-metal strength. Plus it offers good high-temperature oxidation, sulfidation, carburization and chlorination resistance. As a result, 556™ weld rod typically results in performance limited by base metal properties, not weld-metal properties.

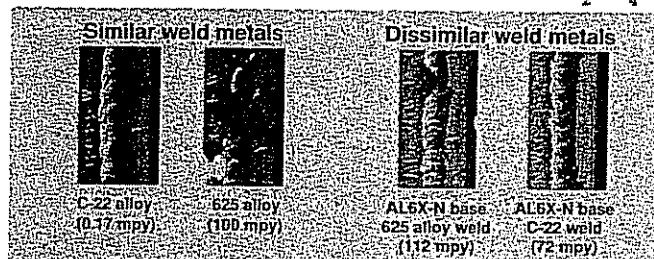
So no matter what your metal combination is—Ni-base to Fe-base, Co-base to Fe-base, stainless steel to Fe-, Ni- or Co-base, carbon steel to Fe-, Ni- or Co-base—556 weld rod is the filler metal for your high-temperature application.



Tensile properties of plate and welded 556 alloy show that the alloy retains its strength when used as a universal weld filler metal.

HASTELLOY® alloy C-22 outlasts C-276 7 to 1 and alloy 625 by 600 times

Tests at the Los Alamos National Laboratories show the superiority of HASTELLOY alloy C-22 weldments over other nickel-base alloys. The environment was 3M NaCl + 0.1M FeCl₃ + 0.1M NaF with the pH adjusted to 1.0 with a mixture of 10M HCl/1M H₂SO₄.



Test coupons show that when welding dissimilar metals, C-22 alloy is 1.5 times more corrosion resistant than 625 alloy.

In actual application, alloy C-276 weldments in a bleach mixer corroded after only three months. But two years after overlaying with C-22™ alloy, there's no corrosion. That's an eight-fold increase in service life.

Both alloys are in stock for fast delivery

HASTELLOY alloy C-22 is available in layer-wound coils, straight lengths and coated electrodes. HAYNES alloy 556 comes in loose and layer-wound coils. The alloys are also offered in plate, sheet, strip, billet, bar, tubing and welded pipe. Four Haynes Service Centers are stocked and ready to ship within 24 hours. For more information, contact the one nearest you.

HAYNES
International

HE 00106

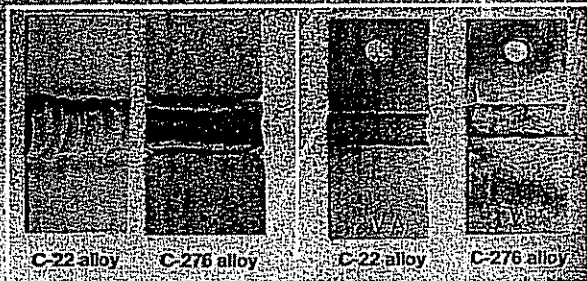
	In state	Toll-free
Anaheim, CA	714-978-1775	1-800-531-0285
Houston, TX	713-937-7597	1-800-231-4548
Kokomo, IN	317-456-6789	1-800-354-0806
Windsor, CT	203-688-7771	1-800-426-1963

HASTELLOY, HAYNES, C-22 and 556 are trademarks of Haynes International Inc. AL6X-N is a registered trademark of Allegheny-Ludlum Corp.

HASTELLOY® alloy C-22 weldments are more corrosion resistant than most base metals

C-22® alloy provides corrosion resistance where you need it most. At the weld.

As a universal weld filler metal, HASTELLOY alloy C-22 can make the most vulnerable parts of your equipment—the welds—the most resistant to corrosion. In both laboratory and field tests, C-22 alloy outperforms other nickel base alloys, demonstrating improved resistance to both localized and general corrosion.

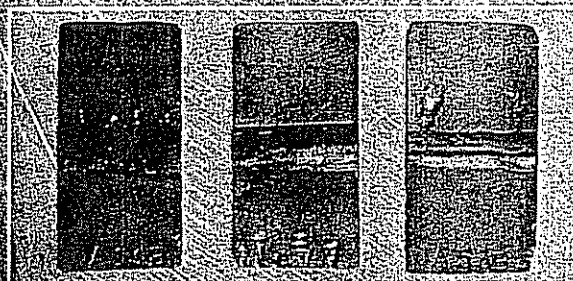


Samples on the left were exposed to 11% H₂SO₄ + 3.9% Fe₂(SO₄)₃, other chemicals and overpressurized with O₂ at 300°F. Samples on the right were exposed to a 3000 ppm Cl⁻ solution, adjusted to a pH of 1.5 with HCl, with Cl₂ gas bubbled through constantly.

Performance has been proven in actual applications. In one instance, alloy C-276 weldments in a bleach mixer were severely corroded in just three months. The weldments were ground back and overlaid with C-22 alloy. Now, after two years, no problems have recurred. With performance like this, HASTELLOY alloy C-22 is your best choice for a wide range of welding applications. C-22 alloy weld metal can provide more corrosion resistance than many less-alloyed base metals such as stainless steels.

Improved welds for stainless steel construction.

Laboratory tests also show the superiority of C-22 alloy welds. Three samples of 317L stainless steel were welded with 317L, alloy 625 and C-22 alloy. They were tested in ASTM G-48 solution (10% FeCl₃) for 120 hours at 95°F. The excellent corrosion resistance of C-22 alloy is evident in the following photographs. And similar results have been seen with other stainless steels and nickel alloys, using either bare-wire filler or coated electrodes of C-22 alloy.



317L stainless steel with (left to right) 317L, 625 and C-22 alloy welds exposed to 10% FeCl₃ at 95°F (ASTM G-48) for 120 hours.

Try C-22 alloy for your toughest weld corrosion problems.

The next time you experience a problem of extreme weld corrosion, why not grind away the corrosion and deposit C-22 alloy? On new construction, too, use of C-22 alloy will help protect the welds of both nickel-alloy and stainless steel equipment.



Alloy C-276 bleach mixer with upgraded C-22 alloy welds for vastly improved service life.

C-22 alloy (layer-wound coils, straight lengths and coated electrodes) is stocked at four conveniently-located Haynes Service Centers and is routinely shipped within 24 hours. C-22 alloy is also available from authorized North American distributors: British Steel Alloys in western Canada and Drummond McCall in eastern Canada; Corrosion Materials, Inc., Baker, LA and TubeSales, Atlanta, GA throughout the United States.

For more details on the laboratory and field tests of HASTELLOY alloy C-22 weldments that prove its superiority, call any of the numbers listed below and ask for Bulletin H-2062.

HAYNES International

	In State	Toll-Free
Anaheim, CA	714-978-1775	1-800-531-0285
Houston, TX	713-937-7597	1-800-231-4548
Kokomo, IN	317-456-6612	1-800-354-0806
Windsor, CT	203-688-7771	1-800-426-1963

HASTELLOY and C-22 are trademarks of Haynes International, Inc.

HE 00107

EVERYTHING IS BIGGER IN TEXAS?

LCRA, LaGrange, Texas
451 MW 100,000 lbs.
HASTELLOY® alloy C-22 for the
30' x 30' x 120' long outlet duct

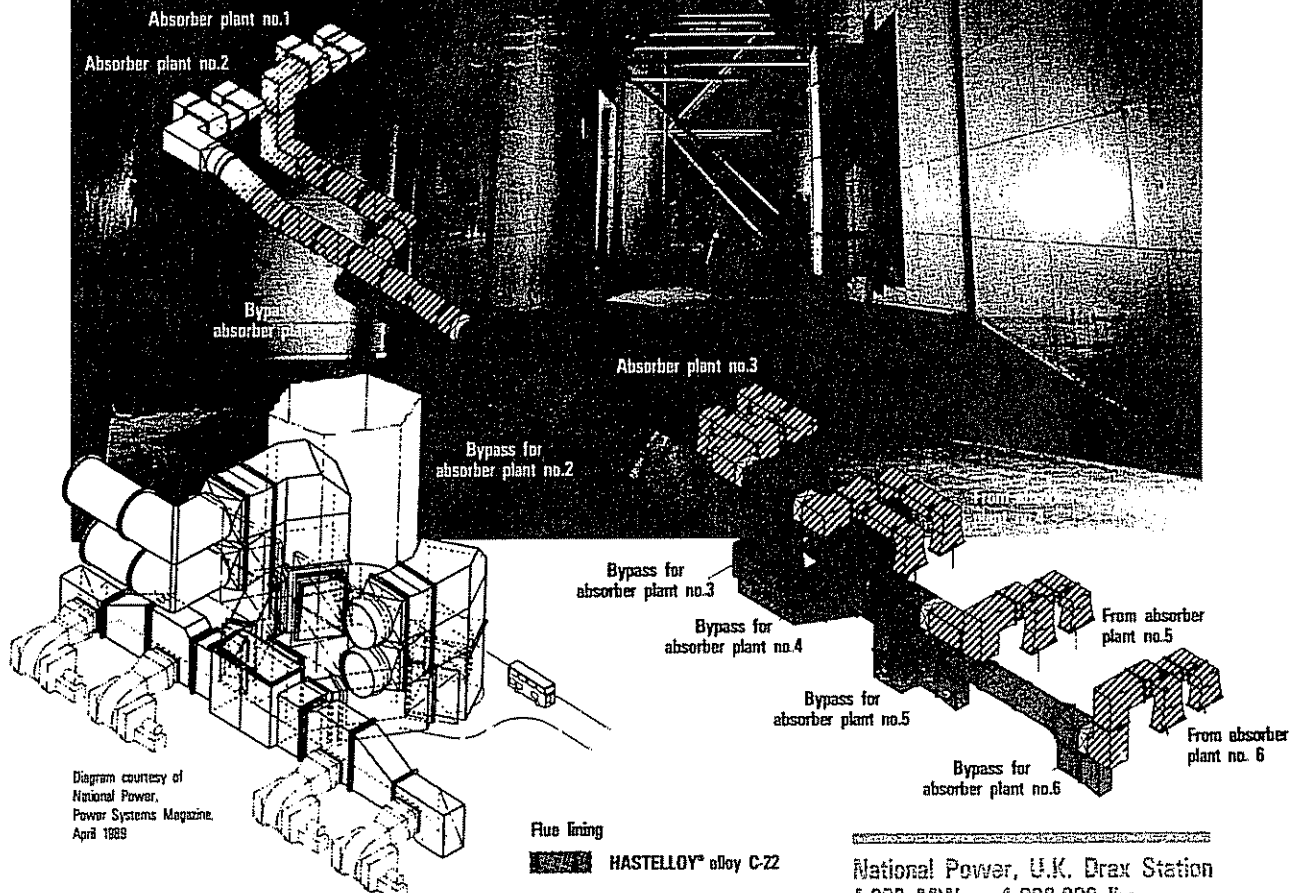


Diagram courtesy of
National Power,
Power Systems Magazine,
April 1989

RELIABILITY:

Over 25 U.S.A. FGD Systems chose HASTELLOY® alloy C-22 based on performance and value.

HASTELLOY® alloy C-22 Performance

- Best weld corrosion resistance, highly improved filler weld material
- Best uniform corrosion resistance important when trace NO_x is present
- Best pitting resistance when sulfur compounds and halide ions (e.g. Cl^-) are present

Haynes International's Performance

- Quality HASTELLOY alloy pacesetter for industry standards
- 75 years experience in manufacturing and competent technical support
- Complete inventory integrated customer service system

Tony Nicholas
FGD Market Manager
Tel (317) 456-6095
FAX (317) 456-6905

HE 00108

HAYNES

International

P.O. Box 9013
1020 W Park Avenue
Kokomo, Indiana 46904-9013

HASTELLOY® alloys outperform all others for corrosion resistance in hazardous waste treatment equipment

Why risk equipment failure, possible injuries, EPA penalties, or liability? For the best equipment reliability, plant designers and operators specify HASTELLOY alloys from Haynes International. C-22™ and G-30™ alloys provide the best corrosion resistance against extreme, and often unpredictable, hazardous waste environments. Consider these examples.



C-22 alloy specified for critical fluid extraction equipment to withstand corrosion and stress cracking

C-22 alloy withstands high pressures and severe corrosives in industrial wastewater processing

C-22 alloy was specified for equipment in a process that uses liquid carbon dioxide at 1000 psi to extract hazardous organic chemicals from wastewater. C-22 alloy resists a variety of corrosives including high chloride levels.



G-30 alloy scrubber withstands chloride corrosion

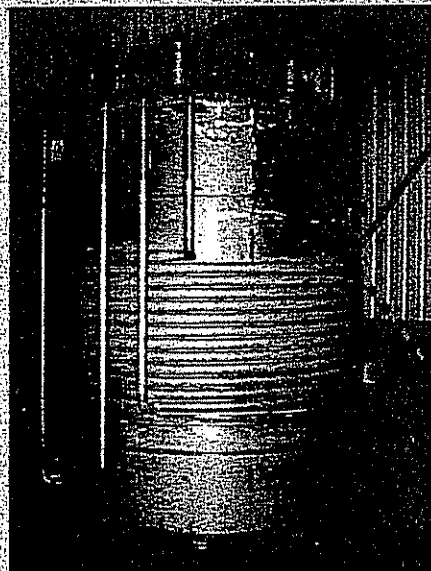
G-30 alloy specified for scrubber after three others fail prematurely

Offgas scrubber components made of 316 stainless steel disintegrated within hours of contact with a chloride-based fuel. And alloys

20Cb-3 and G-3 components lasted less than one year. HASTELLOY alloy G-30 replacement parts, however, show little corrosion more than four years after installation. The scrubber is part of a concrete manufacturing process that burns waste solvents as fuel.

C-22 alloy resists dew point corrosion at elevated temperatures

A scrubber fabricated with C-22 alloy withstands hot gases created as 55-gallon steel drums are heated to red heat to burn away organic residues. This produces gases containing organics and hydrochloric acid which enter the scrubber at 520° F for treatment and cooling.



C-22 alloy was utilized in radioactive waste concentrator vessels

C-22 alloy selected to handle high level radioactive wastes

A radioactive waste disposal system uses a process that heats and concentrates high level radioactive liquid waste. C-22 alloy was specified for the concentrators for its corrosion resistance and reliability.

C-22 alloy: 500 times more resistant than alloy 625; 1000 times better than 316 stainless steel



C-22 base C-22 weld 625 base 625 weld AL6X-N base 625 weld AL6X-N base C-22 weld

Base alloy/weld filler metal	Corrosion Rate (mpy)
C-22 alloy/C-22 alloy	0.17
C-276/C-276 alloy	1.14
alloy 625/alloy 625	100.00
316 stainless/316 stainless	203.00
C-276 alloy/C-22 alloy	1.02
alloy 625/C-22 alloy	94.00
alloy AL6X-N/alloy 625	112.00
alloy AL6X-N/C-22 alloy	72.00
alloy B-2/alloy B-2	95.00
alloy B-2/C-22 alloy	79.00

This table shows results of 39 days of worst case "scrub" condition alloy testing at the Los Alamos National Laboratory. Based on these findings, C-22 alloy was selected for base and weld filler material for incinerator replacement components for a mixed waste incinerator developed for the Department of Energy.

Test HASTELLOY alloys in your plant at no charge

Find out how our alloys stand up to hazardous waste environments at your plant. Just call and our technical experts will send you test coupons. And when you're ready to order, you'll find HASTELLOY alloys in stock and ready to ship, in just the product forms you need. Contact your nearest distribution center at the number below or call 1-800-354-0806.

HAYNES

International

	In state	Toll-free
Anaheim, CA	714-978-1775	1-800-531-0285
Houston, TX	713-937-7597	1-800-231-4548
Kokomo, IN	317-456-6789	1-800-354-0806
Windsor, CT	203-688-7771	1-800-426-1963

HASTELLOY, C-22 and G-30 are trademarks of Haynes International, Inc.

HE 00109

Come to the company that created **HASTELLOY® alloy corrosion resistance...**

... for the ultimate in corrosion-resistant alloys: B-2, B-3™, C-276, C-22®, C-2000™, C-4, D-205™, G-30® and ULTIMET®

Over 100 years ago, Elwood Haynes established the company that was to develop the first commercially produced automobile in the United States. In 1912 he founded the company which developed HAYNES® alloys and the HASTELLOY alloy family. Since then, HAYNES superalloys have served in critical components in gas turbines and the aerospace industry.

And the high performance HASTELLOY alloys? They're being specified in virtually every industrial and chemical process that involves severe corrosion. Over the past five years, Haynes International, Inc. has introduced ULTIMET alloy and three new HASTELLOY alloys. ULTIMET alloy combines excellent corrosion resistance with outstanding wear resistance.

HASTELLOY B-3 alloy offers a level of thermal stability greatly superior to that of its predecessors, e.g. HASTELLOY B-2 alloy. HASTELLOY D-205 alloy exhibits outstanding resistance to hot, highly concentrated sulfuric acid and other highly oxidizing media. And the latest, HASTELLOY C-2000 alloy, provides the broadest range of process environment capabilities to the chemical processing industry.

To get more information on these alloys or the company that has been a leader in superalloys and high performance alloys, call or write:

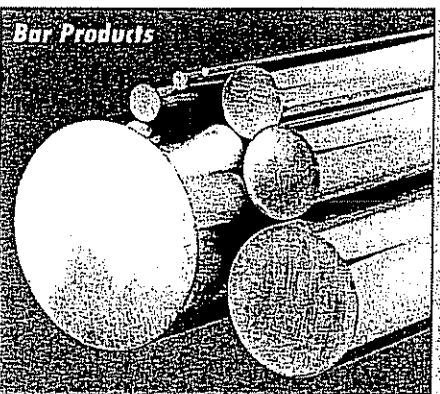
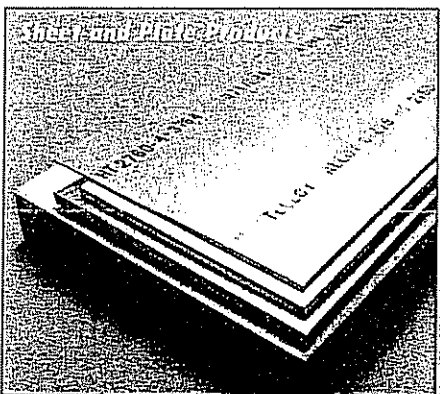
HAYNES **International**

A tradition of innovation spanning a century

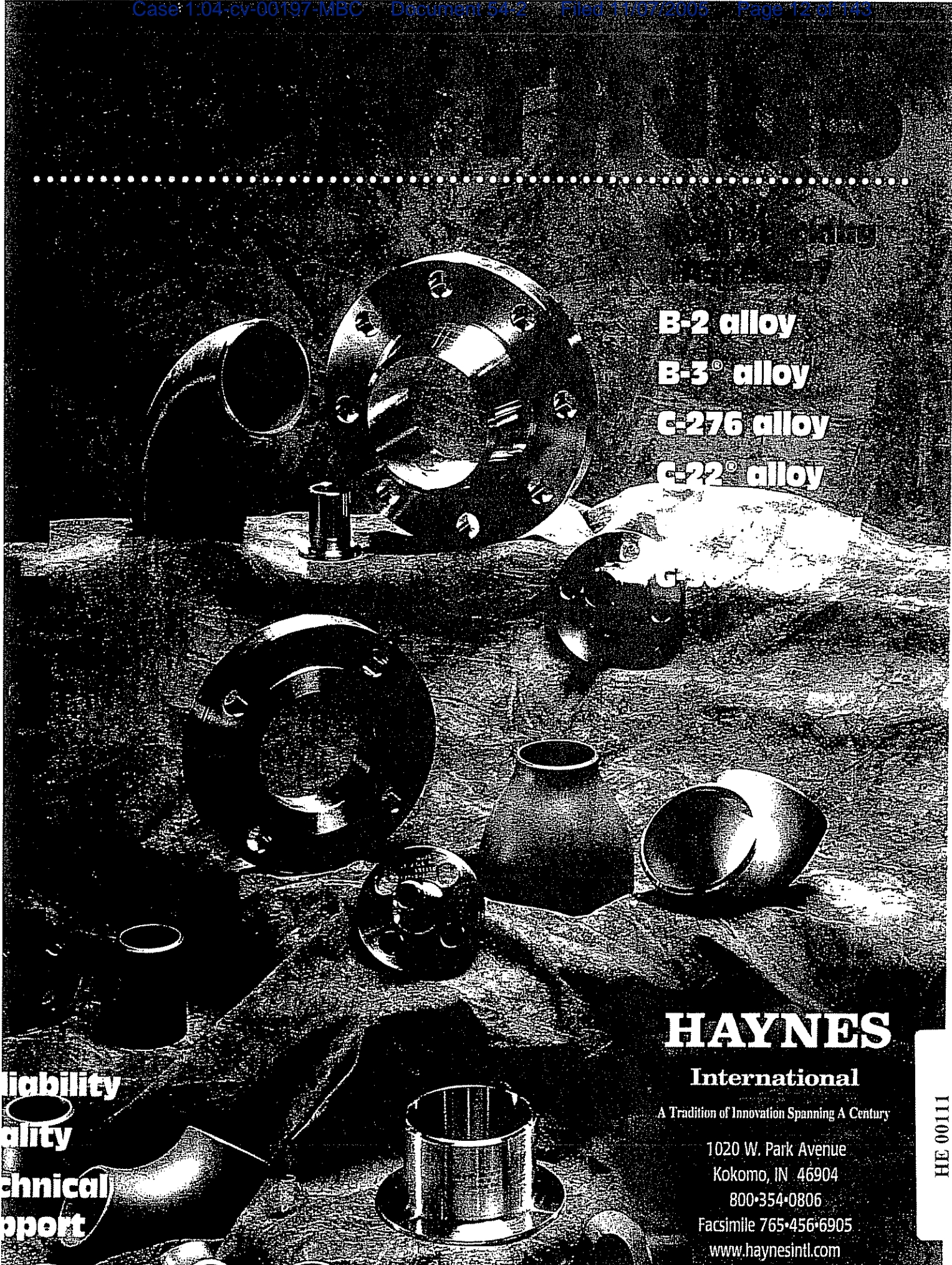
Haynes International, Inc., P.O. Box 9013, Kokomo, Indiana 46904-9013, U.S.A.
Telephone 317-456-6012 FAX 317-456-6079

Haynes International Ltd., P.O. Box 10, Park House Street, Openshaw, Manchester, M11 2ER, U.K. Telephone 44-161-230-7777 FAX 44-161-223-2412

HASTELLOY, HAYNES, B-3, C-22, C-2000, D-205, G-30 and ULTIMET are trademarks of Haynes International, Inc.



HE 00110



B-2 alloy
B-3[®] alloy
C-276 alloy
C-22[®] alloy

HAYNES

International

A Tradition of Innovation Spanning A Century

1020 W. Park Avenue

Kokomo, IN 46904

800-354-0806

Facsimile 765-456-6905

www.haynesintl.com

HE 00111

Reliability
Quality
Technical Support

The Use of New PHACOMP in Understanding the Solidification Microstructure of Nickel Base Alloy Weld Metal

M. J. CIESLAK, G. A. KNOROVSKY, T. J. HEADLEY, and A. D. ROMIG, Jr

The weld metal microstructures of five commercial nickel base alloys (HASTELLOYS* C-4, C-22, and C-276, and INCONELS* 625 and 718) have been examined by electron probe microanalysis and analytical electron microscopy. It has been found that solidification terminates in many of these alloys with the formation of a constituent containing a topologically-close-packed (TCP) intermetallic phase (*i.e.*, σ , μ , Laves). Electron microprobe examination of gas-tungsten-arc welds revealed a solidification segregation pattern of Ni depletion and solute enrichment in interdendritic volumes. New PHACOMP calculations performed on these segregation profiles revealed a pattern of increasing M_d (metal- d levels) in traversing from a dendrite core to an adjacent interdendritic volume. In alloys forming a terminal solidification TCP constituent, the calculated M_d values in interdendritic regions were greater than the critical M_d values for formation of σ as stated by Morinaga *et al.* Implications of the correlation between TCP phase formation and M_d in the prediction of weld metal solidification microstructure, prediction of potential hot-cracking behavior, and applications in future alloy design endeavors are discussed.

I. INTRODUCTION

SOLIDIFICATION during arc welding is an inherently nonequilibrium process. Microstructures generated during arc welding are often not those predicted by applying equilibrium considerations to existing phase diagrams. In some cases, such as the Al-Mg system, the formation of a relatively large volume fraction of a nonequilibrium eutectic constituent makes possible the fabrication of readily weldable alloys such as 5456 (Al-5.2 wt pct Mg). Usually, though, the formation of a low-melting nonequilibrium eutectic constituent is detrimental from a weld hot-cracking viewpoint.

The sequence of solidification reactions in commercial alloys is of prime importance in diagnosing not only hot-cracking propensity but also in understanding subsequent solid-state transformations and materials properties derived from these transformations. Unfortunately, phase diagrams are lacking for virtually every alloy system incorporating more than three components and are generally limited in scope even for ternary systems.

In the case of nickel base alloys, much fundamental and empirical effort has gone into describing phase relationships in the solid state. Nickel base alloys are generally derived from at least ternary systems and more usually quaternary or higher order systems. The face-centered-cubic Ni matrix has a high solubility for many substitutional alloying elements, but commercial alloys often contain a large number of minor phases (carbides, nitrides, borides, intermetallic compounds, *etc.*). The occurrence of certain topologically-close-packed (TCP) intermetallic phases, such as μ , σ , and Laves, has been shown to influence the mechanical properties of nickel and cobalt base superalloys.¹⁻⁴ As phase dia-

grams were not available for complex systems, metallurgists compiled empirical data on the occurrence of these phases in commercial alloys. In the 1950's, several authors⁵⁻⁹ investigating binary and ternary alloy systems applied the electron vacancy concept of Pauling¹⁰ and realized that σ phase was an electron compound,¹¹ the presence of which could be predicted in other alloy systems.

Later, Woodyatt, Sims, and Beattie¹² advanced this predictive capability to complex, commercial alloys through a calculation scheme known by the acronym PHACOMP (for PHase COMPutation). The average electron hole number, defined as N_e , for the austenitic matrix is calculated after accounting for the formation of all phases normally encountered in nickel base superalloys (carbides, γ' , borides, *etc.*). The algebraic definition of N_e is given as follows:

$$N_e = \sum (x_i)(n_i') \quad [1]$$

where x_i is the atomic fraction of element i and n_i' is the electron hole number of element i . Table I lists values of n_i' for the common elements found in nickel-base alloys. A critical electron hole number, based upon studies of binary and ternary alloy systems and upon the collected empirical data from vast numbers of heats of commercial alloys, was established as the " σ -safe" boundary. That is, when the critical value of N_e was exceeded in the residual austenitic matrix, σ would be predicted to form. In a similar manner, " μ -safe" and "Laves-safe" boundaries have been established.¹³ By using this approach, alloy design and chemistries control have been carried out for the past two decades.

It must be pointed out, though, that problems have arisen in predicting the "safe" compositions for some alloys, such as Alloy 713-C.^{3,14} In addition, calculational difficulties have been ascribed to alloys having relatively high Mo or W contents. In general, elements not located in the first long row (transition metals) of the Periodic Table have been simply assigned individual n_e numbers equal to those of the elements at the top of their respective columns. Subsequent attempts to correlate these values with ternary phase diagram data has resulted in, for example, the assigning

*HASTELLOY is a trademark of Cabot Corporation. INCONEL is a trademark of the INCO family of companies.

M. J. CIESLAK and G. A. KNOROVSKY, Org. 1833, Process Metallurgy, T. J. HEADLEY, Org. 1822, Electron Optics and X-ray Analysis, and A. D. ROMIG, Jr., Org. 1832, Physical Metallurgy, are with Sandia National Laboratories, P.O. Box 5800, Albuquerque, NM 87185.

Manuscript submitted March 14, 1986

of n_i^d numbers from 4.66 to 10.¹⁵ A more sophisticated PHACOMP technique, which defines temperature dependent critical N_i values, has also been suggested.¹⁶

Recently, a more fundamental and elegant approach to the problem of austenite phase stability vs TCP phase (and other intermetallic phases) formation in nickel base alloys has been developed by Morinaga *et al.*^{17,18} With a quantum mechanical calculational technique, the DV-X α (discrete variational cluster) method, a different type of PHACOMP, called New PHACOMP, was developed. Instead of calculating an average electron hole number, the average d -electron energy above the Fermi level is calculated for the same residual austenitic matrix. This average d -electron energy is called M_d and is defined algebraically as:

$$M_d = \sum (x_i) (m_i^d) \quad [2]$$

where x_i is the atomic fraction of element i and m_i^d is the metal d -level of element i . Elemental values of m_i^d are given in Table I. In a manner analogous to the original PHACOMP, New PHACOMP calculations are used to predict the occurrence of intermetallic phases such as TCP phases in a nickel-base austenitic matrix. Temperature dependent critical values of M_d , calculated from appropriate binary and ternary phase diagrams, were established for " σ -safe" alloys such that when these values were exceeded, σ would be expected to occur. In addition, other phase boundaries ($\gamma/\gamma + \beta(\text{NiAl})$, $\gamma/\gamma + \gamma'$, and $\gamma/\gamma + \mu$) were also predicted by specific critical M_d values. In particular, the temperature-dependent " σ -safe" expression is given as:¹⁷

$$M_d^{\sigma} = 6.25 \times 10^{-5} T + 0.834 \quad [3]$$

where T is the absolute temperature in Kelvin.

A method for predicting phase stability, microstructure, and solidification sequence in austenitic stainless steel weld metal has also been developed,¹⁹⁻²² based upon a Cr and Ni equivalent concept. It has been determined that alloying elements normally found in stainless steels have similar phase stabilizing behavior as either Cr or Ni. Those elements which act in a manner similar to Cr (Mo, Si, Ti, Nb, W, Ta, V, Al) tend to stabilize the body-centered-cubic ferritic phase. Elements which behave similarly to Ni

(C, N, Mn, Cu, Co) tend to stabilize the face-centered-cubic austenitic phase. An excellent historical review of this development has been recently published by Olson.²² In an analogous manner, an equivalent composition model has recently been proposed by Cieslak *et al.*^{23,24} to describe the solidification and solid state transformation microstructure in austenitic Ni-Cr-Mo-Fe-W weld metals.

It must be remembered that the entire history of the development of PHACOMP-type calculations for austenitic superalloys and equivalency models for austenitic weld metals has been driven by the desire to establish the γ solvus vs a variety of other possible phases in complex, multi-component systems for which phase diagrams are not available. The purpose of this study is to show that a correlation exists between the weld solidification microstructure in the nickel base alloys investigated and critical values of the M_d parameter from the New PHACOMP formalism.¹⁷

II. EXPERIMENTAL PROCEDURE

The mill analyses of the alloys used in this investigation are given in Table II. All alloys tested were in the mill annealed condition prior to welding. All welding was done using the autogenous (no filler metal added) gas-tungsten-arc (GTA) process, direct current, electrode negative. Welds were made using a current of 100 amperes at a travel speed of 20 cm/min (90 amperes at 22 cm/min for INCONEL 718). Argon was the shielding gas.

The weld metal analyzed was obtained from Varestraint Test^{25,26} (a fusion zone hot-cracking test) specimens. Weld metal analysis involved scanning electron microscopy (Hitachi S-520), electron probe microanalysis (Cameca MBX), and transmission electron microscopy (JEOL 100C).

After welding, samples for bulk microstructural analysis were sectioned from Varestraint specimens and included the fusion zone hot cracks present. The samples were mounted in epoxy and polished through 0.05 μm alumina. The microstructures were revealed by a 10 pct chromic acid etchant. Those specimens to be examined in the scanning electron microscope (SEM) were carbon coated prior to examination.

The specimens for electron probe microanalysis had microhardness indentations placed on the specimen surface to bracket areas for analysis. The etched surfaces were then repolished flat with 1 μm diamond paste and carbon coated prior to analysis. Profiles were taken across weld metal dendrites perpendicular to the dendrite growth direction. Care was taken to avoid interdendritic constituents during profiling. The microprobe was operated at an accelerating potential of 15 kV and a beam current of approximately 20 nA. K_{α} X-ray peaks were used to analyze for all elements of interest except for Mo, W, and Nb, where the L_{α} peaks were used. Point count data were reduced to weight percentages with a $\phi(\rho, Z)$ computer algorithm.²⁷

Samples for transmission electron microscopy were sliced from the weld metal of Varestraint specimens with a low-speed carbide saw and ground to a thickness of approximately 125 μm . Standard 3 mm-diameter disks were cut from the thin sheet with a mechanical punch. Thin foils were prepared by electropolishing in a solution of 10 pct perchloric acid in methanol at approximately -65°C . Following electrochemical thinning, the foils were placed in an ion

Table I. Elemental n_i^d and m_i^d Values

Element	n_i^d	m_i^d
Ti	6.66	2.271
V	5.66	1.543
Cr	4.66	1.142
Mn	3.66	0.957
Fe	2.66	0.858
Co	1.71	0.777
Ni	0.66	0.717
Zr	6.66	2.944
Nb	5.66	2.117
Mo	4.66	1.550
Ta	5.66	2.224
W	4.66	1.655
Al	7.66	1.900
Si	6.66	1.900

mill to increase the amount of thin area and to remove any electrolyte residue. The foils were examined in a JEOL 100C AEM operated at 100 kV. Selected-area electron diffraction was used to uniquely identify phases in the weld metals' microstructures.

III. RESULTS

A. Microstructural Analysis

Figures 1 through 5 are SEM secondary electron photomicrographs of the weld metal microstructures of the five alloys studied. In all cases fusion zone hot cracks are present in the figures and terminal solidification constituents can be seen (except in Figure 1. HASTELLOY C-4) associated with the hot cracks. In general, it was observed that INCONEL 718 had the largest volume fraction of terminal solidification constituent, and that HASTELLOY C-4 had the least (none observable in the SEM).

Higher magnification SEM analysis revealed a lamellar, eutectic-like morphology of these terminal solidification constituents. Figure 6 shows this well-developed structure in INCONEL 718 weld metal. A similar morphology can be seen in Figure 7 for INCONEL 625 weld metal. HASTELLOYS C-22 (Figure 8) and C-276 (Figure 9) have a somewhat less well-developed structure, probably the result of a lower volume fraction of terminal solidification constituent in these two alloys.

Electron diffraction experiments performed on these alloys revealed the crystal structure of the terminal solidification constituents. In both INCONELS 625 and 718, the predominant terminal solidification constituent contains a Nb-rich Laves phase (hexagonal, $a = 0.479$ nm, $c = 0.770$ nm). Some NbC/austenite terminal solidification constituent is also observed, especially in INCONEL 718. In HASTELLOY C-22, the terminal solidification phase is

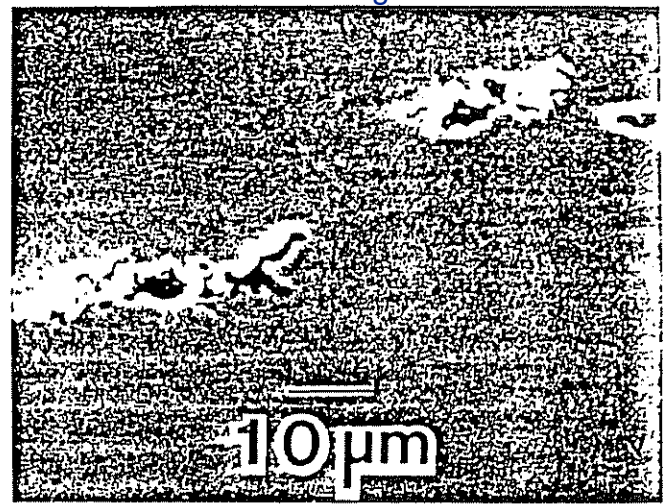


Fig. 1—SEM micrograph of weld hot-cracked region in HASTELLOY C-4

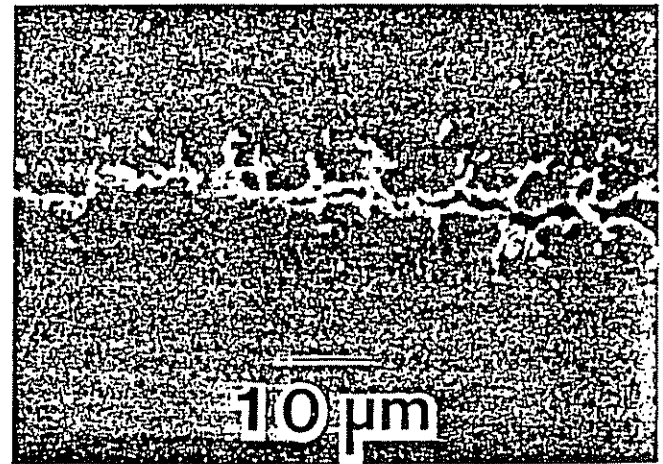


Fig. 2—SEM micrograph of weld hot-cracked region in HASTELLOY C-22.

Table II. Alloy Compositions*

Element	HASTELLOY C-4	HASTELLOY C-22	HASTELLOY C-276	INCONEL 625	INCONEL 718
Al	0.33	0.30	0.30	0.41	0.56
B	<0.002	—	<0.002	0.0012	0.002
C	0.004	0.006	0.003	0.01	0.04
Co	0.10	0.84	0.96	—	0.11
Cr	15.69	21.22	15.83	20.43	18.18
Cu	0.02	0.08	0.16	0.01	0.15
Fe	0.45	3.17	5.44	3.64	18.10
Mg	0.010	—	0.025	—	—
Mn	0.17	0.31	0.50	0.06	0.13
Mo	15.06	13.43	15.56	8.71	3.12
N	—	0.041	0.017	—	—
Nb	—	<0.04	—	3.49	5.25
Ni	67.20	56.96	55.58	62.77	53.20
P	<0.005	0.010	0.014	0.013	0.014
S	<0.002	<0.002	0.002	0.003	0.002
Si	0.03	<0.02	0.03	0.06	0.21
Ta	—	0.06	—	—	—
Ti	0.23	0.03	<0.01	0.27	0.95
V	0.02	0.14	0.18	—	—
W	<0.10	3.29	3.93	—	—

*All concentrations in weight percent

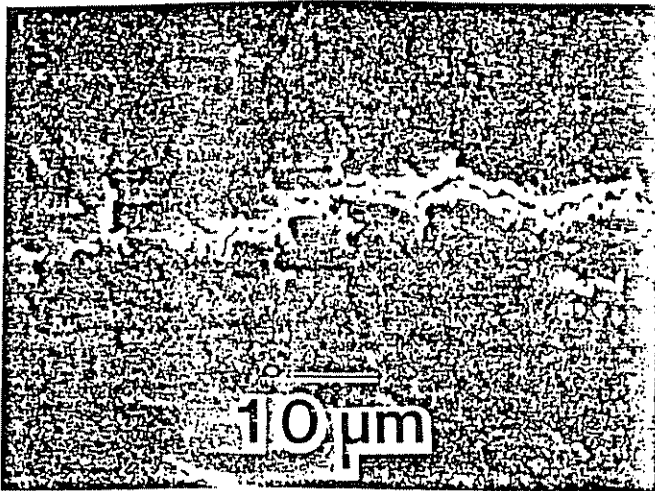


Fig. 3—SEM micrograph of weld hot-cracked region in HASTELLOY C-276

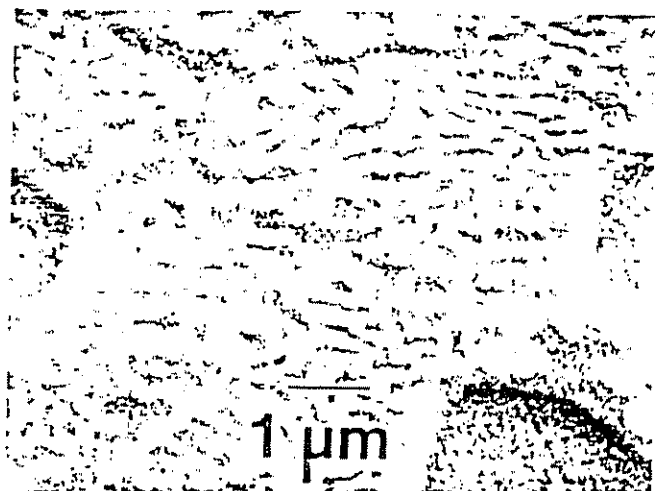


Fig. 6—SEM micrograph of terminal solidification constituent in INCONEL 718

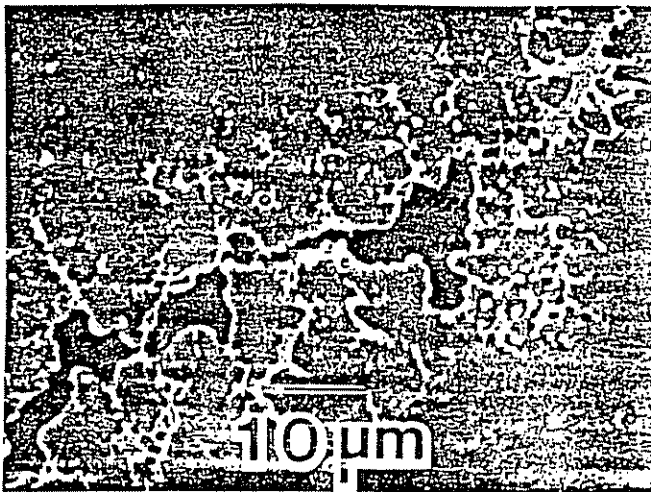


Fig. 4—SEM micrograph of weld hot-cracked region in INCONEL 625



Fig. 7—SEM micrograph of terminal solidification constituent in INCONEL 625

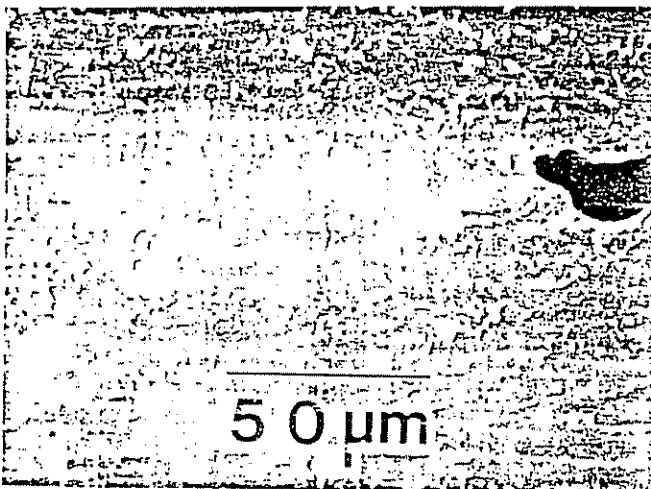


Fig. 5—SEM micrograph of weld non-cracked region in INCONEL 718

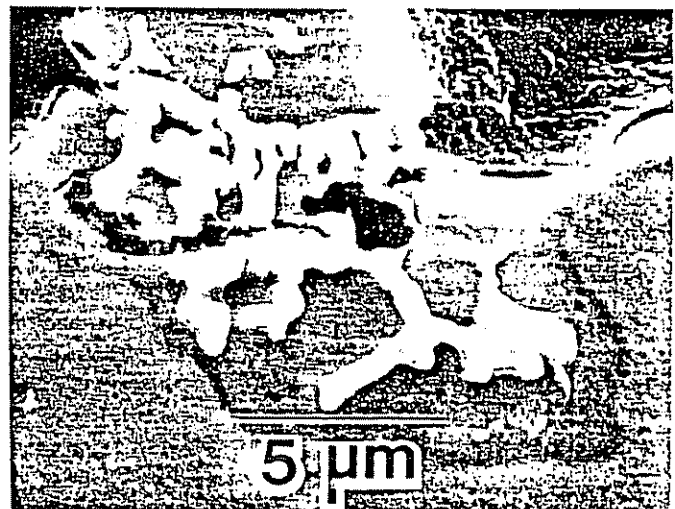


Fig. 8—SEM micrograph of terminal solidification constituent in HASTELLOY C-22

HE 00115



Fig. 9—SEM micrograph of terminal solidification constituent in HASTELLOY C-276

identified as a Mo-rich σ phase (tetragonal, $a = b = 0.908$ nm, $c = 0.475$ nm). In HASTELLOY C-276, the terminal solidification phase is identified as a Mo-rich P phase (orthorhombic, $a = 0.907$ nm, $b = 1.698$ nm, $c = 0.475$ nm). In the cases of Alloys C-22 and C-276, partial transformation of the terminal solidification constituents to other TCP phases occurs^{23,24} on cooling of the weld metal to room temperature. A very small volume fraction of interdendritic TiC is found in HASTELLOY C-4 weld metal.²⁴ The common microstructural feature found in all of the alloys under study (except HASTELLOY C-4) is the occurrence of a terminal solidification constituent involving a TCP phase.

B. Segregation and Chemical Effects

The solidification segregation patterns leading to the formation of these terminal solidification constituents are shown in Figures 10 (a) through (e). All alloys exhibit a depletion of Ni in interdendritic volumes (ID) and an accompanying increase in the concentration of most solute species (Mo, Nb, Ti, etc.) in these same regions, especially those having relatively high m_d^0 values. The reverse pattern can be seen in dendrite core (DC) regions as must be the case to conserve alloy content.

Ni has a very low m_d^0 (Table I), resulting from a relatively full shell of d -band electrons, which results in the well-known ability of Ni to accommodate relatively large amounts of alloying components in solid solution. As the alloys under study solidify, the segregation phenomenon shown in Figure 10 causes the instantaneous value of M_d within a dendrite to increase as it grows out from its central spine (DC). This can be seen in Figures 11 (a) through (c), which plots M_d as a function of position within a dendrite. These M_d values are calculated from the compositional profiles given in Figure 10.

IV. DISCUSSION

The formation of interdendritic terminal solidification constituents involving TCP phases is of fundamental im-

portance during the fusion welding of nickel-base alloys. The formation of terminal solidification constituents accompanies an extension of the solidification temperature range. The presence of a liquid phase, from which terminal constituents form at lower temperatures, has been shown by several investigators^{28,29,30} to be harmful from a weld hot-cracking standpoint.

Recent work^{24,31,32} involving hot-crack testing, differential thermal analysis, and microstructural identification has indicated that even among nickel alloys considered to be readily weldable (HASTELLOYS C-4, C-22, C-276), the presence of a small volume fraction of a terminal solidification constituent involving TCP phases can be detrimental to an alloy's resistance to hot cracking. In several Nb-containing iron-base and nickel-base austenitic alloys, the presence of a Laves phase containing terminal solidification constituent has been shown^{32,33,34} to be detrimental to weld metal hot-cracking resistance.

A. Solidification Considerations

Secondary solidification constituents form when the terminal solid solubility of an alloy is exceeded. That is, the primary solidification phase (in this case, γ) can no longer accommodate the alloy concentration imposed upon it by solidification segregation. At this point, other phases form from the liquid which are more thermodynamically and structurally capable of absorbing this higher alloy concentration. In the case of Ni-base alloys, several secondary solidification constituents are possible, including carbides, borides, nitrides, γ' , and a host of possible intermetallic phases.

With a simple solidification model, Scheil³⁵ showed how, for a simple binary system, the formation of a eutectic constituent could occur when such a solidification product could not be predicted from the application of equilibrium phase diagram principles. His relationship defining the instantaneous composition of solid forming as a function of the fraction solidified, often referred to as the "non-equilibrium lever rule", is given below,

$$C_s = kC_0(1 - f_s)^{k-1} \quad [4]$$

where C_s is the instantaneous solid composition forming at any fraction solid, f_s ; k is the distribution coefficient for the system, defined as the ratio of the composition of the solid to the composition of the liquid with which it is in equilibrium; and C_0 is the nominal alloy composition. If C_0 is defined in terms of weight percent, then C_s has the units of weight percent and f_s is the weight fraction solidified.

For elements which depress the melting point of a pure metal or alloy, $k < 1$. Application of Eq. [4] for the case of $k < 1$ gives the result that the initial solid to form is depleted in that particular alloying element while the last solid to form is enriched in that same alloying element. This can be seen schematically in Figure 12, which shows a partial binary phase diagram for the hypothetical alloy system, A-B. This eutectic-type system has limited solid solubility of element B in a matrix of element A. When this solubility is exceeded, a TCP second phase forms in the microstructure. This system has a distribution coefficient equal to 0.5, which can be determined by taking the ratio of solidus to liquidus concentrations of element B for any hypoeutectic

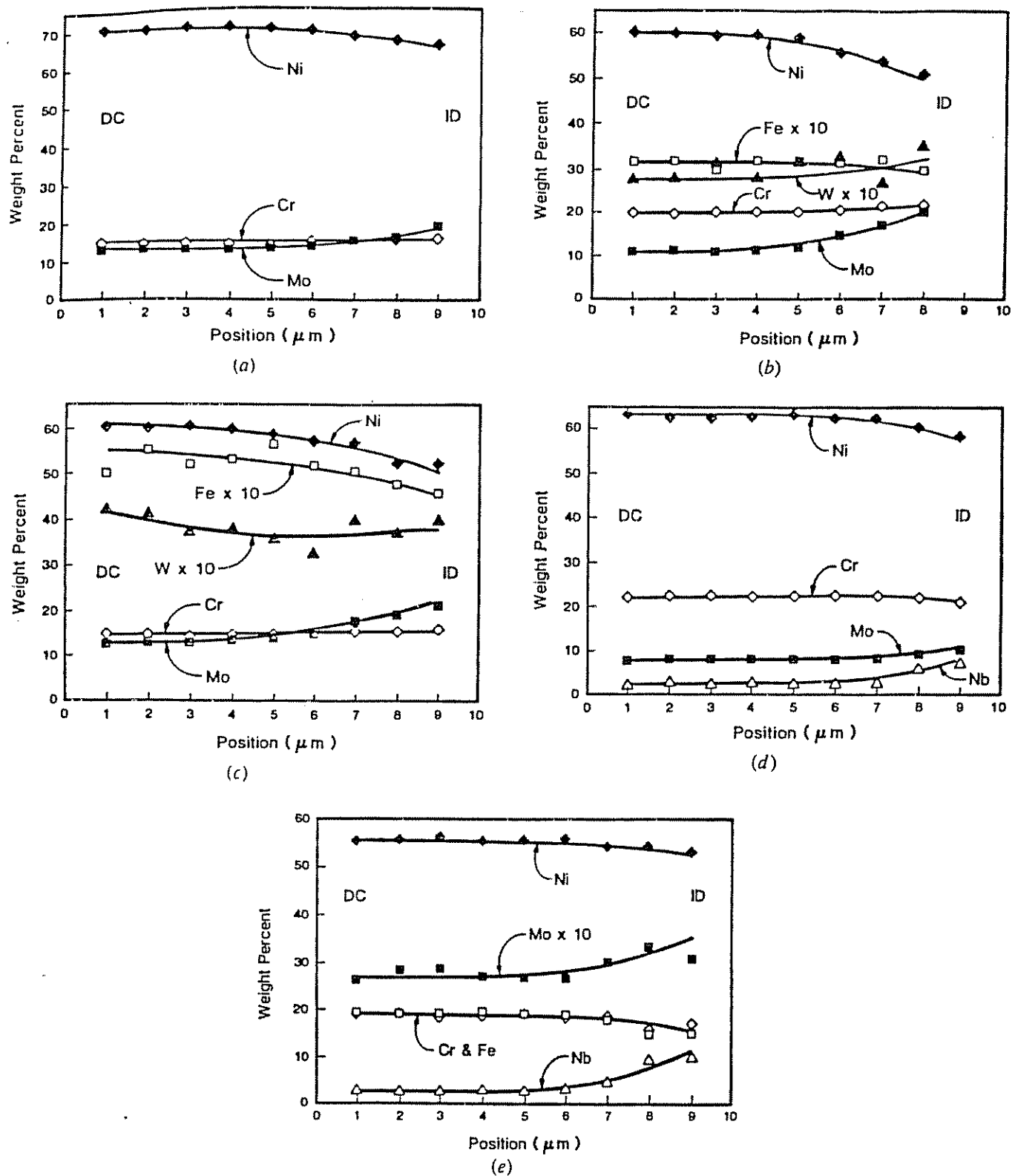


Fig. 10—Weld metal solidification segregation patterns, determined by microprobe, of (a) HASTELLOY C-4, (b) HASTELLOY C-22, (c) HASTELLOY C-276, (d) INCONEL 625, and (e) INCONEL 718

HE 00117

composition at all temperatures above the eutectic temperature, T_E . This alloy system has a maximum solid solubility of element B in the γ matrix of $2C_0$. Application of Eq. [4] to an alloy of composition C_0 would result in an initial solid to form at a composition of $0.5C_0$. Subsequent solid compositions would be those defined by the solidus line at temperatures below T_E , also in accordance with Eq. [4]. The terminal solubility of element B in the γ matrix

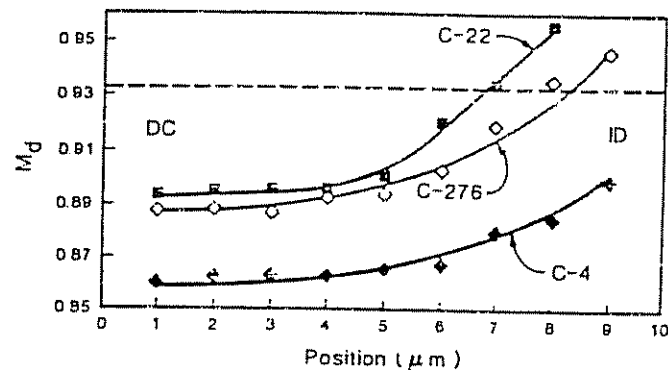
would occur when the solid having a composition of $2C_0$ forms. At this point, the remaining liquid will solidify as the eutectic constituent ($4C_0$), with one of the eutectic phases being the TCP phase. Figure 13 shows graphically the solidification solute profile derived from Eq. [4] for the alloy of composition C_0 given in Figure 12. A reverse pattern of solute element segregation (decreasing C_0 with increasing f) would occur in the case of $k > 1$.

For the alloy C_0 , Eq. [4] predicts that 6.25 wt pct of the microstructure will be composed of the eutectic constituent. In general, less than the predicted amount of eutectic constituent is observed,³⁶⁻³⁷ as diffusion in the solid phase during solidification modifies the interfacial solid and liquid compositions toward those defined by equilibrium solidification (*i.e.*, no eutectic constituent formation).

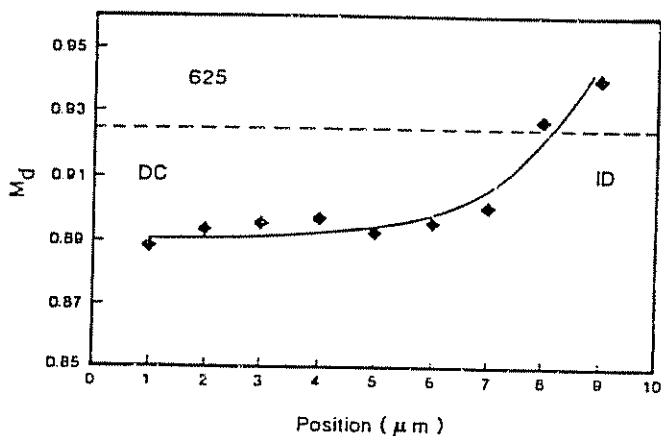
Although this simple model neglects such phenomena as solid-state diffusion during solidification, the effects of undercooling due to interface curvature, and the formation of dendritic side-branching, it is quite useful in illuminating several of the salient features observed during many commercial solidification processes. A similar model has been developed by Bower *et al.*³⁸ for describing cellular dendritic growth. This model reduces to Eq. [4] in its simplest form and predicts the same pattern for interdendritic segregation as that shown in Figure 13. That is, Eq. [4] predicts the segregation profile expected between the center of a dendrite (dendrite core) and its associated interdendritic region. Examination of the shapes of the solute elements' profiles shown in Figure 10 reveals that they are qualitatively similar to those shown in Figure 13 for the hypothetical case. In addition, the weld metal solidification segregation patterns reported by several investigators³⁹⁻⁴¹ for austenitic stainless steels are also in qualitative agreement with a Scheil-type model (Eq. [4]).

B. Correlation between Solidification and New PHACOMP

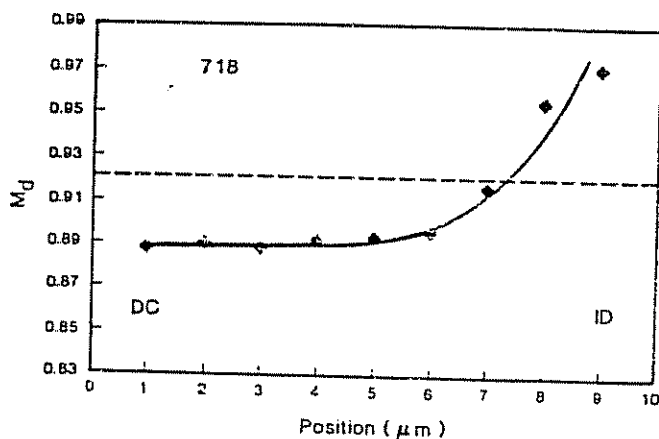
As can be seen in Figure 13, all compositions between $0.5C_0$ and $2C_0$ are predicted to exist in the solidifying γ dendrite. As stated above, the solid forming immediately



(a)



(b)



(c)

Fig. 11— M_D profiles calculated from the data of Fig. 10: (a) HASTELLOYS C-4, C-22, C-276 (b) INCONEL 625, and (c) INCONEL 718. The dotted line is the M_D^0 for the alloy or group of alloys in each figure.

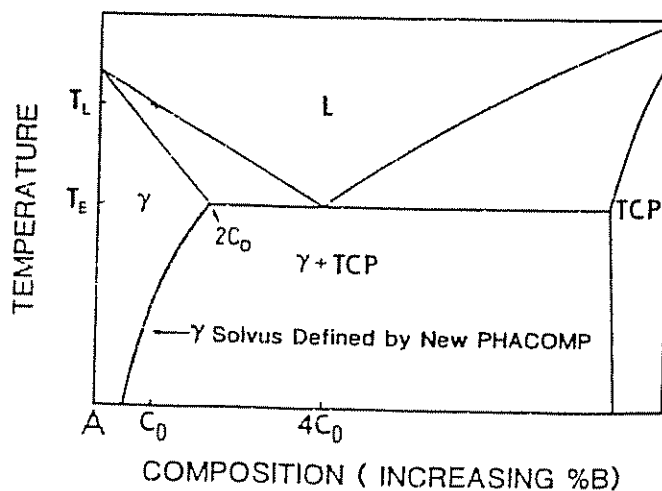


Fig. 12—Hypothetical binary phase diagram of a γ /TCP-type system

prior to the terminal solidification eutectic constituent has the composition of the maximum solid solubility. In addition to being the locus of the lowest solidus temperature, this concentration represents the top (in terms of temperature) of the γ solvus. This solvus line is the locus of points defined by the temperature-dependent New PHACOMP. The commonality of the maximum solid solubility to both lines (solidus and γ solvus) is the link between New PHACOMP and basic solidification theory. That is, New PHACOMP defines the terminal solid solubility during solidification in the same manner as it defines the γ solvus in the solid state.

It is therefore proposed that the critical values of M_2 determined from New PHACOMP calculations can be used to predict the formation of terminal solidification TCP phases in nickel base alloy weldments. Figure 11 shows the M_2 profiles calculated from the microprobe chemistry data (Figure 10 data plus the remainder of the minor alloying elements analyzed with the microprobe during this profiling, but not shown in Figure 10) obtained from GTA weld metal. The horizontal dotted line is the critical M_2 value for the formation of σ as given by Eq. [3]. The temperature values used as input to Eq. [3] are the secondary solidification (formation of TCP phase-containing constituents) temperatures determined by earlier DTA analyses.^{23,31,32} These temperatures are given in Table III. The critical values of M_2 are 0.931 for the HASTELLOYS and 0.926 for INCONELS 625 and 718. According to Morinaga *et al.*,¹⁷ the critical M_2 value for the formation of Laves phase is lower than for σ phase, while that for P phase would be similar to that for σ phase. In the case where Laves forms (INCONELS 625 and 718), the critical M_2 value referenced to σ formation would be an overly conservative test of the application of the New PHACOMP to predicting terminal Laves solidification.

The data of Figure 11 show that terminal solidification involving TCP phases would be predicted (M_2 exceeds the critical values in interdendritic regions) by the New PHACOMP calculations for all alloys except HASTELLOY C-4, where the extent of solidification segregation is such that the maximum solid solubility relative to TCP phase formation is not exceeded. These results are in agreement with the SEM and transmission electron microscopy observations in that only HASTELLOY C-4 was devoid of an interdendritic TCP phase. The high Ni content of HASTELLOY

C-4 results in a bulk M_2 that is lower than that of the other alloys studied. The amount of segregation necessary to initiate TCP phase formation is therefore greater than that for the other alloys studied, and this required segregation does not occur for the welding conditions used in this study.

In performing the New PHACOMP calculations, it was assumed that no other competing terminal solidification constituents (eutectic carbides, nitrides, borides, *etc.*) were present to accommodate the segregating alloying components. For the alloys under consideration, this was generally true except for the case of INCONEL 718, in which some eutectic NbC was observed. In the case of HASTELLOY C-4, the trace amounts of TiC observed would not have affected the calculations, as the bulk Ti content is low. In more complex superalloys containing substantial amounts of eutectic-type carbides, borides, nitrides, *etc.*, a philosophy similar to that used in applying New PHACOMP to the solid state might be envisioned. That is, a net residual composition could be determined after the contributions of the earlier forming eutectic-type constituents are subtracted.

It becomes clear that the class of alloys to which New PHACOMP may be best applied at the present time to predict terminal TCP phase solidification are those which are not likely to form solidification-type carbides, nitrides, or borides. Although this may seem like a serious limitation to the usefulness of New PHACOMP in this application, it is clear that there are many alloy systems for which it could be directly applicable. In fact, its usefulness may become most apparent in considering the prediction of weld solidification microstructures in dissimilar metal joints, when the net alloy formed by the combination of two different alloys, and maybe even a third alloy as a filler metal, is not itself a well-known or commercial composition.

As described in this paper, the New PHACOMP calculations cannot independently predict which TCP phase will occur upon solidification. Even in solid state applications, New PHACOMP does not give a direct prediction of which TCP phase will form in a given alloy. Rather, an available phase diagram, usually of a ternary system which is the closest approximation to a given alloy is referenced to decide which phase may be the most likely to appear. Polar phase diagrams, as described by Sims,³ have also been used as predictive tools. In cases where alloying elements such as Nb and Ta are present, "size-effect" phases such as Laves can often be expected. A judicious use of available phase diagrams should serve equally well in the present case. For example, in the Ni-Cr-Mo system, it could be expected, based upon available data,^{23,34,42} that alloys having a high concentration ratio of Cr to Mo will be likely to form σ as the terminal TCP phase, whereas those alloys having a high concentration ratio of Mo to Cr will form P as the terminal TCP phase.

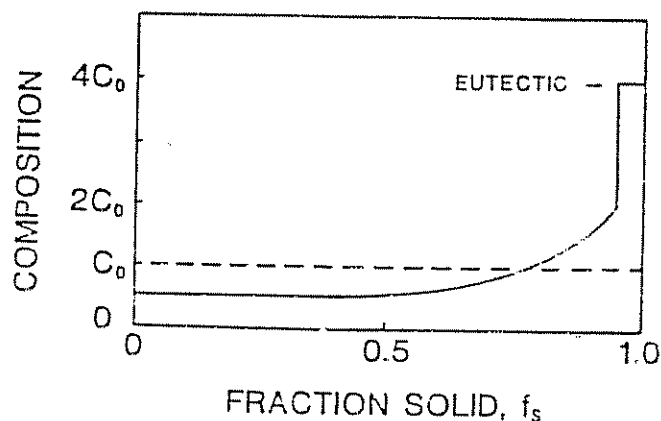


Fig. 13—Plot of the Scheil equation for the alloy C4 shown in Fig. 12

Table III. DTA Terminal Solidification Temperatures

Alloy	TCP Phase Involved	Temperature (°C)
HASTELLOY C-4	none	—
HASTELLOY C-22	σ	≈ 1285
HASTELLOY C-276	P	≈ 1285
INCONEL 625	Laves	≈ 1200
INCONEL 718	Laves	≈ 1200

As the formation of terminal solidification constituents generally implies an extension of the solidification temperature range, to a first approximation the presence of predicted TCP solidification constituents would be undesirable from a weld metal hot-cracking standpoint. Weld metal hot cracking, though, is a more complex process, and requires more than simply the presence of a low melting point liquid from which these constituents appear. Sufficient restraint stress is also necessary to initiate hot cracking. Aside from this, the physical properties of the liquid in final solidification volumes (interdendritic and intergranular regions) is important in determining the hot-cracking susceptibility of an alloy. If this liquid has low surface tension, it will tend to spread out as a continuous thin film and increase the propensity toward cracking. On the other hand, if the residual liquid has a high surface tension, it will have a tendency to spheroidize and remain in isolated pockets and the hot-cracking tendency will be diminished. This theory was established by Borland³⁰ who used it to explain the reduction in hot-cracking tendency imparted by the addition of manganese to mild steels containing sulfur.

More recently, Jolley and Geraghty⁴¹ showed that magnesium additions to Fe-18Cr-13Ni-Nb austenitic stainless steel caused "globularization" of the terminal solidification NbC/austenite eutectic-type constituent, reducing the propensity to hot crack. The ability to predict the formation of a TCP terminal solidification constituent, therefore, is obviously *not* sufficient to predict the hot-cracking behavior of an alloy in a particular situation but rather may serve as an indicator of potential difficulties.

The correlation observed between New PHACOMP calculations and terminal TCP solidification constituents was made through the measurement of solidification segregation patterns. It is clear that for a calculational approach such as this to be effective as a predictive tool, the ability to know these solidification segregation profiles *a priori* is important. This can happen only by incorporating weld solidification modeling into the New PHACOMP analysis. The reality of solid state diffusion during solidification, initially described by Brody and Flemings³² and recently formulated for weld metal solidification by Brooks,³³ must also be included. For alloys more complex than binary systems, essential input parameters for computational modeling efforts, such as distribution coefficients, are generally unknown, and even less is known experimentally about how interactions between alloying elements can affect the values of these parameters. Generation of a fundamental solidification data base for complex nickel alloys should allow for the successful application of a New PHACOMP type approach to the analysis of weld metal solidification structure. A similar predictive capability should also be possible for austenitic iron base alloys as the quantum mechanical calculations similar to those already made for nickel-rich austenitic alloys are performed for these other systems.

C. Closure

Although it is clear that the application of New PHACOMP to predicting solidification behavior is, at the present time, not fully matured, it is equally clear that this new type of approach to predict weld solidification microstructure has merits. In general, any system could be analyzed in this manner as long as the basic calculations for electronic

structure³⁴ are performed and the correlations relative to phase stability are determined. The appeal of this philosophy is in its fundamental nature and its potential application to many multicomponent alloy systems of industrial importance.

V. CONCLUSIONS

1. A variety of nickel base alloys have been found to terminate solidification with the formation of a TCP phase-containing constituent. These constituents are associated with weld metal hot cracks.
2. The solidification segregation pattern observed in all alloys examined was one of Ni depletion and alloy element enhancement in final solidification (interdendritic) volumes.
3. New PHACOMP calculations performed on these segregation profiles revealed a pattern of increasing M_d as one traverses from dendrite core regions to interdendritic volumes.
4. When critical M_d values were exceeded, it was observed that TCP phase-containing terminal solidification constituents were formed. When critical M_d values were not exceeded, no such constituents were observed.
5. It is proposed that the New PHACOMP calculational process can be used as a tool for predicting solidification TCP phases in many nickel base alloys. It may also serve as an indicator of potential weld metal hot-cracking problems in these same alloys.

ACKNOWLEDGMENTS

The authors thank Ms. Ellen Semarge for performing the electron microprobe analyses reported in this paper, Mr. William Hammetter and Mr. Thomas Kollie for performing the DTA tests in the referenced studies, and Mr. Thomas Lienert for assistance with the welding experiments. This work was performed at Sandia National Laboratories, Albuquerque, New Mexico, supported by the United States Department of Energy under contract number DE-AC04-76DP00789.

REFERENCES

1. S. T. Wlodek; *Trans. Am. Soc. Met.*, 1964, vol. 57, pp. 110-19.
2. E. W. Ross; *Journal of Metals*, 1967, vol. 19, No. 12, pp. 12-14.
3. C. T. Sims; *Journal of Metals*, 1966, vol. 18, No. 10, pp. 1119-30.
4. S. T. Wlodek; *Trans. Am. Soc. Met.*, 1963, vol. 56, pp. 287-303.
5. D. K. Das, S. P. Rideout, and P. A. Beck; *Trans. AIME*, 1952, vol. 194, pp. 1071-79.
6. D. S. Bloom and N. J. Grant; *Trans. AIME*, 1953, vol. 197, p. 88.
7. P. Greenfield and P. A. Beck; *Trans. AIME*, 1954, vol. 200, pp. 253-57.
8. P. Greenfield and P. A. Beck; *Trans. AIME*, 1952, vol. 206, pp. 265-75.
9. D. P. Shoemaker, C. B. Shoemaker, and F. C. Wilson; *Acta Crystall.*, 1957, vol. 10, pp. 1-14.
10. L. Pauling; *Physical Review*, Dec. 1, 1938, vol. 54, pp. 899-904.
11. A. H. Sully and T. J. Heal; *Research*, 1948, vol. 1, p. 228.
12. L. R. Woodyatt, C. T. Sims, and H. J. Beattie, Jr.; *Trans. AIME*, 1966, vol. 236, pp. 519-27.
13. C. T. Sims; *The Superalloys*, C. T. Sims and W. C. Hagel, eds., Wiley-Interscience, New York, NY, 1972, p. 276.
14. H. J. Murphy, C. T. Sims, and A. M. Beltran; *Journal of Metals*, 1968, vol. 20, No. 12, pp. 46-54.

- 15 J. R. Mihalasin, C. G. Bieher, and R. T. Grant: *Trans. AIME*, 1968, vol. 242, pp. 2399-2414.
- 16 R. G. Barrows and J. B. Newkirk: *Metall. Trans.*, 1972, vol. 3, pp. 2889-93.
- 17 M. Morinaga, N. Yukawa, H. Adachi, and H. Ezaki: *Superalloys 1984*, pp. 523-32.
- 18 M. Morinaga, N. Yukawa, and H. Adachi: *J. Phys. Soc. Japan*, 1984, vol. 53, No. 2, pp. 653-63.
- 19 A. L. Schaeffler: *Metal Progress*, 1949, vol. 11, No. 56, pp. 680-80B.
- 20 C. J. Long and W. T. DeLong: *Welding Journal*, 1973, vol. 52, No. 7, pp. 281s-97s.
- 21 V. Kujanpaa, N. Suutala, T. Takalo, and T. Moisio: *Welding Research International*, 1979, vol. 9, No. 2, p. 55.
- 22 D. L. Olson: *Welding Journal*, 1985, vol. 64, No. 10, pp. 281s-95s.
- 23 M. J. Cieslak, A. D. Romig, Jr., and T. J. Headley: *Microbeam Analysis—1985*, pp. 179-88.
- 24 M. J. Cieslak, T. J. Headley, and A. D. Romig, Jr.: *Metall. Trans. A*, 1986, vol. 17A, pp. 2035-47.
- 25 W. F. Savage and C. D. Lundin: *Welding Journal*, 1965, vol. 44, No. 10, pp. 433s-42s.
- 26 W. F. Savage and C. D. Lundin: *Welding Journal*, 1966, vol. 45, No. 11, pp. 497s-502s.
- 27 G. F. Bastin, F. J. J. van Loo, and H. J. M. Heijligers: *X-ray Spec.*, 1984, vol. 13, p. 91.
- 28 W. I. Pumphrey and P. H. Jennings: *J. Inst. Met.*, 1948, vol. 75, pp. 235-56.
- 29 W. S. Pellini: *Foundry*, 1952, vol. 80, pp. 124-33, 192, 194, 196, 199.
- 30 J. C. Borland: *British Welding Journal*, 1960, vol. 7, No. 8, pp. 508-12.
- 31 M. J. Cieslak, T. J. Headley, and A. D. Romig, Jr.: Sandia National Laboratories, Albuquerque, NM, unpublished research, 1985.
- 32 G. A. Knorovsky and T. J. Headley: Sandia National Laboratories, Albuquerque, NM, unpublished research, 1985.
- 33 Y. Nakao, H. Oshige, S. Koga, H. Nishihara, and J. Sugitani: *Jour. Japan Weld. Soc.*, 1982, vol. 51, No. 12, pp. 21-27.
- 34 R. Vincent: *Acta Metall.*, 1985, vol. 33, No. 7, pp. 1205-16.
- 35 E. Scheil: *Z. Metallk.*, 1942, vol. 34, p. 70.
- 36 H. D. Brody and M. C. Flemings: *Trans. AIME*, 1966, vol. 236, pp. 615-23.
- 37 J. A. Brooks: *66th AWS Convention Abstracts*, Amer. Weld. Soc., 1985, pp. 194-95.
- 38 T. F. Bower, H. D. Brody, and M. C. Flemings: *Trans. AIME*, 1966, vol. 236, pp. 624-34.
- 39 Y. Arata, F. Matsuda, and F. Katayama: *Trans. JWRI*, 1977, vol. 6, No. 1, pp. 105-16.
- 40 M. J. Cieslak, A. M. Ritter, and W. F. Savage: *Welding Journal*, 1982, vol. 61, No. 1, pp. 1s-8s.
- 41 J. A. Brooks, J. C. Williams, and A. W. Thompson: *Metall. Trans. A*, 1983, vol. 14A, pp. 23-31.
- 42 D. S. Bloom and N. J. Grant: *Journal of Metals*, 1954, vol. 200, pp. 261-68.
- 43 G. Jolley and J. E. Geraghty: *Solidification and Casting of Metals*, The Metals Society, London, 1979, pp. 411-15.

HE 00121

The Welding Metallurgy of HASTELLOY Alloys C-4, C-22, and C-276

M. J. CIESLAK, T. J. HEADLEY, and A. D. ROMIG, Jr

The welding metallurgy (solidification and solid state transformations) of HASTELLOY* Alloys C-4, C-22, and C-276 has been determined. Vareststraint hot-cracking tests performed on commercial alloys revealed a weldability ranking as follows: C-4 > C-22 > C-276. All alloys would be expected to have good weldability, with Alloy C-4 having a very low hot-cracking tendency, comparable to 304L stainless steel. Microstructures of gas-tungsten-arc welds of these alloys have been characterized by scanning electron microscopy and analytical electron microscopy. Intermetallic secondary solidification constituents have been found associated with weld metal hot cracks in Alloys C-276 and C-22. In Alloy C-276, this constituent is a combination of P and μ phases, and in Alloy C-22, this constituent is composed of σ , P , and μ phases. With phase composition data obtained by AEM techniques and available ternary (Ni-Cr-Mo) phase diagrams, an equivalent chemistry model is proposed to account for the microstructures observed in each alloy's weld metal.

I. INTRODUCTION

HASTELLOY Alloys C-4, C-22, and C-276 are highly corrosion-resistant nickel-base alloys derived from the Ni-Cr-Mo ternary system. In addition to the expected impurities (Table I), Alloy C-4 has an intentional Ti alloying addition, and Alloys C-22 and C-276 have W and Fe as additional alloying components. These materials are nominally single-phase, solid-solution strengthened alloys not hardenable by conventional aging treatments.

The thermal stability of these and similar (e.g., HASTELLOY S) alloys in the mill-annealed condition has been investigated in some detail.¹⁻⁸ Long range ordering has been observed¹⁻⁴ in which the disordered face-centered-cubic matrix transforms to an ordered orthorhombic superlattice (isomorphous with Pt₃Mo). This phenomenon generally occurs only after at least several hundred hours in the 600 °C temperature range and hence is not important in the consideration of the fusion zone microstructure generated by cooling rates characteristic of arc welding.⁹

Precipitation of intermetallic phases (μ , P) and carbides has also been observed.^{1,5-8} The intermetallic compounds are the most relevant to the present study. Leonard⁵ has shown that P phase can precipitate in Alloy C-276 within a few minutes of exposure at 875 °C. He also suggests that μ phase is the long-time transformation product of P phase. Hodge and Kirchner⁶ found no evidence of μ phase formation in Alloy C-4 during isothermal heat treatments in the temperature range 650 °C to 1090 °C for times up to 100 hours. Matthews¹ reported that μ phase precipitation occurs in Alloy C-4, but only after extended heat treatment (≥ 1000 hours) in the 800 °C temperature regime.

Recently, Cieslak *et al.*¹⁰ reported on the occurrence of topologically-close-packed phases in Alloy C-22 and Alloy C-276 weld metal. Alloy C-276 contained both the P and μ

phases. Alloy C-22 contained P , μ , and σ phases. All of these phases are possible equilibrium structures in the Ni-Cr-Mo ternary system.^{11,12,13} Raghavan *et al.*¹³ observed that P and σ phases were present in the near-solidus (1250 °C) isothermal section of the Ni-Cr-Mo system; and P , σ , and μ phases were present in the 850 °C isothermal section. Bloom and Grant¹² speculated on the high temperature invariant reactions above 1250 °C in the Ni-Cr-Mo system. In the composition range of importance relative to commercial alloys, the possible equilibrium phases were liquid, austenite (γ), P , and σ .

In this paper we report the results of hot-cracking susceptibility tests on Alloys C-4, C-22, and C-276, and the identification of the minor phases (P , σ , μ , or MC carbide) in the solidified weld microstructures. An equivalent chemistry model is then developed which accounts for the second phases observed in terms of a secondary solidification constituent in each alloy plus subsequent solid-state transformation reactions in Alloys C-22 and C-276.

II. EXPERIMENTAL PROCEDURE

The chemical analyses of the alloys studied are given in Table I. All alloys were sheet products, approximately 0.3 cm thick and all were in the mill-annealed condition prior to welding. All welding was done using the auto-genous (no filler metal added) gas-tungsten-arc (GTA) process. The welding parameters used were 100 A, direct current, electrode negative, at 13.5 V (machine voltage), and a travel speed of 20 cm/min.

The hot-cracking susceptibility was quantified with the Vareststraint test.^{14,15} Earlier work^{16,17} has indicated that this test is a reliable means for differentiating the hot-cracking susceptibility of nickel-base alloys. The Vareststraint test employs a 16.5 cm \times 2.5 cm \times 0.3 cm specimen supported as a cantilever beam as shown schematically in Figure 1(a). A GTA weld is made from left to right as indicated. As the weld pool passes the point marked A, a pneumatic loading system (at point F) bends the specimen to conform to the radiused die block labeled B. The arc continues without stopping to the point labeled C, where it is extinguished. From simple geometric arguments, the longitudinal aug-

*HASTELLOY is a trademark of Cabot Corporation.

M. J. CIESLAK, Div. 1833, Process Metallurgy, T. J. HEADLEY, Div. 1822, Electron Optics and X-Ray Analysis, and A. D. ROMIG, Jr., Div. 1832, Physical Metallurgy, are with Sandia National Laboratories, P.O. Box 5800, Albuquerque, NM 87185.

Manuscript submitted January 2, 1986

Table I Alloy Compositions (Wt Pct)

Element	HASTELLOY C-4	HASTELLOY C-22	HASTELLOY C-276
C	0.004	0.006	0.003
Co	0.10	0.84	0.96
Cr	15.69	21.22	15.83
Fe	0.45	3.17	5.44
Aln	0.17	0.31	0.50
Mo	15.06	13.43	15.56
Ni	67.20	56.96	55.58
P	<0.005	0.010	0.014
S	<0.002	<0.002	0.002
Si	0.03	<0.02	0.03
Ti	0.23	0.03	<0.01
V	0.02	0.14	0.18
W	<0.10	3.29	3.93

mented strain, ϵ , at the top surface of the bar can be calculated from the following relationship.

$$\epsilon = t/2R, \quad (1)$$

where t = specimen thickness and R = die block radius of curvature. Tests were run at various levels of augmented strain (0.8 pct to 2.5 pct) by substituting the appropriately radiused die block. Following testing, the as-welded surface of the specimens was examined under a stereomicroscope

equipped with a filar eyepiece. Fusion zone hot cracks were observed at positions shown schematically in Figure 1(b). The sum of the length of all the cracks emanating back into the fusion zone from the position of the solid/liquid interface at the instant of straining, the total crack length, is the quantitative measure of weldability determined from Varestraint testing. The maximum crack length is the length of the longest hot crack found on a particular specimen. For alloys having similar thermal conductivities and melting temperatures, this value is proportional to the hot-cracking temperature range.¹⁵ Expected scatter parameters (standard deviation/mean) in Varestraint data are 15 pct to 20 pct.

In order to study elemental segregation associated with solidification, *in situ* water spray quenched experiments^{16,17} were performed. Samples of each alloy were welded using the same welding parameters as those used in the Varestraint tests. At the point where strain would normally be imposed upon the specimen, a high pressure water spray quench fixture would both decant the liquid in the weld pool and rapidly cool the dendrites which were then growing into the trailing edge of the weld. This quenching procedure minimizes the extent of solid state diffusion during normal cooling of the weld metal to room temperature and retains the pattern of elemental microsegregation associated with weld solidification.

Subsequent to welding, samples for microstructural analysis were removed from the Varestraint test specimens as shown schematically in Figure 1(b). These samples were mounted in epoxy and polished through 0.05 μm alumina. Microstructures were revealed with a 10 pct chromic acid electroetch. The specimens were then carbon coated and examined in a Hitachi S-520 scanning electron microscope (SEM).

Samples for electron microprobe analysis were taken from the trailing edge of the weld pool of the water-quenched specimens. These were prepared in the same manner as the microstructural analysis specimens except that care was taken to grind as little material as possible off the weld surface. Microhardness indentations were used to bracket areas for microanalysis. Prior to microanalysis, the specimen surface was repolished flat with 1 μm diamond paste and was then carbon coated. Microanalysis was performed with a Cameca MBX electron microprobe operating at an accelerating potential of 15 kV and a beam current of approximately 20 nA. K_α X-ray peaks were used to analyze for all elements of interest except for Mo and W, where the L_α peaks were used. Point count data were reduced to

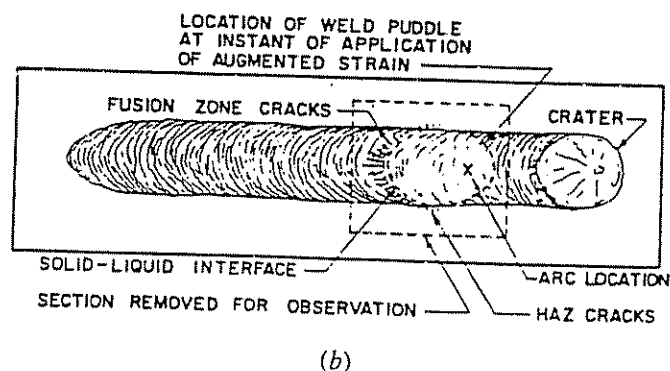
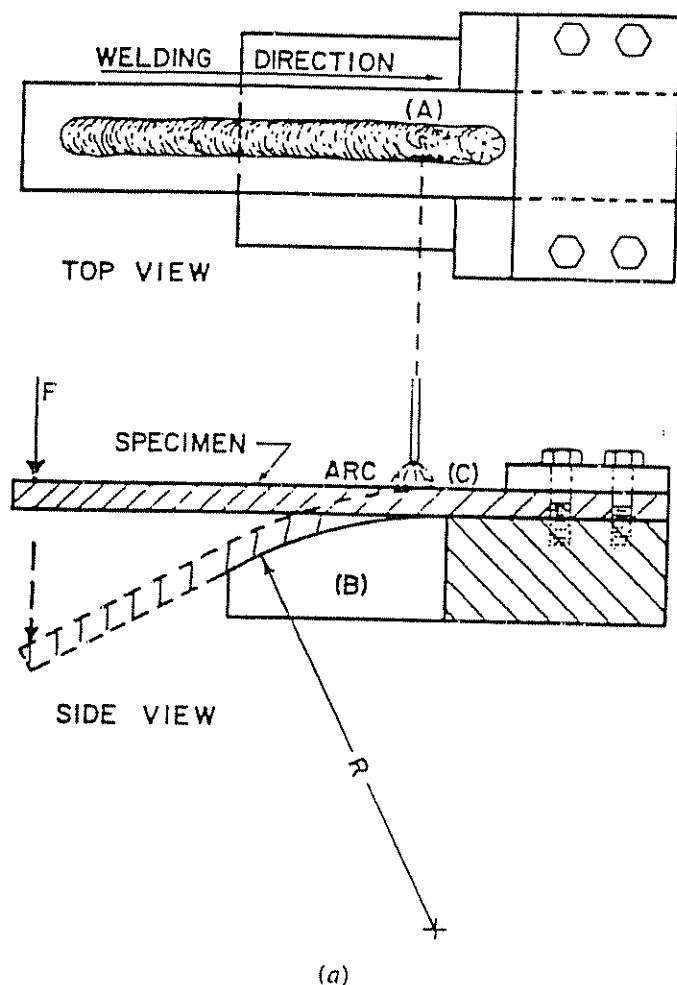


Fig 1—(a) Schematic view of the Varestraint test apparatus; (b) schematic top view of specimen after testing

weight percentages with a computer program. All microprobe data have a scatter of better than ± 2 pct (relative).

The samples for analytical electron microscope (AEM) analysis were sliced from weld metal of Varestraint specimens with a low-speed carbide saw and ground to a thickness of approximately 125 μm . Standard 3 mm-diameter disks were cut from the thin sheet with a mechanical punch. Thin foils were prepared by electropolishing in a solution of 10 pct perchloric acid in methanol at approximately -65°C . Following electrochemical thinning, the foils were placed in an ion mill to increase the amount of thin area and to remove any electrolyte residue. The foils were examined in a JEOL 100C AEM operated at 100 kV, equipped with a side-entry, low take-off angle X-ray detector and a Tracor Northern TN2000 multichannel analyzer.

Electron diffraction was used to identify uniquely each phase prior to X-ray microanalysis. The phases were then analyzed with a focused beam in the scanning transmission electron microscope (STEM) mode. The particles analyzed were all 0.5 to 1.0 μm in diameter. The nominal thickness of the foil at the points of analysis was 50 to 100 nm. Under these experimental conditions, the beam scattering volume was contained entirely within the phase with no contribution from the adjacent matrix.

Phase compositions were determined from AEM X-ray data with the standardless ratio technique, where the weight fractions are related to the measured X-ray intensities by

$$C_X/C_Ni = k_{XNi} \{I_X/I_{Ni}\} \quad (2)$$

where $X = \text{Fe, Cr, Co, Mo, or W}$; C is the composition in weight percent; I is the integrated X-ray intensity; and k_{XNi} is the Cliff-Lorimer sensitivity factor referenced to Ni. The values of the sensitivity factors, k_{XNi} , were determined from a well-homogenized sample of Alloy C-276 with a well-known composition. The k_{XNi} was determined for the family of $W L_B$ lines. It was not possible to integrate over an individual $W L_B$ X-ray line due to line overlap. However, no error is introduced into the analysis if the same integration windows are used for the experimental determination of k_{XNi} and for the analysis of the unknown. Table II lists the sensitivity factors used in this study. The compositions of the unknowns were determined with the experimental values of k_{XNi} in a standard data reduction routine.²¹ X-ray absorption in these samples was not significant. At the 5 pct level of significance, the thin film criterion is violated only at a thickness exceeding 250 nm,²² and foils examined in this study were typically 50 to 100 nm thick.

Differential thermal analysis (DTA) was performed on all alloys with a Dupont differential thermal analyzer. The starting condition of all DTA samples was the mill-annealed condition. Specimen weights ranged from 60 to 100 mg. A platinum standard was used for the control material.

Table II. Sensitivity Factors (k_{XNi})

Elemental Ratio	k_{XNi}
Cr/Ni	0.83 ± 0.02
Mo/Ni	3.41 ± 0.2
Fe/Ni	0.95 ± 0.03
W(L_B)/Ni	9.09 ± 0.6
Co/Ni	1.62 ± 0.08

samples were heated at a rate of $10^\circ\text{C}/\text{min}$ under an argon atmosphere to a temperature of 1450°C . At this temperature, all alloys were completely molten. Specimens were then cooled, also at a rate of $10^\circ\text{C}/\text{min}$, through the solidification temperature range. Primary and secondary solidification reactions on cooling were noted.

III. RESULTS

The results of Varestraint testing are shown in Figure 2. The total crack length data indicate that Alloy C-276 has the poorest resistance to hot cracking of the three alloys and that Alloy C-4 has the best resistance to hot cracking under these test conditions. The cracking response of Alloy C-4 is similar to what would be expected of a 304L stainless steel containing 5 to 10 pct delta-ferrite, that is, a low susceptibility to fusion zone hot cracking. In general, each alloy would be expected to have good weldability when compared to other nickel base alloys such as INCONEL*

*INCONEL is a trademark of the INCO family of companies.

625^{23,24} or INCONEL 718.²⁴ The maximum crack length results are shown in Figure 3. Within experimental deviation, Alloys C-276 and C-22 show similar results and both are different from Alloy C-4, which had maximum crack lengths approximately 60 pct less than the other two alloys.

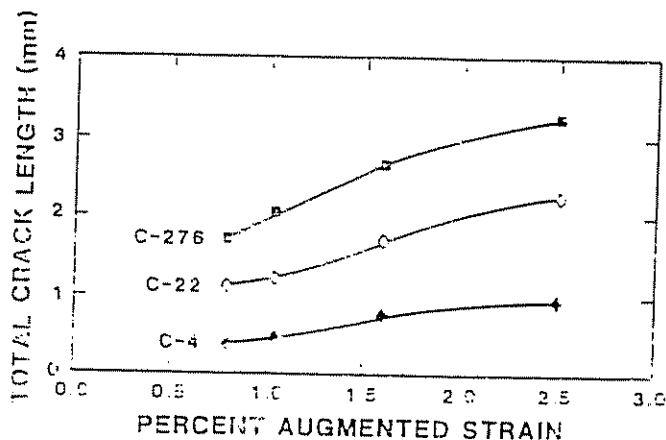


Fig. 2—Varestraint test total crack length data

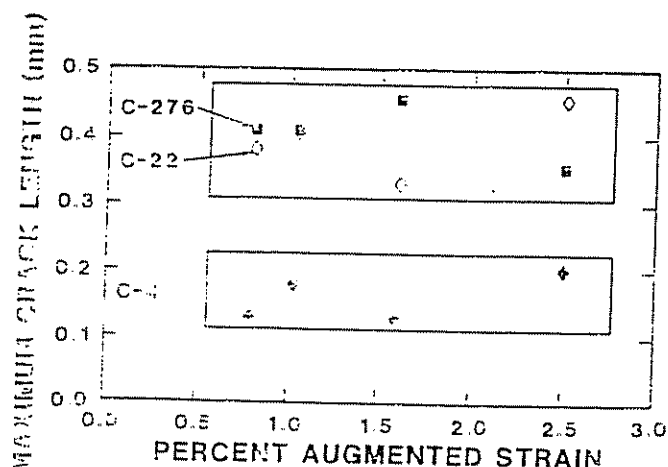
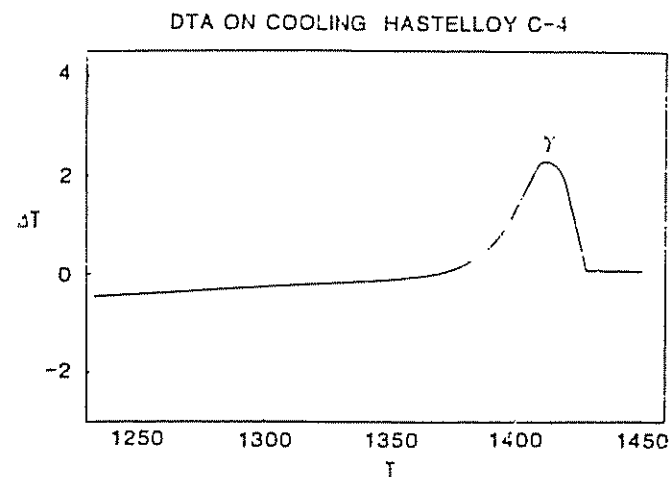
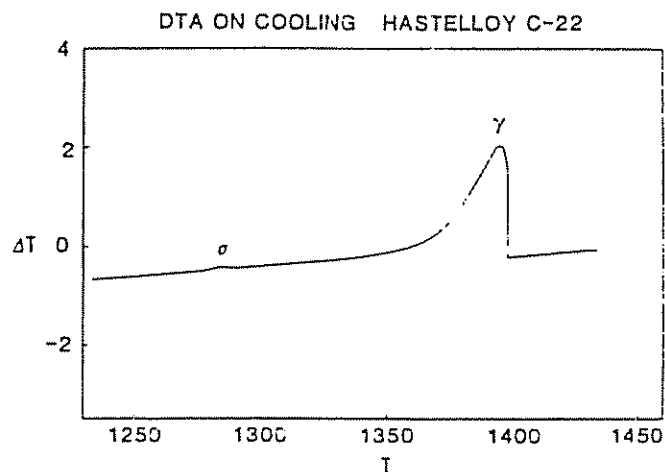


Fig. 3—Varestraint test maximum crack length data

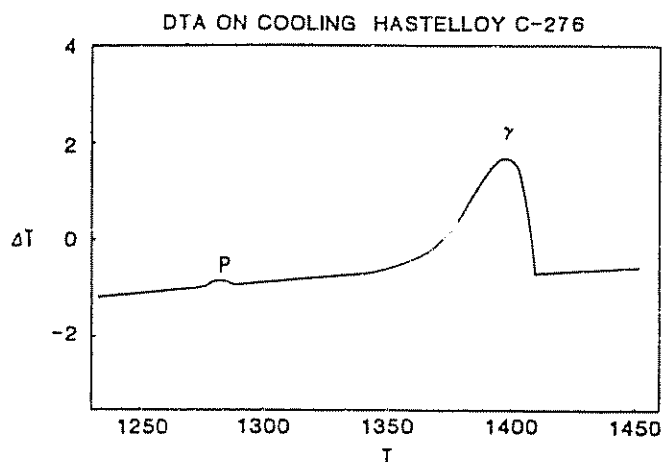
On-cooling DTA results are given in Figure 4. Figure 4(a) shows a single exothermic peak corresponding to the crystallization of austenite (γ) from the melt of Alloy C-4. No other peak was discernible for Alloy C-4, suggesting a simple, single-phase solidification sequence for



(a)



(b)



(c)

Fig 4—(a) DTA profile on cooling for Alloy C-4; (b) DTA profile on cooling for Alloy C-22; (c) DTA profile on cooling for Alloy C-276; all temperatures in °C

this alloy. Figure 4(b) shows the DTA results for Alloy C-22. In addition to the large γ exotherm, there is a second small peak at approximately 1285 °C. As will be described later, this peak corresponds to the secondary solidification of σ phase. Figure 4(c) shows the DTA results for Alloy C-276. In a similar manner to Alloy C-22, this alloy has both a peak corresponding to primary γ solidification and a peak, larger than in the C-22 case, at approximately 1285 °C corresponding to a secondary solidification constituent, identified later as P phase.

Figure 5 shows the microstructure of a water quenched specimen of Alloy C-276. This microstructure was typical of all alloys investigated with the water-quench technique. In the present case, the solidification and welding directions are from left to right in the figure. A series of parallel-growing dendrites can be seen in the center of the figure, the tips of which were growing into the trailing edge of the weld pool at the instant of quenching. Microprobe profiles were taken transverse to the primary growth direction, as indicated by the arrows. The results of these analyses are shown in Figures 6 through 8. A portion of the microprobe profile obtained from each specimen is given, beginning at a particular dendrite core (DC) and terminating at the interdendritic (ID) region between adjacent dendrites. What can be seen as common to all three alloys is that the dendrite cores are enriched in Ni and depleted in Mo relative to the interdendritic regions. This implies that solidification will occur along a path of increasing Mo concentration at the expense of Ni. In addition, it can be observed that there is effectively no Cr segregation associated with solidification in any of the alloys examined.

The segregation profiles of the minor alloying elements (Fe, W, Ti) are somewhat less distinct than those of the major elements. Amongst considerable scatter, segregation of Fe to dendrite cores and Ti to interdendritic volumes in Alloy C-4 is shown in Figure 6(b). The Ti segregation associated with solidification of Alloy C-4 can be seen with greater ease in Figures 9(a) and 9(b). Figure 9(a) is a back-scattered electron image taken in the microprobe of Alloy C-4 weld metal. The interdendritic regions are the light-appearing areas, which have a higher average atomic

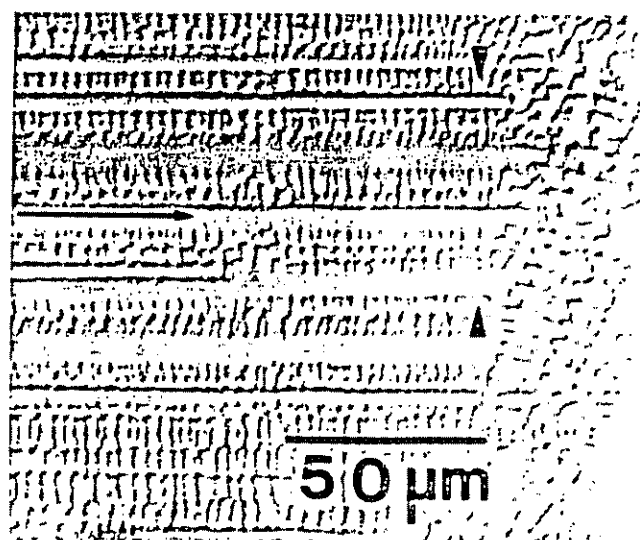


Fig 5—Water-quenched specimen of Alloy C-276

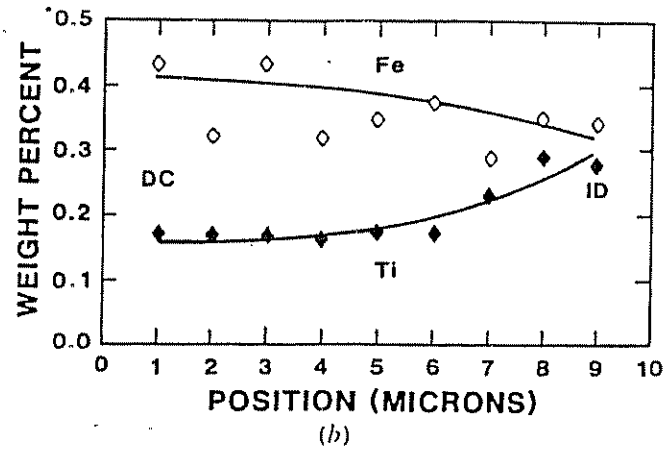
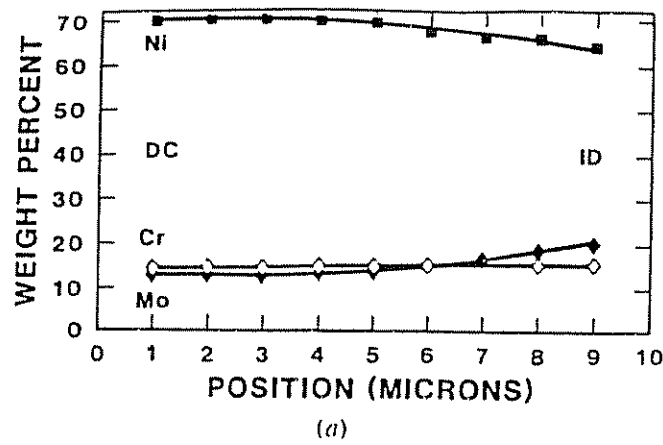


Fig. 6—(a) Major element segregation pattern in Alloy C-4 water-quenched weld metal; (b) minor element segregation pattern along the same profile as (a)

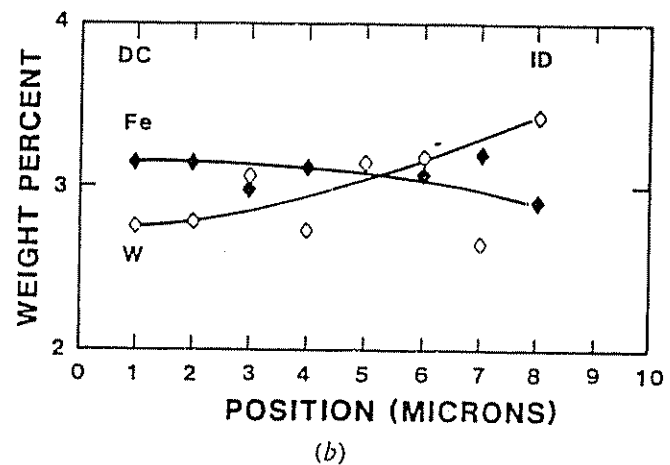
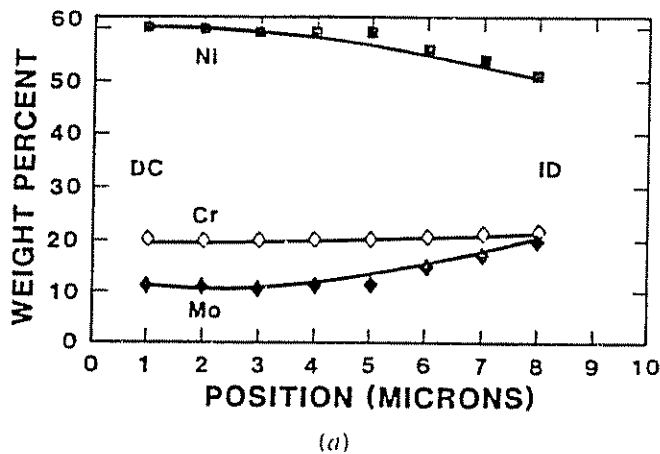


Fig. 7—(a) Major element segregation pattern in Alloy C-22 water-quenched weld metal; (b) minor element segregation pattern along the same profile as (a)

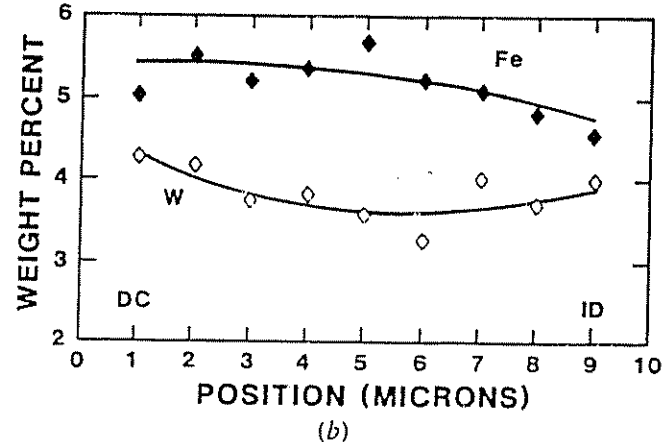
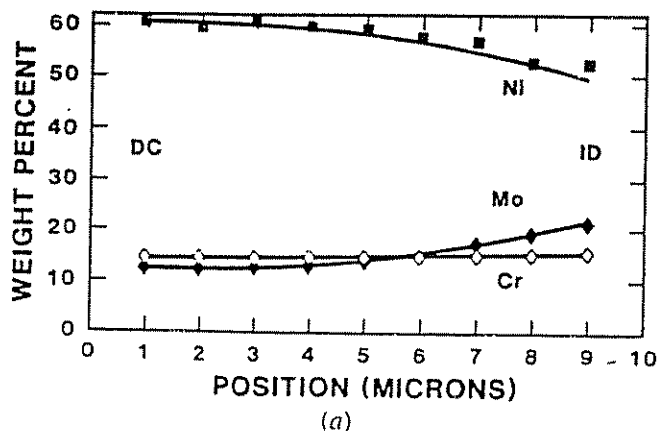
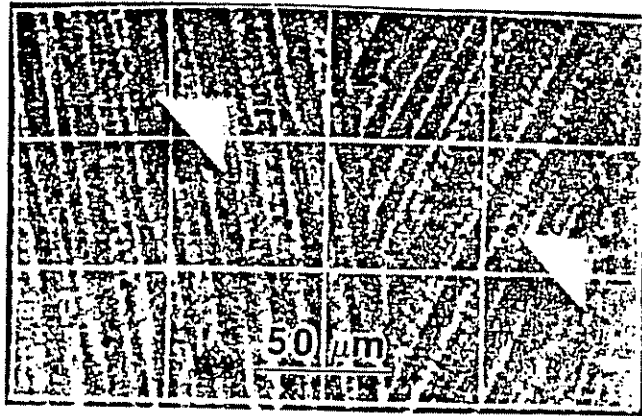
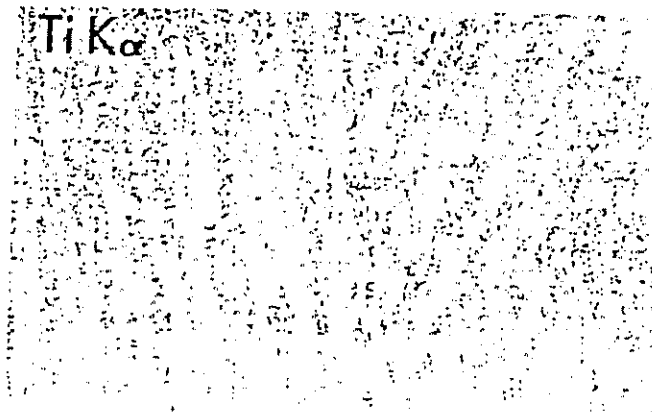


Fig. 8—(a) Major element segregation pattern in Alloy C-276 water-quenched weld metal; (b) minor element segregation pattern along the same profile as (a)



(a)



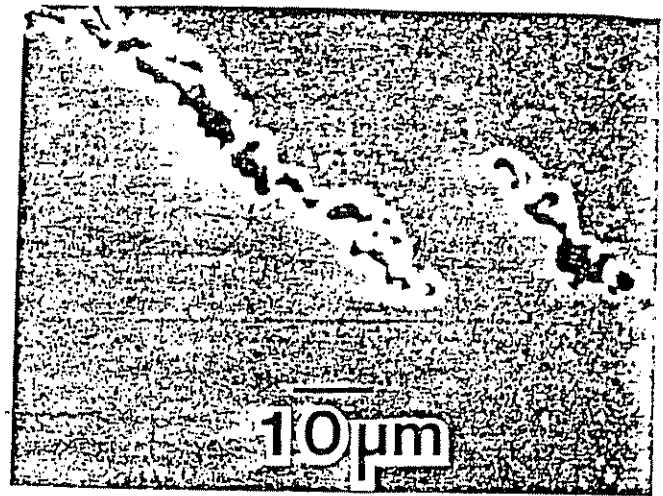
(b)

Fig 9—(a) Backscattered electron image of Alloy C-4 weld metal, un-etched; (b) Ti K_{α} X-ray map of the same region

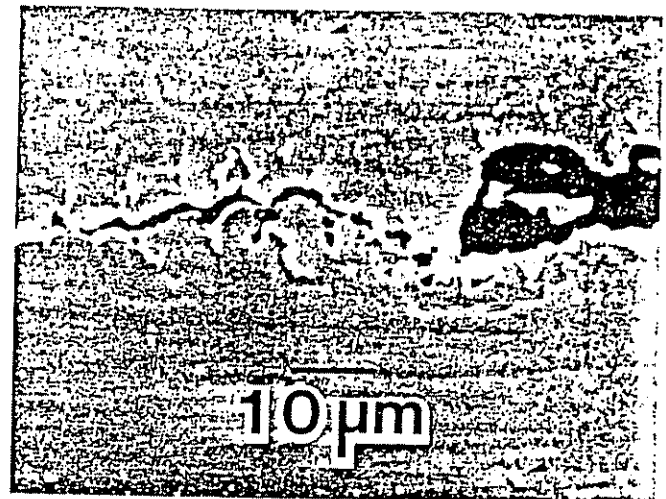
number (higher Mo content) than the dendrite core regions. Figure 9(b) is the corresponding X-ray map of Ti K_{α} radiation which clearly shows the pattern of Ti segregation to interdendritic volumes. In both Alloys C-22 and C-276, Fe appears to segregate to dendrite core regions (Figures 7(b), 8(b)) in a manner similar to Ni. The segregation of W is more difficult to discern against the data scatter, and no distinct pattern was obvious.

Microstructures from the Varestraint test specimens are shown in Figure 10. Figure 10(a) is a SEM micrograph of a hot-cracked region from Alloy C-4. Note the absence of a secondary constituent in the vicinity of the cracks. Figures 10(b) and 10(c) are SEM micrographs of hot-cracked regions in alloys C-22 and C-276, respectively. Note in both cases the presence of a secondary constituent associated with the hot cracks. This kind of microstructure is typical^{25, 26, 27} of weld metal which terminates solidification with the formation of eutectic-like constituents. Also note the presence of these secondary constituents (arrows) at interdendritic regions scattered throughout the microstructures.

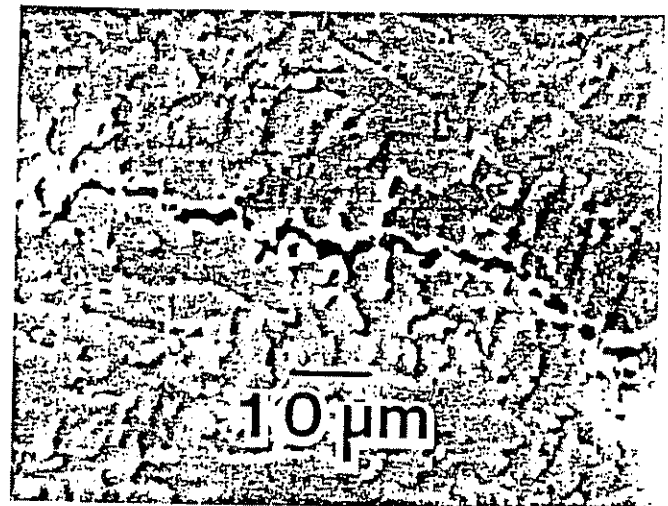
Thin foil micrographs and EDS spectra from minor phases found in the various weld metals are shown in Figures 11 through 13. Figure 11(a) shows the structure found in Alloy C-4 weld metal. The dendritic-shaped second



(a)

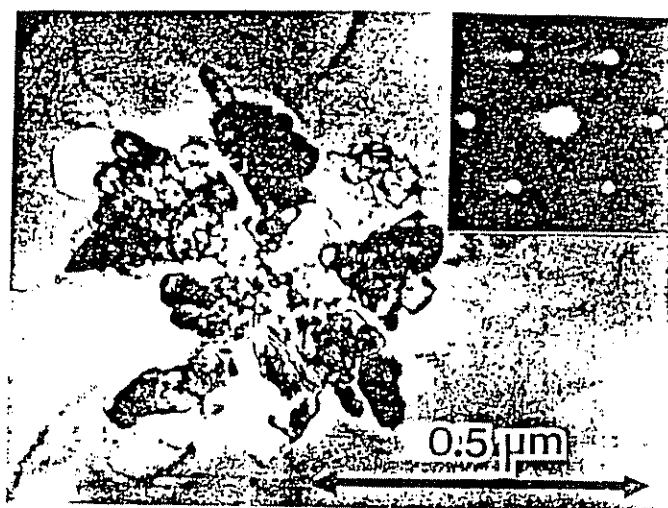


(b)

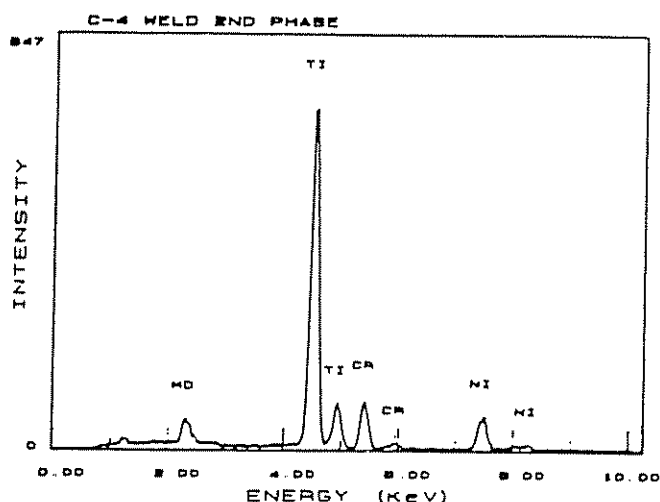


(c)

Fig 10—Secondary electron micrographs of hot-cracked regions in (a) Alloy C-4, (b) Alloy C-22, and (c) Alloy C-276; all specimens etched in 10 pct chromic acid.



(a)



(b)

Fig. 11—(a) Thin foil electron micrograph of TiC, [110] zone, found in Alloy C-4 weld metal; (b) EDS spectrum

phase was indexed to TiC (fcc, $a_0 = 0.427$ nm). This was the only minor phase found in Alloy C-4 by thin foil analysis. Figure 11(b) is the EDS spectrum obtained from this phase and it clearly shows the high Ti concentration expected in TiC.

Figures 12(a) through (c) are thin foil micrographs of the minor phases found in Alloy C-22. Three topologically-close-packed (TCP) intermetallics were observed in this system: σ (tetragonal, $a = b = 0.908$ nm, $c = 0.475$ nm), P (orthorhombic, $a = 0.907$ nm, $b = 1.698$ nm, $c = 0.475$ nm), and μ (hexagonal, $a = 0.476$ nm, $c = 2.591$ nm). Figure 12(d) shows the EDS spectra from the three minor phases. Note the similarity in composition. In addition to large amounts of Ni, Cr, and Mo, smaller amounts of W, Fe, Co, and P can be seen in each phase. It was observed that approximately 80 pct of the total minor constituent population was P , approximately 20 pct was σ , and only a trace amount was μ .

Figures 13(a) and 13(b) are thin foil micrographs of the minor phases found in Alloy C-276. Two topologically-close-packed intermetallics were observed. P and μ , in

approximately equal amounts. The EDS spectra from these two phases are shown in Figure 13(c). These are qualitatively similar to those seen in Figure 12(d) except for generally less intense Cr peaks.

Phase chemistries were determined for the γ matrix and for all of the TCP phases found in weld metal from Alloys C-22 and C-276, using the AEM procedure outlined above. Table III gives the results of these analyses. As can be seen, all of the TCP phases are enriched in Mo and W and depleted in Ni and Fe relative to the γ matrix. The Cr contents of the TCP phases are similar to those of the matrix, and there is no apparent Co partitioning to the TCP phases. There appears to be a somewhat higher Mo content in the TCP phases of Alloy C-276 when compared to those in Alloy C-22. The Cr contents of the TCP phases in Alloy C-276 are less than those of the TCP phases in Alloy C-22. These observations correlate with bulk chemistries in that Alloy C-276 contains more Mo and less Cr than Alloy C-22.

IV. DISCUSSION

The welding metallurgy of these alloys can best be understood by referring to known isothermal sections of the phase diagrams for the ternary system, Ni-Cr-Mo, from which these alloys are derived. Figure 14, developed by Raghavan *et al.*¹³ and Bloom and Grant,¹² shows isothermal sections at 1250 °C and 850 °C. A solidus diagram is not available, nor is a true liquidus diagram. Bloom and Grant¹² measured the liquidus temperatures for the Ni-Cr-Mo system, and proposed a series of possible reactions between 1250 °C and the liquidus. In the composition range corresponding to the alloys under investigation at the present time, the proposed equilibrium phases are liquid, γ , P , and σ .

Several important phase relationships can be discerned by examining Figure 14. The first is that μ is not present as a high temperature (1250 °C) equilibrium constituent. The regions of stability of the TCP phases (neglecting δ , which does not play a role in the present study) are composition dependent. σ is stabilized relative to P by increasing the Cr concentration. The same relationship can be seen for P relative to μ . μ is stabilized relative to P by increasing the Mo concentration. The same relationship is true for P relative to σ .

The phase boundaries move as a function of temperature. On cooling from 1250 °C to 850 °C, both the $\gamma + P$ and the $\gamma + \sigma$ phase fields are displaced to regions of higher Cr content as the $\mu + \gamma$ field appears at lower Cr and higher Mo concentrations. The sequence of possible solid state phase transformations important to this study can be visualized by referring to the points labeled 1 through 3 in Figure 14. The composition corresponding to Point 1 exists in the $P + \gamma$ field at 1250 °C. Upon cooling to 850 °C, this composition is now in the $\mu + \gamma$ field, necessitating the transformation $P \rightarrow \mu$ over that temperature range. The composition corresponding to Point 2 exists in the $\sigma + \gamma$ field at 1250 °C. Upon cooling to 850 °C, this composition now exists in the $P + \gamma$ field, requiring the transformation $\sigma \rightarrow P$ over that temperature range.

An even more complex transformation sequence can be described for the composition corresponding to Point 3. At 1250 °C, this composition resides in the $\sigma + \gamma$ field. At 850 °C, it exists in the $\mu + \gamma$ field. At some temperature

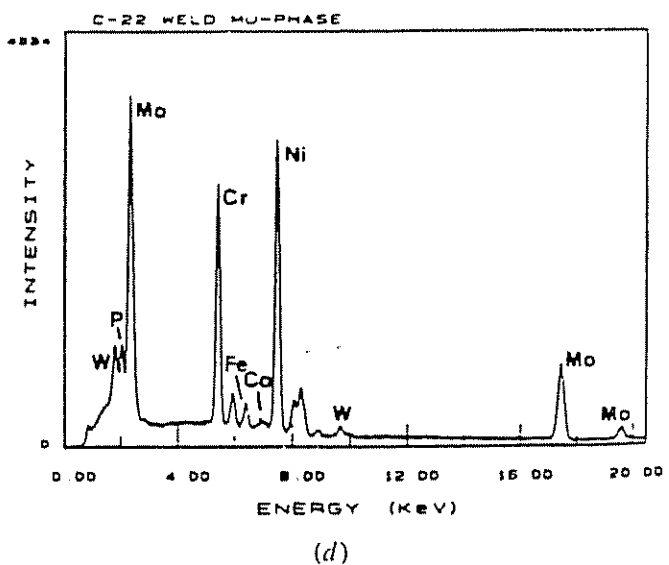
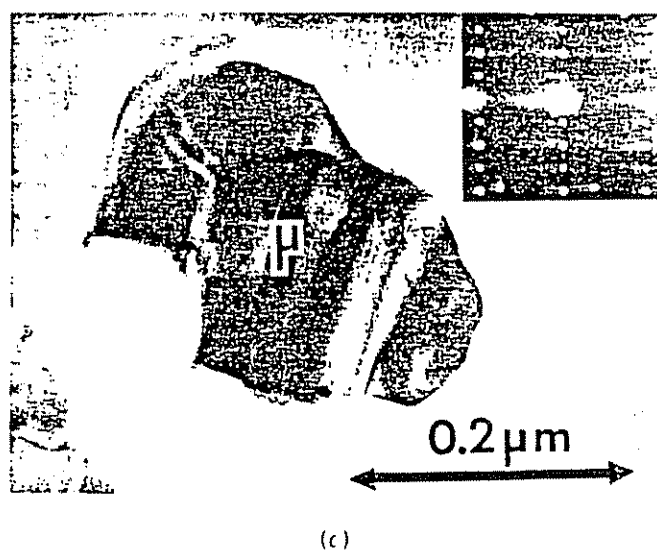
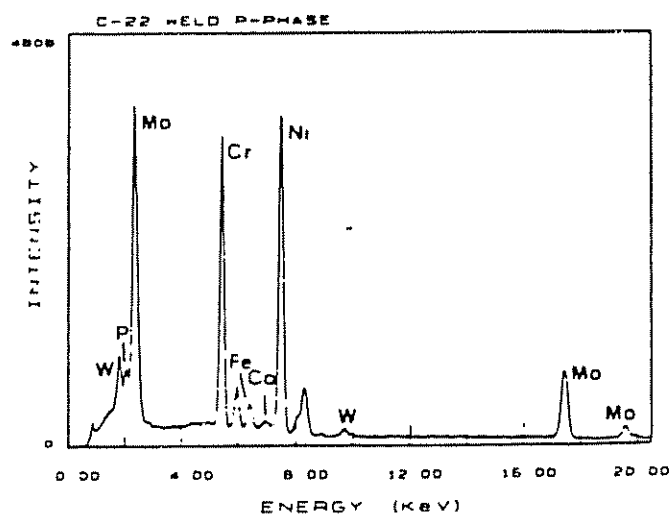
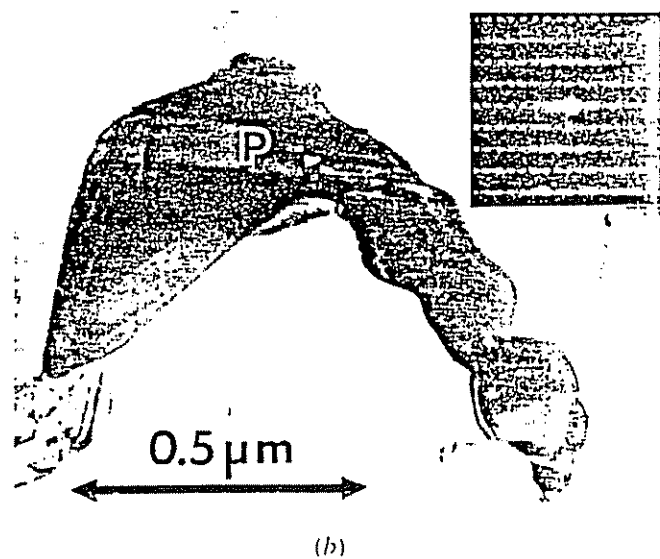
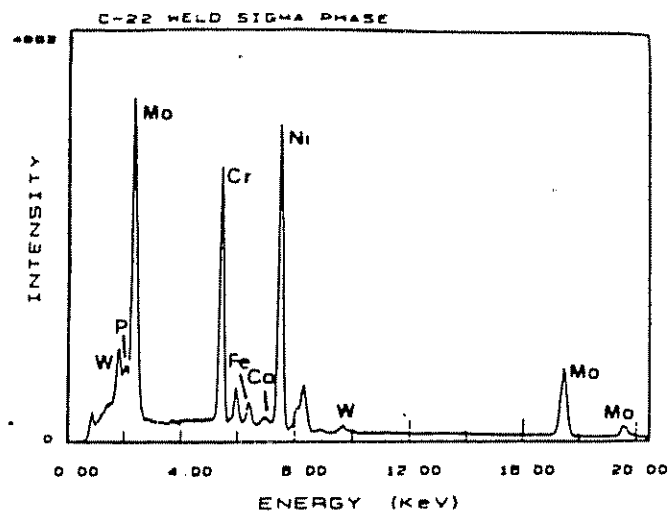
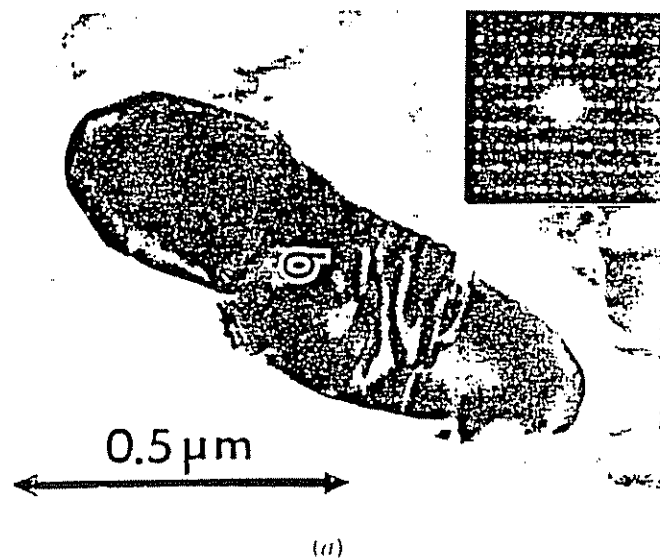


Fig. 12—Thin foil electron micrographs of (a) σ , [001] zone, (b) P , [001] zone, and (c) μ , $[1\bar{1}00]$ zone in Alloy C-22 weld metal; (d) EDS spectra from the three phases

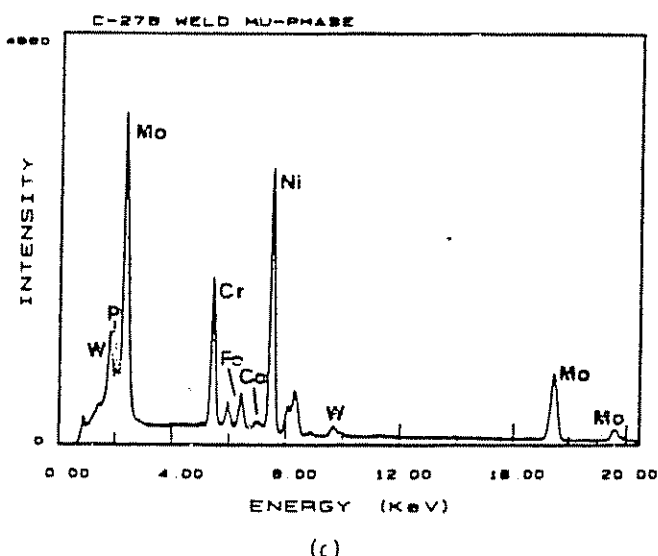
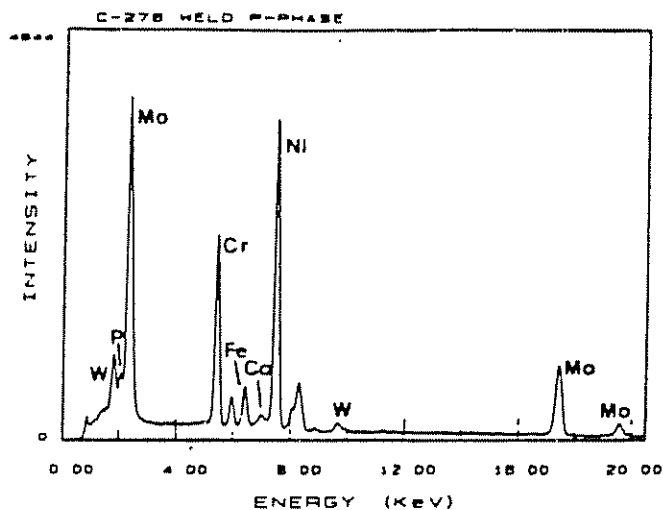
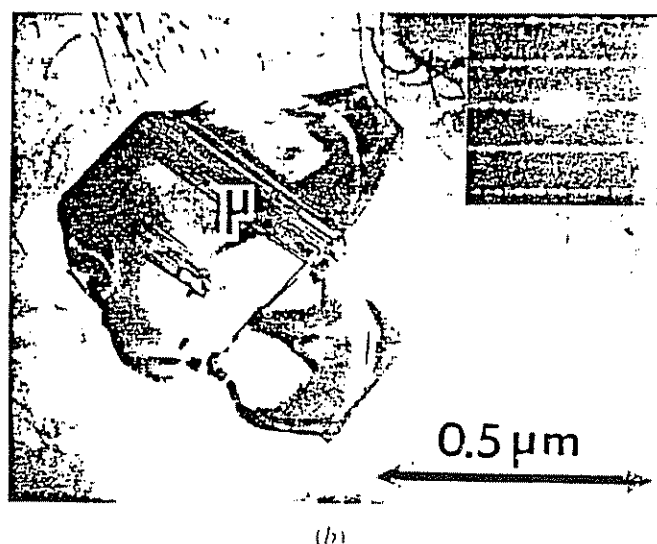
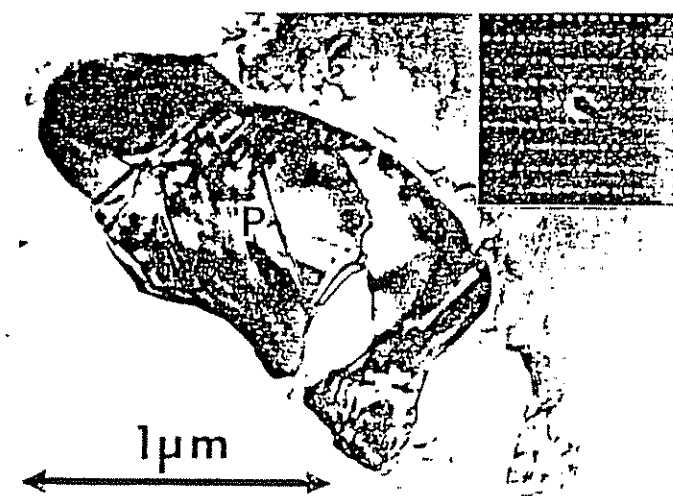


Fig. 13—Thin foil electron micrographs of (a) P [001] zone, and (b) μ [110] zone in Alloy C-276 weld metal; (c) EDS spectra from the two phases

between 1250 °C and 850 °C, this composition would have to pass through a region where P was one of the stable phases. This suggests the following transformation sequence on cooling from 1250 °C to 850 °C: $\sigma \rightarrow P \rightarrow \mu$.

Prediction of the solidification and solid state transformation sequences in the commercial alloys under study is complicated by the fact that they are not pure ternary (Ni-Cr-Mo) systems. A composition model is proposed to treat the remaining minor alloying elements, especially Fe and W, as equivalents of certain of the major alloying elements (Ni, Cr, Mo). This proposal is analogous to the Cr and Ni equivalent concept^{28,29} for predicting the solidification mode³⁰ and room temperature phase stability^{28,29} in austenitic stainless steel weld metal.

First, it is proposed to combine the Mo and W weight fractions to create a Mo equivalent, Mo_{eq} . By referring to Table III, the similarity in partitioning of Mo and W between the TCP phases and the γ matrix is obvious. Both elements partition preferentially to the TCP phases. This is in agreement with the observations of Raghavan *et al.*⁵ for P and μ formation during high-temperature heat treatments of Alloy C-276.

A more subtle similarity in behavior among Mo and W can be seen by examining the Mo and W compositional data for Alloy C-22, in which all three TCP phases are present simultaneously. The average Mo concentration of the TCP phases increases in the order: σ , P , μ , as would be predicted from the phase diagrams of Figure 14. The average W concentration in the TCP phases increases in the same order, mimicking the behavior of Mo. A similarity in the chemical behavior (partitioning and phase stabilization) among Mo and W is not surprising. The refractory nature and body-centered-cubic crystal structure of both elements suggests similarities in bonding characteristics and hence chemical properties.

Second, it is proposed to combine the Fe and Ni weight fractions to create a Ni equivalent, Ni_{eq} . Again, by referring to Table III, the similarity in partitioning behavior of Ni and Fe is obvious. Both elements remain preferentially in the γ matrix. Within most of the high temperature region under consideration, both Ni and Fe have face-centered-cubic (fcc) crystal structures, and so their partitioning to the fcc- γ matrix is also not surprising. The similarity in partitioning behavior among Ni and Fe can be seen in more subtle detail

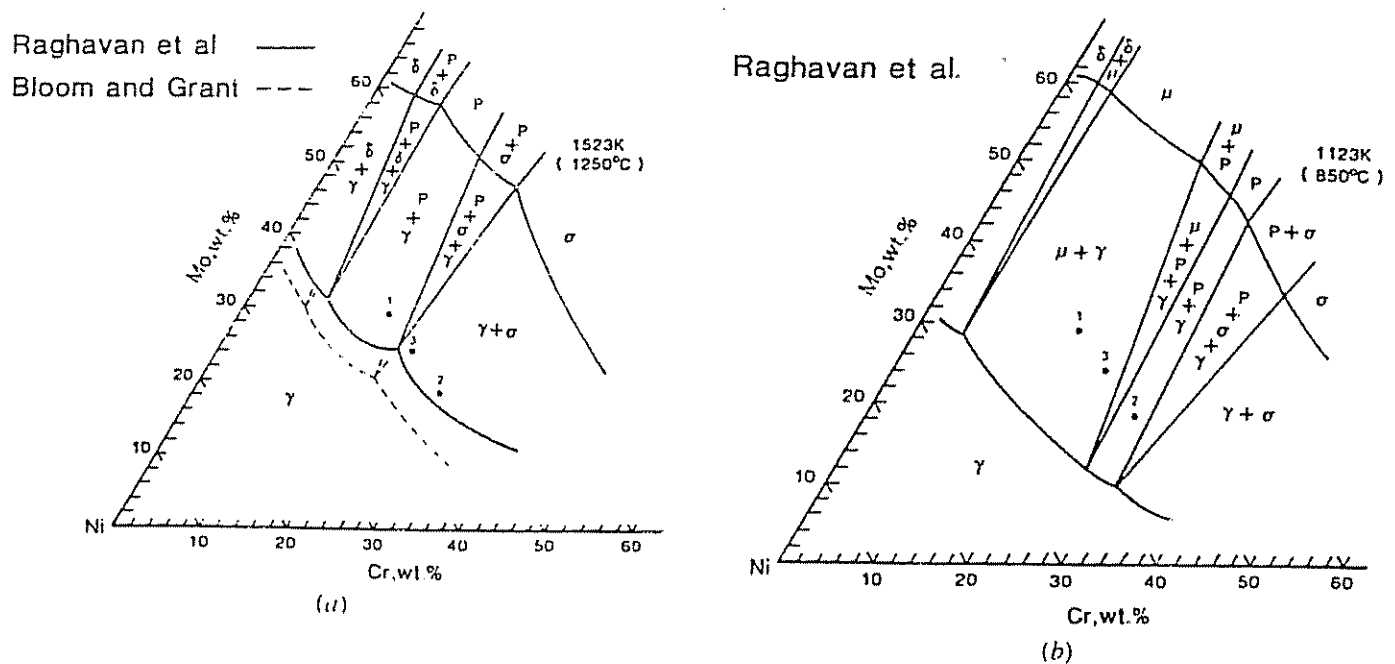


Fig. 14—(a) 1250 °C isothermal section of the Ni-Cr-Mo system; (b) 850 °C section; points 1, 2, and 3 described in text.

by examining the partition ratios: wt pct Fe_{TCP}/wt pct Fe_{γ} , and wt pct Ni_{TCP}/wt pct Ni_{γ} . When the Fe and Ni concentrations are each averaged among all of the TCP phases within a single alloy and ratioed against the concentration of these two elements in the residual matrix, a value of approximately 0.6 is obtained for both elements in both Alloys C-22 and C-276.

Third, it is also proposed that the remainder of the minor alloying elements combine with Ni and Fe as part of the Ni_{eq} . In the present study, Co was found in essentially equal quantities in all phases, suggesting that it is relatively inert. Earlier AEM work by Raghavan *et al.*⁵ indicated that Co remains in the γ matrix and does not partition preferentially to the TCP phases. The Co content of the Alloy C-276 in

the earlier study⁵ was greater than twice that of the present investigation and therefore differences in composition would be simpler to detect. This earlier result, though, supports the grouping of Co in the Ni_{eq} .

No alloying elements were observed to behave similarly to Cr. The Cr contents of the TCP phases were observed to follow the trends predicted by the Ni-Cr-Mo phase diagrams. That is, the Cr content of the TCP phases increased in the order: μ , P , σ . This result is in qualitative agreement with the earlier AEM study⁵ of μ and P phases in Alloy C-276.

In summary, the proposed equivalent composition model is as follows:

$$Mo_{eq} = wt \text{ pct Mo} + wt \text{ pct W} \quad [3]$$

Table III. Phase Compositions (Wt Pct)

Phase	Ni	Mo	Cr	W	Fe	Co
C-22						
μ	33.1 (2.4)*	38.7 (0.2)	19.3 (0.7)	6.3 (1.1)	2.1 (0.2)	0.6 (0.2)
P	32.6 (0.8)	37.4 (1.0)	21.7 (0.7)	5.3 (1.1)	2.2 (0.2)	0.9 (0.4)
σ	34.5 (0.6)	34.9 (0.4)	23.4 (1.3)	4.2 (1.2)	2.2 (0.1)	0.9 (0.2)
γ	58.5 (1.2)	12.7 (0.8)	21.6 (0.5)	2.9 (0.7)	3.4 (0.1)	0.9 (0.2)
Nom	56.96	13.43	21.22	3.29	3.17	0.84
C-276						
μ	33.2 (0.8)	40.9 (0.6)	15.2 (0.9)	6.2 (1.6)	3.5 (0.3)	1.0 (0.5)
P	33.5 (0.6)	39.7 (1.5)	15.7 (0.6)	6.5 (1.6)	3.7 (0.2)	0.8 (0.4)
γ	57.0 (2.3)	16.0 (1.9)	16.3 (0.4)	4.2 (0.8)	5.6 (0.3)	1.0 (0.3)
Nom	55.58	15.56	15.83	3.93	5.44	0.96

*Values in parentheses equal 1 standard deviation

$$Cr_{eq} = wt \text{ pct Cr} \quad [4]$$

$$Ni_{eq} = wt \text{ pct Ni} + wt \text{ pct Fe} + \sum wt \text{ pct X}, \quad [5]$$

where $\sum wt \text{ pct X}$ is the total remaining alloy content not included in the other equivalents. Unlike the case with austenitic stainless steel weld metal Ni and Cr equivalents,^{28,29} no "weighting factors" are included in the equivalents defined here. It was felt that the data base was not extensive enough to attempt to determine appropriate weighting factors. Using the definitions given above to establish an "equivalent" composition for the alloys under study, the sequence of phase transformations leading to the observed room temperature microstructure will be described.

Table IV gives the nominal equivalent compositions for the three alloys under study. These compositions are plotted on the Ni-Cr-Mo isothermal sections in Figure 15. In addition to the nominal compositions, the segregation profiles resulting from solidification, in equivalent terms, are shown as the arrows associated with each nominal composition. The tail of each arrow represents the composition of the initial solid to crystallize from the melt, the dendrite core region. The head of the arrow represents the final solidification composition, that of the interdendritic regions. Although all of the bulk equivalent compositions lie within the single phase γ field at 1250 °C, irrespective of the diagram used, solidification segregation results in the final solidification compositions for Alloys C-22 and C-276 being located within fields of TCP phase stability.

Table IV. Equivalent Compositions*

Equivalent	HASTELLOY C-4	HASTELLOY C-22	HASTELLOY C-276
Cr	15.69	21.22	15.83
Ni	69.25	62.06	64.68
Mo	15.06	16.72	19.49

*All values in weight percent

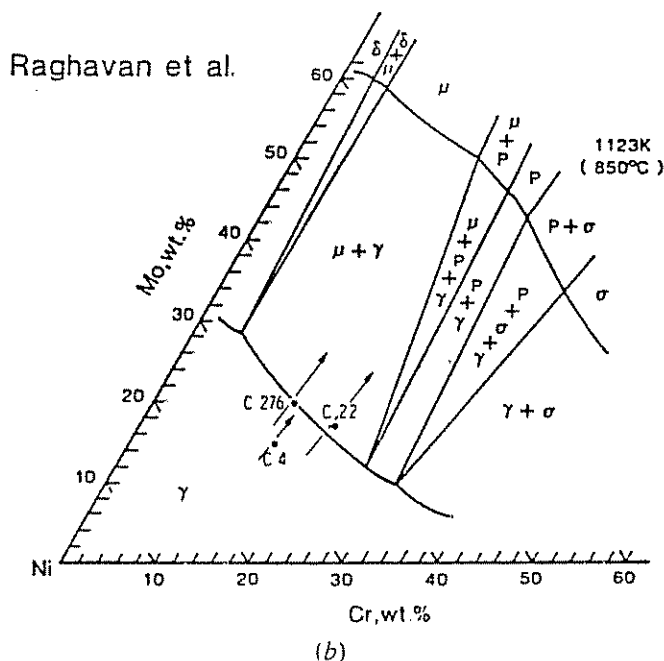
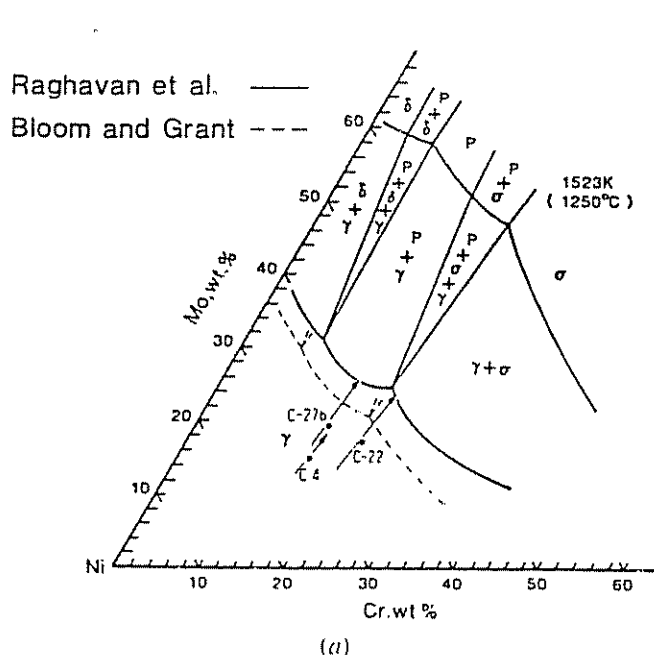


Fig 15 — Isothermal sections: (a) 1250 °C (b) 850 °C showing nominal equivalent compositions and equivalent solidification profiles (arrows)

An experimentally determined solidus section is not available for this system. Kaufman and Nestor³¹ calculated the 1277 °C and 1227 °C sections of the Ni-Cr-Mo system. Although neither diagram contained the experimentally confirmed P phase, the 1277 °C section contained liquid phase in equilibrium with a TCP phase (σ). Bloom and Grant³² indicated that the minimum solidus temperature in the Ni-Cr-Mo system was approximately 1275 °C. These data suggest that the experimentally determined 1250 °C section is quite close to the solidus. This further implies that the phases present in the 1250 °C section are those present at the termination of solidification. Assuming that the presence of the minor alloying elements does not change the phase diagrams much, the 1250 °C section can be used, along with the experimentally determined segregation profiles to predict the solidification microstructure of the alloys under study. The 850 °C section can be used to predict subsequent solid state transformations.

For Alloy C-4, solidification begins and ends within the single phase γ region. There is not sufficient segregation of Mo and Ni to allow this alloy to enter into any $\gamma + TCP$ phase field. TEM analysis revealed the presence of widely dispersed TiC in the weld microstructure. Microprobe analysis showed that Ti does segregate to interdendritic regions, and solidification can terminate locally with the formation of this phase. Lippold³³ identified a TiC constituent in Alloy 800 weld metal that is morphologically identical to the TiC particle shown in Figure 11(a). The TiC in that study was also an interdendritic, terminal solidification constituent. The very low volume fraction of this constituent in Alloy C-4 is such that its formation is not discernible in the DTA profiles.

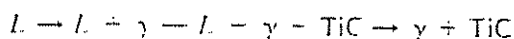
Solidification of Alloy C-276 begins with the crystallization of γ , but ends with the terminal solidification of P phase as the solidification path is such that it enters the region of $\gamma + P$ stability (Figure 15(a)). The DTA curve (Figure 4(c)) shows the presence of a secondary solidi-

ification peak at approximately 1285 °C. This peak corresponds to the crystallization of P phase and it occurs at a temperature in good agreement with those suggested earlier.^{12,11} As the solidified weld metal cools, it enters the region of $\gamma + \mu$ stability (Figure 15(b)) which results in at least partial transformation of P to μ . As in many weld metal transformations, sufficient time at temperature is not available for completion of the $P \rightarrow \mu$ reaction. The weld metal microstructure is then composed of intermediate (P) and final (μ) transformation products in a γ matrix. Figure 16 is a TEM micrograph showing the possible growth of μ on P in Alloy C-276 weld metal. The equivalent composition model used in conjunction with the ternary phase diagrams precludes the formation of σ in Alloy C-276 because of its relatively low Cr_{eq} .

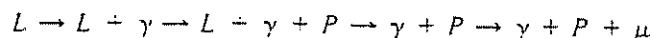
Solidification of Alloy C-22 also begins with the primary crystallization of γ , but this time terminates with the formation of σ phase (Figure 15(a)). The higher Cr_{eq} of this alloy is such that σ forms in preference to P . The DTA profile (Figure 4(b)) reveals a secondary solidification event, also in the range of 1285 °C, this being the crystallization of σ . Subsequent solid state transformation of σ involves a two-step process of $\sigma \rightarrow P$ and $P \rightarrow \mu$, in a manner analogous to that described for Point 3, Figure 14. In this case, assuming neither solid state transformation goes to completion, the final weld metal microstructure will consist of γ plus all three TCP phases: σ , P , and μ .

In summary, the proposed sequences of transformation in the alloys studied are given as follows:

C-4



C-276



C-22

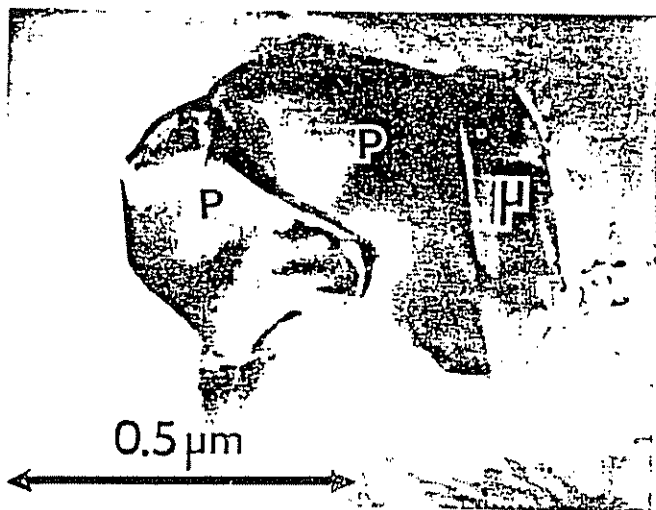
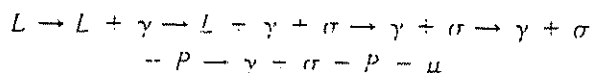


Fig. 16—Thin foil electron micrograph showing growth of μ on P in Alloy C-276 weld metal

Although the weld metal hot-cracking resistance of each alloy was very good, the resistance of Alloy C-4 was the best. This can be attributed to the lack of a TCP terminal solidification constituent. The formation of a TCP constituent accompanies an extension of the solidification temperature range, a situation less desirable from a hot-cracking standpoint. This extension of the solidification temperature range can be seen indirectly in Figure 3. Both Alloys C-22 and C-276 have maximum crack length values greater than those of Alloy C-4 (≈ 0.40 mm vs ≈ 0.15 mm). The similarity in maximum crack length data among Alloys C-22 and C-276 can be understood by reviewing the DTA data of Figures 4(b) and 4(c). Both alloys have very similar curves including temperature range from initiation of solidification to termination of solidification with TCP phase formation. The greater cracking susceptibility of Alloy C-276 can be related to the amount of TCP phase formed (which is also proportional to the amount of liquid phase remaining at 1285 °C) at the termination of solidification. The size of the DTA TCP phase solidification peak was greater for Alloy C-276 than for Alloy C-22. Assuming similar heats of fusion for σ and P phases (they have similar chemical compositions and both are topologically close packed), this implies a larger amount of residual liquid present in Alloy C-276. According to Borland,³³ this would increase the susceptibility to hot cracking.

V. CONCLUSIONS

1. Among the HASTELLOY C-type alloys examined, a resistance to hot-cracking ranking can be given as follows: C-4 > C-22 > C-276. All alloys would be expected to be readily weldable in most situations.
2. Alloys C-22 and C-276 terminate solidification with the formation of a TCP constituent; Alloy C-4 does not.
3. The following equivalent composition model is proposed to account for the behavior of the minor elements (W, Fe, etc.) in these alloys:

$$Mo_{eq} = \text{wt pct Mo} + \text{wt pct W}$$

$$Cr_{eq} = \text{wt pct Cr}$$

$$Ni_{eq} = \text{wt pct Ni} + \text{wt pct Fe} + \sum \text{wt pct } X_i$$

where $\sum \text{wt pct } X_i$ is the total remaining alloy content not included in the other equivalents.

4. The equivalent composition model used in conjunction with available Ni-Cr-Mo phase diagrams correctly predicts the sequence of transformations in the alloys studied (except for the formation of TiC in Alloy C-4).

ACKNOWLEDGMENTS

The authors would like to acknowledge the assistance of Ellen Semarge in performing the microprobe analysis and William Hammett for doing the DTA experiments. This work was performed at Sandia National Laboratories, Albuquerque, New Mexico, and was supported by the United States Department of Energy under contract number DE-AC04-76DP00789.

REFERENCES

- 1 S. J. Mathews: *Superalloys* 1976, pp. 215-26.
- 2 H. M. Tawancy, R. B. Herchenroeder, and A. I. Asphahani: *Jour. of Metals*, 1983, vol. 35, No. 6, pp. 37-43.
- 3 N. Sridhar, J. B. C. Wu, and P. E. Manning: *Jour. of Metals*, 1985, vol. 37, No. 11, pp. 51-53.
- 4 H. M. Tawancy: *Metall. Trans. A*, 1980, vol. 11A, pp. 1764-65.
- 5 M. Raghavan, B. J. Berkowitz, and J. C. Scanlon: *Metall. Trans. A*, 1982, vol. 13A, pp. 979-84.
- 6 F. G. Hodge and R. W. Kirchner: *Corrosion*, Aug. 1976, pp. 332-36.
- 7 F. G. Hodge: *Corrosion*, Oct. 1973, pp. 375-83.
- 8 R. B. Leonard: *Corrosion*, May 1969, pp. 222-28.
- 9 W. A. Owezarski: *Physical Metallurgy of Metal Joining*, TMS/AIME Pub., R. Kossowsky and M. E. Glicksman, eds., June 1980, pp. 166-89.
- 10 M. J. Cieslak, A. D. Romig, Jr., and T. J. Headley: *Microbeam Analysis* 1985, pp. 179-88.
- 11 S. Rideout, W. D. Manly, E. L. Kamen, B. S. Lement, and P. A. Beck: *Trans. AIME*, Oct. 1951, pp. 872-76.
- 12 D. S. Bloom and N. J. Grant: *Trans. AIME*, Feb. 1954, pp. 261-68.
- 13 M. Raghavan, R. R. Mueller, G. A. Vaughn, and S. Floreen: *Metall. Trans. A*, 1984, vol. 15A, pp. 783-92.
- 14 W. F. Savage and C. D. Lundin: *Welding Journal*, Oct. 1965, pp. 433-s-42-s.
- 15 W. F. Savage and C. D. Lundin: *Welding Journal*, Nov. 1966, pp. 497-s-503-s.
- 16 A. C. Lingenfelter: *Welding Journal*, Sept. 1972, pp. 430-s-36-s.
- 17 *Methods of High Alloy Weldability Evaluation*, WRC Pub., Nov. 1970.
- 18 Y. Arata, F. Matsuda, and S. Katayama: *Trans. of JWRI*, Dec. 1976, vol. 5(2), pp. 35-51.
- 19 M. J. Cieslak: Ph.D. Thesis, "Fundamental Metallurgical Investigations of Alloy CN-7M Weldments," Rensselaer Polytechnic Institute, Troy, NY, May 1983.
- 20 G. E. Bastin, H. J. M. Heijligers, and F. J. J. van Looy: *X-ray Spect.* 13, 91, 1984.
- 21 A. D. Romig, Jr.: Sandia National Laboratories Report SAND82-2938, 1983.
- 22 J. I. Goldstein, J. L. Costley, G. W. Lorimer, and S. J. B. Reed: *SEM/1977*, pp. 315-24.
- 23 M. J. Cieslak, T. J. Headley, and A. D. Romig, Jr.: Sandia National Laboratories, Albuquerque, NM, unpublished research, 1985.
- 24 G. A. Knorovsky and T. J. Headley: Sandia National Laboratories, Albuquerque, NM, unpublished research, 1985.
- 25 J. A. Brooks, A. W. Thompson, and J. C. Williams: *Physical Metallurgy of Metal Joining*, R. Kossowsky and M. E. Glicksman, eds., TMS/AIME Pub., June 1980, pp. 117-36.
- 26 R. A. Patterson and J. O. Milewski: *Welding Journal*, Aug. 1985, pp. 227-s-31-s.
- 27 M. J. Cieslak and W. F. Savage: ASTM STP 756, *Stainless Steel Castings*, pp. 241-58.
- 28 A. L. Schaeffer: *Metal Progress*, 1949, vol. 56, No. 11, pp. 680-80B.
- 29 C. J. Long and W. T. DeLong: *Welding Journal*, July 1973, pp. 281-s-97-s.
- 30 N. Suutala and T. Moiso: *Solidification Technology in the Foundry and Casthouse*, The Metals Society, University of Warwick, Coventry, 15-17 Sept., 1980, Session IVa, pp. 1-10.
- 31 L. Kaufman and H. Nestor: *Metall. Trans.*, 1974, vol. 5, pp. 1617-21.
- 32 J. C. Lippold: *Welding Journal*, March 1984, pp. 91-s-103-s.
- 33 J. C. Borland: *British Welding Journal*, Aug. 1960, pp. 508-12.

HE 00134

HAYNES

International

***“The HASTELLOY® trademark -
your assurance of quality”***

Industry often specifies alloys to a Unified Numbering System (UNS) designation unaware that such alloy specifications only address issues of chemical composition, not of corrosion resistance. Haynes International, Inc., the developer of the **HASTELLOY** alloy families, protects the alloys' quality and assures its performance, not merely by close attention to chemical composition and carefully selected thermomechanical processing, but also by **systematic corrosion testing**.

Every heat of HASTELLOY C-276 and C-22™ alloys is subjected to the ASTM G-28A and B test methods. Only products exhibiting corrosion rates lower than the established internal Quality Control limits are shipped to customers by Haynes. A typical example is given below for maximum allowable corrosion rates, in mils per year:

<u>ASTM B 575 Products</u>	<u>ASTM G-28A</u>	<u>ASTM G-28B</u>
HASTELLOY alloy C-276	410	110
HASTELLOY C-22 alloy	80	10

Specify these tests to ensure the level of performance on which you have come to depend, from your HASTELLOY products.

HE 00164

NICKEL

Alloys for Corrosive Environments

A wide range of nickel-base alloys is available for applications in highly aggressive environments.

Raúl B. Rebak*

Paul Crook*

Haynes International Inc.
Kokomo, Indiana

Nickel-base alloys provide outstanding resistance to specific chemicals, and some are extremely versatile and able to handle complex process and waste streams. In particular, the versatile alloys are much less subject than stainless steels to stress corrosion cracking, pitting, and crevice attack in hot chloride-bearing solutions. Also, nickel alloys are among the few materials able to withstand hot hydrofluoric acid, a chemical that is very corrosive to the reactive metals (titanium, zirconium, niobium, and tantalum).

The aim of this article is to describe the general characteristics of nickel-base alloys and to examine the effects of different aggressive environments on the corrosion behavior of these alloys.

Nickel alloy types

The nickel alloys can be categorized according to the main alloying elements, as follows:

- *Nickel*: primarily for caustic solutions.
- *Nickel-copper*: primarily for mild, reducing solutions, especially hydrofluoric acid.
- *Nickel-molybdenum*: primarily for strong, reducing media.
- *Nickel-iron-chromium*: primarily for oxidizing solutions.
- *Nickel-chromium-silicon*: primarily for super-oxidizing media.
- *Nickel-chromium-molybdenum*: versatile alloys for all environments.

The terms "reducing" and "oxidizing" refer to the nature of the reaction at cathodic sites during corrosion. Reducing solutions such as hydrochloric acid generally induce hydrogen evolution at cathodic sites. Oxidizing solutions such as nitric acid induce cathodic reactions with higher potentials.

*Member of ASM International

Copper, molybdenum, and tungsten all increase the inherent corrosion resistance of nickel. In addition, molybdenum and tungsten are significant strengthening agents, due to their large atomic sizes. The compositions of a few nickel alloys are given in Table 1. These are all wrought alloys, available in the form of plates, sheets, bars, pipes, tubes, forgings, and wires.

The role of chromium is the same as that in the stainless steels: it enhances the formation of passive surface films, in the presence of oxygen. These passive films impede the corrosion process. Iron, if added to the nickel alloys, also affects passivation. Silicon is beneficial at high corrosion potentials, where chromium-rich passive films cannot be maintained. It offers extended protection through the formation of protective (silicon-rich) oxides.

Nickel alloy metallurgy

Most of the corrosion-resistant nickel alloys have a single-phase atomic structure. In common with the austenitic stainless steels, this is face-centered cubic. To optimize performance, designers of the nickel alloys have taken advantage of the fact that greater quantities of elements such as chromium and molybdenum are soluble in this face-centered cubic structure at temperatures in excess of 1000°C (1830°F) than at lower temperatures. Furthermore, added elements can be retained within this phase if the materials are water-quenched from the high temperatures. Therefore, such alloys are solution annealed to dissolve any unwanted second phases, and water quenched to "freeze-in" the high-temperature structure.

Second phases are possible, if they are subjected to elevated temperature excursions, for example during welding. The kinetics of second-phase for-

Table 1—Nominal compositions of nickel alloys

Group	Alloy	Ni	Cu	Mo	Fe	Cr	Others
Ni	200	99.5	—	—	—	—	—
Ni-Cu	400	67	31.5	—	12	—	—
Ni-Mo	B-3	68.5	—	28.5	1.5	1.5	—
Ni-Fe-Cr	825	43	2.2	3	30	21.5	0.9 Ti
Ni-Fe-Cr	G-30	44	2	5	15	30	2.5W, 4Co
Ni-Cr-Si	D-205	65	2	2.5	6	20	5 Si
Ni-Cr-Mo	C-276	57	—	16	5	16	4 W
Ni-Cr-Mo	C-4	68	—	16	—	16	—
Ni-Cr-Mo	C-22	56	—	13	3	22	3 W
Ni-Cr-Mo	C-2000	60	1.6	16	—	23	—

HE 00269

Chemical processes most often involve a few aggressive chemicals.

mation depend critically on the amount of over-alloying and the content of minor elements, such as carbon and silicon. Carbon is kept as low as possible in the wrought alloys by special melting techniques. Silicon is also held at low levels in most of the wrought alloys, since it is a strong promoter of second phases. Indeed, this is why the Ni-Cr-Si materials are not more highly alloyed. In cast nickel alloys, a small quantity of silicon is necessary for fluidity during pouring. However, it heightens the importance of the solution annealing and quenching processes with castings.

Nickel alloy performance

Although the number of environments encountered within the chemical process industries is vast, the performance of metallic materials is most often based on their resistance to a few aggressive inorganic chemicals. These are predominantly hydrochloric acid, sulfuric acid, and hydrofluoric acid. Also very important are the effects of residuals such as ferric ions.

• **Caustic solutions:** The most common caustic solutions are sodium hydroxide or caustic soda (NaOH) and potassium hydroxide or caustic potash (KOH). When contamination with iron or stress corrosion cracking is not a problem, these substances are sometimes handled in carbon steel; how-

ever, nickel and nickel alloys are the metals that offer the highest resistance to corrosion in caustic solutions. Figure 1 shows the corrosion rate of several alloys in boiling 50% NaOH solution. The higher the nickel content in the alloy, the lower the corrosion rate. The corrosion resistance of nickel is a consequence of the formation of insoluble metal hydroxides and salts, which slow down the dissolution rate of the alloy.

Figure 2 shows the corrosion rate of three alloys in 30% NaOH as a function of the temperature. Ni-200 offers the best resistance to corrosion, especially at the higher temperatures.

Sodium hypochlorite (bleach) can be considered a mildly oxidizing alkaline salt that can also be successfully handled by a nickel alloy, especially of the Ni-Cr-Mo group (C-276 or C-2000 alloys).

• **Hydrochloric acid:** Hydrochloric acid (HCl) is very corrosive, and its aggressiveness can change drastically depending on the acid concentration, temperature, and contamination of the acid (e.g. ferric ions). In general, steels, stainless steels, and copper alloys cannot tolerate HCl. Of the reactive metals, titanium does not resist HCl well, zirconium is satisfactory for pure acid, and tantalum offers excellent performance. Figure 3 shows the cor-

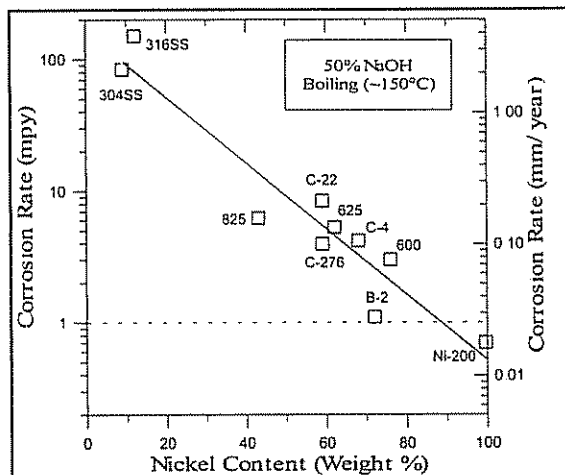


Fig 1 — The higher the content of nickel, the lower the corrosion rate in caustic solutions

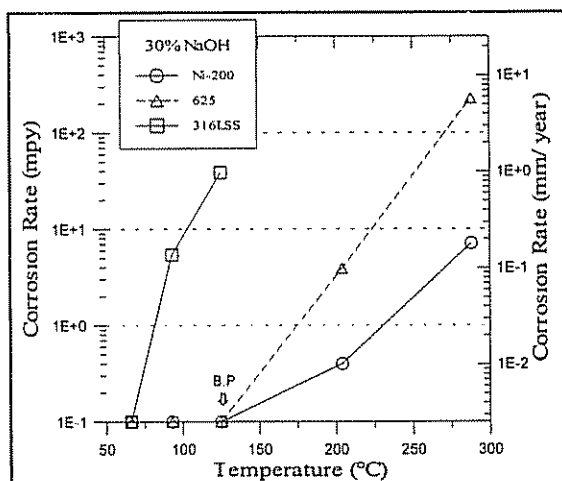


Fig 2 — Corrosion rate of three nickel alloys in 30% NaOH as a function of the temperature

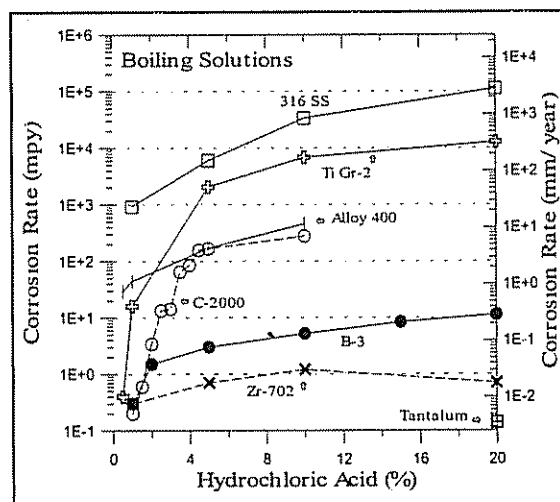


Fig 3 — This graph shows the corrosion of commercial alloys of stainless steel, titanium, nickel, and zirconium in boiling HCl solution

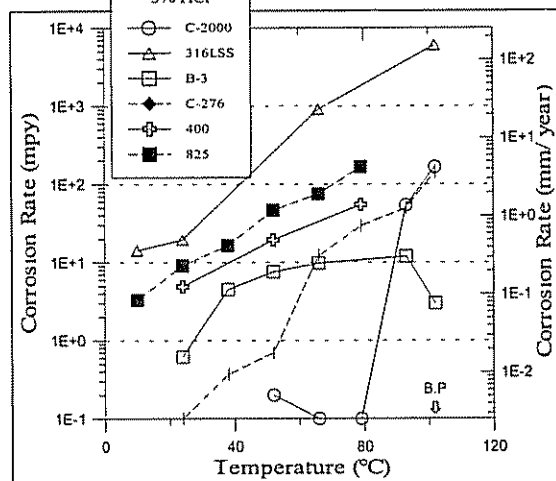


Fig 4 — Effect of the temperature on the corrosion rate of nickel-base alloys and 316L stainless steel in 5% HCl

rosion behavior of several alloys in boiling solutions of pure hydrochloric acid. At intermediate acid concentrations, the corrosion rate of 316 SS can be more than four orders of magnitude higher than the corrosion rate of zirconium or B-3 alloy.

Figure 4 shows the effect of temperature on the corrosion rate of several nickel-base alloys and 316L SS. For most of the alloys, the corrosion rate gradually increases as the temperature increases.

For C-2000 alloy, a threshold temperature is reached, below which the corrosion rate is negligible due to passivation of the alloy; above the threshold temperature, the corrosion rate increases rapidly as the temperature increases.

However, for the B-3 alloy, the corrosion rate does not depend strongly on temperature. The fact that the corrosion rate of the B-3 alloy at the boiling temperature is lower than the corrosion rate at temperatures below the boiling point, could be related to the amount of dissolved oxygen at each temperature (which decreases as the temperature increases).

The nickel alloys that should be considered for service in pure hydrochloric acid are shown in Table 2, a nine-segment chart organized by concentration and temperature. The selections are based on evidence that alloys from the chosen groups exhibit rates of 0.5 mm/y (20 mpy) or less over significant concentration and temperature ranges, within those segments. Table 2 covers only concentrations up to 20 wt%, the maximum that can be sustained in a boiling solution. It indicates that, of the nickel alloys, only those from the nickel-molybdenum group are suitable at high concentrations and temperatures.

In fact, molybdenum is the most important alloying element for good performance of nickel-base alloys in pure hydrochloric acid (reducing conditions). The corrosion rate in boiling HCl decreases as the content of molybdenum in the alloy increases.

Oxidizing impurities in hydrochloric acid, such as ferric ions (Fe^{3+}), are detrimental to the performance of the nickel-molybdenum and nickel-copper alloys. Under such conditions, the nickel-chromium-molybdenum alloys constitute the best choice, because they are tolerant of residuals, although they are temperature-limited at the higher acid concentrations.

Figure 5 shows the corrosion rate of several alloys in boiling 2.5% HCl solution as a function of the concentration of ferric ions in the solution. The corrosion rates of 316L SS and alloy 825 are high, and are not affected significantly by the presence of ferric ions. The corrosion rate of the B-3 alloy in the pure boiling acid is low, but it gradually increases as the content of ferric ions in the solution increases. The corrosion rate of C-2000 in pure acid is higher than that of the B-3 alloy; however, a content of only 3 ppm Fe^{3+} produces a decline in its corrosion rate by almost two orders of magnitude. The oxidizing ferric ions promote the passivation of C-2000 by the formation of a chromium-rich oxide film that reduces the uniform dissolution rate.

Figures 3, 4, and 5 show that the nickel-chromium-molybdenum alloys such as C-2000 are resistant to HCl in a moderately broad range of con-

Table 2 — Nickel alloy selection for pure HCl*

Temperature	0 to 5% HCl	5% to 10% HCl	10% to 20% HCl
79°C to B.P. (175°F to B.P.)	Ni-Mo (B-3)	Ni-Mo (B-3)	Ni-Mo (B-3)
52°C to 79°C (125°F to 175°F)	Ni-Mo (B-3) Ni-Cr-Mo (C-2000) Ni-Cu (400)	Ni-Mo (B-3)	Ni-Mo (B-3)
RT to 52°C (RT to 125°F)	Ni-Mo (B-3) Ni-Cr-Mo (C-2000) Ni-Fe-Cr (G-30) Ni-Cu (400)	Ni-Mo (B-3) Ni-Cr-Mo (C-2000)	Ni-Mo (B-3) Ni-Cr-Mo (C-2000)

*For each alloy group, one example is given
B.P. = boiling point. RT = room temperature

centrations and temperatures, whereas 316L stainless steel is generally unsuitable for hydrochloric acid service. Alloys 400 and 825 may be adequate at room temperature.

Titanium Grade 2, as well as the stainless steels containing 6% molybdenum (such as 254SMO), are resistant to low concentrations of HCl. The resistance of zirconium (Zr-702 alloy) to pure hydrochloric acid is exceptional; however, in the presence of ferric ions Zr-702 would be subjected to pitting corrosion. Tantalum also exhibits excellent resistance to pure HCl solutions up to 175°C (350°F), but it is unacceptable if the HCl solution is contaminated with fluorides. Fluoride ion impurities are also damaging to titanium and zirconium alloys.

• **Sulfuric acid:** Sulfuric acid is the most widely used acid in all branches of industry. Sulfuric acid is less corrosive than hydrochloric acid, and its aggressiveness is highly dependent on acid concentration, temperature, and the presence of impurities. Figure 6 shows the corrosion rate of several alloys in boiling pure sulfuric acid. Sulfuric acid aqueous solutions up to 96 wt% are stable at the boiling point.

However, these boiling points increase dramatically at the medium and high concentrations. For example, at 20% sulfuric acid, the boiling point is 104°C (220°F), at 50% is 123°C (253°F), and at 80% is 202°C (395°F). Titanium Grade 2 and 316L stainless steel are not adequate for sulfuric acid service.

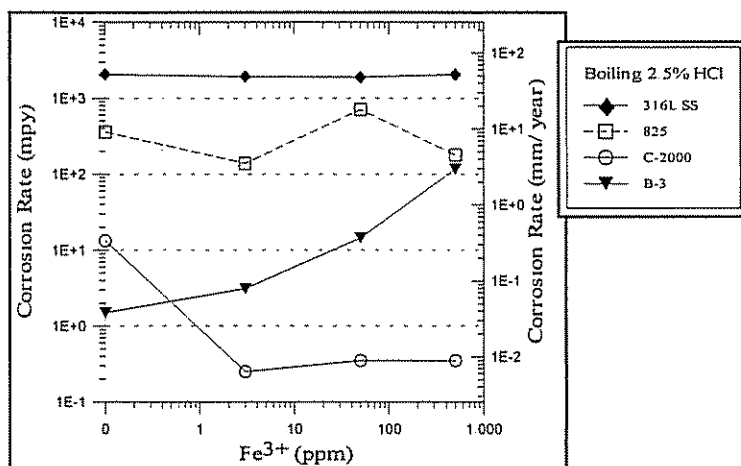


Fig 5 — Corrosion rate of commercial alloys in a solution of HCl contaminated with ferric ions.

Oxidizing impurities such as ferric ions are detrimental to Ni-Mo and Ni-Cu alloys.

Hydrofluoric
acid is
extremely
corrosive.

Figure 6 shows that the B-3 alloy has the lowest corrosion rate of the nickel alloys in boiling sulfuric acid. Only at the highest acid concentration (>70%) does the corrosion rate of B-3 start to increase. The strong concentration effect on the corrosion rate of zirconium alloy 702 is also revealed.

Figure 7 shows the effect of temperature at a constant acid concentration. As in the case of HCl solutions (Fig. 4), the temperature has a strong influence on the corrosion rate of Ni-Cr-Mo and Ni-Cr-Mo-Fe alloys such as C-2000 and G-30; however, the corrosion rate of a Ni-Mo alloy (B-3) is almost unaffected by the temperature (low activation energy).

Table 3 shows the types of nickel alloy that should be considered for service in pure sulfuric acid, depending on the acid concentration and temperature. The selections are based on evidence that alloys from the chosen groups exhibit rates of 0.5 mm/y (20 mpy) or less over significant concentration and temperature ranges, within those segments. The important revelations of this chart are the excellent corrosion resistance of the nickel-molybdenum alloys in pure sulfuric acid, the good resistance of the nickel-chromium-molybdenum materials, and the usefulness of several groups at lower concentrations and temperatures.

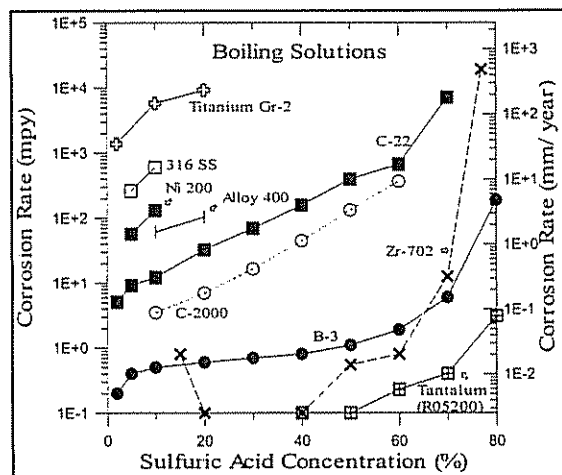


Fig 6 — Corrosion rate in boiling sulfuric acid.

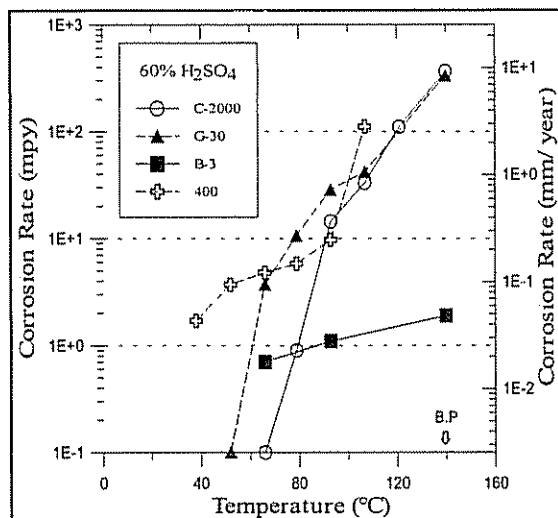


Fig. 7 — This graph shows the effect of temperature on the corrosion rate of several nickel-base alloys

The presence of contaminants in sulfuric acid could change the corrosion rate of the alloys. Figure 8 shows the corrosion rate of alloys B-3 and C-2000 in pure sulfuric acid and in sulfuric acid contaminated with 200 ppm chloride ions (as NaCl). The corrosion rate of both alloys increases if the solution is contaminated; however, the effect seems more pronounced for the Ni-Cr-Mo alloy.

• *Hydrofluoric acid:* Hydrofluoric acid is extremely corrosive and unique in its corrosion behavior. Many industries use it as an aqueous solution, as a fluorinating agent, for metal pickling, and in the manufacturing of semiconductors.

Nickel alloys are the only alloys that are widely chosen for handling aqueous solutions of hydrofluoric acid, because stainless steels, titanium, zirconium, and tantalum are not adequate for this application. The most common alloy for handling aqueous hydrofluoric acid is wrought Monel 400. This alloy has excellent corrosion resistance in the absence of air or other oxidizing species; however, if oxygen is present, it is subject to accelerated intergranular attack, especially in the vapor phase.

Figure 9 shows the corrosion rate of three nickel alloys in the liquid phase (immersed conditions), and in the vapor phase where vapor condenses on the coupons (for these tests, the ingress of air to the testing kettles was not restricted).

Alloy 400 corrodes at high rates in the vapor phase, because of intergranular attack. The corrosion rate of alloy 400 is higher at the higher temperature, both for the liquid and vapor phases.

The corrosion rate of the B-3 alloy is lower in the vapor phase than in the liquid phase. Moreover, at the higher temperature, its corrosion rate in both phases is lower. In general, the corrosion rate of B-3 is not highly influenced by the temperature; therefore, the lower corrosion rate at the higher temperature can be the result of a lower availability of oxygen both in the liquid and vapor phases. The B-3 alloy is subject to pitting corrosion in HF environments, both in the liquid and vapor phases.

The C-2000 alloy showed the lowest corrosion rate in all the tested conditions. Laboratory testing has also shown that the corrosion rate of C-2000 in

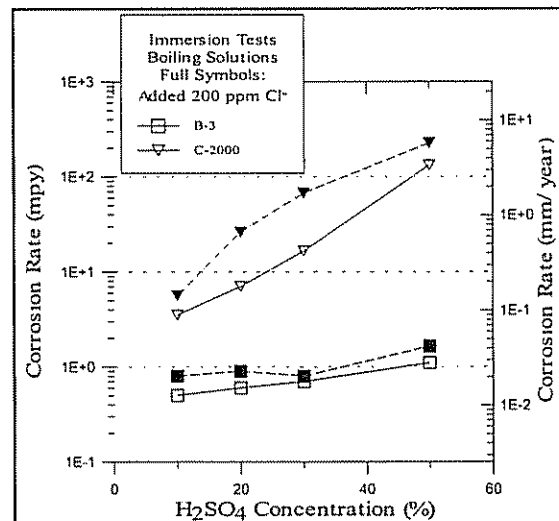


Fig 8 — This graph shows the effect of contamination by chlorides in sulfuric acid on alloys B-3 and C-2000

HE 00272

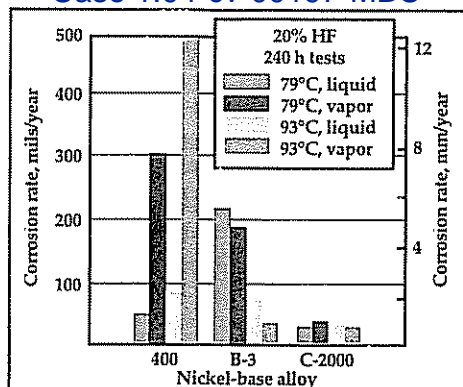


Fig. 9 — Corrosion of nickel alloys in hydrofluoric acid liquid and vapor.

the vapor phase is time dependent; that is, the rate decreases as the test duration increases. This is probably due to the gradual development of a protective film on the surface. The corrosion rates of alloys 400 and C-2000 in the liquid phase do not depend on the testing time.

Nickel-base alloys are susceptible to stress corrosion cracking in the presence of aqueous solutions of hydrofluoric acid. Not all nickel alloys are equally susceptible to SCC under the same conditions; that is, cracking is strongly dependent on several variables, such as alloy composition, temperature, presence of oxygen, and liquid vs. vapor phase.

Mixtures of hydrofluoric and nitric acid are typical in the metal industry for pickling processes. In a solution of 20% HNO_3 containing different amounts of hydrofluoric acid, the lowest corrosion rate corresponds to G-30, a Ni-Cr-Fe alloy containing 30% chromium. The high chromium content promotes the formation of a passive film in the oxidant nitric acid, and does not seem to be readily attacked by the hydrofluoric acid.

• *Other acids:* Phosphoric acid (H_3PO_4) is not highly corrosive to nickel alloys. Two distinct types of phosphoric acid are encountered in the industry. The pure (reagent grade) acid is made from elemental phosphorus, derived from phosphate rock. This is oxidized, then reacted with water. On the other hand, the preferred type of phosphoric acid in the agricultural industries is made by reacting phosphate rock with sulfuric acid. This contains several impurities, notably sulfuric acid, silica, and chloride and fluoride ions, which markedly affect the corrosion behavior of the acid. The levels of these impurities vary depending on the source of the rock, and different batches of this so-called "wet process" acid can vary considerably in their corrosivity.

The G-30 alloy is generally preferred to handle the "wet process" phosphoric acid. For pure phosphoric acid, Ni-Mo (B-3), Ni-Cr-Mo (C-276, C-2000) and Ni-Fe-Cr (G-30) alloys can function in up to 85% acid up to the boiling point.

The corrosion behavior of hydrobromic acid (HBr) is similar to that of hydrochloric acid; however, HBr is less aggressive. Therefore, when pure and hot, HBr is best handled by a Ni-Mo alloy such as the B-3 alloy. A Ni-Cr-Mo alloy such as C-2000 is versatile and is suitable for most applications containing HBr, especially in solutions contaminated

Table 3 — Nickel alloys for pure sulfuric acid*

Temperature	0 to 30% H_2SO_4	30% to 70% H_2SO_4	70% to 96% H_2SO_4
79°C to B. P. (175°F to B.P.)	Ni-Mo (B-3) Ni-Cr-Mo (C-2000) Ni-Fe-Cr (G-30) Ni-Cr-Si (D-205) Ni-Cu (400)	Ni-Mo (B-3)	Ni-Mo (B-3)
52°C to 79°C (125°F to 175°F)	Ni-Mo (B-3) Ni-Cr-Mo (C-2000) Ni-Fe-Cr (G-30) Ni-Cr-Si (D-205) Ni-Cu (400)	Ni-Mo (B-3) Ni-Cr-Mo (C-2000) Ni-Fe-Cr (G-30) Ni-Cr-Si (D-205) Ni-Cu (400)	Ni-Mo (B-3) Ni-Cr-Mo (C-2000)
RT to 52°C (RT to 125°F)	Ni-Mo (B-3) Ni-Cr-Mo (C-2000) Ni-Fe-Cr (G-30) Ni-Cr-Si (D-205) Ni-Cu (400)	Ni-Mo (B-3) Ni-Cr-Mo (C-2000) Ni-Fe-Cr (G-30) Ni-Cr-Si (D-205) Ni-Cu (400)	Ni-Mo (B-3) Ni-Cr-Mo (C-2000) Ni-Fe-Cr (G-30) Ni-Cr-Si (D-205)

*For each alloy group, one example is given

with oxidizing species.

Organic acids such as formic and acetic acids are not highly corrosive for nickel alloys. At temperatures higher than 100°C (212°F), the B-3 alloy (Ni-Mo) would offer the lowest corrosion rate.

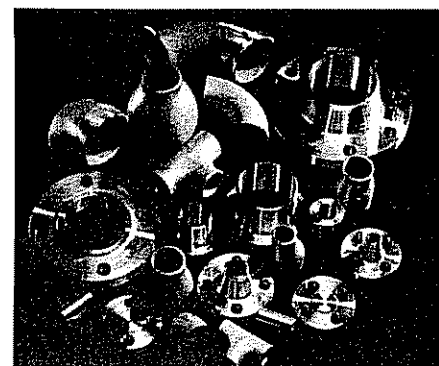
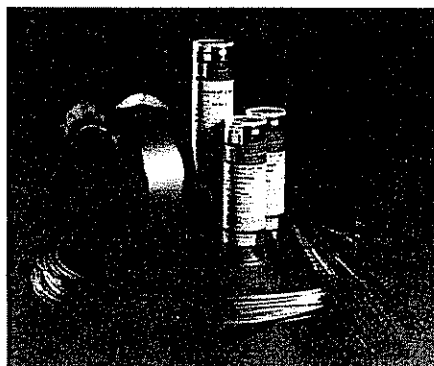
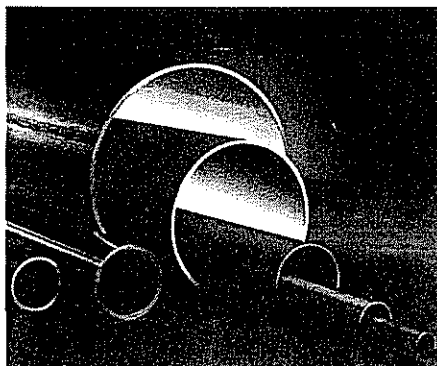
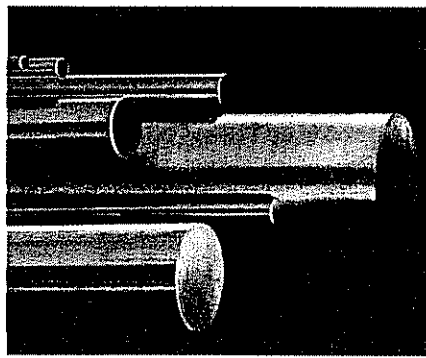
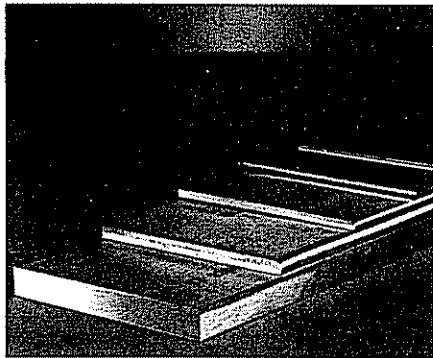
Nitric acid is a strong oxidizing acid which, besides zirconium and titanium alloys, can be handled with stainless steels or nickel alloys containing at least 15% chromium (other nickel alloys such as B-3, Ni-200, and Monel 400 cannot be used in nitric acid). For most purposes, a nickel alloy is not required to handle nitric acid; however, nickel alloys resist corrosion better than stainless steels in cases where the nitric acid is contaminated with chlorides.

Phosphoric acid is not highly corrosive to nickel alloys.

For more information: Dr. Raúl B. Rebak (765/456-6262), is a Corrosion Engineer; Paul Crook (765/456-6241) is Manager, Technical Services, at Haynes International, 1020 W. Park Ave., Kokomo, IN 46904; e-mail: rrebak@haynesintl.com; pcrook@haynesintl.com; Web site: www.haynesintl.com.

References

1. *Corrosion Engineering*, by M.G. Fontana: McGraw-Hill, Inc., New York, N.Y., 1986.
2. *Process Industries Corrosion — Theory and Practice*, by J.K. Nelson: NACE International, Houston, Texas, 1986.
3. *Corrosion Control in the Chemical Process Industries*, by C.P. Dillon: NACE International, Houston, Texas, 1994.
4. *Corrosion Resistance Tables*, by P.A. Schweitzer, (New York, NY; Marcel Dekker, Inc., 1995).
5. "Paper 382," by J.R. Crum, G.D. Smith, M.J. McNallan, and S. Hirnyj: Corrosion/99, NACE International, Houston, Texas, 1999.



For More Information, Contact:

Kokomo, Indiana 46904-9013
1020 W. Park Avenue
P.O. Box 9013
Tel: 765-456-6012
800-354-0806
FAX: 765-456-6905

Windsor, Connecticut 06095
430 Hayden Station Road
Tel: 860-688-7771
800-426-1963
FAX: 860-688-5550

England
Haynes International, Ltd.
P.O. Box 10
Parkhouse Street
Openshaw
Manchester, M11 2ER
Tel: 44-161-230-7777
FAX: 44-161-223-2412

Italy
Haynes International, S.R.L.
Viale Brianza, 8
20127 Milano
Tel: 39-2-2614-1331
FAX: 39-2-282-8273

Anaheim, California 92806
Stadium Plaza
1520 South Sinclair Street
Tel: 714-978-1775
800-531-0285
FAX: 714-978-1743

Houston, Texas 77041
The Northwood Industrial Park
12241 FM 529
Tel: 713-937-7597
800-231-4548
FAX: 713-937-4596

France
Haynes International, S A R L
Z1 des Bethunes
10 rue de Picardie
95310 Saint-Ouen l'Aumone
Tel: 33-1-34-48-3100
FAX: 33-1-30-37-8022

Switzerland
Nickel Contor AG
Hohlstrasse 534
CH-8048 Zurich
Tel: 41-1-434-7080
FAX: 41-1-431-8787

Arcadia, Louisiana 71001-9701
3786 Second Street
Tel: 318-263-9571
800-648-8823
FAX: 318-263-8088

Check out our website: www.haynesintl.com

All trademarks are owned by Haynes International, Inc.

HAYNES

International

A Tradition Of Innovation Spanning A Century

HE 00274

Corrosion behavior of nickel alloys in wet hydrofluoric acid*

Korrosionsverhalten von Nickellegierungen in feuchter Fluorwasserstoffsäure

R. B. Rebak**, J. R. Dillman, P. Crook and
C. V. V. Shawber

Wet hydrofluoric acid at concentrations below approximately 60% is highly corrosive to glass, reactive metals, carbon steel and stainless steels. Nickel alloys offer moderate corrosion resistance over a wide range of acid concentration and temperature. The corrosion behavior of eleven commercial alloys was quantified through laboratory testing. Variables that were studied included testing time, acid concentration, temperature, vapor and liquid phases and the presence of residual stresses. Results show that the corrosion rate of a Ni-Cu and a Ni-Cr-Mo-Cu alloy increased with the acid concentration and the temperature. However, both for increasing acid concentration and temperature, the corrosion rate of the Ni-Cu alloy increased faster than the corrosion rate of the Ni-Cr-Mo-Cu alloy, especially in the vapor phase. Even in unstressed coupons, nickel alloys showed internal penetration in presence of wet HF; the mode of this internal penetration varied from alloy to alloy. Considering all the studied variables that influence corrosion, the highest ranked material for wet HF service was a Ni-Cr-Mo-Cu alloy.

Feuchte Fluorwasserstoffsäure mit Konzentrationen unterhalb von etwa 60% ist hochkorrosiv für Glas, reaktive Metalle, Kohlenstoffstahl sowie nichtrostenden Stahl. Nickellegierungen bieten einen moderaten Korrosionswiderstand über einen weiten Bereich an Säurekonzentrationen und Temperatur. Das Korrosionsverhalten von 11 kommerziellen Legierungen wurde mittels Laborversuchen quantifiziert. Die untersuchten Variablen beinhalteten die Versuchszeit, Säurekonzentration, Temperatur, Dampf- und Flüssigphasen und die Anwesenheit von Restspannungen. Die Ergebnisse zeigen, dass die Korrosionsgeschwindigkeit von Ni-Cu- und Ni-Cr-Mo-Cu-Legierungen mit der Säurekonzentration und der Temperatur zunahm. Sowohl für steigende Säurekonzentration als auch für steigende Temperatur nahm jedoch die Korrosionsgeschwindigkeit der Ni-Cu-Legierung schneller zu als die Korrosionsgeschwindigkeit der Ni-Cr-Mo-Cu-Legierung, besonders in der Dampfphase. Sogar in den ungespannten Proben zeigten die Nickellegierungen interne Penetration in Anwesenheit von feuchter HF; der Modus dieser internen Penetration variierte von Legierung zu Legierung. Unter Berücksichtigung aller untersuchten Variablen, die die Korrosion beeinflussen, war eine Ni-Cr-Mo-Cu-Legierung der am höchsten eingestufte Werkstoff für den Einsatz in feuchter HF.

1 Introduction

Hydrofluoric acid is a water solution of hydrogen fluoride (HF). Hydrofluoric acid is used widely in diverse types of industrial applications; traditionally, it is used in pickling solutions in the metal industry and as an etching agent in the industry of glass. In recent years, hydrofluoric acid has extensively been used in the manufacture of semiconductors and microelectronics during the wet chemical cleaning of silicon wafers. Although hydrofluoric acid is chemically classified as an acid weaker than, for example, sulfuric or hydrochloric acids, it is extremely corrosive.

The choices of engineering alloys to handle hydrofluoric acid are limited. Glass and the reactive metals such as titanium, zirconium and tantalum are readily attacked by hydrofluoric acid. Hydrofluoric acid at concentrations higher than 64% can be handled with carbon steel; however, at lower concentrations, this acid attacks the steel rapidly [1, 2]. Nickel alloys are a popular choice for wet hydrofluoric acid [3]. For example, a wrought Ni-Cu material (alloy 400) has been used in most of the applications of hydrofluoric acid even though its corrosion resistance is greatly diminished by the presence of air or oxidizing salts [1–3].

Recent publications dealing with the laboratory testing and/or alloy performance in hydrofluoric acid environments are scarce [4–7]. Laboratory characterization of nickel based alloys in hydrofluoric acid has not been as extensive as it has with other common, inorganic acids. This is largely because tests using hydrofluoric acid can not be run in standard laboratory equipment and because of the dangerous nature of hydrofluoric acid. Moreover, short-term weight loss laboratory corrosion tests in hydrofluoric acid can be frustrating since the results are not as highly reproducible as in the case of other acids such as sulfuric or hydrochloric.

The aim of the present work was to study the corrosion behavior of several engineering alloys which might be used in the handling of hydrofluoric acid. Variables that were studied

* Paper presented atACHEMA 2000, Frankfurt am Main, Germany, May 22–27, 2000.

** R. B. Rebak
Haynes International Inc., Engineering and Technology
P.O. Box 9013, Kokomo IN 46904-9013 (USA)
now with: Swagelok
6060 Cochran Rd., Solon, OH 44139 (USA)

J. R. Dillman, P. Crook, C. V. V. Shawber
Haynes International Inc., Engineering and Technology
P.O. Box 9013, Kokomo IN 46904-9013 (USA)

Table 1. Approximate chemical composition of the tested alloys (alloys are arranged in alphabetical order by UNS number)

Tabelle 1. Ungefähre chemische Zusammensetzung der untersuchten Legierungen (die Legierungen sind in der Reihenfolge der UNS Nummerierung aufgelistet)

Alloy	UNS	Approximate chemical composition in weight %
MONEL [®] 400	N04400	67Ni-31.5Cu-1.2Fe
HASTELLOY [®] C-22 [®]	N06022	59Ni-22Cr-13Mo-3W-3Fe
HASTELLOY G-30 [®]	N06030	44Ni-30Cr-15Fe-5Mo-4Co-2.5W-2Cu
HASTELLOY C-2000 [®]	N06200	59Ni-23Cr-16Mo-1.5Cu
INCONEL [®] 600	N06600	76Ni-15.5Cr-8Fe
HAYNES [®] 625	N06625	62Ni-21Cr-9Mo-5Fe-3.7(Cb + Ta)
CARPENTER 20Cb-3 [®]	N08020	37Fe-34Ni-20Cr-3.5Cu-2.5Mo
HAYNES 242 [™]	N10242	65Ni-25Mo-8Cr
HASTELLOY C-276	N10276	57Ni-16Cr-16Mo-4W
HASTELLOY B-3 [®]	N10675	65Ni-28.5Mo-1.5Cr-1.5Fe
AVESTA 254SMO [®]	S31254	56Fe-20Cr-18Ni-6.1Mo-0.2N

HASTELLOY, HAYNES, C-22, G-30, C-2000, 242 and B-3 are registered trademarks of Haynes International Inc., INCONEL and MON-EL are registered trademarks of Special Metals. 20Cb-3 is a registered trademark of Carpenter Technologies and 254SMO is a registered trademark of Avesta Sheffield.

included testing time, acid concentration, temperature, vapor vs. liquid phase and presence of residual stresses.

2 Experimental procedures

Most of the studied engineering alloys were nickel based (Table 1). Two types of coupons were used for laboratory tests: (1) Plain or unstressed coupons to study the effect of time, acid concentration and temperature and (2) U-bend coupons to study the effect of residual stresses. The coupons were prepared using 1/8 inch thick sheets (3.175 mm). Testing procedures for coupon preparation, cleaning and assessment of corrosion rate were conducted according to ASTM standards. All the corrosion rates reported in this paper were measured by weight loss. Tests were carried out in kettles made of nickel alloy N10276 and lined with PTFE (polytetrafluorethylene). Some coupons were immersed in the aqueous acid solutions (reported as liquid phase or L) and others were suspended through a drilled hole by PTFE threads above the liquid level (vapor phase or V). The kettles were open to the atmosphere of the laboratory scrubber through a small orifice at the top of a PTFE lined condenser, that is, the ingress of air into the kettles was not restricted. Tests were conducted at the free potential and the evolution of the corrosion potential of the coupons during the tests was not monitored. The reported acid concentrations and testing temperatures correspond to the conditions of the liquid solution. After the tests were complete, the coupons were studied in a SEM (scanning electron microscope) and/or were metallographically sectioned, to determine the depth and mode of internal penetration or crack propagation. In the case of the stressed coupons, the crack propagation rate was calculated by dividing the longest crack by the total testing time; that is, the effect of induction time on crack propagation was not considered.

3 Results and discussion

3.1 Effect of testing time

It has been reported in the literature that the resistance to corrosion of engineering alloys in wet HF service was a consequence of the formation of insoluble fluoride salts on the

surface of these alloys [1, 2, 4]. Ciaraldi et al. reported that the corrosion rate of C-276 alloy in the vapor phase of 0.5% HF at 93 °C decreased as the time increased between 2 days and 14 days [4]. They attributed this behavior to the formation of partially protective fluoride films [4]. Fig. 1 shows the corrosion rates of alloy 400 in 20% HF at 79 °C and 93 °C as a function of testing time. The corrosion rate of alloy 400 in the vapor phase was not a simple function of the testing time while in the liquid phase the corrosion rate slowly increased as the testing time increased (Fig. 1).

Fig. 2 shows the corrosion rates of C-2000 alloy in 20% HF at 79 °C and 93 °C as a function of testing time. In the vapor phase, the corrosion rate of C-2000 alloy decreased as the testing time increased. In the liquid phase, the corrosion rate was not a strong function of the testing time (Fig. 2). Figs. 1 and 2 also show that the corrosion rate for both alloys was higher in the vapor phase than in the liquid phase, probably influenced by the higher availability of oxygen in the vapor phase. After

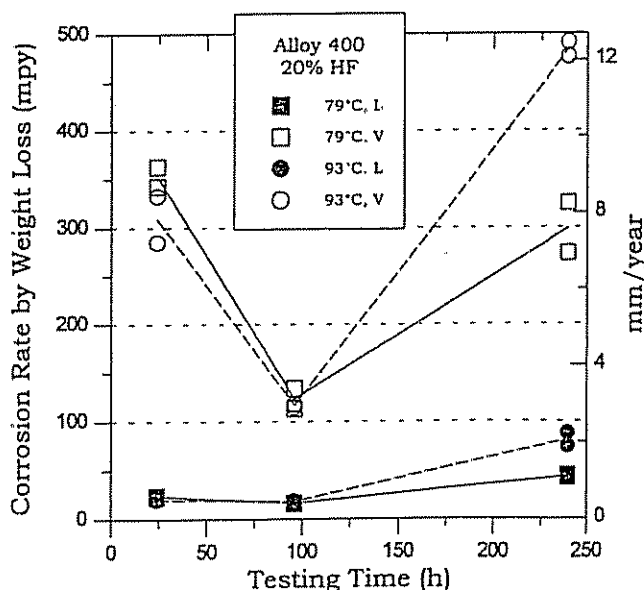


Fig. 1. Corrosion rate of alloy 400 as a function of testing time
Abb. 1. Korrosionsgeschwindigkeit der Legierung 400 als Funktion der Versuchszeit

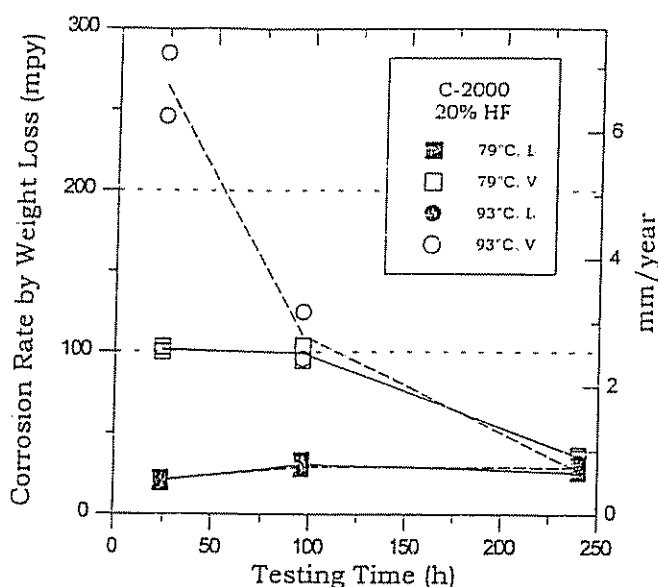


Fig. 2. Corrosion rate of C-2000 alloy as a function of testing time
Abb. 2. Korrosionsgeschwindigkeit der Legierung C-2000 als Funktion der Versuchszeit

240 h of testing, the corrosion rate of alloy 400 was higher than the corrosion rate of C-2000 alloy, both in the liquid and vapor phases (Figs. 1 and 2). Observation of the metallic coupons after testing showed that, both at 79 °C and 93 °C, alloy 400 suffered grain boundary etching in the liquid phase and deep extended intergranular attack in the vapor phase, while C-2000 alloy suffered uniform corrosion both in the liquid and vapor phases. Some crystalline green corrosion products formed on the C-2000 alloy coupon exposed to the vapor phase. X-ray diffraction determined that this crystalline corrosion product was $\text{NiCrF}_5 \cdot 7\text{H}_2\text{O}$. In the alloy 400 coupons exposed to the liquid phase the intergranular attack was only 25 μm deep both at 79 °C and 93 °C. In the vapor phase, the intergranular attack was approximately 350–370 μm deep both at 79 °C and 93 °C. In the C-2000 alloy coupons, after 240 h of testing, a lace-like penetration was observed both for the vapor and liquid phases. At 79 °C the penetration was approximately 100 μm in the liquid phase and approximately 40 μm in the vapor phase. At 93 °C, the lace-like penetration in C-2000 alloy was approximately 220 μm in the liquid phase and approximately 65 μm in the vapor phase. More details of the physical appearance and depth of internal penetration in the coupons of alloy 400 and C-2000 alloy are given in Table 2.

Table 2. Effect of temperature on the corrosion behavior of unstressed coupons. Alloys 400 and C-2000 exposed in 20% HF for 240 h
Tabelle 2. Einfluss der Temperatur auf das Korrosionsverhalten von ungespannten Coupons. Legierungen 400 und C-2000 in 20% HF 240 h ausgelagert

Alloy	T °C	Exp.	Average corrosion rate by weight loss in mpy (mm/year)	Rolled face internal penetration in mils (μm)	Observations
Alloy 400	38	L	10.5 (0.27)	0.5 (13)	Uniform corrosion. Light gray sample. Depth of roughness reported as internal penetration.
		V	45.15 (1.15)	9.5 (241)	IGA. Cracks at the perforated hole and from the edges.
	52	L	18.05 (0.46)	0.5 (13)	Uniform corrosion. Shiny original color metallic sample. IG etching. Depth of roughness reported as internal penetration.
		V	130.5 (3.31)	24.5 (622)	Severe IGA. Some cracks from edges. Light blue corrosion products.
	66	L	8.5 (0.22)	0.5 (13)	Uniform corrosion. Original metallic color.
		V	69.45 (1.76)	7.5 (191)	IGA. Cracks along drilled hole.
	79	L	43.35 (1.10)	1 (25)	Uneven corrosion. Grain boundary etching.
		V	299 (7.59)	14 (356)	Deep IGA. Dark gray and green color.
	93	L	80.95 (2.06)	1 (25)	Uneven corrosion. Grain boundary etching. Bright original metallic color.
		V	483.5 (12.3)	14.5 (368)	Deep IGA and uneven corrosion.
C-2000	38	L	8.3 (0.21)	0.5 (13)	Uniform corrosion. Bright original color metallic sample.
		V	7.55 (0.19)	9.5 (241)	Uniform corrosion. Bright original color metallic sample. Traces of Cu on surface.
	52	L	18.8 (0.48)	0.5 (13)	Uniform corrosion. Light gray sample. Layers of Cu on surface.
		V	14.35 (0.36)	0.5 (13)	Uniform corrosion. Small amount of green corrosion product.
	66	L	33.5 (0.85)	1.5 (38)	Uneven general corrosion. Delamination type corrosion. Small dealloyed layer. Sample plated with Cu and probably Ni.
		V	33.45 (0.85)	0.5 (13)	Minimal corrosion. Sample plated with Ni and traces of Cu. Micropits on edges of sample.
	79	L	26.25 (0.67)	4 (102)	Fine lace or shadow-like penetration. Light Cu color.
		V	36.1 (0.92)	1.5 (38)	Shallow isolated lace penetration. Blue stains of surface.
	93	L	29.25 (0.74)	8.5 (216)	Fine lace-like penetration. Isolated light gray spots on surface.
		V	27.3 (0.69)	2.5 (64)	Isolated lace-like penetration. Metallic color. Isolated spots of corrosion. Green corrosion products.

The behavior of alloys C-276 and 600 (Table 1) in 20% HF at 79 °C was similar to that of C-2000 alloy, that is, they showed a higher corrosion rate in the vapor phase than in the liquid phase and, in the vapor phase, the corrosion rate continuously decreased as the testing time increased while in the liquid phase there was little influence of the testing time. A metallographic cross section of the specimens after 240 h of testing showed that alloy 600 suffered intergranular attack in the liquid phase with a final corrosion rate of approximately 1 mm/year; cracking, internal voids and intergranular attack occurred in the vapor phase with a final corrosion rate of approximately 2–3 mm/year. In the liquid phase, the deepest internal attack was approximately 100 μ m and in the vapor phase the thin transgranular cracks were up to 500 μ m deep. After 240 h of testing in 20% HF at 79 °C, alloy C-276 suffered lace-like internal penetration which was approximately 180 μ m deep in the coupon exposed to the liquid phase and approximately 90 μ m in the coupon exposed to the vapor phase. In both the liquid and vapor phases, the final corrosion rate of alloy C-276 was approximately 1–2 mm/year.

For alloys 254SMO and G-30, the corrosion rates in 20% HF at 79 °C were higher in the liquid phase than in the vapor phase and they were not a strong function of the testing time. The coupons of 254SMO that were exposed to the liquid phase showed severe uneven general corrosion with an average corrosion rate of approximately 50–60 mm/year. In the vapor phase, the corrosion rate of 254SMO was in the order of 10 mm/year. For G-30 alloy, the corrosion rate in the liquid phase was approximately 4–5 mm/year and in the vapor phase approximately 1 mm/year. After 240 h of testing, the G-30 alloy coupons showed an internal penetration that consisted of intergranular attack and voids in the liquid phase approximately 600 μ m deep, and in the vapor phase an apparent dealloyed layer approximately 90 μ m deep.

For alloy 20Cb-3 in 20% HF at 79 °C the corrosion rate in the vapor phase decreased as the testing time increased from approximately 5 mm/year for 24 h testing to approximately 2 mm/year for 240 h testing. In the liquid phase, the dependence of the corrosion rate with testing time was erratic. The average corrosion rate was approximately 2–3 mm/year. After 240 h of testing, the coupons exposed to the liquid phase showed a lace-type internal penetration as well as internal voids and intergranular attack. Some of these voids contained small amounts of metallic copper in them. The deepest attack was approximately 190 μ m. In the vapor phase, the coupons suffered intergranular attack and thin deep transgranular cracks. These cracks were up to 940 μ m deep.

For B-3 alloy in 20% HF, the corrosion rate was in general higher in the vapor phase than in the liquid phase both at 79 °C and 93 °C at least for the two shorter periods. At both temperatures, the corrosion rate in the vapor phase was approximately 4 mm/year and in the liquid phase was approximately 2 mm/year. After 240 h of testing, the samples appeared dark gray with uneven general corrosion. This uneven or serrated corrosion penetration was approximately 100 μ m both for the liquid and vapor phases and at both temperatures.

In the majority of the tested coupons (especially in alloys such as 600, B-3 and 20Cb-3) the dissolution rate, grain drop and internal attack in the direction across the thickness of the coupon (perpendicular to the rolling direction) was higher than the attack from the rolled face. Moreover, this deeper lamination attack seemed to follow the pattern associated to the parallel lines or directions produced during rolling. The internal penetrations reported in Table 2 and in Figs. 7 and 9 correspond to the penetration from the rolled face of the coupon

because this is the more likely front or side that could be found in practical engineering applications.

3.2 Effect of acid concentration

Figs. 3 and 4 show the effect of the acid concentration on the average corrosion rate by weight loss of alloys 400 and C-2000 at 79 °C in the liquid and vapor phases, respectively. In the liquid phase (Fig. 3) the corrosion rate of alloy 400 increased approximately two times as the acid concentration changed from 1% to 20%. The corrosion rate of C-2000 alloy

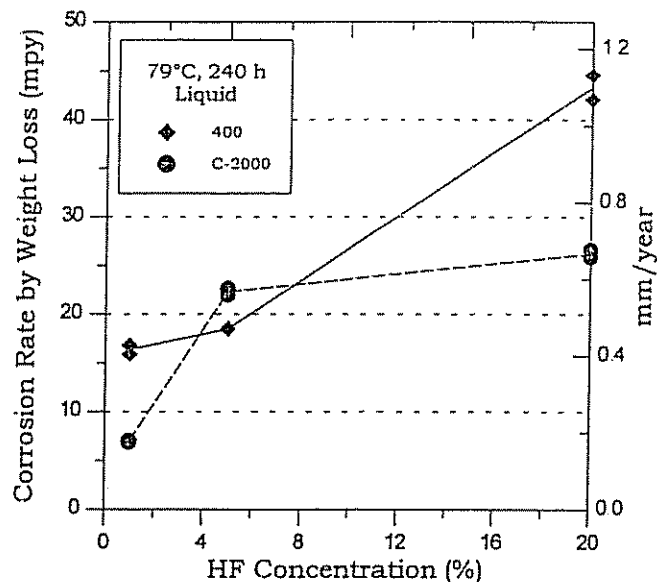


Fig. 3. Effect of acid concentration on the corrosion rate in the liquid phase

Abb. 3. Einfluss der Säurekonzentration auf die Korrosionsgeschwindigkeit in der flüssigen Phase

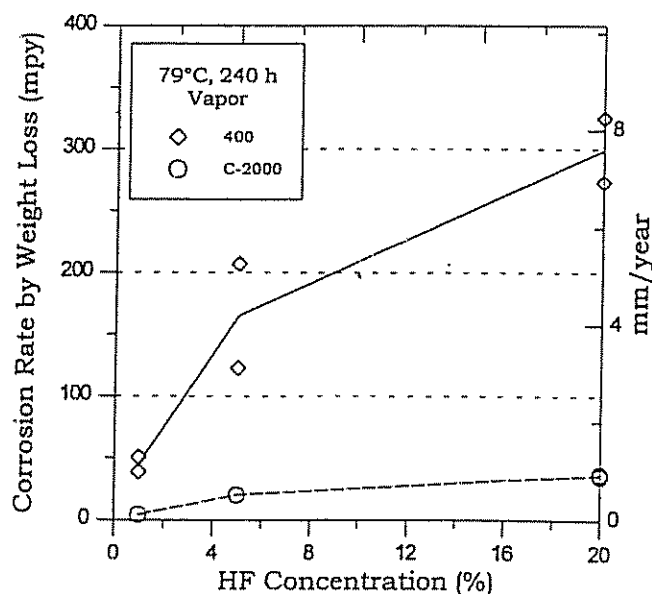


Fig. 4. Effect of acid concentration on the corrosion rate in the vapor phase

Abb. 4. Einfluss der Säurekonzentration auf die Korrosionsgeschwindigkeit in der Dampfphase

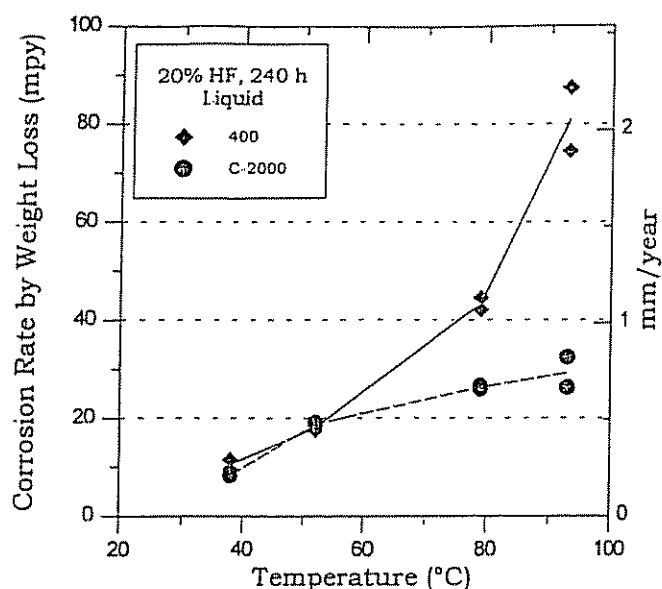


Fig. 5. Effect of the temperature on the corrosion rate in the liquid phase

Abb. 5. Einfluss der Temperatur auf die Korrosionsgeschwindigkeit in der flüssigen Phase

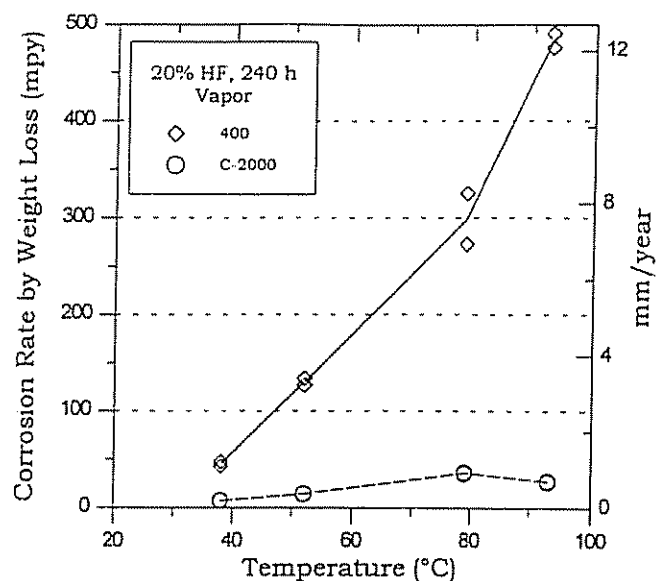


Fig. 6. Effect of the temperature on the corrosion rate in the vapor phase

Abb. 6. Einfluss der Temperatur auf die Korrosionsgeschwindigkeit in der Dampfphase

was less affected by the acid concentration between 5% and 20%. In the vapor phase, the corrosion rate of alloy 400 increased from approximately 1 mm/year at 1% HF to 8 mm/year at 20% HF. On the other hand, the corrosion rate of C-2000 alloy in the vapor phase remained below 1 mm/year for the entire range of acid concentration investigated (Fig. 4).

3.3 Effect of temperature

Figs. 5 and 6 and Table 2 show the effect of the temperature on the average corrosion rate of alloys 400 and C-2000 in 20% HF in the liquid and vapor phases, respectively. In the liquid phase (Fig. 5) the corrosion rates by weight loss of alloys 400 and C-2000 were similar at 38 °C and 52 °C. However, at higher temperatures the corrosion rate of alloy 400 increased faster, as the temperature increased, than the corrosion rate for C-2000 alloy. In the vapor phase, the corrosion rate of alloy 400 was higher than the corrosion rate of C-2000 alloy, especially at the higher temperatures (Fig. 6). Fig. 7 and Table 2 show the internal penetration of the coupons after they were exposed to 20% HF for 240 h (this penetration does not account for the material that was dissolved by general corrosion). Fig. 7 shows that alloy 400 had a high internal penetration (intergranular attack) in the vapor phase while in the liquid phase the internal penetration was small. The opposite behavior was observed for C-2000 alloy; that is, the internal attack (lace-like penetration) was higher in the liquid phase than in the vapor phase. Moreover, the internal penetration seemed to have higher thermal activation in C-2000 alloy than in alloy 400.

3.4 Effect of alloy composition

Fig. 8 shows the average corrosion rate by weight loss in the liquid and vapor phases of nine engineering alloys in 20% HF

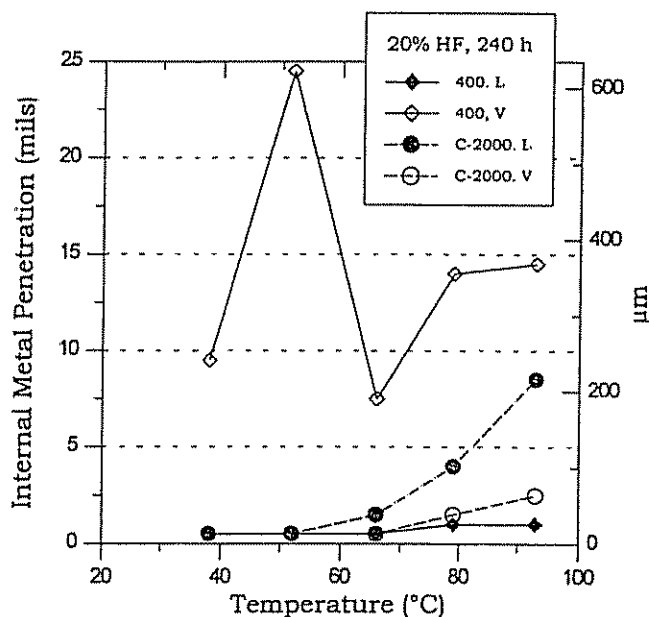


Fig. 7. Effect of the temperature on the internal penetration of alloys 400 and C-2000

Abb. 7. Einfluss der Temperatur auf die interne Penetration der Legierungen 400 und C-2000

at 79 °C. There are seven nickel base alloys and two iron base alloys (stainless steels). Ni-Cu (400) and Ni-Mo (B-3) alloys have high corrosion rate in the vapor phase. These alloys do not contain chromium (Table 1) which seems to be a beneficial alloying element for the vapor phase where there existed a higher availability of oxygen. Alloys that contained a relatively high amount of iron such G-30 (Table 1) had a higher corrosion rate in the liquid phase. The nickel alloy that had the lowest corrosion rate under the tested conditions both in the

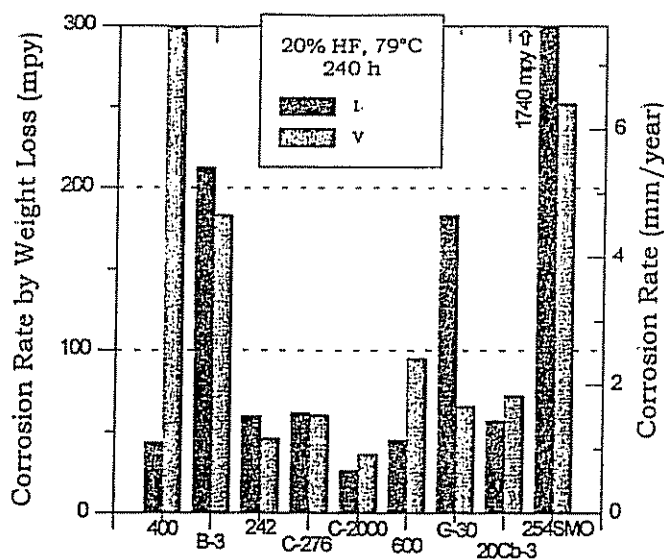


Fig. 8. Corrosion rate by weight loss of engineering alloys in wet HF

Abb. 8. Mittels Gewichtsverlust ermittelte Korrosionsgeschwindigkeit von technischen Legierungen in feuchter HF

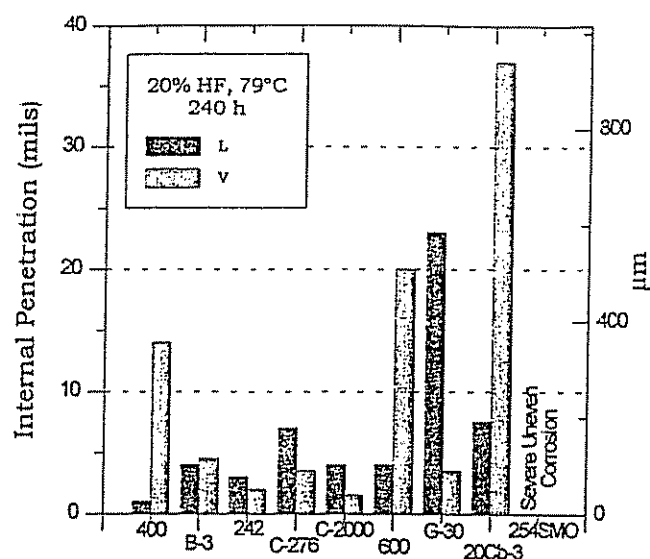


Fig. 9. Internal penetration in engineering alloys when exposed to wet HF

Abb. 9. Interne Penetration von technischen Legierungen, die feuchter HF ausgesetzt waren

liquid and vapor phases was C-2000 alloy. Of the stainless steels, alloy 20Cb-3 had a lower corrosion rate than alloy 254SMO probably because the former had a higher amount of nickel and also contained copper which seems to be a beneficial alloying element for wet HF service.

Fig. 9 shows the internal penetration in the coupons that were exposed for 240 h in 20% HF in the liquid and vapor phases. This internal penetration could be: (1) Intergranular attack such as for alloy 400 in the vapor phase and alloy 600 in the liquid and vapor phases; (2) Lace-like penetration such as for C-276 and C-2000 in the liquid and vapor phases; (3) Uneven serrated penetration such as for B-3 alloy; (4) Wasp nest-like penetration such as for alloy 242; (5) Deep thin transgranular cracks such as for alloy 600 and 20Cb-3 in the vapor phase; (6) Voids such as for alloy 600 in the vapor phase and G-30 and 20Cb-3 in the liquid phase; (7) Dealloying such as for G-30 in the vapor phase. The ranking of alloys from Fig. 9 (which measures the internal penetration) is similar to the ranking of alloys from Fig. 8 (which measures the corrosion rate by weight loss). Again, it appears that C-2000 alloy offers a good relative performance in wet HF service.

3.5 Unique corrosive attack of wet HF

Sulfuric and hydrochloric acids tend to corrode metallic alloys in a uniform way, producing an even thinning. The total weight loss (or corrosion rate) is different for different conditions of temperature or alloy composition, for example, but the thinning of the coupons is rather uniform. On the other hand, in hydrofluoric acid, the tested coupons seemed more attacked in certain areas than in others and this uneven mode of corrosion was highly dependent on the composition of the alloy, temperature, acid concentration, if the wet acid is in the liquid or vapor state, and on the level of oxygen that was present. It was commonly observed that, in the attacked areas, corrosion did not advance by regular thinning of the material but the attack progressed underneath the exposed surface of the alloy

leaving behind uncorroded material. This behavior was reported before by Pawel for alloys including alloys 600, 400 and C-276 [5]. Hydrofluoric acid also tended to dissolve and reprecipitate some elements of the alloy preferentially. Sometimes, corroded coupons appeared to have been plated with either nickel or copper or both. The color appearance of the coupons was different for each alloy under each set of test conditions and, even for the same alloy, under different test conditions. The mode of internal attack was also different for each alloy. For the unstressed coupons several modes of internal attack were identified for the studied nickel alloys. These modes of attack included uneven corrosion or serration of the surface, dealloying, intergranular attack, lace-like or cobweb penetration, internal voids, pits or cavities, wasp nest appearance and long and thin transgranular cracks. For each alloy, the mode of internal attack did not depend strongly on external variables; however, the extent of this attack was different depending, for example, on temperature, vapor versus liquid phases, etc.

The corrosion rate of alloys in hydrofluoric acid depended on the testing time, especially in the vapor phase. For example, in the vapor phase, the corrosion rate of nickel alloys containing chromium (e.g. C-2000) decreased as the testing time increased. For these same alloys, there was little influence of the testing time on the corrosion rate in the liquid phase. For alloys that did not contain chromium (e.g. B-3, alloy 400) the corrosion rate in the vapor phase was erratic as the time increased; however, in the liquid phase, the corrosion rate tended to slightly increase as the testing time increased. The corrosion rate depended on the testing time probably because of the formation of pseudo passivating surface films and/or the subsequent breakdown of these films.

3.6 Effect of residual stresses

The susceptibility of five nickel alloys to stress corrosion cracking or stress assisted internal penetration in wet HF

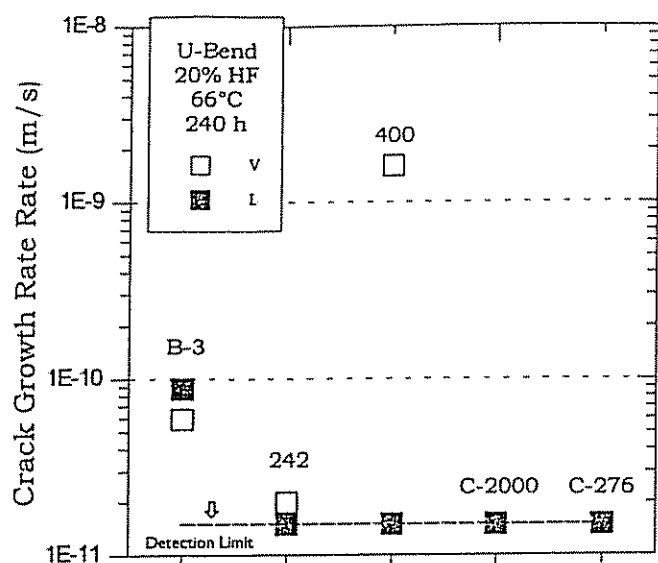


Fig. 10. SCC susceptibility of nickel alloys in 20% HF at 66 °C. For C-2000 and C-276 alloys the symbols for the L and V phases overlap (no detected cracking)

Abb. 10. SCC-Empfindlichkeit der Nickellegierungen in 22% HF bei 66 °C. Für die Legierungen C-2000 und C-276 überschneiden sich die Symbole für die L und V Phasen (Risse wurde nicht festgestellt)

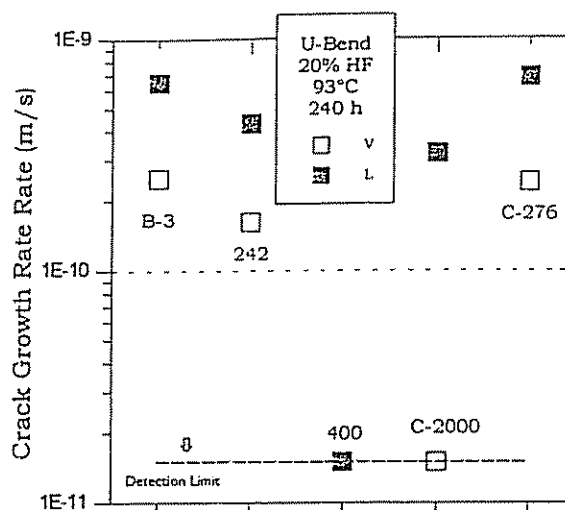


Fig. 11. SCC susceptibility of nickel alloys in 20% HF at 93 °C. For alloy 400, the symbols for the L and V phases overlap (no detected cracking)

Abb. 11. SCC-Empfindlichkeit der Nickellegierungen in 22% HF bei 93 °C. Für die Legierung 400 überschneiden sich die Symbole für die L und V Phasen (Risse wurde nicht festgestellt)

was determined using U-bend specimens. Data on average crack propagation and corrosion rate by weight loss are given in Table 3. Figs. 10 and 11 show the average crack or penetration in specimens that were exposed for 240 h to 20% HF at 66 °C and 93 °C, respectively. At 66 °C, the highest penetration (intergranular cracking) corresponded to alloy 400, while, for example, alloy C-276 was not susceptible to cracking (In Fig. 10, the L and V symbols for C-276 and C-2000 alloys overlap). These findings confirm previous published results. Pawel reported that U-bend specimens of alloy 400 cracked after a 48 h test in the vapor phase of 10% HF at 24 °C [5]. Pawel also reported that C-276 alloy was free of cracking after the same exposure time even in 24% HF at 76 °C [5]. At 93 °C (Fig. 11), the roles appeared reversed, that is, alloy 400 was free from cracking (L and V symbols overlap) while C-276 alloy was susceptible to cracking. In general, the liquid phase was more aggressive than the vapor phase for C-276 and C-2000 alloys and the vapor phase was more aggressive than the liquid phase for alloy 400. Average corrosion rate by weight loss (Table 3) shows again that the corrosion of C-2000 was consistently low both in the liquid and vapor phases while the corrosion rate of alloy 400 was high in the vapor phase.

In another set of experiments, U-bend specimens of five engineering alloys were exposed to the liquid and vapor spaces of 20% HF at 93 °C for 336 h (the acid solution was changed after 168 h exposure). These alloys were: C-22, C-2000, 600, 625 and 20Cb-3. Alloy 20Cb-3 was exposed for only one period of 168 h since it had severe transgranular (TG) cracking after this testing time. In the liquid phase the average TG crack growth rate in alloy 20Cb-3 was 5.3×10^{-9} m/s and in the vapor phase was 2.3×10^{-9} m/s. Alloy 20Cb-3 also exhibited internal penetration in form of voids that seemed to be aligned following rolling planes in the U-bend specimen. The average corrosion rate by weight loss of the 20Cb-3 U-bend specimens was 134 mpy (3.4 mm/

year) in the liquid phase and 205 mpy (5.2 mm/year) in the vapor phase. The U-bend specimen of alloy 20Cb-3 that was exposed to the vapor phase had small amounts of crystalline green corrosion product as well as deposited metallic copper. Fig. 8 shows that the average corrosion rate by weight loss of alloy 20Cb-3 at 79 °C was comparable to the corrosion rate of some nickel alloys; however, alloy 20Cb-3 had a higher susceptibility to stress corrosion cracking. The average penetration rate in alloy 600 U-bend specimens after 336 h testing was approximately 4×10^{-10} m/s both in the liquid and vapor phases. The mode of internal penetration was TG cracks, IGA and voids. The average corrosion rate by weight loss of the alloy 600 U-bend specimens was 174 mpy (4.4 mm/year) in the liquid phase and 136 mpy (3.5 mm/year) in the vapor phase. Alloy 625 had severe uneven general corrosion but did not exhibit internal penetration. The average corrosion rate by weight loss of the alloy 625 U-bend specimens was 1890 mpy (48 mm/year) in the liquid phase and 442 mpy (11 mm/year) in the vapor phase. After 336 h, the average TG cracking rate in C-22 alloy was 6.3×10^{-10} m/s in the liquid phase and 3.4×10^{-10} m/s in the vapor phase. The average corrosion rate by weight loss of the C-22 alloy U-bend specimens was 54.9 mpy (1.4 mm/year) in the liquid phase and 75.3 mpy (1.9 mm/year) in the vapor phase. Similarly, after 336 h test, the average TG cracking rate in C-2000 alloy was 4.2×10^{-10} m/s in the liquid phase and 2.9×10^{-10} m/s in the vapor phase. The average corrosion rate by weight loss of the C-2000 alloy U-bend specimens was 16.2 mpy (0.41 mm/year) in the liquid phase and 15.1 mpy (0.38 mm/year) in the vapor phase. C-2000 alloy also exhibited internal penetration in the form of voids. The TG cracking in C-22 alloy had more branching than the TG cracking in C-2000 alloy. The cracks in C-2000 alloy were particularly thin, what made them almost indiscernible even in the metallographically polished coupons. After the tests, the U-bend specimens of both C-22 and C-2000 alloy that were exposed to the vapor phase had isolated spots of green crystalline corrosion products on their surface. The C-2000 alloy had also metallic

Table 3. Stress corrosion cracking of nickel alloys using U-bend specimens

Tabelle 3. Spannungsrisskorrosion von Nickellegierungen mittels Biegeproben

Alloy	U-bend specimens in 20% HF, 240 h	Average general corrosion rate (weight loss), mpy (mm/year)	Average crack or preferential pene- tration rate, m/s	Observations
400	66 °C, L	6.5 (0.165)	$< 1.5 \times 10^{-11}$	Shiny original metallic. Shallow IGA.
	66 °C, V	255 (6.48)	1.6×10^{-9}	Black. Severe IGA, fissures
	79 °C, L	$< 0.1 (< 0.003)$	$< 1.5 \times 10^{-11}$	Intense Cu color. 0.05 mm thick layer of Cu on surface
	79 °C, V	267 (6.78)	1.5×10^{-10}	IGA.
	93 °C, L	$< 0.1 (< 0.003)$	$< 1.5 \times 10^{-11}$	Cu color. Crystalline lumps of Cu on the surface.
	93 °C, V	150 (3.81)	$< 1.5 \times 10^{-11}$	Ni plated appearance. Shallow IGA.
C-276	66 °C, L	116 (2.95)	$< 1.5 \times 10^{-11}$	Ni plated appearance. Uniform corrosion.
	66 °C, V	42.6 (1.08)	$< 1.5 \times 10^{-11}$	Small corrosion pits. Green corrosion product ($\text{NiCrF}_5 \cdot 7\text{H}_2\text{O}$)
	79 °C, L	239 (6.07)	1.2×10^{-10}	Dark gray sample. Uneven general corrosion especially in stressed areas. Crevice corrosion.
	79 °C, V	94 (2.39)	3.0×10^{-11}	Light gray sample. Uneven penetration. Small corrosion pits
	93 °C, L	28.8 (0.732)	6.8×10^{-10}	Green corrosion product ($\text{NiCrF}_5 \cdot 7\text{H}_2\text{O}$). Ni plated appearance. SCC, pitting and crevice corrosion.
	93 °C, V	31.4 (0.798)	2.4×10^{-10}	Black corrosion products in creviced area. Compressive side attack. Ni plated appearance. SCC. Green corrosion products ($\text{NiCrF}_5 \cdot 7\text{H}_2\text{O}$)
C-2000	66 °C, L	33.7 (0.856)	$< 1.5 \times 10^{-11}$	Dark gray color. Shallow sponge like surface appearance.
	66 °C, V	34 (0.864)	$< 1.5 \times 10^{-11}$	Ni plated appearance. Uniform corrosion. Green corrosion products ($\text{NiCrF}_5 \cdot 7\text{H}_2\text{O}$)
	79 °C, L	16.2 (0.411)	1.3×10^{-10}	Light Cu color. Small crevice corrosion. Thin band of forest like penetration.
	79 °C, V	14.3 (0.363)	5.9×10^{-11}	Bluish color with dotted areas of Cu color. Small crevice corrosion. Thin hair like penetration.
	93 °C, L	13.9 (0.353)	3.2×10^{-10}	SCC. In compressive side cracks parallel to surface.
	93 °C, V	14.8 (0.376)	$< 1.5 \times 10^{-11}$	Ni plated appearance. Small crevice corrosion. $< 1 \mu\text{m}$ Cu granules on surface.
242	66 °C, L	71.6 (1.82)	$< 1.5 \times 10^{-11}$	Light gray color. Sponge like surface (metal flaking). Crevice corrosion.
	66 °C, V	26.9 (0.683)	2.0×10^{-11}	Sponge like appearance. Uneven corrosion in the stressed areas.
	79 °C, L	65.4 (1.66)	1.3×10^{-10}	Dark gray color. Uneven sponge like corrosion in stressed areas. Small crevice corrosion. Pitting
	79 °C, V	19.8 (0.503)	3.5×10^{-11}	Bluish color. Small crevice corrosion. SCC.
	93 °C, L	17.1 (0.434)	4.3×10^{-10}	Dark gray color. SCC, pitting and crevice corrosion.
	93 °C, V	24.2 (0.615)	1.6×10^{-10}	Ni plated appearance. Shallow crevice and pitting corrosion.
B-3	66 °C, L	112 (2.84)	8.8×10^{-11}	Dark gray color. Uneven sponge like corrosion. Small crevice and pitting corrosion.
	66 °C, V	73.6 (1.87)	5.9×10^{-11}	Dark gray color. Uneven sponge like corrosion especially in the stressed area. Crevice corrosion.
	79 °C, L	393 (9.98)	7.3×10^{-11}	Dark gray color. Uneven sponge like corrosion especially in the stressed area. Crevice corrosion
	79 °C, V	179 (4.55)	1.2×10^{-10}	Dark gray color. Uneven sponge like corrosion especially in the stressed area. Crevice corrosion
	93 °C, L	103 (2.62)	6.5×10^{-10}	Dark gray color. Fissures, crevice and pitting corrosion
	93 °C, V	94.2 (2.39)	2.5×10^{-10}	Ni plated appearance. Fissures, crevice and pitting corrosion.

copper on the surface of the U-bend specimens that were exposed to both the liquid and vapor phases.

Overall, considering resistance to general corrosion by weight loss and to stress assisted crack propagation, both in the liquid and vapor phases of wet HF, C-2000 alloy was the highest ranked material (For a pool of materials that included eleven different corrosion resistant engineering alloys).

4 Conclusion

1. For nickel alloys containing high chromium and which were exposed to the vapor phase, the corrosion rate decreased as the testing time increased. The corrosion rate was not highly dependent on the testing time when the coupons were exposed to the liquid phase.
2. The corrosion rate of both alloy 400 and C-2000 alloy increased with the acid concentration and the temperature. However, both for increasing acid concentration and tem-

HE 00282

perature, the corrosion rate of alloy 400 increased faster than the corrosion rate of C-2000 alloy, especially in the vapor phase.

3. Even in unstressed coupons, nickel alloys show internal penetration in presence of wet HF. The mode of internal penetration is different for each alloy.
4. Nickel alloys are susceptible to stress corrosion cracking in the presence of wet HF service and this susceptibility is strongly influenced by alloy composition, temperature and phase of exposure.
5. Considering factors such as corrosion rate by weight loss, internal penetration and susceptibility to stress cracking, C-2000 alloy had the best performance of all the tested alloys.

5 References

- [1] *M. G. Fontana*. Corrosion Engineering, 3rd Ed., McGraw-Hill, New York, 1986. p. 353.
- [2] *T. F. Degnan*. Process Industry Corrosion – The Theory and Practice NACE International. 1986, p. 275–282.
- [3] NACE International publication 5A171 "Materials for Receiving, Handling and Storing Hydrofluoric Acid", NACE International, 1995.
- [4] *S. W. Ciaraldi, R. M. Berry, J. M. Johnson*: CORROSION/82, NACE International, 1982, Paper 98.
- [5] *S. J. Pavel*: Corrosions 50 (1994) 963.
- [6] *C. M. Schillmoller*: Chem. Eng. Progress (1998) 49.
- [7] *J. R. Crum, G. D. Smith, M. J. McNallan, S. Hirnyj*: CORROSION/99, NACE International, 1999, Paper 382.

(Received: May 9, 2000)

W 3496

HE 00283

WELD CORRO

Preventing

Filler metals containing specific amounts of nickel, chromium, titanium, tungsten, and molybdenum provide outstanding corrosion resistance characteristics, and also impart corrosion protection to welded assemblies.

Samuel D. Kiser

*Special Metals Welding Products Company
Newton, North Carolina*

Welding products that have the most effective resistance to pitting and crevice corrosion contain specific amounts of nickel, chromium, titanium, tungsten, and molybdenum. These elements not only provide outstanding corrosion resistance characteristics, but also impart corrosion protection to welded assemblies. Details of corrosion testing with a variety of alloys reveal the breadth and magnitude of these advantages. This article discusses how various elements in the composition affect corrosion resistance, and explains how to calculate the pitting corrosion resistance of nickel welding alloys.

Chemical composition

The chemical compositions of several widely selected corrosion-resistant alloys are given in Table 1, along with a simple summation of %Cr+%Mo+%W for each alloy. The workhorse alloys in this list contain a substantial percentage of nickel, which provides good general corrosion resistance and serves as the matrix or solvent to contain the active elements chromium, molybdenum, and sometimes niobium, tungsten, and titanium. Most of these alloys and their welding

products have very low carbon contents. However, Inco-Weld 686CPT and Inconel Alloy 686 contain almost imperceptible, but nevertheless critical, additions of the stabilizer titanium, along with robust additions of tungsten. The titanium serves to protect the other active ingredients against the formation of deleterious combinations with carbon, while the tungsten is beneficial to weldability and crack-resistance.

The tendency toward elemental segregation in NiCrMo alloy welds is reduced when niobium is replaced with tungsten. When compared with niobium, tungsten promotes improved deployment of the active ingredients by enhancing elemental homogeneity of the weld, even in dissimilar welds. Tungsten is similar to molybdenum in structure and refractory nature, and in nickel alloy welds, it participates similarly to molybdenum in corrosion resistance. Superior pitting resistance of 686 CPT in the aggressive test medium of green death (Fig. 1) is provided by titanium, tungsten, and very low carbon contents, along with major additions of chromium and molybdenum.

The composition of green death is 11.9% H_2SO_4 + 1.3% HCl + 1% $FeCl_3$ + 1% $CuCl_2$, and testing was carried out in a solution at 103°C (boiling). In most cases, triplicate specimens were exposed for three days at boiling temperature, and the side that showed greatest attack was photographed. Although 686CPT welding products do not completely eliminate corrosion in every test, they provide corrosion resistance that is shown to be superior to other matching-composition welds. This exceptional resistance to preferential weld corrosion is not limited to pitting environments; the protection extends to crevice corrosion resistance as well. Figure 2 depicts the crevice-corrosion resistance of several alloys in green death at various temperatures.

Pitting resistance equivalent

Rather than drawing inferences or estimating corrosion resistance, some designers prefer actual equations that predict pitting or crevice corrosion performance by calculating a PREN (pitting resistance equivalence number). A variety of PRE equations have been developed, and are helpful in predicting the corrosion performance of members of a particular group of alloys or welds.

Within a given PRE equation, higher values of PREN correspond to greater corro-

Table 1 — Chemical compositions of selected corrosion-resistant alloys

UNS Designation	Alloy	Fe	Ni	Cr	Mo	W	Cr+Mo+W
UNS N06625*	625	1	64	21.5	9.0	—	30.5
UNS N10276	C-276	6	57	16.0	15.7	3.7	35.4
UNS N06455	C-4	3	57	16.0	16.0	-	32.0
UNS N06022	622	2.3	59	20.5	14.2	3.2	37.9
UNS N06022	C-22	4.5	58	21.6	13.0	3.0	37.6
UNS N06200	C-2000	2	58	23.0	16.0	(Cu 1.5)	39
UNS N06059	59	1.5	58	23.0	16.0	—	39
UNS N06686	686	1	57	20.5	16.3	3.9	40.7
INCO-WELD 686CPT welding product	686	1	57	20.5	16.3	3.9	40.7

*N06625 has 3.6Nb and no tungsten

SION

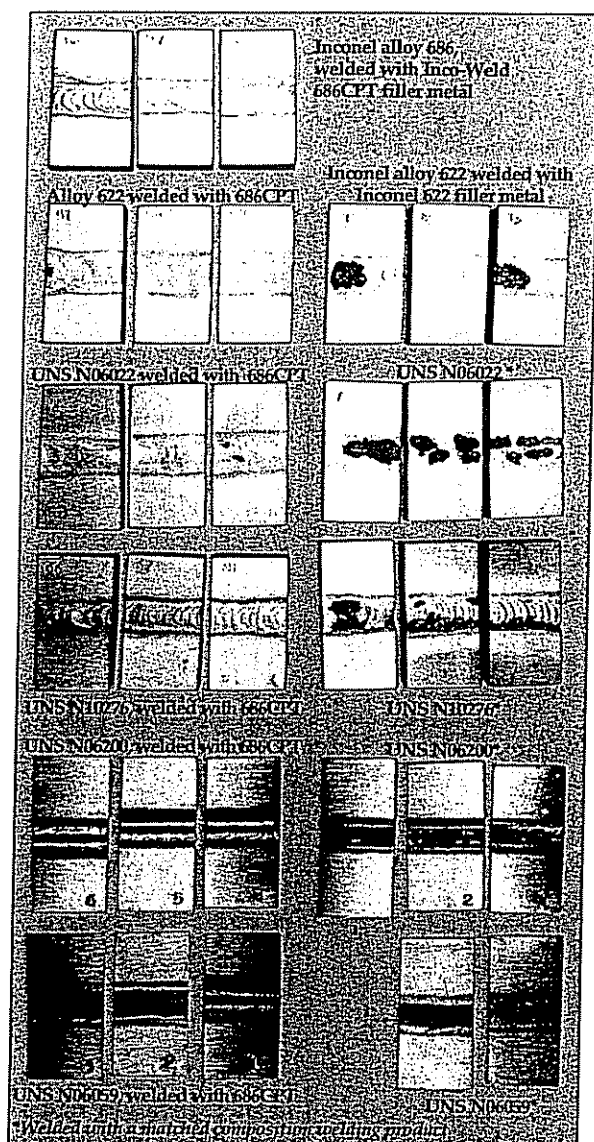


Fig. 1 — Pitting resistance in welded joints for range of high-performance nickel-chromium-molybdenum alloys. GTAW welds of various sizes of plate and sheet, laboratory tested in a "Green Death" solution: 11.9% H_2SO_4 + 1.3% HCl + 1% $FeCl_3$ + 1% $CuCl_2$. Three days at boiling (103°C) temperature. Samples turned to show the most severe attack.

sion resistance. A realistic PREN for stainless steels is:

$$PREN = \%Cr + 3.3 (\%Mo) + 30N.$$

Sometimes nitrogen is correctly included in the equations for stainless steels. It has been proposed that dissolved nitrogen in the matrix of a stainless steel weld metal or base metal has a capability of reducing the acidity of the media at the bottom of an incipient pit and reducing the pitting action. Of course, the solubility for nitrogen is much lower in nickel alloys than in stainless steels, with the result

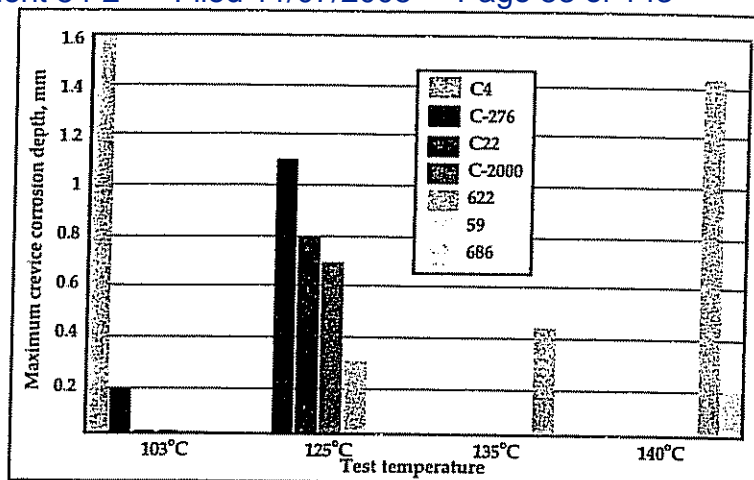


Fig. 2 — Relative resistance of nickel-base alloys to crevice corrosion in "Green Death" as a function of temperature. Tungsten enhances resistance to crevice corrosion.

Table 2 — PRE numbers derived via different formulas

A	B	C	D
UNS Number	Alloy	PREN	PREN
N06686	686CPT	87.16	50.8
N10276	C-276	80.02	45.1
N06022	622	77.92	46.6
N06022	C-22	74.40	45.6
N06059	59	75.80	47.0
N06200	C-2000	75.80	45.8
N06455	C-4	68.80	40.0
N06625	625	51.20	35.0

that dissolved nitrogen in the matrix of nickel alloys is typically very low.

When nitrogen exceeds these very low solubility limits, the excess nitrogen forms either porosity or solid solutions of nitrides or carbo-nitrides. Because of these three possibilities, the appropriate equation for calculating PRE in stainless steels is not the same as that for calculating PRE in nickel alloys or nickel alloy welds.

Therefore, it would not be appropriate to use $PRE = \%Cr + 3.3(\%Mo) + 30N$ to predict the pitting resistance of nickel alloy welds. Rather, researchers have found that tungsten is a potent pit and crevice corrosion-resistant elemental addition. Streicher was one of the first to show the beneficial effect of tungsten on corrosion resistance in wrought alloys. More recently, in their paper, "Improved Pitting and Crevice Corrosion Resistance of Nickel and Cobalt Based Alloys," Rebak and Crook report that "Some researchers have proposed a different PRE to explain the influence of alloying elements in nickel base alloys than in stainless steels." That PRE equation is

$$PRE = Cr + 3.3 (Mo + W) + 30N$$

HE 00285

and is presented in Reference 12 of their paper as

$$PRENW = \%Cr + 3.3(Mo + W) + 16N$$

Tungsten behavior is similar to that of molybdenum in several respects, such as enhancing resistance to pitting and crevice corrosion. The effect of tungsten can be demonstrated by the perfor-

The Salt River Project at Navajo Station in Page, Arizona

The largest FGD project ever built in North America required nearly 4,500,000 pounds of Inconel alloy C-276 sheet, plate, and clad-steel, as well as Inconel Filler Metal C-276 and Inco-Weld 686CPT welding products. Navajo Station pumps a major amount of electrical power to the southwest while burning very high sulfur coal delivered by conveyor from a mine directly beneath it. The six scrubbers and three chimneys protect the nearby Grand Canyon from haze and acid rain by removing 98% of the polluting emissions from the plant.



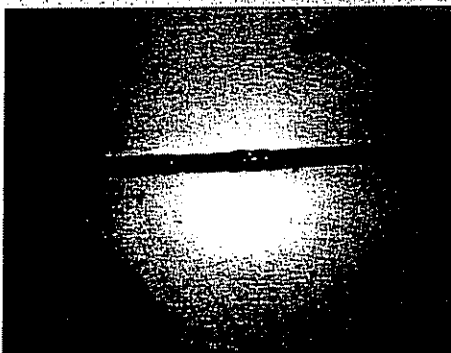
Salt River Project at Navajo Station in Page, Arizona.

Seminole Electric Co-op in Palatka, Florida

A "green death" corrosion medium was being naturally generated by a re-boiler effect at the bypass duct damper in this power generation plant. The corrosion medium was formed when a continuous supply of flue gas was delivered to the closed bypass duct at the chimney. The cold duct condensed the unscrubbed products of combustion, but then the closed damper conducted heat from the chimney, thus reheating the condensate. The environment was so severe that C-276 welds completely disappeared in less than six months. Figure 4 shows the floor of the damper after the C-276 welds were replaced with Inco Weld 686CPT. The C-276 plate continued to corrode at greater than 40 mils per year and was replaced with Alloy 686 Plate. Figure 5 shows the repair weld after six years.



By-pass duct floor after 6 months at 71°C. Alloy C-276 was welded with Inco-Weld Filler Metal 686CPT.



This shows the repair made with Inconel Alloy 686 welded with Inco-Weld 686CPT after six years of continued service with no corrosion.

mance of similar alloys with and without tungsten (Fig. 2). Note the difference between the depth of crevice attack at 103°C for UNS N06455 (alloy C-4), which contains no tungsten, and UNS N06276 (alloy C-276), a similar alloy that contains 4% tungsten. The depth of crevice attack for C-4 is nearly ten times greater than for C-276.

Again, compare the performance of UNS N06059 (alloy 59), which contains no tungsten, to that of Inconel alloy 686 (UNS N06686) with 4% tungsten, at 135°C and 140°C. Alloy 59 experiences over seven times greater depth of crevice attack than alloy 686 at 140°C. The beneficial effect of tungsten is also validated in the pitting results of weldments shown in Fig. 1. Note that outstanding pitting resistance of welds in the punishing green death environment is provided only by alloy 686CPT welds, which also contain 4% tungsten.

The results shown in Fig. 1 are reported numerically in Table 3. Although the PRE equation proposed by Charles, Audourd, and Verneau properly includes a term for tungsten, it fails to accurately predict the performance of nickel alloys and welds shown in Fig. 1 and 2, and Table 3.

Based on the equation

$$PREN = \%Cr + 3.3 (\%Mo + \%W) + 30N$$

to calculate indices for the compositions in Table 1, values are given in Column C of Table 2. Note that C-276 and C-2000 are overestimated, while alloy 59 is underestimated when compared to their actual performances. According to Fig. 1 and Table 3, Alloy 59 marginally outperforms C-2000 as a weld metal in pitting resistance. According to Fig. 2, it outperforms C-2000 as a base metal in crevice corrosion resistance.

Because Alloys 59 and C-2000 are nearly identical except for copper, it would appear that copper has a negative influence on localized corrosion resistance. Note the disparities between the predictions for alloys C-276, C-2000, and 59, and the experimental results for these alloys. These disparities can be corrected by reducing the significance of the term (Mo + W) relative to chromium by reducing its coefficient from 3.3 to 1.5.

Furthermore, the difference between prediction and performance caused by the presence of copper may be addressed by inserting a negative term to account for the deleterious effect of copper. These changes result in:

$$PREN = \%Cr - 0.8\%Cu + 1.5 (\%Mo + \%W)$$

The values shown in Table 2, Column D were calculated by this equation.

Because the calculated values given in Column D fit the data presented in Fig. 1 and 2, and in Table 3, we would propose that the equation

$$PREN = \%Cr - 0.8\%Cu + 1.5 (\%Mo + \%W)$$

be used to predict future performance of unknown nickel alloys. Note that the absolute values given in Table 2 column D are considerably lower than

HE 00286

Base metal alloy	Filler metal	Base metal max pit depth, mm	Filler metal max pit depth, mm	Overall, corrosion rate, mm/y	Comments
686	686CPT	0	0	N/A	No attack
686	686CPT	0	0	N/A	No attack
686	686CPT	0	0	N/A	No attack
622	686CPT	0	0	N/A	No attack
622	686CPT	0	0	N/A	No attack
622	686CPT	0	0	N/A	No attack
622	622FM	0	1.7	N/A	Severe attack of weld metal
622	622FM	0	0	N/A	No attack
622	622FM	0	2.9	N/A	Severe attack of weld metal
C-22	686CPT	0	0.6	N/A	Light attack of weld metal
C-22	686CPT	0	0	N/A	No attack
C-22	686CPT	0	0.6	N/A	Light attack of weld metal
C-22	C-22	0	2.8	N/A	Severe attack of weld metal
C-22	C-22	0	2.4	N/A	Severe attack of weld metal
C-22	C-22	0	2.1	N/A	Severe attack of weld metal
C-276	686CPT	1.5	1.5	N/A	Severe attack of base and weld
C-276	686CPT	0.6	0.1	N/A	Light attack of base/Very light attack of weld
C-276	686CPT	0.5	0	N/A	Light attack of base/No attack of weld
C-276	C-276	0.5	2	N/A	Light attack of base/Severe attack of weld
C-276	C-276	1.2	2.5	N/A	Severe attack of base and weld
C-276	C-276	0.5	2	N/A	Light attack of base/Severe attack of weld
C-2000	686CPT	N/A	0	0.1	No attack
C-2000	686CPT	N/A	0	0.1	No attack
C-2000	686CPT	N/A	0	0.1	No attack
C-2000	C-2000	N/A	2.6	11.3	Severe attack of weld metal
C-2000	C-2000	N/A	2.3	9.8	Severe attack of weld metal
C-2000	C-2000	N/A	2.4	10.6	Severe attack of weld metal
59	686CPT	N/A	0	0.1	No attack
59	686CPT	N/A	0	0.1	No attack
59	686CPT	N/A	0	0.1	No attack
59	59	N/A	1.5	6.5	Severe attack of weld metal
59	59	N/A	1.6	6.7	Severe attack of weld metal

* In 11.9% H₂SO₄ + 1.3% HCl + 1% FeCl₃ + 1% CuCl₂, "Green Death" 3 days, 103° C (Boiling)

those generated by the stainless steel PREN shown in column C, but the relationships among the alloys shown in Table 2 are accurately portrayed. A term could be added for %N, but given the low solubility for nitrogen in nickel, it would be superfluous. (Note that values calculated with one PRE equation should not be compared with the values calculated from a different PRE equation.)

Applications and locations

Because of the exceptional performance in very low pH acid-chloride environments, nickel-base wrought alloys and welding products have been widely selected for components in the pollution-control industry. These applications involve both solid and clad-steel welded fabrications in wet-limestone scrubbing systems in flue gas desulfurization (FGD) equipment for power plants, and other industrial flue gas treatment systems. Specific types of applications include scrubbers and absorber towers, breeching and by-pass ducting, dampers and turning vanes, chimney liners and expansion joints, and recovery heat exchangers and welded tubing. Other applications include chemical reactor vessels, process piping, and other related equipment. These welded fabrications have been combating corrosion throughout the United States, Eastern Europe, the Middle East, Western Europe, and Canada. ■

For more information: Samuel D. Kiser, P.E., is Director of Technology, Special Metals Welding Products Company, 1401 Burris Road, Newton, NC 28658; tel: 828/465-0352, ext. 205; fax: 828/464-8993; e-mail: skiser@iaiwpc.com.

(Inconel and Inco-Weld are trademarks of Special Metals Corp.)

References

1. Rebak, R.B. and Crook, P. "Improved Pitting and Crevice Corrosion Resistance of Nickel and Cobalt Based Alloys" Electrochemical Society Proceedings Volume 98-17, The Electrochemical Society, Pennington, NJ 1998, pp. 290.
2. Streicher, M.A., Corrosion, Vol. 32, March 1976.
3. Op. cit. (Ref. 1), p299.
4. Charles, J and Audourd, J.-P, and Verneau, M, "Paper 480," Corrosion/98, NACE International, Houston (1998).
5. Special Metals Corporation, "High-Performance Alloys for Resistance to Aqueous Corrosion," 2000, p. 55.

HE 00287

How useful did you find the information presented in this article?
 Very useful, Circle 273
 Of general interest, Circle 274
 Not useful, Circle 275

Corrosion Resistance of a New, Wrought Ni-Cr-Mo Alloy

Paul Crook, M.L. Caruso, and D.A. Kingseed
Haynes International, 1020 West Park Ave., P O Box 9013, Kokomo, IN 46904-9013

HE 00288

A new, nickel-based alloy resistant to a very wide range of corrosive media is described. The main alloying additions are chromium and molybdenum; however, the alloy also contains ~1.6% copper, which significantly enhances its resistance to dilute sulfuric and hydrochloric acids. The safe operating regimes for the alloy in these two acids are defined, as are its current and potential applications in the chemical process industries.

Of the materials available to chemical process industry engineers, the wrought Ni-Cr-Mo alloys are among the most versatile. Not only do they resist uniform attack in a wide range of acidic and alkaline environments, but they also withstand stress corrosion cracking, pitting, and crevice corrosion. In addition, they can be formed and welded, without difficulty, into complex components.

Many of the attractive properties of the wrought Ni-Cr-Mo alloys stem from the physical properties of nickel. First, it is more noble than iron; second, it exhibits a ductile, face-centered cubic structure at all temperatures; and third, it is very tolerant of useful solutes, such as chromium and molybdenum, which enhance passivity and nobility.

The chromium contents of the wrought Ni-Cr-Mo alloys range from ~16 wt% to 23 wt% (Table 1). The higher the chromium content, the better is the performance in oxidizing acids. The performance of the wrought Ni-Cr-Mo alloys in reducing acids, on the other hand, is largely

a function of the levels of molybdenum and tungsten, which range from ~13 wt% to 16.5 wt% and 0 wt% to 4 wt%. Reducing acids include hydrochloric, hydrofluoric, phosphoric, and dilute sulfuric; however, when these acids contain sufficient quantities of ferric ions, cupric ions, or dissolved oxygen they become oxidizing. Nitric acid and concentrated sulfuric acid are naturally oxidizing to nickel-based alloys, although the relation-

ship between chromium content and resistance to corrosion do not hold in the case of concentrated sulfuric.

Solubility constraints at the solution annealing temperatures define how much chromium, molybdenum, and tungsten can be retained in solution, assuming that the materials are quenched after annealing. For a given amount of chromium, only certain quantities of molybdenum and tungsten can be added; further additions then partition to primary precipitates. The same is true if the molybdenum and tungsten levels are fixed, and chromium is added. Thus, only certain levels of resistance to both oxidizing and reducing acids can be

TABLE 1
Typical Compositions of New and Existing Wrought Ni-Cr-Mo Alloys (wt%)

Alloy Designation	Ni	Cr	Mo	W	Fe	Mn	Si	C	Others
Existing									
C-276	Bal	16	16	4	5	0.5	0.02	0.002	V-0.15 Al-0.25
C-4	Bal	16	16	—	0.5	0.2	0.02	0.002	Ti-0.2 Al-0.2
C-22	Bal	22	13	3	3	0.3	0.02	0.002	V-0.15 Al-0.25
59	Bal	23	15.75	—	0.3	0.2	0.02	0.002	Al-0.25
666	Bal	20.5	16.5	4	1	0.2	0.02	0.002	Al-0.25
New									
C-2000	Bal	23	16	—	0.5	0.2	0.02	0.002	Cu-1.6 Al-0.25

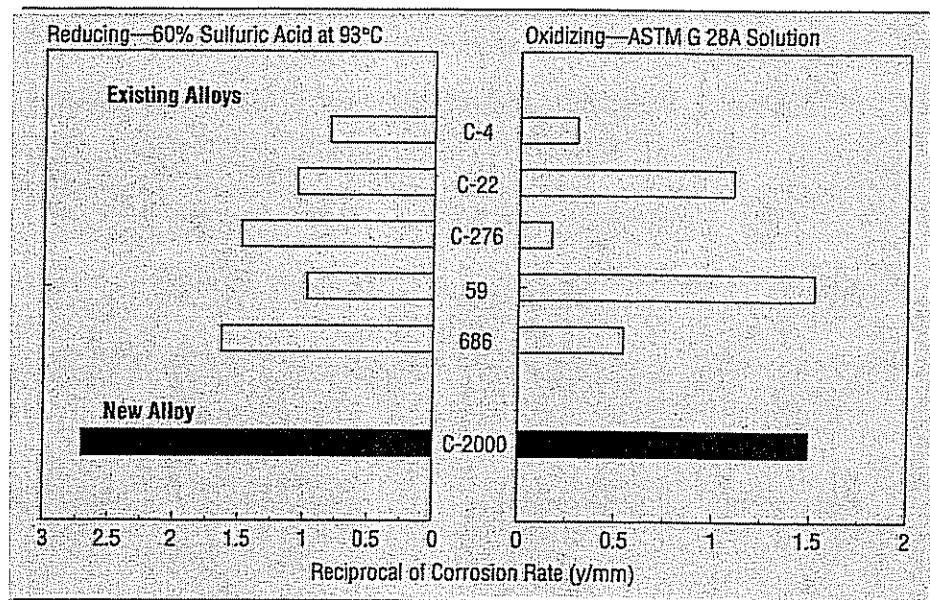


FIGURE 1
Application ranges of existing and new Ni-Cr-Mo alloys

attained using only chromium, molybdenum, and tungsten additions. The compositions of the existing alloys reflect the type of media for which they were designed, since none span the entire Ni-Cr-Mo alloys capability range, as illustrated using corrosion rate reciprocals in strong oxidizing and reducing solutions (Figure 1).

A new, wrought Ni-Cr-Mo alloy was designed along slightly different lines. The technical objective during development was a wider application range, i.e., increased versatility. The development goal was to equal the performance of the existing high chromium alloys in oxidizing acids, and to equal the high molybdenum and tungsten alloys in reducing acids. To achieve this, a combination of molybdenum and copper was used. Copper was found not only to be more effective than tungsten in enhancing nobility under active corrosion conditions, but also it allowed the use of a high chromium content.¹ The success of this approach is evident in comparing the application range of the new material with those of the existing alloys, as defined by the same two media (Figure 1). The composition of the new material, which is known commercially as alloy C-2000, and designated UNS N06200 is given in Table 1.

Resistance to Corrosion

In common with the existing, wrought Ni-Ti-Cr-Mo materials, alloy C-2000 is very resistant to pitting, crevice corrosion, and stress corrosion cracking, in the presence of chlorides.

As part of the assessment of its uniform corrosion resistance, alloy C-2000 was tested extensively in sulfuric and hydrochloric acids, since these are among the most corrosive and common compounds encountered in the chemical process industries. The results of the tests in sulfuric acid are summarized in the iso-corrosion diagram (Figure 2). This diagram, which

indicates the "very safe," "moderately safe," and "unsafe" regimes, was constructed from 80 data points, i.e., two test results at each of 40 concentration and temperature combinations. The tops of the bars represent the boiling points. This diagram shows that alloy C-2000 is usable in pure sulfuric acid up to ~100°C at concentrations up to 70 wt%, this being a significant advance over the most widely used Ni-Cr-Mo material, alloy C-276 (UNS N10276). The new alloy also possesses advantages over other existing Ni-Cr-Mo alloys in sulfuric acid.¹

The performance of alloy C-2000 in hydrochloric acid is depicted by the iso-corrosion diagram (Figure 3). This chart was constructed from 90 data points, i.e., two test results at each of 45 concentration and temperature combinations. From this chart, it is evident that the alloy can be used in boiling solutions up to a concentration of 3 wt%, which is beyond the capability of existing Ni-Cr-Mo alloys,¹ and up to a temperature of ~60°C in the concentration range 7 wt% to 20 wt%. Concentrations in excess of 20 wt% were not studied because of the volatility of hydrochloric acid, i.e., it is not possible to maintain a boiling solution at concentrations >20 wt% in a flask/condenser system, due to the evolution of hydrogen chloride gas.

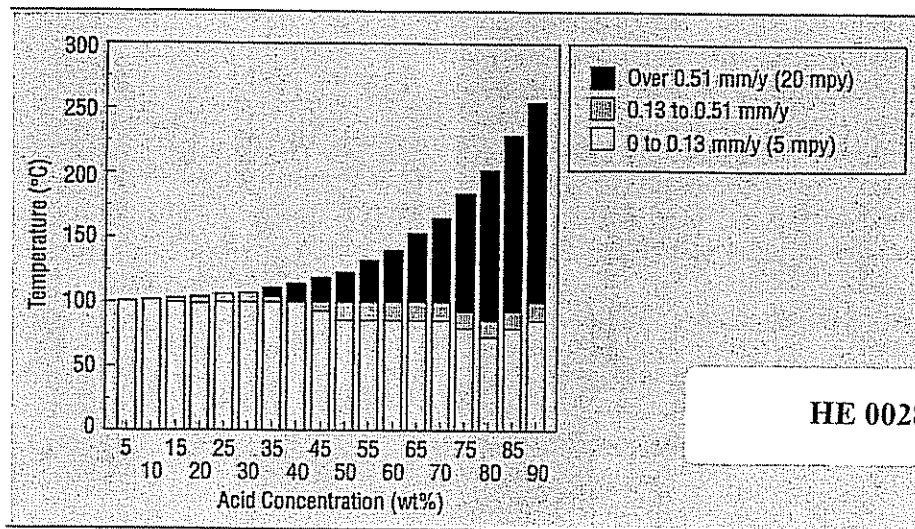


FIGURE 2
Iso-corrosion diagram for alloy C-2000 in sulfuric acid.

HE 00289

Alloy C-2000 is also resistant to hydrofluoric acid, phosphoric acid, nitric acid, organic acids, mixed inorganic acids, and sodium hydroxide.

Physical Metallurgy

The wrought Ni-Cr-Mo alloys are typically used in the solution annealed and water quenched condition. At the solution annealing temperature, which is normally in the range 1,120°C to 1,150°C, secondary phases dissolve in the fcc structure. The effect of the quench is to "freeze in" the high temperature structure. Only when the alloys are subsequently raised to a temperature sufficient to cause appreciable diffusion, e.g., during welding is there need for concern.

Several precipitates can occur in alloy C-276, for example, when it is exposed to elevated temperatures. In the range 300°C to 650°C, an ordered phase of the type $Ni_2(Cr,Mo)$ can form homogeneously throughout the microstructure, although the reaction kinetics are slow. At temperatures above 650°C, precipitates of μ phase, M_6C carbide, and P phase can form heterogeneously at the grain boundaries and twin boundaries in the microstructure.² Of these precipitates, μ phase is the most abundant, and M_6C the second most abundant. They are both rich in molybdenum and can quickly form continuous grain boundary networks, which render the alloy prone to intergranular attack, since they possess different compositions from the alloy solid solution, and in forming, deplete the surrounding matrix of molybdenum. To reduce the tendency of the wrought Ni-Cr-Mo alloys to form such precipitates, special melting procedures are used to minimize the contents of carbon and silicon (a known promoter of intermetallics).

The issues of thermal stability and intergranular attack are complex. Not only are the kinetics of the precipitation reactions important, but also the nature of the corrosive environment, and the electrochemical effects of the precipitates must be taken into account.

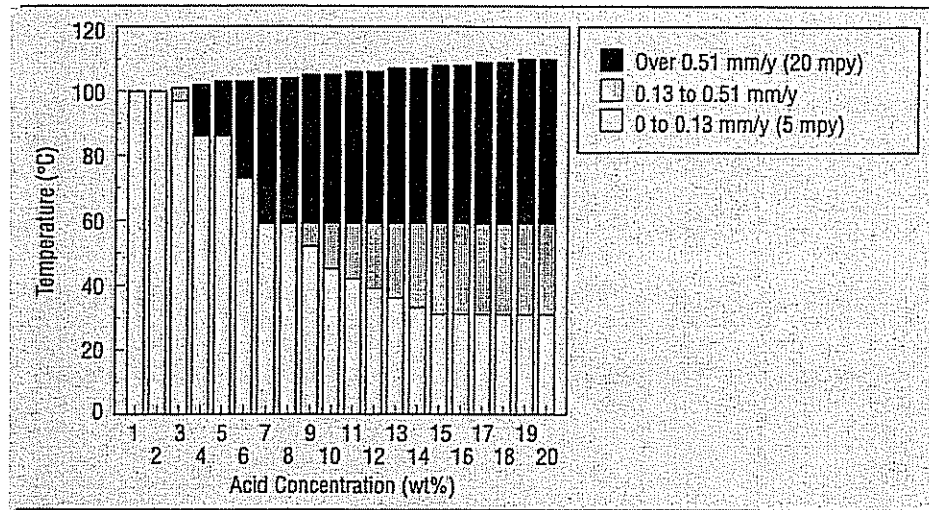


FIGURE 3
Iso-corrosion diagram for alloy C-2000 in hydrochloric acid.

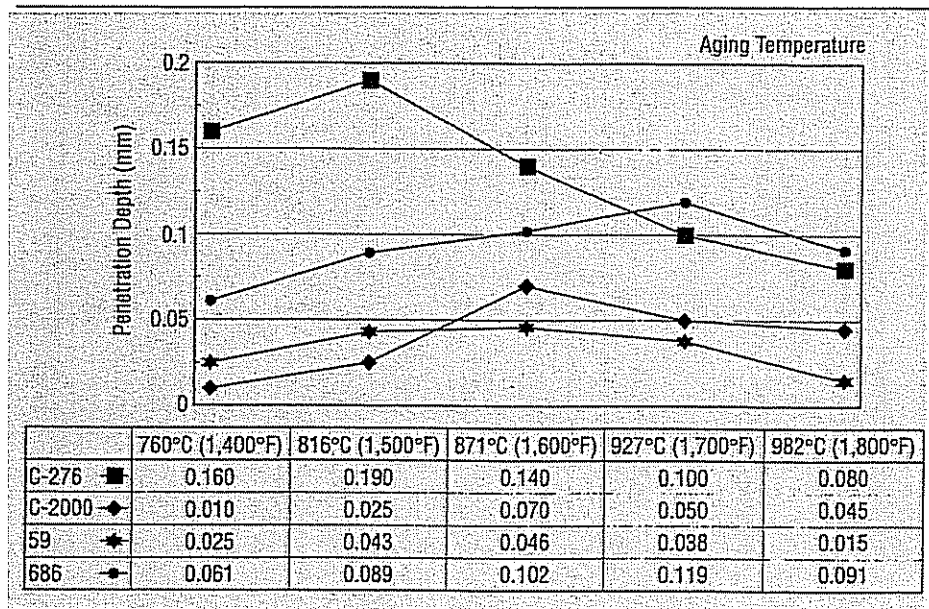


FIGURE 4
ASTM G 28A penetration depth as a function of aging temperature (3 min age)

To determine the effects of elevated temperature precipitation on alloy C-2000, samples were held (aged) for three minutes at temperatures ranging from 760°C to 982°C, then tested according to the ASTM G 28A.³ These procedures were designed specifically to detect the susceptibility of wrought nickel-based chromium-bearing alloys to intergranular corrosion, which have been used before to establish the time-temperature-sensitization characteristics of the wrought Ni-Cr-Mo alloys.^{3,4} The heating cycle in each case was 13 min (10 min to reach the precipita-

tion temperature, and 3 min at this temperature, followed by water quenching). To assess the level of grain boundary attack at each temperature, the samples were studied metallographically, in section, and the maximum depths of attack recorded. For comparison, similar tests were performed on alloys C-276, 59 (N06059), and 686 (N06686). The results of these tests are shown in Figure 4. Those alloys with the highest chromium contents (alloys C-2000 and 59) exhibit the highest resistance to intergranular corrosion after aging.

HE 00290

Applications

As a result of its ease of forming and welding, alloy C-2000 is suitable for many types of hardware, including reaction vessels, heat exchangers, piping and fittings, valves, and pumps. ASME approval, for use in pressurized systems, has been applied for. Its superiority over alloy C-276 has so far led to two chemical process industry applications, one involving the handling of sulfuric acid over a wide range of acid concentrations, the other involving a mixture of acids, including hydrofluoric. Field tests also indicate alloy C-2000 possesses advantages in brominated water and in chloride-containing acid mixtures.

Summary

The wrought Ni-Cr-Mo alloys are extremely versatile materials, resistant to many forms of corrosive attack. By using copper in alloy C-2000, this versatility has been extended significantly. Copper provides greatly enhanced nobility in certain reducing acids, and allows the use of a high chromium content, for optimum passivity in oxidizing media.

References

1. P. Crook, CORROSION/96, paper no. 412 (Houston, TX: NACE, 1996).
2. M. Raghavan, B.J. Berkowitz, J.C. Scanlon, Metallurgical Transactions A, 13A (1982): p. 979.
3. ASTM G 28, "Standard Test Methods of Detecting Susceptibility to Intergranular Corrosion in Wrought Nickel-Rich Chromium Bearing Alloys," Annual Book of ASTM Standards, Vol. 03.02 (Philadelphia, PA: ASTM)
4. Material Data Sheet No. 4030, NICROFER 5923 hMo - Alloy 59, (Werdohl, Germany: Krupp VDM, 1993)

Paul Crook is Manager of Commercial Technical Services (Corrosion) with Haynes International. He has more than 23 years' experience with corrosion resistant alloys and is a member of NACE and ASM International.

Martin Caruso is Market Development Manager with Haynes International. He has more than 10 years' experience with corrosion resistant materials and is a member of NACE and ASTM.

Dale Kingseed is a Sales/Marketing Consultant with Haynes International. He has 40 years' experience working in metals related fields and has held positions in engineering manufacturing, sales, and marketing.

HE 00291

Buchanan Ingersoll PC

ATTORNEYS

Lynn J. Alstadt
412 562 1632
alstadtjl@bipc.com

One Oxford Centre
301 Grant Street, 20th Floor
Pittsburgh, PA 15219-1410
T 412 562 8800
F 412 562 1041
www.buchananingersoll.com

July 19, 2004

Intellectual Property Rights Branch
U.S. Customs Service
1300 Pennsylvania Avenue, NW
Washington, DC 20229

Re: *Haynes International, Inc.*

Dear Sirs:

Pursuant to 19 C.F.R. § 133.1 et. seq., please record United States Trademark Registration No. 1953864 for the trademark C-22 with the United States Customs Service. The goods bearing the trademark C-22 are unwrought and partly wrought common metals and their alloys in various forms. The information required under 19 C.F.R. § 133.2 is as follows:

- (a) The trademark owner is Haynes International, Inc. whose address is 1020 West Park Avenue, Kokomo, Indiana 46902-9013. Haynes International, Inc. was incorporated in Delaware.
- (b) Haynes International, Inc. manufactures the goods bearing the trademark "C-22" in Kokomo, Indiana and Arcadia, Louisiana. The alloy is melted in Kokomo, Indiana and sold in various forms from that facility. The facility in Arcadia, Louisiana obtains the alloy from the Kokomo facility and forms it into tubular products.
- (c) There are no foreign persons or business entities authorized or licensed to use the trademark.
- (d) There is no parent or subsidiary company or other foreign company under common ownership or control which uses the trademark abroad.
- (e) Lever-rule protection is inapplicable in this recordation.

Three foreign business entities are selling in foreign markets, without authorization from applicant, alloys not manufactured by applicant that bear the mark C-22. These foreign business entities may attempt to import these infringing products into the United States. These companies are (1) Hart B.V., Post Office Box 144, 3860 AC Nijkerk, The Netherlands; (2) Clama Trade, via Montecatini 14-20144, Milan, Italy; (3) ThyssenKrupp VDM GmbH, Postfach 18 20, 58778 Werdohl, Plettenberger Straße 2, D-58791 Werdohl, Germany.

Intellectual Property Rights Branch
U.S. Customs Service
July 19, 2004
Page - 2 -

Enclosed is a check in the amount of \$190 to cover the fee for recordation. Also, enclosed herewith is a status copy of the certificate of registration, certified by the U.S. Patent and Trademark Office, showing title to be presently in the name of applicant, Haynes International, Inc. and five copies of this certification of registration.

Very truly yours,



Lynn J. Alstadt

Enclosures

HE 00300

HAYNES

International

cc: R. W. Clemens
A. I. Asphahani
J. L. Nickerson
S. Walden
~~and Joseph J. Phillips~~
File C-22

August 29, 1988

Mr. Frank Modic
Stooddy Deloro Stellite, Inc.
610 West Ash Street
Suite 1510
San Diego, CA 92101

Dear Frank:

A copy of your Material Safety Data Sheet (MSDS) No. P2277, copy enclosed, has come to my attention. It relates to your metal powder product identified as "NISTELLE C-22".

For your information, C-22 is a trademark of Haynes International, Inc. Our registration of the mark has been filed and is pending in the U.S. Patent and Trademark Office.

It appears that your identification of NISTELLE C-22 is a combination of two trademarks suggesting two different sources of product, which is misleading and improper. We suggest as an example, that you may avoid this problem by using your powder product identification: NISTELLE Powder No. P2277" and, if you wish, the added notation "made from C-22" alloy" to indicate the alloy was produced by Haynes International, Inc.

As you know, we must use our trademarks properly to keep them as valuable property.

May we have your comments regarding this matter.

Very truly yours,



Joseph J. Phillips
Manager, Patent & Trademark Dept.

vlw

0431n

HE 00474

stellite

COATINGS DIVISION

SAFETY DIRECTOR 1201 Eisenhower Dr., North Carmel, IN 46526-3256	Telephone (219) 534-2585
MATERIAL IDENTIFICATION NUMBER P2277	ORIGINAL DATE 7-22-1985 REVISED DATE 11-22-1987

MATERIAL SAFETY DATA SHEET	ALLOY POWDERS
----------------------------	------------------

SECTION 1 - PRODUCT			SECTION 2 - PHYSICAL PROPERTIES		
PRODUCT IDENTIFICATION TRADE NAME ALLOY NUMBER	CHEMICAL FAMILY ALLOY	FORMULA Alloy composed of varying concentrations of elements listed in Section 3.	FREEZING POINT °F: 2475 MELTING POINT °F: 2550 BOILING POINT: N/A SUBLIMES: N/A EVAPORATION RATE: N/A APPEARANCE: Powder, Gray Color	ODOR: None VAPOR PRESSURE: N/A VAPOR DENSITY(AIR=1): N/A SPECIFIC GRAVITY(H ₂ O=1): 8.69 SOLUBILITY IN WATER: None % VOLATILES BY VOLUME: None	
WISTELLE C-22 2277					

SECTION 3 - TLV DATA ON PRINCIPAL ALLOY INGREDIENTS					
CONSTITUENT	* NOMINAL PERCENT	CAS NUMBER	NIOSH RTECS NUMBER	EXPOSURE LIMITS (AS mg/m ³) **	
				OSHA PEL	ACGIH TLV
B	-----	7440-42-8	ED3750000	NONE	NONE
C	.08 MAX.	7440-44-0	PP5250100	3.5	7
Co	2.5 MAX.	7440-48-4	GF8750000	.1	.1
Cr	21.3	7440-47-3	GB4200000	1.0	.5
Cu	-----	7440-50-8	GL5325000	DUST 1.0 PUME .1	DUST 1.0 (2.0 STEL) PUME .2
Fe	4.0	1309-37-1	HO7400000	10.0	5.0 FOR IRON OXIDE PUME
Mn	.5 MAX.	7439-96-5	OO9275000	5.0 CEILING	DUST 5.0 CEILING PUME 1.0 (3.0 STEL)
Mo	13.5	7439-98-7	QA4680000	15.0	10.0 (20.0 STEL)
Ni	BALANCE	7440-02-0	QR5950000	1.0	1.0
Si	1.0 MAX.	7440-21-3	VW0400000	NONE	TOTAL DUST 10.0 RESPIRABLE DUST 5.0
V	.35 MAX.	7440-62-2	YW1355000	DUST .5 PUME .1 CEILING (V205)	0.5 AS V205 (DUST AND PUME)
W	3.0	7440-33-7	Y07175000	NONE	5.0 (10.0 STEL)

* Nominal percent content of elemental constituent for alloy.

** Many substances do not have a unique exposure limit. The absence of an exposure limit does not lessen consideration for exposure risk. In the absence of specific information, professional judgement may be required.

SECTION 4 - FIRE AND EXPLOSION HAZARD DATA

FLASH POINT (WITH TEST METHOD) NONE	FLAMMABLE (EXPLOSIVE) LIMITS V/V% LEL=NONE UEL=NONE
EXTINGUISHING MEDIA	This alloy is noncombustible. Use extinguishing media appropriate to the surrounding fire.
SPECIAL FIREFIGHTING PROCEDURES	If this powder is attritioned or reduced in particle size, caution must be used to prevent fire by avoiding sources of ignition, flames, etc. To extinguish a metal powder fire use dry sand, dry graphite or other class "D" fire extinguishing powder.
UNUSUAL FIRE AND EXPLOSION HAZARDS	No unusual fire or explosion hazards are associated with this material.
GENERAL REACTIVITY	This alloy is a stable material.
INCOMPATIBILITY (MATERIALS TO AVOID)	Avoid contact with mineral acids and oxidizing agents which may generate hydrogen gas; the evolution of hydrogen may be an explosion hazard.
HAZARDOUS DECOMPOSITION PRODUCTS	Various elemental metals and metal oxides may be generated during thermal spraying, welding, metallizing or similar operations. Refer to Section 3 for permissible exposure limits.

HE 00475

SECTION 5 - HEALTH HAZARD INFORMATION

PRIMARY ROUTE(S) OF EXPOSURE	INHALATION	Inhalation of metal dust, fume or powder may result from thermal spraying, welding, metalizing or similar operations which generate airborne metal particulate during use of this material.
	INGESTION	Hand, clothing, food and drink contact with metal dust, fume or powder can cause ingestion of particulate during hand to mouth activities such as eating, drinking, smoking, nail biting, etc.
	SKIN	Skin contact with this material may cause, in some sensitive individuals an allergic response if elements such as chromium, cobalt, copper and nickel are present. In the form of metal dust or powder, skin contact or abrasion may also cause irritation or dermatitis.
	EYES	Particulate metal (dust, fume or powder) may be dangerous to the eye and surrounding tissue. Airborne particulate (chips, dust or powder) is always a potential problem as well as inserting fingers into the eye socket if the hand or clothing is contaminated with metal particulate.

SECTION 6 - EMERGENCY AND FIRST AID PROCEDURES

INHALATION	Breathing difficulty caused by inhalation of dust or fume requires removal to fresh air. If breathing has stopped, perform artificial respiration and obtain medical assistance at once.
INGESTION	Swallowing metal powder or dust can be treated by having the affected person swallow large quantities of water and attempting to induce vomiting if conscious. Obtain medical assistance at once.
SKIN	Skin cuts and abrasions can be treated by standard first aid. Skin contamination with dust or powder can be removed by washing with soap and water. If irritation persists obtain medical assistance.
EYES	Dust or powder should be flushed from the eyes with copious amounts of clean water. If irritation persists obtain medical assistance. Contact lenses should not be worn if working with metal dusts and powders.

SECTION 7 - INDUSTRIAL HYGIENE CONTROL MEASURES

VENTILATION	Local exhaust ventilation should be used to control exposure to airborne dust and fume whenever possible.	
RESPIRATORY PROTECTION	Use NIOSH approved respirators as specified by an Industrial Hygienist or qualified Safety Professional. Lung function tests are recommended for users of negative pressure devices.	
PROTECTIVE GLOVES	Wear gloves to prevent metal cuts and skin abrasions.	
EYE PROTECTION	Wear safety glasses when risk of eye injury is present particularly during powder handling.	
OTHER PROTECTIVE EQUIPMENT	Protective clothing such as uniforms, disposable coveralls, safety shoes, etc. may be required during metal handling operations as appropriate to the circumstances of exposure.	
RECOMMENDED MONITORING PROCEDURES	ENVIRONMENTAL SURVEILLANCE	Exposure to the elements identified in Section 3 can be best determined by having air samples taken in the employee breathing zone, work area or department.
	MEDICAL SURVEILLANCE	Lung function tests, chest X-rays and routine physical examinations may be useful to determine effects of dust or fume exposure.

SECTION 8 - ENVIRONMENTAL PROTECTION INFORMATION

STEPS TO BE TAKEN IF MATERIAL IS RELEASED OR SPILLED	In powder or dust form, clean-up should be conducted with a vacuum system utilizing a high efficiency particulate air filtration system. Caution should be taken to minimize airborne generation of powder or dust and avoid contamination of air and water. Properly label all materials collected in waste container.
WASTE DISPOSAL METHOD	Prior to disposal consider if the material has recovery value. State or federal regulations may require specific labeling, packing, storage, transportation and disposal procedures. Contact an Environmental Engineer or consultant familiar with waste disposal regulations.
ENVIRONMENTAL HAZARDS	Metal powders or dusts may have significant impact on air and water quality. Airborne emissions, spills and releases to the environment (discharge to streams, sewer systems, ground water, surface soil, etc.) should be controlled immediately. If such potential for a spill or release exists it is advisable to develop an emergency spill response plan.

SECTION 9 - SPECIAL PRECAUTIONS

HANDLING PRECAUTIONS	This product must be handled according to the size, shape and quantity of material involved. Powders should be moved or transported to minimize spill or release potential.
STORAGE PRECAUTIONS	Store metal and metal powder in a dry area. Do not store adjacent to mineral acids. This is not regarded as a flammable material, however, if this powder is attritioned or reduced in particular size, caution should be taken to keep away from flames and sources of ignition.

SECTION 10 - DOT SHIPPING REQUIREMENTS

NONE

STROMBERG STELLITE, INC. assumes no responsibility and makes no warranty, express or implied, representation, promise or statement that the data provided is complete, accurate or current.

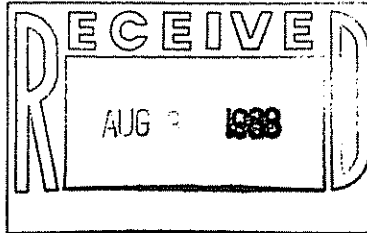
HE 00476

S-1733A

Haynes International, Inc.

1020 West Park Avenue
P.O. Box 9013
Kokomo, Indiana 46902-9013
317-456-6000

DATE: August 3, 1988
TO: J. J. Phillips
FROM: J. L. Nickerson
RE: Stellite C-22 Powder



I have checked my files and the only documented/formal communication I've had with Stellite in Goshen, Indiana, regarding the sale of alloy C-22 powder is attached. My current contact at this company is Nancy Sporn since Vidhu left the company.

To reiterate, Vidhu and I informally agreed that we would recommend customers to them for atomized alloy C-22 powder and they could sell it as such only if they bought our material as feedstock. In return, they would communicate to us who the customers were they sold it to.

Also, in some phone conversation notes I wrote while communicating with Vidhu on February 29, 1988, he said that their C-22 powder was high in carbon content (0.05-0.08).

J. L. Nickerson

bls
5550b

Attachment

HE 00477



1201 Eisenhower Dr., North
Goshen, Indiana 46526-5311
Telephone (219) 534-2585
800-235-9353
Telex: 6711857 CSD
Fax: (219) 534-3417

June 17, 1988

Ms. Jessica Nickerson
Haynes International
1020 West Park Avenue
Kokomo, IN 46901

Dear Jessica:

In checking our records on the C-22 alloy, we sold some powder to a customer in Japan last year and sent another sample to a customer in Pittsburgh. In both instances, the mesh size was 100/325. I do not know what the application was.

We will be sending you a small sample of the C-22 (100/325 mesh).

I will try to keep you informed of any further sales of this alloy.

Sincerely,

A handwritten signature in cursive script, appearing to read "Nancy".

Nancy A. Sporn
Customer Service Supervisor
STELLITE COATINGS DIVISION

NAS/sw

HE 00478



COATINGS DIVISION

SAFETY DIRECTOR
1201 Eisenhower Dr., North
Cassan, IN 46526-3396

Telephone
(219)
534-2585

MATERIAL SAFETY DATA SHEET

ALLOY
POWDERS

MSDS IDENTIFICATION NUMBER
P2277

ORIGINAL DATE 7-22-1985

REVISED DATE 11-22-1987

SECTION 1 - PRODUCT

PRODUCT IDENTIFICATION
TRADE NAME
NISTELLE C-22
ALLOY NUMBER
2277

CHEMICAL FAMILY
ALLOY

FORMULA
Alloy composed of
varying concentra-
tions of elements
listed in Section 3.

SECTION 2 - PHYSICAL PROPERTIES

FREEZING POINT °F: 2475
MELTING POINT °F: 2550
BOILING POINT: N/A
SUBLIMES: N/A
EVAPORATION RATE: N/A
APPEARANCE: Powder, Gray Color

ODOR: None
VAPOR PRESSURE: N/A
VAPOR DENSITY(AIR=1): N/A
SPECIFIC GRAVITY(H₂O=1): 8.69
SOLUBILITY IN WATER: None
VOLATILES BY VOLUME: None

SECTION 3 - TLV DATA ON PRINCIPAL ALLOY INGREDIENTS

CONSTITUENT	* NOMINAL PERCENT	CAS NUMBER	NIOSH RTECS NUMBER	EXPOSURE LIMITS (AS M ₂ /M ³) **			
				OSHA PEL		ACGIH TLV	
B	-----	7440-42-8	ED3750000	NONE		NONE	
C	.08 MAX.	7440-44-0	PP5250100	3.5		7	
Co	2.5 MAX.	7440-48-4	GP8750000	.1		.1	
Cr	21.3	7440-47-3	GB4200000	1.0		.5	
Cu	-----	7440-50-8	GL5325000	DUST 1.0	FUME .1	DUST 1.0 [2.0 STEL]	FUME .2
Fe	4.0	1309-37-1	HO7400000	10.0		5.0 FOR IRON OXIDE FUME	
Mn	.5 MAX.	7439-96-5	OO9275000	5.0 CEILING		DUST 5.0 CEILING	FUME 1.0 [3.0 STEL]
Mo	13.5	7439-98-7	QA4680000	15.0		10.0 [20.0 STEL]	
Ni	BALANCE	7440-02-0	QR5950000	1.0		1.0	
Si	1.0 MAX.	7440-21-3	VW0400000	NONE		TOTAL DUST 10.0	RESPIRABLE DUST 5.0
V	.35 MAX.	7440-62-2	YW1355000	DUST .5	FUME .1 CEILING [V205]	0.5 AS V205 [DUST AND FUME]	
W	3.0	7440-33-7	YO7175000	NONE		5.0 [10.0 STEL]	

* Nominal percent content of elemental constituent for alloy.

** Many substances do not have a unique exposure limit. The absence of an exposure limit does not lessen consideration for exposure risk. In the absence of specific information, professional judgement may be required.

SECTION 4 - FIRE AND EXPLOSION HAZARD DATA

FLASH POINT (WITH TEST METHOD) NONE		FLAMMABLE (EXPLOSIVE) LIMITS V/VZ LEL=NONE UEL=NONE	
EXTINGUISHING MEDIA	This alloy is noncombustible. Use extinguishing media appropriate to the surrounding fire.		
SPECIAL FIREFIGHTING PROCEDURES	If this powder is attritioned or reduced in particle size, caution must be used to prevent fire by avoiding sources of ignition, flames, etc. To extinguish a metal powder fire use dry sand, dry graphite or other class "D" fire extinguishing powder.		
UNUSUAL FIRE AND EXPLOSION HAZARDS	No unusual fire or explosion hazards are associated with this material.		
GENERAL REACTIVITY	This alloy is a stable material.		
INCOMPATIBILITY (MATERIALS TO AVOID)	Avoid contact with mineral acids and oxidizing agents which may generate hydrogen gas; the evolution of hydrogen may be an explosion hazard.		
HAZARDOUS DECOMPOSITION PRODUCTS	Various elemental metals and metal oxides may be generated during thermal spraying, welding, metallizing or similar operations. Refer to Section 3 for permissible exposure limits.		

HE 00479

SECTION 5 - HEALTH HAZARD INFORMATION

PRIMARY ROUTE(S) OF EXPOSURE	INHALATION	Inhalation of metal dust, fume or powder may result from thermal spraying, welding, metallizing or similar operations which generate airborne metal particulate during use of this material.
	INGESTION	Hand, clothing, food and drink contact with metal dust, fume or powder can cause ingestion of particulate during hand to mouth activities such as eating, drinking, smoking, nail biting, etc.
	SKIN	Skin contact with this material may cause, in some sensitive individuals an allergic response if elements such as chromium, cobalt, copper and nickel are present. In the form of metal dust or powder, skin contact or abrasion may also cause irritation or dermatitis.
	EYES	Particulate metal (dust, fume or powder) may be dangerous to the eye and surrounding tissue. Airborne particulate (chips, dust or powder) is always a potential problem as well as inserting fingers into the eye socket if the hand or clothing is contaminated with metal particulate.

SECTION 6 - EMERGENCY AND FIRST AID PROCEDURES

INHALATION	Breathing difficulty caused by inhalation of dust or fume requires removal to fresh air. If breathing has stopped, perform artificial respiration and obtain medical assistance at once.
INGESTION	Swallowing metal powder or dust can be treated by having the affected person swallow large quantities of water and attempting to induce vomiting if conscious. Obtain medical assistance at once.
SKIN	Skin cuts and abrasions can be treated by standard first aid. Skin contamination with dust or powder can be removed by washing with soap and water. If irritation persists obtain medical assistance.
EYES	Dust or powder should be flushed from the eyes with copious amounts of clean water. If irritation persists obtain medical assistance. Contact lenses should not be worn if working with metal dusts and powders.

SECTION 7 - INDUSTRIAL HYGIENE CONTROL MEASURES

VENTILATION	Local exhaust ventilation should be used to control exposure to airborne dust and fume whenever possible.	
RESPIRATORY PROTECTION	Use NIOSH approved respirators as specified by an Industrial Hygienist or qualified Safety Professional. Lung function tests are recommended for users of negative pressure devices.	
PROTECTIVE GLOVES	Wear gloves to prevent metal cuts and skin abrasions.	
EYE PROTECTION	Wear safety glasses when risk of eye injury is present particularly during powder handling.	
OTHER PROTECTIVE EQUIPMENT	Protective clothing such as uniforms, disposable coveralls, safety shoes, etc. may be required during metal handling operations as appropriate to the circumstances of exposure.	
RECOMMENDED MONITORING PROCEDURES	ENVIRONMENTAL SURVEILLANCE	Exposure to the elements identified in Section 3 can be best determined by having air samples taken in the employee breathing zone, work area or department.
	MEDICAL SURVEILLANCE	Lung function tests, chest X-rays and routine physical examinations may be useful to determine effects of dust or fume exposure.

SECTION 8 - ENVIRONMENTAL PROTECTION INFORMATION

STEPS TO BE TAKEN IF MATERIAL IS RELEASED OR SPILLED	In powder or dust form, clean-up should be conducted with a vacuum system utilizing a high efficiency particulate air filtration system. Caution should be taken to minimize airborne generation of powder or dust and avoid contamination of air and water. Properly label all materials collected in waste container.
WASTE DISPOSAL METHOD	Prior to disposal consider if the material has recovery value. State or federal regulations may require specific labeling, packing, storage, transportation and disposal procedures. Contact an Environmental Engineer or consultant familiar with waste disposal regulations.
ENVIRONMENTAL HAZARDS	Metal powders or dusts may have significant impact on air and water quality. Airborne emissions, spills and releases to the environment (discharge to streams, sewer systems, ground water, surface soil, etc.) should be controlled immediately. If such potential for a spill or release exists it is advisable to develop an emergency spill response plan.

SECTION 9 - SPECIAL PRECAUTIONS

HANDLING PRECAUTIONS	This product must be handled according to the size, shape and quantity of material involved. Powders should be moved or transported to minimize spill or release potential.
STORAGE PRECAUTIONS	Store metal and metal powder in a dry area. Do not store adjacent to mineral acids. This is not regarded as a flammable material, however, if this powder is attritioned or reduced in particular size, caution should be taken to keep away from flames and sources of ignition.

SECTION 10 - DOT SHIPPING REQUIREMENTS

NONE

STONBY BEARD STELLITE, INC. assumes no responsibility and makes no warranty, express or implied, representation, promise or statement that the data provided is complete, accurate or current.

HE 00480

HAYNESInternational

cc: R. W. Clemens
A. I. Asphahani
J. L. Nickerson
~~S. Walden~~
J. J. Phillips
File

August 29, 1987

Mr. Frank Modic
Stoody Deloro Stellite, Inc.
610 West Ash Street
Suite 1510
San Diego, CA 92101

Dear Frank:

A copy of your Material Safety Data Sheet (MSDS) No. P2277, copy enclosed, has come to my attention. It relates to your metal powder product identified as "NISTELLE C-22".

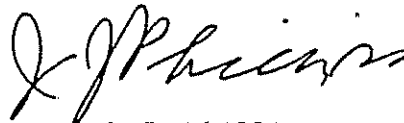
For your information, C-22 is a trademark of Haynes International, Inc. Our registration of the mark has been filed and is pending in the U.S. Patent and Trademark Office.

It appears that your identification of NISTELLE C-22 is a combination of two trademarks suggesting two different sources of product, which is misleading and improper. We suggest as an example, that you may avoid this problem by using your powder product identification: NISTELLE Powder No. P2277" and, if you wish, the added notation "made from C-22" alloy" to indicate the alloy was produced by Haynes International, Inc.

As you know, we must use our trademarks properly to keep them as valuable property.

May we have your comments regarding this matter.

Very truly yours,



Joseph J. Phillips
Manager, Patent & Trademark Dept.

vlw

043ln

HE 00481



COATINGS DIVISION

SAFETY DIRECTOR
1281 Eisenhower Dr., North
Goshen, IN 46526-5336

Telephone
(219)
534-2585

MATERIAL SAFETY DATA SHEET	ALLOY POWDERS	MATERIAL IDENTIFICATION NUMBER P2277	ORIGINAL DATE 7-22-1985 REVISED DATE 11-22-1987
----------------------------	------------------	---	--

SECTION 1 - PRODUCT			SECTION 2 - PHYSICAL PROPERTIES		
PRODUCT IDENTIFICATION TRADE NAME NISTELLE C-22 ALLOY NUMBER 2277	CHEMICAL FAMILY ALLOY	FORMULA Alloy composed of varying concentra- tions of elements listed in Section 3.	FREEZING POINT °F: 2475 MELTING POINT °F: 2550 BOILING POINT: N/A SUBLIMING: N/A EVAPORATION RATE: N/A APPEARANCE: Powder, Gray Color	ODOR: None VAPOR PRESSURE: N/A VAPOR DENSITY(AIR=1): N/A SPECIFIC GRAVITY(H ₂ O=1): 8.69 SOLUBILITY IN WATER: None % VOLATILES BY VOLUME: None	

SECTION 3 - TLV DATA ON PRINCIPAL ALLOY INGREDIENTS					
CONSTITUENT	* NOMINAL PERCENT	CAS NUMBER	NIOSH RTECS NUMBER	EXPOSURE LIMITS (AS mg/m ³) **	
				OSHA PEL	ACGIH TLV
B	-----	7440-42-8	ED3750000	NONE	NONE
C	.08 MAX.	7440-44-0	PF5250100	3.5	7
Co	2.5 MAX.	7440-48-4	GP8750000	.1	.1
Cr	21.3	7440-47-3	GB4200000	1.0	.5
Cu	-----	7440-50-8	GL5325000	DUST 1.0 FUME .1	DUST 1.0 (2.0 STEL) FUME .2
Fe	4.0	1309-37-1	NO7400000	10.0	5.0 FOR IRON OXIDE FUME
Mn	.5 MAX.	7439-96-5	OD9275000	5.0 CEILING	DUST 5.0 CEILING FUME 1.0 (3.0 STEL)
Mo	13.5	7439-98-7	QA4680000	15.0	10.0 (20.0 STEL)
Ni	BALANCE	7440-02-0	QR5950000	1.0	1.0
Si	1.0 MAX.	7440-21-3	VW0400000	NONE	TOTAL DUST 10.0 RESPIRABLE DUST 5.0
V	.35 MAX.	7440-62-2	YW1355000	DUST .5 FUME .1 CEILING (V205)	0.5 AS V205 (DUST AND FUME)
W	3.0	7440-33-7	YO7175000	NONE	5.0 (10.0 STEL)

* Nominal percent content of elemental constituent for alloy.

** Many substances do not have a unique exposure limit. The absence of an exposure limit does not lessen consideration for exposure risk. In the absence of specific information, professional judgement may be required.

SECTION 4 - FIRE AND EXPLOSION HAZARD DATA	
FLASH POINT (WITH TEST METHOD) NONE	FLAMMABLE (EXPLOSIVE) LIMITS V/V% LEL-NONE UEL-NONE
EXTINGUISHING MEDIA	This alloy is noncombustible. Use extinguishing media appropriate to the surrounding fire.
SPECIAL FIREFIGHTING PROCEDURES	If this powder is attritioned or reduced in particle size, caution must be used to prevent fire by avoiding sources of ignition, flames, etc. To extinguish a metal powder fire use dry sand, dry graphite or other class "D" fire extinguishing powder.
UNUSUAL FIRE AND EXPLOSION HAZARDS	No unusual fire or explosion hazards are associated with this material.
GENERAL REACTIVITY	This alloy is a stable material.
INCOMPATIBILITY (MATERIALS TO AVOID)	Avoid contact with mineral acids and oxidizing agents which may generate hydrogen gas; the evolution of hydrogen may be an explosion hazard.
HAZARDOUS DECOMPOSITION PRODUCTS	Various elemental metals and metal oxides may be generated during thermal spraying, welding, metallizing or similar operations. Refer to Section 3 for permissible exposure limits.

HE 00482

PRIMARY ROUTE(S) OF EXPOSURE	INHALATION	Inhalation of metal dust, fume or powder may result from thermal spraying, welding, metallizing or similar operations which generate airborne metal particulate during use of this material.
	INGESTION	Hand, clothing, food and drink contact with metal dust, fume or powder can cause ingestion of particulate during hand to mouth activities such as eating, drinking, smoking, nail biting, etc.
	SKIN	Skin contact with this material may cause, in some sensitive individuals an allergic response if elements such as chromium, cobalt, copper and nickel are present. In the form of metal dust or powder, skin contact or abrasion may also cause irritation or dermatitis.
	EYES	Particulate metal (dust, fume or powder) may be dangerous to the eye and surrounding tissue. Airborne particulate (chips, dust or powder) is always a potential problem as well as inserting fingers into the eye socket if the hand or clothing is contaminated with metal particulate.

SECTION 6 - EMERGENCY AND FIRST AID PROCEDURES

INHALATION	Breathing difficulty caused by inhalation of dust or fume requires removal to fresh air. If breathing has stopped, perform artificial respiration and obtain medical assistance at once.
INGESTION	Swallowing metal powder or dust can be treated by having the affected person swallow large quantities of water and attempting to induce vomiting if conscious. Obtain medical assistance at once.
SKIN	Skin cuts and abrasions can be treated by standard first aid. Skin contamination with dust or powder can be removed by washing with soap and water. If irritation persists obtain medical assistance.
EYES	Dust or powder should be flushed from the eyes with copious amounts of clean water. If irritation persists obtain medical assistance. Contact lenses should not be worn if working with metal dusts and powders.

SECTION 7 - INDUSTRIAL HYGIENE CONTROL MEASURES

VENTILATION	Local exhaust ventilation should be used to control exposure to airborne dust and fume whenever possible.	
RESPIRATORY PROTECTION	Use NIOSH approved respirators as specified by an Industrial Hygienist or qualified Safety Professional. Lung function tests are recommended for users of negative pressure devices.	
PROTECTIVE GLOVES	Wear gloves to prevent metal cuts and skin abrasions.	
EYE PROTECTION	Wear safety glasses when risk of eye injury is present particularly during powder handling.	
OTHER PROTECTIVE EQUIPMENT	Protective clothing such as uniforms, disposable coveralls, safety shoes, etc. may be required during metal handling operations as appropriate to the circumstances of exposure.	
RECOMMENDED MONITORING PROCEDURES	ENVIRONMENTAL SURVEILLANCE	Exposure to the elements identified in Section 3 can be best determined by having air samples taken in the employee breathing zone, work area or department.
	MEDICAL SURVEILLANCE	Lung function tests, chest X-rays and routine physical examinations may be useful to determine effects of dust or fume exposure.

SECTION 8 - ENVIRONMENTAL PROTECTION INFORMATION

STEPS TO BE TAKEN IF MATERIAL IS RELEASED OR SPILLED	In powder or dust form, clean-up should be conducted with a vacuum system utilizing a high efficiency particulate air filtration system. Caution should be taken to minimize airborne generation of powder or dust and avoid contamination of air and water. Properly label all materials collected in waste container.
WASTE DISPOSAL METHOD	Prior to disposal consider if the material has recovery value. State or federal regulations may require specific labeling, packing, storage, transportation and disposal procedures. Contact an Environmental Engineer or consultant familiar with waste disposal regulations.
ENVIRONMENTAL HAZARDS	Metal powders or dusts may have significant impact on air and water quality. Airborne emissions, spills and releases to the environment (discharge to streams, sewer systems, ground water, surface soil, etc.) should be controlled immediately. If such potential for a spill or release exists it is advisable to develop an emergency spill response plan.

SECTION 9 - SPECIAL PRECAUTIONS

HANDLING PRECAUTIONS	This product must be handled according to the size, shape and quantity of material involved. Powders should be moved or transported to minimize spill or release potential.
STORAGE PRECAUTIONS	Store metal and metal powder in a dry area. Do not store adjacent to mineral acids. This is not regarded as a flammable material, however, if this powder is attritioned or reduced in particular size, caution should be taken to keep away from flames and sources of ignition.

SECTION 10 - DOT SHIPPING REQUIREMENTS

NONE

STELLITE INC. assumes no responsibility and makes no warranty, express or implied, representation, promise or statement that the data provided is complete, accurate or current.

HE 00483

HAYNES**International****HASTELLOY®**
Corrosion-Resistant Alloys**HASTELLOY® and ULTIMET™ Castings**

In a continuing effort to satisfy the growing need for HASTELLOY quality castings, Haynes International, Inc. has licensed its technology to certain premier producers of sand and investment castings. The companies listed below are the approved foundries offering corrosion- and wear-resistant castings **with specified quality control programs**. The products include *ULTIMET* and *HASTELLOY B-2, C-4C, C-22™, C-276, and G-30®* castings.

CASTING LICENSEES
HASTELLOY and ULTIMET alloys

Maggotteaux S.A.
B-4601 Vaux-sous-Chevremont
BELGIUM

J. Gaspar
Tel: 32 41 67 47 04
Fax: 32 41 67 08 46

Magalloy Ltd.
10 Pine Street
Stratford, Ontario N5A 1W3
CANADA

Al Batten
Tel: 519 273-2330
Fax: 519 273-4088

Otto Junker GmbH
D-5107 Simmerath
Postfach 1180
Lammersdorf
GERMANY

G. Knoppke
Tel: 49 24 73 601 452
Fax: 49 24 73 601 286

Deloro Stellite GmbH
Zur Bergpflege 53
D-5400 Koblenz
GERMANY

E. Reinbacher
Tel: 49 261 80 880
Fax: 49 261 80 8823

Fondinox S.p.A.
Via Marconi 46-48
26010 Sergnano (CR)
ITALY

A. Morini
Tel: 39 373 455050
Fax: 39 373 455100

Goodwin Steel Castings Ltd.
Ivy House Foundry
Hanley
Stoke on Trent
ST1 3NR, **UNITED KINGDOM**

S. Birks
Tel: 44 78 220 8040
Fax: 44 78 220 8060

REMELT CASTING LICENSEES
HASTELLOY and ULTIMET alloys**HE 00563**

Cannon-Muskegon
P.O. Box 506
Muskegon, MICHIGAN 49443
USA

Ted Klemp
Tel: 616 755-1681
Fax: 616 755 4016

HASTELLOY, ULTIMET, C-22, and G-30 are trademarks of Haynes International, Inc.

BUDGET UNIT	NAME	QTY	UNIT PRICE	TOTAL
532	MARKET DEVELOPMENT	110	EXEMPT SALARY	
532	MARKET DEVELOPMENT	111	NON-EXEMPT SALARY	
532	MARKET DEVELOPMENT	112	EXCESS OF BASE	
532	MARKET DEVELOPMENT	141	FRINGE BENEFITS	
532	MARKET DEVELOPMENT	224	REWORK	
532	MARKET DEVELOPMENT	508	ALL OTHER B & G	
532	MARKET DEVELOPMENT	538	OUTSIDE PURCHASE VEHICLE	
532	MARKET DEVELOPMENT	508	ALL OTHER FREIGHT	
532	MARKET DEVELOPMENT	740	DEPRECIATION	
532	MARKET DEVELOPMENT	751	ENVIRONMENT - PERMIT	
532	MARKET DEVELOPMENT	803	ALL OTHER ADVERTISING	
532	MARKET DEVELOPMENT	813	SALES AIDS & SERVICES	
532	MARKET DEVELOPMENT	816	SAMPLES & DISPLAYS	
532	MARKET DEVELOPMENT	822	PHONE-EQUIP	
532	MARKET DEVELOPMENT	823	TELEPHONE - LOCAL	
532	MARKET DEVELOPMENT	827	TELEPHONE - MOBILE	
532	MARKET DEVELOPMENT	829	OTHER	
532	MARKET DEVELOPMENT	882	OUTSIDE PRINTING	
532	MARKET DEVELOPMENT	910	CONSULTANTS	
532	MARKET DEVELOPMENT	912	CLERICAL AGENCY FEES	
532	MARKET DEVELOPMENT	913	CONTRACTED SERVICES	
532	MARKET DEVELOPMENT	920	PROFESSIONAL	
532	MARKET DEVELOPMENT	921	CONF. SCHOOLS &	
532	MARKET DEVELOPMENT	928	EMP DEVELOPMENT	
532	MARKET DEVELOPMENT	930	OFFICE SUPPLIES	
532	MARKET DEVELOPMENT	933	OFFICE EQUIP	
532	MARKET DEVELOPMENT	938	OUTER OFFICE SUP & EQP	
532	MARKET DEVELOPMENT	943	ENTRANCE MOVING	
532	MARKET DEVELOPMENT	943	HOUSING PROGRAM	
532	MARKET DEVELOPMENT	945	PER	
532	MARKET DEVELOPMENT	960	AUTO OPERATION -	
532	MARKET DEVELOPMENT	961	AUTO OPER - COMPANY	
532	MARKET DEVELOPMENT	962	AUTO OPER - EMPLOYEE	
532	MARKET DEVELOPMENT	963	AIR/AUT TEMPORARY	
532	MARKET DEVELOPMENT	964	TRAVEL MEALS	
532	MARKET DEVELOPMENT	966	TRAVEL LODGING	
532	MARKET DEVELOPMENT	966	GUEST ENTERTAINMENT	
532	MARKET DEVELOPMENT	967	BUSINESS MEALS	
532	MARKET DEVELOPMENT	969	ALL OTHER TRAVEL &	
532	MARKET DEVELOPMENT	981	INTERNAL PROD-	
		988	Label	
532	MARKET DEVELOPMENT	999	ALL OTHER ADMIN COSTS	
532				
538	ADVERTISING	124	MAINTENANCE MATERIAL	
538	ADVERTISING	800	ADVERTISING SPACE	
538	ADVERTISING	801	ADVERTISING	
538	ADVERTISING	802	AUDIOVISUALS	
538	ADVERTISING	803	PHOTOGRAPHIC	
538	ADVERTISING	804	PUBLICITY	
538	ADVERTISING	805	NEW PRODUCT	
538	ADVERTISING	808	ALL OTHER ADVERTISING	
538	ADVERTISING	810	SALES LITERATURE	
538	ADVERTISING	811	CATALOGS & DIRECTORS	
538	ADVERTISING	812	DIGEST	
538	ADVERTISING	813	SALES AIDS & SERVICES	
538	ADVERTISING	814	TRADE SHOWS	
538	ADVERTISING	816	SAMPLES & DISPLAYS	
538	ADVERTISING	817	TECHNICAL SKILLINGS	
538	ADVERTISING	822	OUTSIDE PRINTING	
538	ADVERTISING	832	BOOKS, PAMPHLETS, & PER	
538	ADVERTISING	866	GUEST ENTERTAINMENT	

This copy redacted for Court filing.
Unredacted version produced to Defendant.

VENDOR LOG OF PRINT JOBS

JOB#	VENDOR	PO #	REL #	INVOICE	QUANTITY	SUBJECT	PRICE	# OF PAGES
940127	MODERN	1030783	99	165646-01	5000	H-2069 C-22 REFERENCE GUIDE	1157.00	
950137	KOKOMO LITHO	80504	99	35832	2262	H-2019D C-22 BROCHURE	5202.60	
960180	KOKOMO LITHO	80504		36551	1990	H-2019D C-22 BROCHURE	4676.50	
970348	XEROX				15	HIGHEST VOLTAGE FOR C-22, G-30 & TI-2		
970681	HUMPHREY	63219		9331P	2000	h-2019e c-22	12,118.00	
980572	HUMPHREY	63219		5194	2000	h-2019e c-22	9286.00	
982260	HUMPHREY	63219		5194	2000	h-2019e c-22	7931.89	
982451	XEROX				1	ALLOY C-22		
983001	XEROX				5	C-22 STRIP WITH TEARS		
983002	XEROX				5	C-22 STRIP WITH TEARS		
983003	XEROX				5	C-22 STRIP WITH TEARS		
983352	IKON				1000	H-2066C C-22 Welding Data Technical Information		
984482	SHEAFER	1035042	138		7000	H-2120 G-22 H&A Alloy at a Glance-	1221.98	

13

41593.32
 -1221.98
 40371.34
 1992-2004
 1342415
 211554/41
 total for C-22
 H-2019d
 H-2069
 H-2120

HE 00567

HAYNES INTERNATIONAL, INC.

Printing Request

Shelly Morris 456-6204
John Browning 456-6444

JOB# 984172 DATE IN 2/5/2004

PO # 63219

REL #

NB PO#

C=COLOR, BW=BLACK/WHITE, B=BOTH
BWC=BLACK & WHITE ON COLOR MACHINE,

VENDOR HUMPHREY
INVOICE

COPIER
REQUESTOR STEVE COREY

JOB OUT TO PRINTER

/COPYROOM

2/5/2004

DEPT 810
CHARGE 810

JOB COMPLETE

3/24/2004

PRIORITY 1

H-1101A Specifications - CRA

ORDER SENT TO PRINTER BY
ENTER CLOCK NUMBER

SUBJECT
STOCK
OF PAGES
PAGE DEFINITION
OF COLOR
BINDERY
PACKAGING
PRICE
\$LAYOUT

QUANTITY ORIGINALS SIDES IMPRESSIONS

2000

0

80# GLOSS COVER

OF PAGES

TXT PG

PCT PG

8-1/2

4 - COLOR PROCESS PLUS LOGO RED 032 & GRAY

SHRINK WRAP IN 50'S

BINDERY

PACKAGING

PRICE 1453.16

\$LAYOUT

PRINT ONE SIDE

PRINT TWO SIDES

HEAD TO HEAD

HEAD TO FOOT

SADDLE STITCH

LEFT HAND GATHER

PUNCH

PAD

X

X

/PAD

COMMENTS **LAYOUT PROVIDED ON DISK like old invoice 21482**

Please provide blueline proof before printing, WILL PAY ONLY FOR 3% OVERRUN,
ARTWORK TO BE RETURNED TO HAYNES UPON COMPLETION OF JOB

STATUS

HIE 00568

HAYNES INTERNATIONAL, INC.

Printing Request

Shelly Morris 456-6204
John Browning 456-6444

JOB# 982948 DATE IN 2/12/2001

PO # 63219

REL #

NB PO#

C=COLOR, BW=BLACK/WHITE, B=BOTH
BWC=BLACK & WHITE ON COLOR MACHINE,

VENDOR HUMPHREY

INVOICE 21482

COPIER

REQUESTOR STEVE COREY

DEPT 810

CHARGE 810

PRIORITY 1

JOB OUT TO PRINTER

/COPYROOM

2/12/2001

JOB COMPLETE

4/11/2001

H-1101 Specifications - CRA

ORDER SENT TO PRINTER BY
ENTER CLOCK NUMBER

SUBJECT	2000	0
STOCK	80# GLOSS COVER	
# OF PAGES	2	# TXT PG
PAGE DEFINITION	8-1/2	# PCT PG
# OF COLOR	4 - COLOR PROCESS PLUS LOGO RED 032 & GRAY	
BINDERY	SHRINK WRAP IN 50'S	
PACKAGING		
PRICE	1453.16	
\$LAYOUT		

QUANTITY	ORIGINALS	SIDES	IMPRESSIONS
----------	-----------	-------	-------------

PRINT ONE SIDE	
PRINT TWO SIDES	X
HEAD TO HEAD	X
HEAD TO FOOT	
SADDLE STITCH	
LEFT HAND GATHER	
PUNCH	
PAD	/PAD

COMMENTS

LAYOUT PROVIDED ON DISK - Lotus document WORD PRO

Please provide blue line proof before printing, WILL PAY ONLY FOR 3% OVERRUN,
ARTWORK TO BE RETURNED TO HAYNES UPON COMPLETION OF JOB

STATUS

HE 00569

HAYNES INTERNATIONAL, INC.

Printing Request

Shelly Morris 456-6204
John Browning 456-6444

JOB# 940127

DATE IN

PO # 1030783

REL # 99

NB PO#

COPIER

C=COLOR, BW=BLACK/WHITE, B=BOTH
BWC=BLACK & WHITE ON COLOR MACHINE,

VENDOR

MODERN GRAPHICS

REQUESTOR

MIKE ROTHMAN

INVOICE

165646-01

DEPT

588

JOB OUT TO PRINTER

/COPYROOM

8/22/1994

CHARGE

588-810

JOB COMPLETE

9/8/1994

PRIORITY

H-2069 C-22 REFERENCE GUIDE

ORDER SENT TO PRINTER BY
ENTER CLOCK NUMBER

SUBJECT:
STOCK
OF PAGES
PAGE DEFINITION
OF COLOR
BINDERY
PACKAGING
PRICE
LAYOUT

QUANTITY	ORIGINALS	SIDES	IMPRESSIONS
5000			0
80# TAHOE GLOSS			
# TXT PG			# PCT PG

PRINT ONE SIDE
PRINT TWO SIDES
HEAD TO HEAD
HEAD TO FOOT
SADDLE STITCH
LEFT HAND GATHER
PUNCH
PAD

/PAD

1157.00

COMMENTS

REFER TO OLD INV# 144604-01 FOR
PRINTING SPECS AND QUOTE EST.
12921 FOR CURRENT PRICE

STATUS

JAYNES INTERNATIONAL, INC.

Printing Request

Shelly Morris 456-6204
John Browning 456-6444

JOB #	940127	DATE IN		PO #	1030783	REL #	99
-------	--------	---------	--	------	---------	-------	----

NB PO#

COPIER	C=COLOR, BW=BLACK/WHITE, B=BOTH	VENDOR	MODERN GRAPHICS
REQUESTOR	MIKE ROTHMAN	INVOICE	165646-01
DEPT	588	JOB OUT TO PRINTER	/COPYROOM
CHARGE	588-810	JOB COMPLETE	8/22/1994
PRIORITY			9/8/1994

H-2069 C-22 REFERENCE GUIDE

QUANTITY	ORIGINALS	SIDES	IMPRESSIONS
----------	-----------	-------	-------------

SUBJECT	H-2069 C-22 REFERENCE GUIDE
STOCK	80# TAHOE GLOSS
# OF PAGES	5000
# OF COLOR	0
BINDERY	
PACKAGING	
PRICE	1157.00
SLAYOUT	

ORDER SENT TO PRINTER BY
ENTER CLOCK NUMBER

PRINT ONE SIDE
PRINT TWO SIDES
HEAD TO HEAD
HEAD TO FOOT
SADDLE STITCH
LEFT HAND GATHER
PUNCH
PAD

/PAD

COMMENTS
REFER TO OLD INV# 144604-01 FOR
PRINTING SPECS AND QUOTE EST.
12921 FOR CURRENT PRICE

STATUS

JAYNES INTERNATIONAL, INC.

Printing Request

Shelly Morris 456-6204
John Browning 456-6444

JOB #	950137	DATE IN	8/25/1995	PO #	80504	REL #	99
-------	--------	---------	-----------	------	-------	-------	----

NB PO #

COPIER	C=COLOR, BW=BLACK/WHITE, B=BOTH	VENDOR	KOKOMO LITHO
REQUESTOR	MIKE ROTHMAN	INVOICE	35832
DEPT	588	JOB OUT TO PRINTER	/COPYROOM 8/25/1995
CHARGE	588-810	JOB COMPLETE	9/7/1995

PRIORITY

SUBJECT: H-2019D C-22 BROCHURE

QUANTITY	ORIGINALS	SIDES	IMPRESSIONS
----------	-----------	-------	-------------

2262

0

STOCK

80# NORTHWEST GLOSS TEXT THROUGHOUT

OF PAGES

TXT PG

PCT PG

PAGE DEFINITION

8-1/2 X 11

OF COLOR

BINDERY

SADDLESTICH

PACKAGING

SHRINKWRAP IN 25'S

PRICE

5202.60

LAYOUT

ORDER SENT TO PRINTER BY
ENTER CLOCK NUMBER

PRINT ONE SIDE

PRINT TWO SIDES

HEAD TO HEAD

HEAD TO FOOT

SADDLESTICH

LEFT HAND GATHER

PUNCH

PAD

X
X
X
X
X
X
/PAD

COMMENTS

STATUS

HAYNES INTERNATIONAL, INC.

Printing Request

Shelly Morris 456-6204
John Browning 456-6444

JOB# 960180 DATE IN 8/9/1996

PO # 80504

REL #

NB PO#

COPIER

C=COLOR, BW=BLACK/WHITE, B=BOTH
BWC=BLACK & WHITE ON COLOR MACHINE,

VENDOR KOKOMO LITHO
INVOICE 36551

REQUESTOR JIM LAIRD

DEPT 588

JOB OUT TO PRINTER

/COPYROOM

8/9/1996

CHARGE 588-810

JOB COMPLETE

10/1/1996

PRIORITY

H-2019D C-22 BROCHURE

ORDER SENT TO PRINTER BY
ENTER CLOCK NUMBER

SUBJECT	QUANTITY	ORIGINALS	SIDES	IMPRESSIONS
STOCK	1990			0
# OF PAGES	80#	NORTHWEST GLOSS TEXT THROUGHOUT		
PAGE DEFINITION		# TXT PG		# PCT PG
# OF COLOR	8-1/2 X 11			
BINDERY	~PMS 301, 430, BLK			
PACKAGING	SADDLESTICH			
	SHRINKWRAP IN 25'S			
PRICE	4676.50			
LAYOUT				

PRINT ONE SIDE	
PRINT TWO SIDES	X
HEAD TO HEAD	X
HEAD TO FOOT	
SADDLE STICH	
LEFT HAND GATHER	
PUNCH	X
PAD	/PAD

COMMENTS REPRINT OF YOUR INVOICE 35832

PLEASE CHANGE BACK COVER PROVIDED ON DISK FORMAT BY

HAYNES

PLEASE PROVIDE BLUE LINE PROOF TO SHELLY MORRIS
COVER COLOR TO MATCH SAMPLE PROVIDED

STATUS

HE 00573

HAYNES INTERNATIONAL, INC.

Printing Request

Shelly Morris 456-6204
John Browning 456-6444

JOB# 970681 DATE IN 10/10/1997 PO # 63219 REL #

NB PO#

COPIER C=COLOR, BW=BLACK/WHITE, B=BOTH
REQUESTOR STEVE COREY BWC=BLACK & WHITE ON COLOR MACHINE,
DEPT 588 VENDOR HUMPHREY
CHARGE 588-910 INVOICE 9331P
JOB OUT TO PRINTER /COPYROOM 10/10/1997
JOB COMPLETE 11/3/1997

PRIORITY h-2019e c-22

QUANTITY ORIGINALS SIDES IMPRESSIONS

SUBJECT: h-2019e c-22
STOCK 24 PAGE BROCHURE
OF PAGES 2000
PAGE DEFINITION 0
OF COLOR # TXT PG # PCT PG
BINDERY
PACKAGING
PRICE 12,118.00
\$LAYOUT

ORDER SENT TO PRINTER BY
ENTER CLOCK NUMBER

PRINT ONE SIDE
PRINT TWO SIDES
HEAD TO HEAD
HEAD TO FOOT
SADDLE STITCH
LEFT HAND GATHER
PUNCH
PAD /PAD

COMMENTS humphrey's did layout and printing

STATUS

HAYNES INTERNATIONAL, INC.

Printing Request

Shelly Morris 456-6204
John Browning 456-6444

JOB #	980572	DATE IN	8/18/1998	PO #	63219	REL #	
-------	--------	---------	-----------	------	-------	-------	--

NB PO#

COPIER	C=COLOR, BW=BLACK/WHITE, B=BOTH	VENDOR	HUMPHREY
REQUESTOR	STEVE COREY	INVOICE	5194
DEPT	588	JOB OUT TO PRINTER	/COPYROOM 8/18/1998
CHARGE	588-910	JOB COMPLETE	10/14/1998

PRIORITY

h-2019e c-22

QUANTITY	ORIGINALS	SIDES	IMPRESSIONS
----------	-----------	-------	-------------

2000			0
STOCK	24 PAGE BROCHURE		
# OF PAGES	# TXT PG		# PCT PG

PAGE DEFINITION

# OF COLOR	BINDERY
PACKAGING	PRICE
\$LAYOUT	

ORDER SENT TO PRINTER BY
ENTER CLOCK NUMBER

PRINT ONE SIDE
PRINT TWO SIDES
HEAD TO HEAD
HEAD TO FOOT
SADDLE STITCH
LEFT HAND GATHER
PUNCH
PAD

/PAD

COMMENTS YOUR LAST TICKET NUMBER 9331P

humphrey's did layout and printing

Case 1:04-cv-00197-MBC Document 54-1 Filed 11/07/2005 Page 88 of 143

STATUS

HE 00575

HAYNES INTERNATIONAL, INC.

Printing Request

Shelly Morris 456-6204
John Browning 456-6444

JOB# 982260 DATE IN 4/28/2000

PO # 63219

REL #

NB PO#

C=COLOR, BW=BLACK/WHITE, B=BOTH
BWC=BLACK & WHITE ON COLOR MACHINE.

VENDOR HUMPHREY

INVOICE 5194

COPIER

REQUESTOR STEVE COREY

DEPT 588

CHARGE 588-910

JOB OUT TO PRINTER

/COPYROOM

4/28/2000

JOB COMPLETE

5/12/2000

PRIORITY

h-2019e c-22

ORDER SENT TO PRINTER BY
ENTER CLOCK NUMBER

SUBJECT:	h-2019e c-22
QUANTITY	2000
ORIGINALS	24 PAGE BROCHURE
SIDES	
IMPRESSIONS	0
# OF PAGES	
# TXT PG	
# PCT PG	
PAGE DEFINITION	
# OF COLOR	
BINDERY	
PACKAGING	
PRICE	
\$LAYOUT:	

PRINT ONE SIDE
PRINT TWO SIDES
HEAD TO HEAD
HEAD TO FOOT
SADDLE STITCH
LEFT HAND GATHER
PUNCH
PAD

/PAD

COMMENTS Reprint same except use new art for the back page.

YOUR LAST TICKET NUMBER 5194

Will pay for only #% overrun

Artwork & Films to be returned to haynes when job is complete.

STATUS

HAYNES INTERNATIONAL, INC.

Printing Request

Shelly Morris 456-6204
John Browning 456-6444

JOB# 984482 DATE IN 10/4/2004

PO # 1035042

REL # 138

NB PO# 1032247

COPIER

C=COLOR, BW=BLACK&WHITE, B=BOTH
BWC=BLACK & WHITE ON COLOR MACHINE,

VENDOR SHEARER
INVOICE

REQUESTOR STEVE COREY

DEPT 588-810

JOB OUT TO PRINTER

/COPYROOM

10/4/2004

CHARGE

JOB COMPLETE

7/15/2004

PRIORITY

H-2120 C-22HS Alloy at a Glance

ORDER SENT TO PRINTER BY
ENTER CLOCK NUMBER

SUBJECT	QUANTITY	ORIGINALS	SIDES	IMPRESSIONS
STOCK	7000			0
# OF PAGES	1	# TXT PG	# PCT PG	
PAGE DEFINITION	8-1/2 X 11			
# OF COLOR	2-COLOR (BLACK AND PROCESS BLUE)			
BINDERY				
PACKAGING	SHRINK WRAP IN 50			
PRICE				
\$LAYOUT	602.49			

PRINT ONE SIDE	X
PRINT TWO SIDES	X
HEAD TO HEAD	X
HEAD TO FOOT	
SADDLE STITCH	
LEFT HAND GATHER	
PUNCH	X
PAD	/PAD

COMMENTS Print to 100% (I needed to print at 98% to get boarders off Haynes color printer).

Please send proof to Shelly Morris before printing.

3-hole punch

Artwork on disk provided - Created on PC in PageMaker 6.5 - Most fonts are Helvetica

STATUS

HE 00577

Printing Request

HAYNES INTERNATIONAL, INC.

Shelly Morris 456-6204
John Browning 456-6444

JOB# 930127 DATE IN 6/29/1993

PO # 80504

REL # 93

NB PO#

COPIER C=COLOR, BW=BLACK/WHITE, B=BOTH
REQUESTOR STEVE COREY BWC=BLACK & WHITE ON COLOR MACHINE.

VENDOR KOKOMO LITHO
INVOICE

DEPT 588

JOB OUT TO PRINTER

/COPYROOM

6/29/1993

CHARGE 588-810

JOB COMPLETE

7/12/1993

PRIORITY

SUBJECT:

H-2092B

QUANTITY ORIGINALS SIDES IMPRESSIONS

ORDER SENT TO PRINTER BY
ENTER CLOCK NUMBER

STOCK
OF PAGES
PAGE DEFINITION
OF COLOR
BINDERY
PACKAGING
PRICE
\$LAYOUT

TXT PG

PCT PG

1290.00

PRINT ONE SIDE
PRINT TWO SIDES
HEAD TO HEAD
HEAD TO FOOT
SADDLE STITCH
LEFT HAND GATHER
PUNCH
PAD

/PAD

COMMENTS PRINTING DIRECTIONS ON PO

STATUS

Printing Request

HAYNES INTERNATIONAL, INC.

Shelly Morris 456-6204
John Browning 456-6444

JOB# 970772 DATE IN 11/17/1997

PO # 63219

REL #

NB PO#

COPIER

C=COLOR, BW=BLACK/WHITE, B=BOTH
BWC=BLACK & WHITE ON COLOR MACHINE,

VENDOR HUMPHREY
INVOICE 9672P

REQUESTOR

STEVE COREY

DEPT

588

JOB OUT TO PRINTER

/COPYROOM

11/17/1997

CHARGE

588-810

JOB COMPLETE

12/15/1997

PRIORITY

H-2092C CRA POCKET GUIDE

ORDER SENT TO PRINTER BY
ENTER CLOCK NUMBER

SUBJECT	QUANTITY	ORIGINALS	SIDES	IMPRESSIONS
STOCK	2000			0
# OF PAGES	80# WHITE NORTHWEST GLOSS			
PAGE DEFINITION	9X16			
# OF COLOR	4-COLOR PROCESS			
BINDERY				
PACKAGING				
PRICE	1842.00			
SLAYOUT				

PRINT ONE SIDE	PRINT TWO SIDES
HEAD TO HEAD	HEAD TO FOOT
SADDLE STITCH	LEFT HAND GATHER
PUNCH	PAD
	/PAD

COMMENTS HUMPHREY'S ASSUMED OLD JOBS FROM KOKOMO LITHO NEGATIVES ON FILE.
STRIP IN NEW CHANGES ON OLD NEGS, NO COMPUTER ART AVAILABLE

STATUS

HE 00579

Printing Request

HAYNES INTERNATIONAL, INC.

Shelly Morris 456-6204
John Browning 456-6444

JOB# 940127

DATE IN

PO # 1030783

REL # 99

NB PO#

COPIER

C=COLOR, BW=BLACK/WHITE, B=BOTH
BWC=BLACK & WHITE ON COLOR MACHINE,

VENDOR

MODERN GRAPHICS

REQUESTOR

MIKE ROTHMAN

INVOICE 165646-01

DEPT

588

JOB OUT TO PRINTER

/COPYROOM

8/22/1994

CHARGE

588-810

JOB COMPLETE

9/8/1994

PRIORITY

H-2069 C-22 REFERENCE GUIDE

ORDER SENT TO PRINTER BY
ENTER CLOCK NUMBER

SUBJECT:	
STOCK	80# TAHOE GLOSS
# OF PAGES	5000
PAGE DEFINITION	
# OF COLOR	
BINDERY	
PACKAGING	
PRICE	1157.00
LAYOUT	

QUANTITY	ORIGINALS	SIDES	IMPRESSIONS
5000			0

PRINT ONE SIDE	
PRINT TWO SIDES	
HEAD TO HEAD	
HEAD TO FOOT	
SADDLE STITCH	
LEFT HAND GATHER	
PUNCH	
PAD	

/PAD

COMMENTS

REFER TO OLD INV# 144604-01 FOR
PRINTING SPECS AND QUOTE EST.
12921 FOR CURRENT PRICE

STATUS

Printing Request

HAYNES INTERNATIONAL, INC.

Shelly Morris 456-6204
John Browning 456-6444

JOB# 982948 DATE IN 2/12/2001

PO # 63219

REL #

NB PO#

COPIER

C=COLOR, BW=BLACK/WHITE, B=BOTH
BWG=BLACK & WHITE ON COLOR MACHINE,

VENDOR HUMPHREY

REQUESTOR STEVE COREY

INVOICE 21482

DEPT 810

JOB OUT TO PRINTER

/COPYROOM

2/12/2001

CHARGE 810

JOB COMPLETE

4/11/2001

PRIORITY 1

H-1101 Specifications - CRA

ORDER SENT TO PRINTER BY
ENTER CLOCK NUMBER

SUBJECT	H-1101 Specifications - CRA		
QUANTITY	ORIGINALS	SIDES	IMPRESSIONS
2000			0
STOCK	80# GLOSS COVER		
# OF PAGES	2	# TXT PG	# PCT PG
PAGE DEFINITION	8-1/2		
# OF COLOR	4 - COLOR PROCESS PLUS LOGO RED 032 & GRAY		
BINDERY	SHRINK WRAP IN 50'S		
PACKAGING			
PRICE	1453.16		
LAYOUT			

PRINT ONE SIDE	X
PRINT TWO SIDES	X
HEAD TO HEAD	X
HEAD TO FOOT	
SADDLE STITCH	
LEFT HAND GATHER	
PUNCH	
PAD	/PAD

COMMENTS **LAYOUT PROVIDED ON DISK - Lotus document WORD PRO**

Please provide blue-line proof before printing, WILL PAY ONLY FOR 3% OVERRUN, ARTWORK TO BE RETURNED TO HAYNES UPON COMPLETION OF JOB

STATUS

HE 00581

Printing Request

HAYNES INTERNATIONAL, INC.

Shelly Morris 456-6204
John Browning 456-6444

JOB# 984172 DATE IN 2/5/2004

PO # 63219

REL #

NB PO#

COPIER C=COLOR, BW=BLACK/WHITE, B=BOTH
REQUESTOR STEVE COREY BWC=BLACK & WHITE ON COLOR MACHINE,

VENDOR HUMPHREY
INVOICE

DEPT 810

JOB OUT TO PRINTER

/COPYROOM 2/5/2004

CHARGE 810

JOB COMPLETE 3/24/2004

PRIORITY 1

SUBJECT: H-1101A Specifications - CRA

QUANTITY ORIGINALS SIDES IMPRESSIONS

2000 0

STOCK 80# GLOSS COVER

OF PAGES 2 # TXT PG # PCT PG

PAGE DEFINITION

8-1/2

OF COLOR 4 - COLOR PROCESS PLUS LOGO RED 032 & GRAY

BINDERY SHRINK WRAP IN 50'S

PACKAGING

PRICE 1453.16

\$LAYOUT

ORDER SENT TO PRINTER BY
ENTER CLOCK NUMBER

PRINT ONE SIDE X
PRINT TWO SIDES X
HEAD TO HEAD X
HEAD TO FOOT
SADDLE STITCH
LEFT HAND GATHER
PUNCH
PAD /PAD

COMMENTS LAYOUT PROVIDED ON DISK like old invoice 21482

Please provide blueine proof before printing, WILL PAY ONLY FOR 3% OVERRUN,
ARTWORK TO BE RETURNED TO HAYNES UPON COMPLETION OF JOB

STATUS

HE 00582

Printing Request

JAYNES INTERNATIONAL, INC.

Shelly Morris 456-6204
John Browning 456-6444

JOB# 980703 DATE IN 9/28/1998

PO # 63219

REL #

NB PO#

COPIER C=COLOR, BW=BLACK/WHITE, B=BOTH
BWC=BLACK & WHITE ON COLOR MACHINE,
REQUESTOR STEVE COREY
DEPT 588
CHARGE 588-810

VENDOR HUMPHREY
INVOICE TICKET NO 5944

JOB OUT TO PRINTER /COPYROOM

JOB COMPLETE 9/28/1998
10/5/1998

PRIORITY

H-2092C CRA POCKET GUIDE

ORDER SENT TO PRINTER BY
ENTER CLOCK NUMBER

SUBJECT	QUANTITY	ORIGINALS	SIDES	IMPRESSIONS
STOCK	3500			0
# OF PAGES	80# WHITE NORTHWEST GLOSS			
PAGE DEFINITION	# TXT PG			# PCT PG
# OF COLOR	9X16			
BINDERY	4-COLOR PROCESS			
PACKAGING				
PRICE				
SLAYOUT				

PRINT ONE SIDE
PRINT TWO SIDES
HEAD TO HEAD
HEAD TO FOOT
SADDLE STITCH
LEFT HAND GATHER
PUNCH
PAD
/PAD

COMMENTS REPEAT OF YOUR OLD JOB NUMBER 9672P

REQUESTED 2500, THEY RAN 3500

STATUS

LAYNES INTERNATIONAL, INC.

Printing Request

Shelly Morris 456-6204
John Browning 456-6444

JOB#	970348	DATE IN	5/8/1997	PO #		REL #	
------	--------	---------	----------	------	--	-------	--

NB PO#

COPIER	BWC	C=COLOR, BW=BLACK/WHITE, B=BOTH	VENDOR	XEROX
REQUESTOR	BECKY HORNER	BWC=BLACK & WHITE ON COLOR MACHINE.	INVOICE	
DEPT	816		JOB OUT TO PRINTER	/COPYROOM
CHARGE	816-96-892		JOB COMPLETE	5/8/1997

PRIORITY

HIGHEST VOLTAGE FOR C-22,G-30 & T1-2

QUANTITY	ORIGINALS	SIDES	IMPRESSIONS
----------	-----------	-------	-------------

STOCK	15	1	1	15
# OF PAGES	8 1/0 X 11 20#	WHITE		
# TXT PG			# PCT PG	

PAGE DEFINITION

# OF COLOR	
BINDERY	
PACKAGING	
PRICE	
SLAYOUT	

ORDER SENT TO PRINTER BY
ENTER CLOCK NUMBER

PRINT ONE SIDE	X
PRINT TWO SIDES	
HEAD TO HEAD	
HEAD TO FOOT	
SADDLE STITCH	
LEFT HAND GATHER	
PUNCH	
PAD	/PAD

COMMENTS

STATUS

LAYNES INTERNATIONAL, INC.

Printing Request

Shelly Morris 456-6204
John Browning 456-6444

JOB#	982451	DATE IN	6/30/2000	PO #		REL #	
------	--------	---------	-----------	------	--	-------	--

NB PO#

COPIER	C	C=COLOR, BW=BLACK/WHITE, B=BOTH	VENDOR	XEROX
REQUESTOR	ED BICKEL	BWC=BLACK & WHITE ON COLOR MACHINE,	INVOICE	
DEPT	532			
CHARGE	532-96-892			
PRIORITY				
		JOB OUT TO PRINTER	/COPYROOM	6/30/2000
		JOB COMPLETE		6/30/2000

ORDER SENT TO PRINTER BY	
ENTER CLOCK NUMBER	

SUBJECT	ALLOY C-22		
QUANTITY	ORIGINALS	SIDES	IMPRESSIONS
1	21	1	21
STOCK	60#	WHITE	
# OF PAGES		# TXT PG	# PCT PG
PAGE DEFINITION	8.5 X 11		
# OF COLOR	4		
BINDERY			
PACKAGING			
PRICE			
LAYOUT			

PRINT ONE SIDE	X
PRINT TWO SIDES	
HEAD TO HEAD	
HEAD TO FOOT	
SADDLE STITCH	
LEFT HAND GATHER	
PUNCH	
PAD	/PAD

COMMENTS

STATUS

LAYNES INTERNATIONAL, INC.

Printing Request

Shelly Morris 456-6204
John Browning 456-6444

JOB# 983001 DATE IN 2/21/2001

PO #

REL #

NB PO#

COPYER BWC

C=COLOR, BW=BLACK/WHITE, B=BOTH
BWC=BLACK & WHITE ON COLOR MACHINE.

VENDOR XEROX
INVOICE

REQUESTOR MARK ROWE

DEPT 814

JOB OUT TO PRINTER

/COPYROOM

2/21/2001

CHARGE 814-96-892

JOB COMPLETE

2/21/2001

PRIORITY

SUBJECT

C-22 STRIP WITH TEARS

ORDER SENT TO PRINTER BY
ENTER CLOCK NUMBER

QUANTITY	ORIGINALS	SIDES	IMPRESSIONS
5	3	1	15
STOCK	24#	WHITE	
# OF PAGES	# TXT PG	# PCT PG	
PAGE DEFINITION	8.5 X 11		
# OF COLOR	BLACK		
BINDERY			
PACKAGING			
PRICE			
\$LAYOUT			

PRINT ONE SIDE	X
PRINT TWO SIDES	
HEAD TO HEAD	
HEAD TO FOOT	
SADDLE STITCH	
LEFT HAND GATHER	
PUNCH	
PAD	/PAD

COMMENTS

Case 1:04-cv-00197-MBC Document 54-1 Filed 11/07/2005
STATUS

HE 00586

HAYNES INTERNATIONAL, INC.

Printing Request

Shelly Morris 456-6204
John Browning 456-6444

JOB# 983002 DATE IN 2/21/2001

PO #

REL #

NB PO#

COPIER C C=COLOR, BW=BLACK/WHITE, B=BOTH
REQUESTOR MARK ROWE BWC=BLACK & WHITE ON COLOR MACHINE,
DEPT 814
CHARGE 814-96-892

VENDOR XEROX
INVOICE

JOB OUT TO PRINTER /COPYROOM 2/21/2001
JOB COMPLETE 2/21/2001

PRIORITY

C-22 STRIP WITH TEARS

ORDER SENT TO PRINTER BY
ENTER CLOCK NUMBER

SUBJECT	QUANTITY	ORIGINALS	SIDES	IMPRESSIONS
STOCK	5	3	1	15
# OF PAGES	24#	WHITE		
PAGE DEFINITION	8.5 X 11			
# OF COLOR	BLACK			
BINDERY				
PACKAGING				
PRICE				
\$LAYOUT				

PRINT ONE SIDE X
PRINT TWO SIDES
HEAD TO HEAD
HEAD TO FOOT
SADDLE STITCH
LEFT HAND GATHER
PUNCH
PAD /PAD

COMMENTS

STATUS

JAYNES INTERNATIONAL, INC.

Printing Request

Shelly Morris 456-6204
John Browning 456-6444

JOB#	983003	DATE IN	2/21/2001	PO #		REL #	
------	--------	---------	-----------	------	--	-------	--

NB PO#

COPIER	BW	C=COLOR, BW=BLACK/WHITE, B=BOTH	VENDOR	XEROX
REQUESTOR	MARK ROWE	BWC=BLACK & WHITE ON COLOR MACHINE,	INVOICE	
DEPT	814		JOB OUT TO PRINTER	/COPYROOM
CHARGE	814-96-892		JOB COMPLETE	2/21/2001
PRIORITY				2/21/2001

C-22 STRIP WITH TEARS

SUBJECT	QUANTITY	ORIGINALS	SIDES	IMPRESSIONS
STOCK	5	1	1	5
# OF PAGES	24#	WHITE		
PAGE DEFINITION		# TXT PG		# PCT PG
# OF COLOR	8.5 X 11			
BINDERY	BLACK			
PACKAGING				
PRICE				
\$LAYOUT				

ORDER SENT TO PRINTER BY
ENTER CLOCK NUMBER

PRINT ONE SIDE	X
PRINT TWO SIDES	
HEAD TO HEAD	
HEAD TO FOOT	
SADDLE STITCH	
LEFT HAND GATHER	
PUNCH	
PAD	/PAD

COMMENTS

STATUS

Printing Request

HAYNES INTERNATIONAL, INC.

Shelly Morris 456-6204
John Browning 456-6444

JOB# 983352 DATE IN 8/9/2001

PO #

REL #

NB PO#

COPIER BW C=COLOR, BW=BLACK/WHITE, B=BOTH
REQUESTOR STEVE COREY BWC=BLACK & WHITE ON COLOR MACHINE,
DEPT 588-810
CHARGE
PRIORITY

VENDOR IKON
INVOICE

JOB OUT TO PRINTER /COPYROOM 8/9/2001
JOB COMPLETE 8/10/2001

H-2066C C-22 Welding Data Technical Information

QUANTITY	ORIGINALS	SIDES	IMPRESSIONS
1000	4	1	4000

STOCK 1st PAGE PRINTED ON TECHNICAL LETTERHEAD

OF PAGES # TXT PG # PCT PG

PAGE DEFINITION 8.5 X 11 20# WHITE ON REST

OF COLOR BLACK

BINDERY STAPLED

PACKAGING

PRICE

LAYOUT

ORDER SENT TO PRINTER BY
ENTER CLOCK NUMBER

PRINT ONE SIDE
PRINT TWO SIDES

HEAD TO HEAD

HEAD TO FOOT

SADDLE STITCH

LEFT HAND GATHER

PUNCH

PAD

/PAD

COMMENTS

STATUS

HAYNES INTERNATIONAL, INC.

Printing Request

Shelly Morris 456-6204
John Browning 456-6444

JOB # 983352 DATE IN 8/9/2001

PO #

REL #

NB PO#

COPIER BW

C=COLOR, BW=BLACK/WHITE, B=BOTH
BWC=BLACK & WHITE ON COLOR MACHINE,

VENDOR IKON
INVOICE

REQUESTOR STEVE COREY

DEPT 588-810

JOB OUT TO PRINTER

/COPYROOM

8/9/2001

CHARGE

JOB COMPLETE

8/10/2001

PRIORITY

H-2066C C-22 Welding Data T echnical Information

QUANTITY ORIGINALS SIDES IMPRESSIONS

1000 4 1 4000

1st PAGE PRINTED ON TECHNICAL LEETERHEAD

OF PAGES # TXT PG # PCT PG

PAGE DEFINITION 8.5 X 11 20# WHITE ON REST

OF COLOR BLACK

BINDERY STAPLED

PACKAGING

PRICE

\$LAYOUT:

ORDER SENT TO PRINTER BY
ENTER CLOCK NUMBER

PRINT ONE SIDE

PRINT TWO SIDES

HEAD TO HEAD

HEAD TO FOOT

SADDLE STITCH

LEFT HAND GATHER

PUNCH

PAD

/PAD

COMMENTS

Case 1:04-cv-00197-MBC Document 54-1 Filed 11/07/2005 Page 9 of 148

STATUS

HE 00590

Printing Request

HAYNES INTERNATIONAL, INC.

Shelly Morris 456-6204
John Browning 456-6444

JOB# 983779 DATE IN 9/6/2002

PO #

REL #

NB PO#

COPIER BW C=COLOR, BW=BLACKWHITE, B=BOTH
REQUESTOR SHELLY MORRIS BWC=BLACK & WHITE ON COLOR MACHINE,
DEPT 706 INVOICE
CHARGE 706-96-892
PRIORITY

JOB OUT TO PRINTER /COPYROOM 9/6/2002
JOB COMPLETE 9/7/2002

SUBJECT H-2053A

QUANTITY	ORIGINALS	SIDES	IMPRESSIONS
500	4	2	4000
STOCK	20# WHITE	IT LETTER HEAD	
# OF PAGES	# TXT PG	# PCT PG	
PAGE DEFINITION	8.5 X 11		
# OF COLOR			
BINDERY	STAPLED		
PACKAGING			
PRICE			
SLAYOUT			

ORDER SENT TO PRINTER BY
ENTER CLOCK NUMBER

PRINT ONE SIDE
PRINT TWO SIDES
HEAD TO HEAD
HEAD TO FOOT
SADDLE STITCH
LEFT HAND GATHER
PUNCH
PAD /PAD

COMMENTS

STATUS

HE 00591

Printing Request

HAYNES INTERNATIONAL, INC.

Shelly Morris 456-6204
John Browning 456-6444

JOB# 980703 DATE IN 9/28/1998

PO # 63219

REL #

NB PO#

COPIER C=COLOR, BW=BLACK/WHITE, B=BOTH
REQUESTOR STEVE COREY BWC=BLACK & WHITE ON COLOR MACHINE,

VENDOR HUMPHREY
INVOICE TICKET NO 5944

DEPT 588
CHARGE 588-810

JOB OUT TO PRINTER

/COPYROOM 9/28/1998
JOB COMPLETE 10/5/1998

PRIORITY

SUBJECT H-2092C CRA POCKET GUIDE

QUANTITY ORIGINALS SIDES IMPRESSIONS

3500 0

STOCK 80# WHITE NORTHWEST GLOSS

OF PAGES # TXT PG # PCT PG

PAGE DEFINITION 9X16

OF COLOR 4-COLOR PROCESS

BINDER

PACKAGING

PRICE

\$LAYOUT

ORDER SENT TO PRINTER BY
ENTER CLOCK NUMBER

PRINT ONE SIDE

PRINT TWO SIDES

HEAD TO HEAD

HEAD TO FOOT

SADDLE STITCH

LEFT HAND GATHER

PUNCH

PAD

/PAD

COMMENTS REPEAT OF YOUR OLD JOB NUMBER 9672P

REQUESTED 2500, THEY RAN 3500

STATUS

HAYNES INTERNATIONAL, INC.

Printing Request

Shelly Morris 456-6204
John Erowning 456-6444

NB PO#

JOB# 983165 DATE IN 4/19/2001

PO #

REL #

COPIER

C

C=COLOR, BW=BLACK/WHITE, B=BOTH
BWC=BLACK & WHITE ON COLOR MACHINE,

VENDOR

CANNON

REQUESTOR

MONICA HARP

INVOICE

DEPT

532

JOB OUT TO PRINTER

/COPYROOM

4/19/2001

CHARGE

532-96-892

JOB COMPLETE

4/19/2001

PRIORITY

SUBJECT

H-1101 & 02

ORDER SENT TO PRINTER BY
ENTER CLOCK NUMBER

QUANTITY ORIGINALS SIDES IMPRESSIONS

1

4

1

4

STOCK

TRANSPARENCY

OF PAGES

TXT PG

PCT PG

PAGE DEFINITION

8.5 X 11

OF COLOR

4

BINDERY

PACKAGING

PRICE

\$LAYOUT

X

PRINT ONE SIDE

PRINT TWO SIDES

HEAD TO HEAD

HEAD TO FOOT

SADDLE STITCH

LEFT HAND GATHER

PUNCH

PAD

/PAD

COMMENTS

STATUS

Date of last revision is 5/21/90

The years where no report is attached are years we did not advertise!

HAYNES INTERNATIONAL MEDIA SCHEDULE
FROM: OCTOBER 1, 1989 TO: SEPTEMBER 30, 1990

PUBLICATION	Close Date	SIZE OF AD	OCT	NOV	DEC	JAN	FEB	MAR	APR	MAY	JUN	JUL	AUG	SEP
CHEMICAL ENGINEERING	1st prec month	4-c, 7x full page bleed						CC-89 133	CC-89 133	CA-90 144	CA-90 144	CA-90 143	CA-90 144	CC-26109 143
Circ. 71,089								\$5,975.50	CC-89 133	\$5,975.50	\$5,975.50	\$2,397.0	\$5,975.50	\$5,975.50
WELDING JOURNAL	4 wks. prior to pub	4-c, 4x full page bleed							CC-89 133	\$2,397.0	CA-90 143	CA-90 143		\$2,397.0
Circ. 34,190								CC-90 141		CA-90 140	\$2,397.0	CC-90 141A		
HAZARDOUS WASTE MANAGEMENT	15th prec month	4-c, 3x full page bleed						\$3,587.0		\$3,587.0		\$3,587.0		
Circ. 20,797														
SOLID WASTE AND POWER		4-c, 3x full page bleed						CC-90-141 Extension March 6 \$1,799.88	CA-90-140 Close April 15 \$1,799.88	CA-90-140 Close June 15 \$1,799.88				
Circ. 14,674										CA-90 142	CA-90 142		CA-90 142	CA-90 142
AEROSPACE ENGINEERING	1st prec month	4-c, 4x full page bleed								\$4,798.25	\$4,798.25		\$4,798.25	\$4,798.25
Circ. 61,163														
* 3x rate combined with Automotive Engineering														
INDUSTRIAL HEATING	1st prec month	4-c, 7x full page bleed	CA-89 137	CA-89 137		CA-89 137	CA-89 137	CA-89 137			CA-89 137		CA-26106 145	CA-90 145
Circ. 22,397			\$2,800.75	\$2,800.75		\$2,800.75	\$2,800.75	\$2,800.75			\$2,800.75		\$2,800.75	\$616.25
AMERICAN CERAMIC SOCIETY BUL.	1st prec month	b/w, 6x 1/4 pg						CA-90 145	CA-90 145	CA-90 145	CA-90 145	CA-90 145	CA-90 145	CA-90 145
Circ. 14,839								\$616.25	\$616.25	\$616.25	\$616.25	\$616.25	\$616.25	\$616.25
CPI PURCHASING	5th prec month	4-c, 1x full page bleed					CC-88 131							
Circ. 36,706							\$4,811							
MATERIALS PERFORMANCE	5th prec month	4-c, 1x full page bleed		CC-88 131				CC-89 121						
Circ. 15,418				\$1,819				\$1,819						

HE 00594

Date of last revision
5/21/90

HAYNES INTERNATIONAL MEDIA SCHEDULE
FROM: OCTOBER 1, 1989 TO: SEPTEMBER 30, 1990

PUBLICATION	SIZE	OCT	NOV	DEC	JAN	FEB	MAR	APR	MAY	JUN	JUL	AUG	SEP
AUTOMOTIVE ENGINEERING	5th prec. month	4-c, 1x full page bleed							CA-89 137				
Circ. 81,979									\$5,567.50				
* 3x rate combined with Aerospace Engineering													
CHEMICAL ENGINEERING PROGRESS	1st prec month	4-c, 1x full page bleed							CC-90 141A				
Circ. 46,367									\$4,088.50				
ADVANCED MATERIALS & PROCESSES	5th prec. month	4-c, 1x full page bleed							CA-90 140				
Circ. 50,236									\$4,203.25				

CC-89-121 "See how HASTELLOY alloy C-22 Weldment..."
 CC-88-131 "HASTELLOY alloy G-30 outlasts..."
 CC-89-133 "HASTELLOY alloy C-22 weldments..."
 CA-89-137 "Cutting corners on heat treating..." *Uberg*
 CA-90-140 "HAYNES alloy 556: the best..."
 CA-90-141A "HASTELLOY alloys outperform..." (Hazardous Waste)
 CA-90-142 "For more than 50 years..." (Aerospace)
 CA-90-143 "Here are two of the best..." (Universal Weld) - *Uberg*
 CA-90-144 "Superior high-temp design..." (230 CP1)
 CA-90-145 "Clean firing through 2200F..."
 CC-26109 New G-30/C-22 CP1 ad

HE 00595

(10)

	Feb	Mar	Apr	May	June	July	Aug	Sep	Oct	Nov	De
Chemical Equip.						<u>#2</u> #32350 1-10-10 #3		<u>24935</u> #10-11			
Mechanical Eng.		<u>#2 C</u>									<u>#12</u> K
Aerospace Eng.								<u>#12</u> 11-2-10 10-29-1			
Automotive Eng.											
Power					<u>#2</u> 7-1-10 #32350						
Plastics Act. Crds.											<u>#16</u>
Chemical Eng.									<u>#12</u> 11-2-10 11-11		
NASA Tech Briefs	<u>#3</u> 1-9 DRC				<u>#32353</u> 9515 #1-2-5-10						
Aerospace America	<u>#12</u> 1-5 DRC										
NACE (Mat. Perf.)				<u>#2</u> 10-3-11 #32324 1-10-10 #2 (See Attached)					<u>#7</u> 682-50 10-10-10 E-12 card (See Attached)		
Power Engineering											
Industrial Mktg			<u>#2</u> 10-1-10 #32350								
Pollution Equipment News			<u>#4</u> 1-10-10 #32350								
Advanced Matl + Process											
Mechanical Eng.				<u>#11</u> 11-11							

HE 00596

4-25

	Feb	Mar	Apr	May	June	July	Aug	Sep	Oct	Nov	Dec	Jan
Chemical Equip.												
Mechanical Eng.												
Chemical Eng.												
Automotive Eng.												
Power												
Plastics Act. Cds.												
Chemical Eng.												
NASA Tech Briefs												
Aerospace America												
NACE (Mat. Perf.)												
Power Engineering												
Industrial Mfg.												
Pollution Equipment												
Advanced Matl + Process												
Mechanical Eng.												

#2 2-3110

3-3219 #3

#2

#12

#12

10-1-1

#16

2-3219 #2

3-3219 #12

3-3186 #2

2-3112 #2
#1-3054 #4 have

2-3111

2-3187 #11

#6

(A1)

Deck Cards 1-71

Chemical Equip.

Mechanical Eng.

Aerospace Eng.

Power

Plastics Act. Cards

Chemical Eng.

NASA Tech Briefs

Aerospace America

ACE (Mat. Perf.)

Power Eng.

Industrial Heating

Pollution Eng. News

Society of Plastics Engineers

Adv. Mat. & Proc.

Hazard. Waste Mgmt.

Chemical Processing

Automotive Eng.

Oct

Nov

Dec

Jan

Feb

Mar

Apr

May

June

July

Aug

Sep

#12

#16
New #42
CABO
#2112

#3

#2
2401.95
injected # 32439

#16
10-25-50
11/8/91

#3
30345
7/30/91

#2
Cancelled
11/15/91
Dane

#3

#3
A
Dane
8-30
11/8/91

#12
A

#12
A

#2
202105
11/8/91

NEW
FIRE
3337-#376-PU
HE-120 CABO
3383-#452-4-100

#12
A

#1
Dane
8-30
11/8/91

#11c
Applied Polym. Eng.
3/30/91
11/8/91

#20
NEW
HE-120 CABO
10/7/91
New
HE-120 CABO
10/7/91

#2
177A
3513
11/8/91

#7
CABO
11/8/91

#19
NEW
CABO
11/8/91

(over)

FY-96 Journal Ads

Journal	Oct 95	Nov 95	Dec 95	Jan 96	Feb 96	Mar 96	Apr 96	May 96	Jun 96	Jul 96	Aug 96	Sep 96
Chemical Engineering		Ad			Ad		Deck			Ad		
Chemical Processing		Ad	Ad	Deck						Ad		
Chem Engr Progress		Ad	BW		Ad				BW		Ad	
Chemical Equipment												
Materials Performance										Ad		
					X							X

Ad = Full Page Color Ad
 BW = Reduced full page Black & White
 Deck = Black & White Deck Card

"HISTORY" AD w/CHEM SHOW #5719

"HANDS" AD WITHOUT CHEM SHOW #5920

"HISTORY" AD WITHOUT CHEM SHOW #5919

Oct 96

Ad

FY-97 Journal Ads

Journal	Jan 97	Feb 97	Mar 97	Apr 97	May 97	Jun 97	Jul 97	Aug 97	Sep 97	Oct 97	Nov 97	Dec 97
Chemical Engineering		Ad			beck		Ad			Ad		
Chemical Processing		Ad			Ad					Ad	Ad	
Chem Engr Progress			Ad			Ad	Ad				Ad	
Materials Performance		Ad					Ad					
Industrial Heating					Ad				Ad			

HARD'S

13545557

FY-98 Journal Ads

Journal	Jan 98	Feb 98	Mar 98	Apr 98	May 98	Jun 98	Jul 98	Aug 98	Sep 98	Oct 98	Nov 98	Dec 98
Chemical Engineering		Ad 7/14/98			Deck 4/29/98		Ad 7/17/98			Ad 10/1/98		
Chemical Processing		Ad 7/14/98		8/15/98 Ad						Ad 10/1/98		
Chem Engr Progress			Ad 7/14/98		Lit	Ad 7/14/98	Ad 7/17/98			Lit	Ad 7/17/98	
Materials Performance		Ad 7/14/98			Ad 7/14/98		Ad 7/17/98			Buyer		
Industrial Heating				Ad 8/15/98					Ad 10/1/98			

Charles E. Grier
Heat Treating Program
Stainless Steel weld
VS ductility Today

AD 7/14/98

AD - 10/1/98
AD - 10/1/98
AD - 10/1/98
AD - 10/1/98

AD

FY-99 Journal Ads

Journal	Jan 99	Feb 99	Mar 99	Apr 99	May 99	Jun 99	Jul 99	Aug 99	Sep 99	Oct 99	Nov 99	Dec 99	Cost
Chemical Engineering		Ad-1			Ad-2					Ad-3			14,500
Chemical Processing			Ad-2				Ad-3			Ad-1			18,000
Chemical Engr Progress			Ad-3		Ad-1						Ad-2		12,000
Materials Performance			Ad-1				Ad-2						6,000
Industrial Heating				Ad-4					Ad-5				8,700
Heat Treating Progress						Ad-6				Ad-5			6,000
Tube and Pipe								Ad-7					6,000
Stainless Steel World					Ad-8						Ad-8		6,300
													77,500

CY98- Journal	Responses	Survey	Ads
Chemical Engineering	250	1	1 = C-2000 Hands
Chemical Processing	345		2 = Fittings and Flanges
Chemical Engr Progress	115		3 = HASTELLO Y
Materials Performance	60		4 = HR-120 Eggs in a Basket
Industrial Heating	125	1	5 = HR-120 No Future
Heat Treating Progress	25		6 = High Temperature
Stainless Steel World	0	1	7 = Tubular
			8 = HASTELLO Y (International)

New Service Center: Customer Mailing, Tour, News Release

HE 00602

Date: 6/21/2000

HAYNES INTERNATIONAL
FY-2000 Journal Ads

Journal	Jan 00	Feb 00	Mar 00	Apr 00	May 00	Jun 00	Jul 00	Aug 00	Sep 00	Oct 00	Nov 00	Dec 00	Cost
Chemical Engineering				Ad-2				Ad-9		Ad-10			15,000
Chemical Processing			Ad-3		Ad-2				Ad-9				15,300
Chemical Engr Progress					Ad-3							Ad-10	6,200
Materials Performance			Ad-3								Ad-9		6,000
Chemical Equipment								Ad-2					8,100
Industrial Heating				Ad-6					Ad-9				8,700
Heat Treating Progress						Ad-5			Ad-9				6,000
Tube and Pipe													
Stainless Steel World					Ad-8					Ad-8			6,300
													71,600

CY99- Journal

Responses

Survey

Ads

Chemical Engineering 369
 Chemical Processing 115
 Chemical Engr Progress 59
 Materials Performance 40
 Industrial Heating 108
 Heat Treating Progress 25
 Stainless Steel World 0

1 = C-2000 Hands
 2 = Fittings and Flanges
 3 = HASTELLOX
 4 = HR-120 Eggs in a Basket
 5 = HR-120 No Future
 6 = High Temperature
 7 = Tubular
 8 = HASTELLOX (International)
 9 = Haynes Products
 10 = Welded Pipe & Fittings

HE 00603

Date: 4/10/2001

HAYNES INTERNATIONAL
FY-2001 Journal Ads

Journal	Jan 01	Feb 01	Mar 01	Apr 01	May 01	Jun 01	Jul 01	Aug 01	Sep 01	Oct 01	Nov 01	Dec 01	Cost \$
Chemical Engineering			10				9		9				15,000
Chemical Processing			9				10			10			15,300
Materials Performance		9			10							9	9,000
Chemical Equipment			10					10					16,200
Industrial Heating						9				12			8,700
Heat Treating Progress						9				12			6,000
AWS Journal				12									6,000
Stainless Steel World					9					9			6,300
Total													82,500

Ad Code:

1 = C-2000 Hands
 2 = Fittings and Flanges
 3 = HASTELLOX
 4 = Egg in a Basket
 5 = HR-120 No Future
 6 = High Temperature
 7 = Tubular
 8 = HASTELLOX (International)
 9 = Haynes Products
 10 = Welded Pipe & Fittings
 11 = Heat Treat (New)
 12 = Welding Consumables (New)

HE 00604

HAYNES INTERNATIONAL
CY-2002 Journal Ads

Journal	Jan 02	Feb 02	Mar 02	Apr 02	May 02	Jun 02	Jul 02	Aug 02	Sep 02	Oct 02	Nov 02	Dec 02	Cost \$ Full	Cost \$ Island	Cost \$ 1/2
Chemical Engineering	2		10			9 13			F9	10			10,200	13,900	
Chemical Processing	2				13					10					
Chemical Engr Progress															
Materials Performance	3		9		10						B9		8,800		
Chemical Equipment	2		10							10				12,600	
Industrial Heating	1		12				B13				F13		9,000		
Purchasing	2														
Heat Treating Progress						9 13						B9	6,000		
AWS Journal	1														
Stainless Steel World	2				9					9			6,800		
SSW Buyer Guide	1										B9		6,000		
Asia Chemical News	2														
Total	18												46,800	26,500	
Full Cost													2,000	800	
1/2 Page Development														200	

B= Buyers Guide F= Free Insert (Full Page)

Ad Code:

- 1 = C-2000 Hands
- 2 = Fittings and Flanges
- 3 = HASTELLO
- 4 = Egg in a Basket
- 5 = HR-120 No Future
- 6 = High Temperature
- 7 = Tubular
- 8 = HASTELLO (International)
- 9 = Haynes Products
- 10 = Welded Pipe & Fittings

- 11 = Heat Treat (New)
- 12 = Welding Consumables
- 13 = Service Center (New)

AC: PEM

TYPE OF DISBURSEMENT - Cashier will "X" one

CASH FUND	PAYROLL	NOT TO BE REIMBURSED	RECEIPTS REMITTED
-----------	---------	----------------------	-------------------

CASH VOUCHER ➔

CASHIER PLEASE PAY ➔

NUMBER

AMOUNT

\$80 00

DOLLARS

WRITE OUT AMOUNT FOR CASH DISBURSEMENTS ONLY

To Central Iowa Chapter of ASM InternationalBy Currency ☐ or Check ☒ Number _____In Payment Of Advertisement in Yearbook

CHARGE TO			
DEPT. OR ACCOUNT	I.E.A.	ORDER NUMBER	AMOUNT
589	96	= 800	\$80 00

Requested by E. K. Maddox Date 7/9/91Approved by E. Buckle Date 7/9/91

Paid by _____ Date _____

(LOCATION NUMBER)

Received by _____

S-620A

(SIGNED)
ORIGINAL (Auditor's Copy)

HE 00606

*Elaine Maddox**Phone: 317-456-6017*

Central Iowa Chapter of ASM International Yearbook Advertising

Advertisements should be camera ready, if possible.

1 Full page ads @ \$80 each = \$ 80⁰⁰

8.5" tall x 5.5" wide.

(Our ad size is 4 7/8 tall x 7" wide)

 Half page ads @ \$50 each = \$

4.25" tall x 5.5" wide

Total Amount Due = \$ 80⁰⁰

The deadline for submittal is August 16, 1991.

Please send your advertisements and a check payable to the
Central Iowa Chapter of ASM International to:

Tim Landgraf
Eaton Corporation
700 Luick's Lane
Belmond, Iowa 50421

7/8/91

589-96-800

(1/2 pr. Btw CRA ad per yr)

HE 00607

HAYNES
 International

**World's Largest Inventory of
 HASTELLOY® Corrosion-Resistant Alloys**


Alloy	ASME/ASTM Specifications					AWS/ASME Specifications	
	Plate Sheet Strip	Bar Rod	Welded Pipe	Welded Tubes	Seamless Pipe & Tube	Coated Electrodes	Bare Weld Wire
HASTELLOY B-2 alloy (Ni-28Mo) UNS: N10665	SB333/ B333	SB335/ B335	SB619/ B619	SB626/ B626	SB622/ B622	A 5.11/ SFA 5.11 (ENiMo-7)	A 5.14/ SFA 5.14 (ERNiMo-7)
HASTELLOY C-276 alloy (Ni-16Cr-16Mo-4W-5Fe) UNS: N10276	SB575/ B575	SB574/ B574	SB619/ B619	SB626/ B626	SB622/ B622	A 5.11/ SFA 5.11 (ENiCrMo-4)	A 5.14/ SFA 5.14 (ERNiCrMo-4)
HASTELLOY C-22™ alloy (Ni-22Cr-13Mo-3W-3Fe) UNS: N06022	SB575/ B575	SB574/ B574	SB619/ B619	SB626/ B626	SB622/ B622	A 5.11/ SFA 5.11* (ENiCrMo-10)	A 5.14/ SFA 5.14* (ERNiCrMo-10) ASME 2094 Code
HASTELLOY G-30* alloy (Ni-30Cr-5.5Mo-2.5W-15Fe) UNS: N06030	SB582/ B582	SB581/ B581	SB619/ B619	SB626/ B626	SB622/ B622	A 5.11/ SFA 5.11* (ENiCrMo-11)	A 5.14/ SFA 5.14* (ERNiCrMo-11) ASME 2095 Code

*Pending

SALES OFFICES/SERVICE CENTERS

Arcadia, Louisiana Tel: 800-648-8823 Fax: 318-263-8088	Kokomo Indiana Tel: 800-354-0806 Fax: 317-456-6810	Houston, Texas Tel: 800-231-4548 Fax: 713-937-4596	Anaheim, California Tel: 800-531-0285 Fax: 714-978-1743	Windsor, Connecticut Tel: 800-426-1963 Fax: 203-688-5550
--	--	--	---	--

In addition to over 3M pounds of stock for immediate delivery, Haynes International allows you to get the best technical service and support that may be required for use of these advanced alloys.

Also Available:

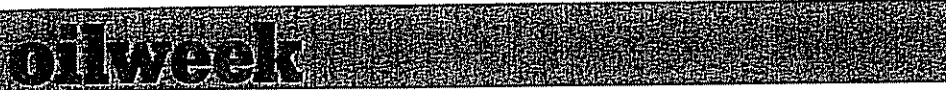
Corrosion-Resistant Alloys
 HASTELLOY alloys
 H-9M™ alloy (UNS pending)
 G-50™ alloy (UNS N06950)
 C-4 (UNS N06455)
 N (UNS N10003)
 S (UNS N06635)
 W (UNS N10004)
 FERRALUM®
 alloy 255 (UNS-S32550)

**Corrosion- and
 Wear-Resistant Alloy**
 ULTIMET™
 alloy (UNS-pending)

High-Temperature Alloys
 HAYNES® alloys:
 214 (UNS pending)
 X (UNS N06002)
 230 (UNS N06230)
 625 (UNS N06625)
 718 (UNS N07718)
 X-750 (UNS N07500)
 556 (UNS R30556)
 25 (UNS R30605)
 188 (UNS R30188)
 HR-160™ alloy
 HR-120™ alloy
 242

HE 00608

7/8/91
Susan Brown
Checked
9-15
Shirley Miller



A MACLEAN HUNTER PUBLICATION
"CENTRE 1015", SUITE 200, 1015 CENTRE ST. N., CALGARY, ALBERTA T2E 2P8 • TELEPHONE 276-7881

July 2, 1991

JUL 8 1991

Haynes International
P.O. Box 9013
Kokomo, IN 46904 - 9013
Att: Elaine Maddox

Dear Ms. Maddox:

Please find enclosed a copy of the invoice originally sent to your advertising agency, Stairtop Studios.

We have since been informed that this invoice should have been sent directly to you. As we are unable to re-address original invoices, could you please make arrangements to pay the enclosed statement from your office.

Thank you so much for your assistance in this matter.

Sincerely,

Susan Brown
Office Manager
Oilweek Magazine

HE 00609

Branch Offices:

7 Bay Street
Toronto, Ont. M5W 1A7
(416) 596-5827

Suite 1000
1001 De Maisonneuve Blvd. West
Montreal, Que. H3A 3E1
Tel. (514) 845-5141

11504 - 170 St. #102
Edmonton, Alta. T5S 1J7
Tel (403) 454-0377

700 - 1111 Melville Street
Vancouver, B.C. V6E 3V6
Tel (604) 683-8254



Macleon Hunter

Macleon Hunter Limited / Limitee
 Maclean Hunter Building
 777 Bay Street
 Toronto Canada M5W 1A7

INVOICE / FACTURE

STAIRTOP STUDIOS
 100 E. Broadway
 P.O. Box 824
 KOKOMO, IN 46903-0824

1438 57

INVOICE NO. N° DE FACTURE		
A48360		
DAY JOUR	MO. MOIS	YR. AN
17	06	91

INVOICE DATE
DATE DE FACTURE

PAGE *

OILWEEK 661-01-001

ADVERTISER
ANNONCEUR

HAYNES, INTERNATIONAL

VE-PUBLICATION Y MO. R	MO. YEAR AN	EDITION EDITION	CLASS	ITEM DESCRIPTION - DESCRIPTION D'ITEM	CARD RATE - TAUX CARTE	NET AMOUNT - MONTANT NET
17	06	91		1/2 Page Horizontal Black & White Less 15% Agency Commission I.O. 5-4019, Two Tearsheets Please. COPY	\$1,965.00 -294.75	
TOTAL						\$1,670.25

HISTORY COPY / COPIE D'HISTOIRE

HE 00610

DATE DAY MONTH YEAR	QUANTITY UNIT EA	DESCRIPTION ITEM	PRICE UNIT EA	TOTAL AMOUNT DOLLARS
17 06 91		1/2 Page Horizontal Black & White Less 15% Agency Commission		\$1,965.00 -294.75
		I.O. 6-4019, Two Tearsheets Please.		
		VENDOR NO: INVOICE NO: INVOICE DATE: DUE DATE: ACCOUNT NO: _____ ACCOUNTING NO: APPROVAL: _____		
TOTAL				\$1,670.25

INVOICE / FACTURE

HE 00611

INSERTION ORDER

Case 1:04-cv-00197-MBC

Document 54-2

Filed 11/07/2005

FED. X INFO -
Page 119 of 143
MAY HAVE HUNT
SEND VIA FED-X
DIRECT TO MAG.

Date: 6.4.91

OILWEEK, ATTN: ANDREA
#200, 1015 CENTRE ST. N
CALGARY, ALBERTA, CANADA
T2E 2P8

DEH

Insertion Order No 6-4019 Client HAYNES, INT.

This is your authorization to insert ATTACHED 1/2 P. AD
into 6.17 ISSUE OF OILWEEK
Confirmed _____ X rate of \$ 1530.00

Reproduction materials attached ☒ (y) ☐ (n)

~~Reproduction materials coming ☒ (y) ☐ (n)~~

CLIENT

Please invoice this ~~order~~ direct using the above insertion authorization number as all insertion orders

HE 00612

Gulf Canada Resources Ltd.	3,766,500	5	4,171,500	9
Mobil Oil Canada Ltd.	3,567,708	6	3,494,156	6
Imperial Oil Limited	3,075,344	8	3,110,920	8
PanCanadian Petroleum Ltd.	2,264,800	9	2,275,735	9
Texaco Canada Petroleum Inc.	1,900,000	10	1,800,000	10
Home Oil Company Limited	1,671,200	11	1,592,800	12
Norcen Energy Resources Ltd.	1,627,532	12	1,352,404	13
Saskatchewan Oil & Gas Corp.	1,516,118	13	1,659,826	11
Husky Oil Ltd.	1,342,397	14	1,291,450	14
A E C Oil and Gas	1,105,197	15	1,024,000	15
Canadian Hunter Exploration	994,111	16	869,467	18
North Canadian Oils	897,757	17	946,559	16
Encor Inc.	879,000	18	869,700	17
Sceptre Resources Limited	789,000	19	760,200	19
Bow Valley Industries Ltd.	637,380	20	512,737	26
Renaissance Energy Ltd.	602,596	21	588,023	21
B P Resources Canada	580,400	22	570,800	22
Mark Resources Inc.	560,969	23	598,616	20
Unocal Canada Ltd.	535,798	24	528,013	23
C/N Exploration Inc.	502,133	25	338,412	32
Amerada Hess Canada Ltd.				

Stock motors ready for immediate shipment includes: triple rated high slip pump motors, explosion-proof motors, chemical processing motors, "Dirty-Duty" motors, and a wide variety of general-purpose motors.

For more information, call the Baldor District Office in your area, or contact BALDOR, Fort Smith, Arkansas 72902, USA. Phone (501) 646-4711. TELEX 53-7425

BALDOR

HAYNES
International

World's Largest Inventory of
HASTELLOY® Corrosion-Resistant Alloys

Alloy	ASME/ASTM Specifications				AWS/ASME Specifications		
	Plate Sheet Strip	Bar Rod	Welded Pipe	Welded Tubes	Seamless Pipe & Tube	Coated Electrodes	Bare Weld Wire
HASTELLOY B-2 alloy (Ni-28Mo) UNS: N10665	SB333/ B333	SB335/ B335	SB619/ B619	SB626/ B626	SB622/ B622	A 5 11/ SFA 5 11 (ENiMo-7)	A 5 14/ SFA 5.14 (ERNiMo-7)
HASTELLOY C-276 alloy (Ni-16Cr-16Mo-4W-5Fe) UNS: N10276	SB575/ B575	SB574/ B574	SB619/ B619	SB626/ B626	SB622/ B622	A 5 11/ SFA 5 11 (ENiCrMo-4)	A 5 14/ SFA 5.14 (ERNiCrMo-4)
						A 5 11/ SFA 5 11	A 5 14/ SFA 5.14



Also Available:

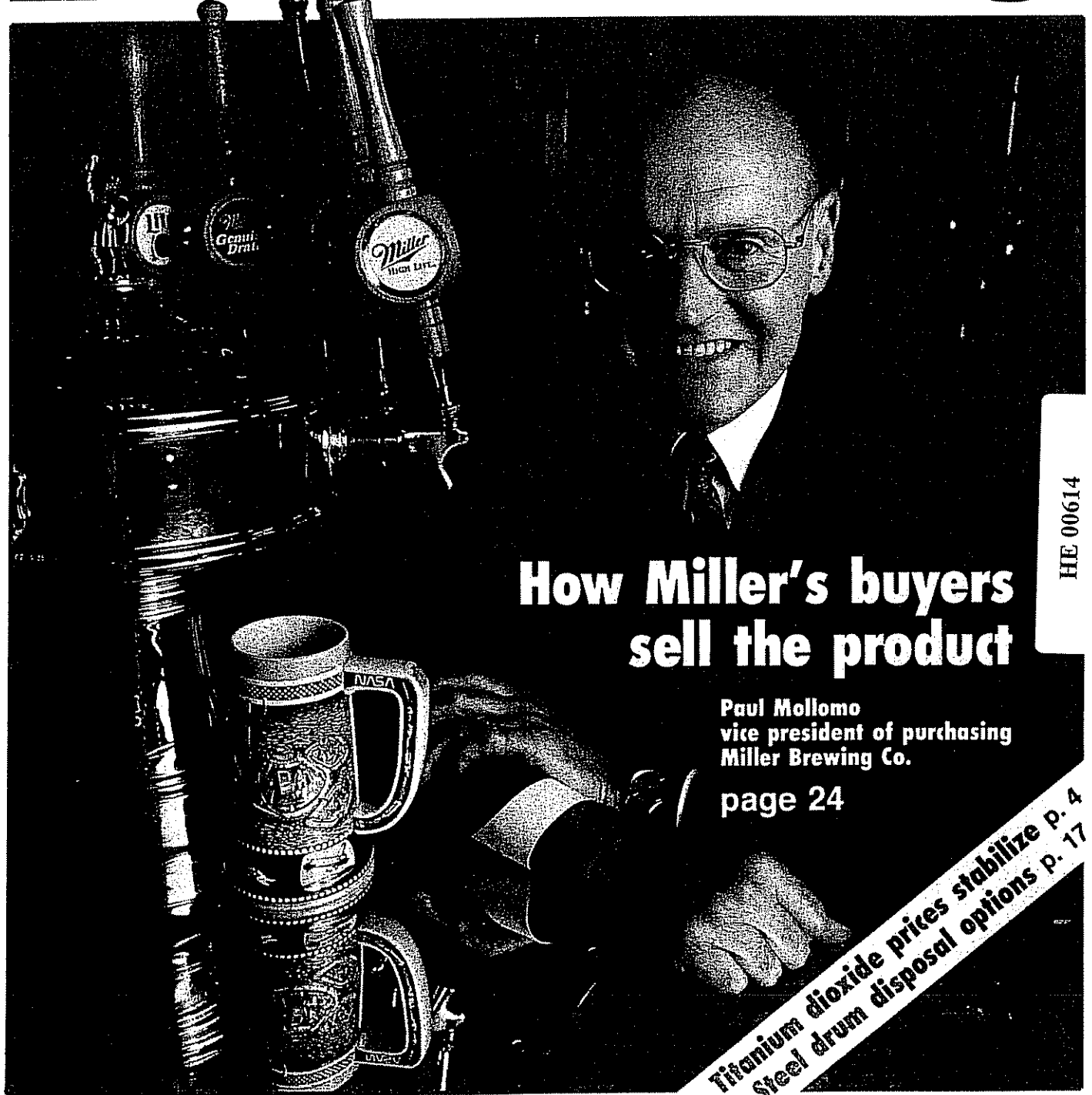
Corrosion-Resistant Alloys
HASTELLOY alloys
H-9M™ alloy (UNS pending)
G-50™ alloy (UNS N06950)
C-4 (UNS N06455)
N (UNS N10003)
S (UNS N06635)
W (UNS N10004)
FERRALIUM®
alloy 255 (UNS-S32550)

CPI Purchasing

► New regs bring new
► How to buy storage
► Transaction price sur

*Miss
can*

THE MAGAZINE ABOUT BUYING FOR THE CHEMICAL/PROCESS INDUSTRIES



**How Miller's buyers
sell the product**

Paul Mollomo
vice president of purchasing
Miller Brewing Co.

page 24

**Titanium dioxide prices stabilize p. 4
Steel drum disposal options p. 17**

HE 00614

CPI PRODUCT NEWS

used in Lubricomp composites including polytetrafluoroethane (PTFE), silicone, glass, carbon and aramid fibers, as well as graphite powders and molybdenum disulfide (Moly) that are used in specialty applications are described in the brochure. LNP Engineering Plastics, 215-363-4500.

Gas Filters

Literature on the Model 6119 ceramic membrane micro-filter suited for gas purification is now available. Included is a complete description of the physical and performance characteristics of the filter, which is ideal for use in applications with stringent purity requirements including microelectronics, hydrocarbon processing, food and beverage processing, bioprocessing, chemical processing and water and wastewater treatment applications. Matheson Gas Products, 201-867-4100.

Hazardous materials shipping regulations

The "Orange Book" overview of United Nations (U.N.) Packaging and U.S. Department of Transportation (DOT) hazardous materials shipping regulations defines classes of dangerous goods, outlines performance-oriented packaging, explains testing requirements for U.N. containers, clarifies commodity qualification for U.N. packaging, provides guidelines for recommended methods of pail closing and lists permit-issuing Competent Authorities in 48 countries. Philips Container, 216-541-2444.

Bearings

The Dodge S-2000 spherical set-screw mounted bearing is detailed in an eight-page, full-color brochure. In addition to illustrating

the S-2000's features with photographs and drawings, the brochure includes radial load rating charts and detailed selection tables that act as a reference guide for the specifier. Problems and solutions are explored with example calculations. Dodge, 803-297-4800.

Steam traps

A free catalog describing the features, applications and benefits of Filled Thermal Element (FTE) steam traps is now available. In addition to detailing the five configurations of FTE traps and their applications including drying and process, a selection with pressure, temperature application information also provided. Yarway Corp., 215-812-1100.

A free paper entitled 'Sim, Techniques for Surveying Steam Traps' details the visual, sound

HAYNES
International

**World's Largest Inventory of
HASTELLOY® Corrosion-Resistant Alloys**

Alloy	ASME/ASTM Specifications				AWS/ASME Specifications		
	Plate Sheet Strip	Bar Rod	Welded Pipe	Welded Tubes	Seamless Pipe & Tube	Coated Electrodes	Bare Weld Wire
HASTELLOY B-2 alloy (Ni-28Mo) UNS: N10665	SB333/ B333	SB335/ B335	SB619/ B619	SB626/ B626	SB622/ B622	A 5.11/ SFA 5.11 (ENiMo-7)	A 5.14/ SFA 5.14 (ERNiMo-7)
HASTELLOY C-276 alloy (Ni-16Cr-16Mo-4W-5Fe) UNS: N10276	SB575/ B575	SB574/ B574	SB619/ B619	SB626/ B626	SB622/ B622	A 5.11/ SFA 5.11 (ENiCrMo-4)	A 5.14/ SFA 5.14 (ERNiCrMo-4)
HASTELLOY C-22™ alloy (Ni-22Cr-13Mo-3W-3Fe) UNS: N06022	SB575/ B575	SB574/ B574	SB619/ B619	SB626/ B626	SB622/ B622	A 5.11/ SFA 5.11* (ENiCrMo-10)	A 5.14/ SFA 5.14* (ERNiCrMo-10) ASME 2094 Code
HASTELLOY G-30® alloy (Ni-30Cr-5.5Mo-2.5W-15Fe) UNS: N06030	SB582/ B582	SB581/ B581	SB619/ B619	SB626/ B626	SB622/ B622	A 5.11/ SFA 5.11* (ENiCrMo-11)	A 5.14/ SFA 5.14* (ERNiCrMo-11) ASME 2095 Code

*Pending

SALES OFFICES/SERVICE CENTERS

Arcadia, Louisiana Tel: 800-648-8823 Fax: 318-263-8088	Kokomo Indiana Tel: 800-354-0806 Fax: 317-456-6810	Houston, Texas Tel: 800-231-4548 Fax: 713-937-4596	Anaheim, California Tel: 800-531-0285 Fax: 714-978-1743	Windsor, Connecticut Tel: 800-426-1963 Fax: 203-688-5550
--	--	--	---	--

In addition to over 3M pounds of stock for immediate delivery, Haynes International allows you to get the best technical service and support that may be required for use of these advanced alloys.



Also Available:

Corrosion-Resistant Alloys
HASTELLOY alloys
H-9M™ alloy (UNS pending)
G-50™ alloy (UNS N06950)
C-4 (UNS N06455)
N (UNS N10003)
S (UNS N06635)
W (UNS N10004)
FERRALIUM® alloy 255 (UNS-S32550)

**Corrosion- and
Wear-Resistant Alloy**
ULTIMET™ alloy (UNS-pending)

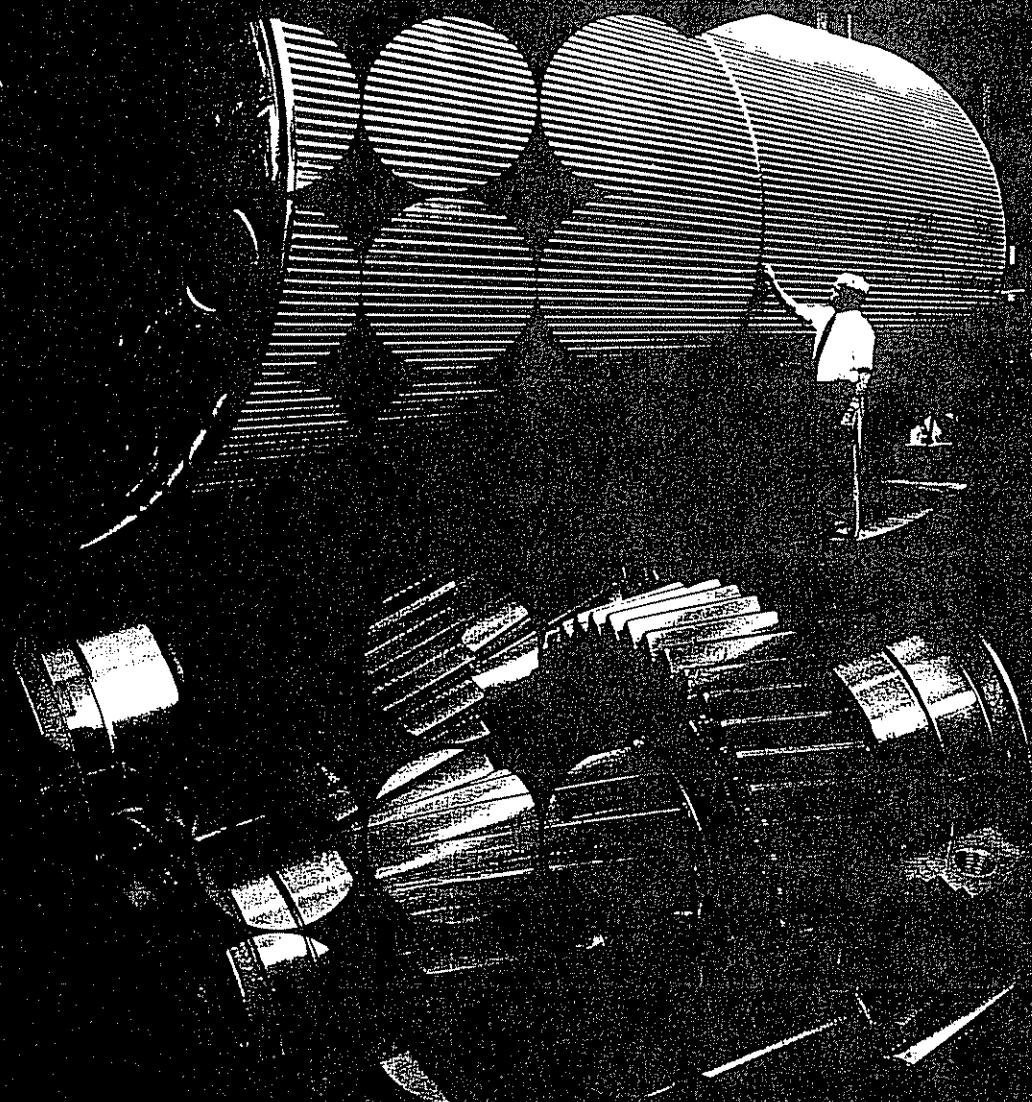
High-Temperature Alloys
HAYNES® alloys:
214 (UNS pending)
X (UNS N06002)
230 (UNS N06230)
625 (UNS N06625)
718 (UNS N07718)
X-750 (UNS N07500)
556 (UNS R30556)
25 (UNS R30605)
188 (UNS R30188)
HR-160™ alloy
HR-120™ alloy
242

HE 00615

MOLYBDENUM Mosaic

The Journal of Molybdenum Technology

Volume 10, Number 1, 1987



Continued

Alloy Type

PS (EX)
PS (EX)
PS 31 + ca
PS (EX) 55
PS (EX) 55

PS 55

Information Data

Weight Percent

Si Mn P

0.79
0.18
0.27
0.17
0.17

0.17

0.17

0.16

0.16

Sheets for Carbonizing Steels

Weight Percent

S Cr Ni Mo B

0.019 0.56 0.86 0.47
0.022 0.54 0.85 0.51
0.023 0.40 0.84 0.54
0.007 0.59 1.75 0.73
0.023 0.49 1.84 0.74

0.023 0.49 1.84 0.74

0.022 0.15 3.58 0.26

0.025 0.50 0.53 0.36

0.014 0.49 0.54 0.54

Data Sheet No.

I-255
I-49
I-260
I-256
I-254

I-261

I-257

I-50

I-259

I-51

HE 00644

MOLYBDENUM Mo

The Journal of Molybdenum Technology

ISSN 0163-1888

Volume 10, Number 1, 1987

Contents

- Page 1
New Advances in
Molybdenum-containing
Corrosion Resistant Alloys
- Page 6
Molybdenum Carburizing Steel
Provides Performance Edge
- Page 11
New CCT Diagrams for Carburizing
Steels
- Page 13
New Literature

Molybdenum Mosaic is published by AMAX Metal Products, 1370 Washington Pike, Bridgeville, Pennsylvania 15017, U.S.A.

Permission is granted to reprint material appearing in this publication provided appropriate credit is given to *Molybdenum Mosaic* and AMAX Metal Products. Where material not originally written by AMAX Metal Products is involved, permission to reprint or use must be requested from the appropriate writer, editor or publication.

Molybdenum Mosaic is presented as a public service. While every effort is made to avoid error, AMAX Metal Products does not verify all of the data presented and disclaims any liability and responsibility for the information contained herein.

The editor of *Molybdenum Mosaic* welcomes letters from readers pertaining to material appearing in *Molybdenum Mosaic* or other subjects of interest.

Editor's Note:

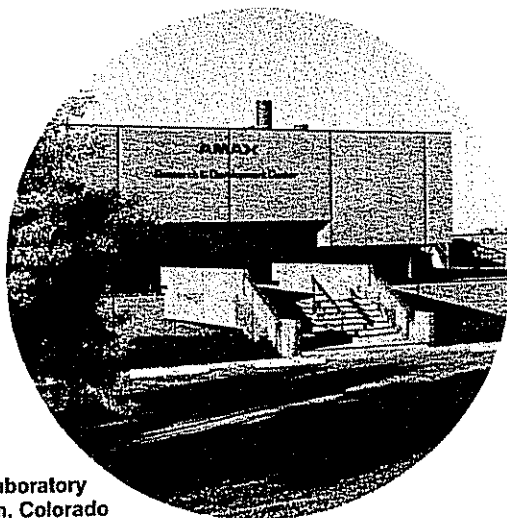
Many of our readers have inquired about the number of issues per volume. Here is the information:

Volume 1, Numbers 1, 2, 3 and 4
Volume 2, Numbers 1, 2, 3 and 4
Volume 3, Numbers 1, 2 and 3
Volume 4, Numbers 1, 2 and 3
Volume 5, Numbers 1, 2, 3 and 4
Volume 6, Numbers 1, 2 and 3
Volume 7, Numbers 1, 2 and 3
Volume 8, Numbers 1 and 2
Volume 9, Number 1

AMAX Consolidates Laboratory Facilities; Opens New Office in Michigan

It has been called the end of an era by some, but AMAX prefers to think of it as a move to make better and more efficient use of its research facilities. As of June 30, 1987, the AMAX Materials Research Center in Ann Arbor, Michigan was shut down and a significant portion of its staff will have transferred to the company's other laboratory site in Golden, Colorado. The address for the Golden laboratory is:

AMAX R&D Center
5950 McIntyre Street
Golden, Colorado 80403
Telephone (303) 279-7636



AMAX Laboratory
in Golden, Colorado

At the same time, the company has established a new business unit in Ann Arbor, Michigan. This new unit, known as AMAX Specialty Businesses, has been established to develop a wide range of specialty chemical markets ranging from polymer additives to electronic materials. The address of this new AMAX unit is:

AMAX Specialty Businesses
Atrium Office Center, Suite 320
900 Victors Way
Ann Arbor, Michigan 48108
Telephone (313) 665-0100

New Advances in Molybdenum-containing Corrosion Resistant Alloys

by Aziz Asphahani, Paul Manning, and John Straatmann*

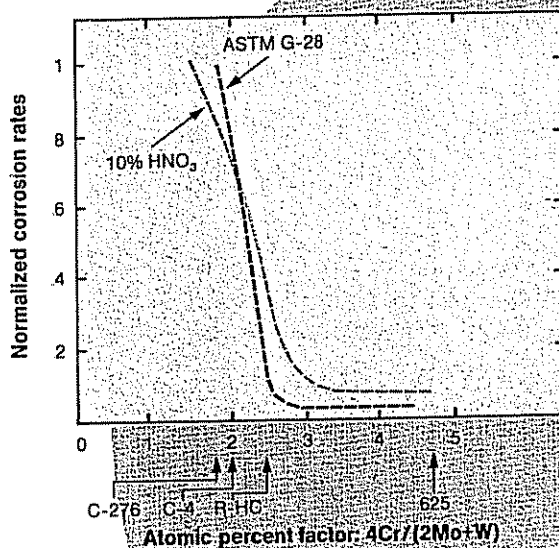
A new, versatile, nickel-chromium-molybdenum-tungsten alloy, produced by Haynes International and designated HASTELLOY® alloy C-22, finds applications in highly corrosive environments found in the pulp and

paper, pickling acid process, the production of pesticides and agrichemicals, plastics, oil and gas. The alloy also finds uses in marine environments and chemical process industries.

Over the last 25 years, there has been a continuous evolution of corrosion resistant alloys arising from the well established HASTELLOY alloy C family. Initial development resulted from a need for a solution anneal after fabrication with HASTELLOY alloy C and the inherent problems associated with

*Dr. Asphahani is General Manager and Dr. Manning is Marketing Manager of Corrosion Resistant Alloys Business at Haynes International, Inc., Kokomo, Indiana. For further information, contact them at (317) 456-6000. Mr. Straatmann is General Manager of Sales Development for AMAX Metal Products. For further information contact him at (412) 257-1560.

Figure 1—Range for best resistance to oxidizing environments.



New Advances in Molybdenum-containing Corrosion Resistant Alloys

this practice led to the introduction of HASTELLOY alloy C-276. The critical role of extra carbon and silicon contents were defined and newly developed melting technology made it possible to achieve the alloy C-276 chemistry. However, this composition was not completely free of preferential weld and heat affected zone (HAZ) attack due to precipitation of Mo- and W-rich intermetallic phases.¹ This problem led to the development of HASTELLOY alloy C-4.² Thermal stability was obtained in this alloy by minimizing the W, Fe, Co and V contents. While preferential weld and HAZ attack problems were eliminated, the localized corrosion resistance and, in some cases, the uniform corrosion resistance of C-4TM alloy were impaired vs C-276 alloy.³

Even though HASTELLOY alloys C-276 and C-4 possess versatile corrosion resistance, both alloys exhibit limited resistance to oxidizing acid environments. Advances in corrosion science and better understanding of the specific roles of Cr, Mo and W in imparting corrosion resistance to the Ni-base alloys have led to a new generation of this versatile Ni-Cr-Mo/W family, i.e. HASTELLOY alloy C-22.⁴

The criticality of the proper amounts of Cr, Mo and W in C-22TM alloy is based on the fact that in reducing acids, molybdenum and tungsten are beneficial additions for uniform and intergranular corrosion resistance. Molybdenum and tungsten, however, are ineffective additions for uniform corrosion resistance in oxidizing acid environments.³ The role of chromium is just the opposite of molybdenum and

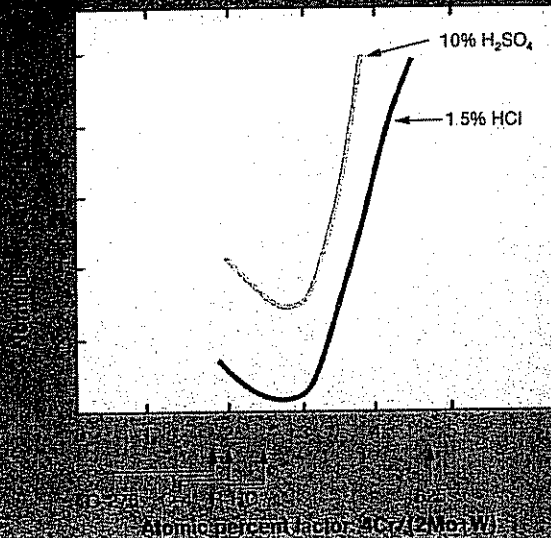


Figure 3—Optimum range for best resistance to both oxidizing and reducing environments.

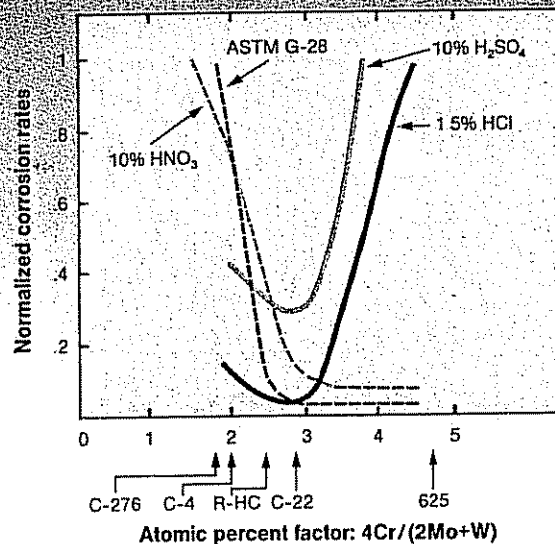
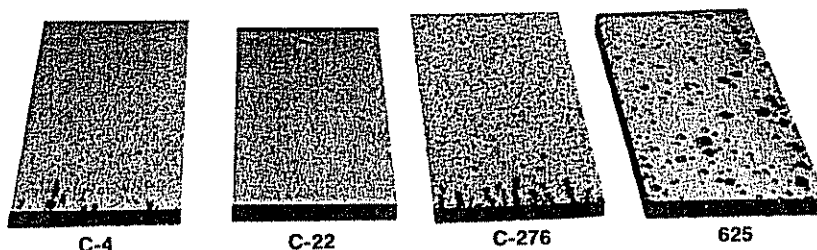


Figure 4—Critical temperature above which pitting is observed. 24-hr exposure. Samples were subjected to a solution of 12% H₂SO₄, 1.2% HCl, 1% FeCl₂, and 1% CuCl₂. Solutions for coupons 625 and C-4 were at 102°C, while C-276 and C-22 were at 125°C.



tungsten, i.e. chromium is ineffective in reducing acids and beneficial in oxidizing acids. In view of these concepts, a logical basis for comparison of corrosion resistance of the various compositions is the atomic percent factor (APF) which reflects the opposing role of chromium to that of molybdenum and tungsten. The APF is defined as the ratio of four times the chromium weight percent over the sum of twice the molybdenum weight percent and one times the tungsten weight percent

$$APF = 4Cr / (2Mo + 1W)$$

In oxidizing environments, such as nitric acid and sulfuric acid plus ferric sulfate (ASTM G 28), the higher the chromium content (i.e. the higher the APF), the lower the corrosion rates (Figure 1). On the other hand, in reducing environments, such as boiling hydrochloric acid and dilute sulfuric acid, the higher the molybdenum and tungsten contents (i.e. the lower the APF), the lower are the corrosion rates (Figure 2).

The ultimate versatility providing the best resistance to both oxidizing and

reducing environments is achieved by careful adjustment of alloying elements to yield an APF in the range of 2.5 to 3.3 (Figure 3). HASTELLOY alloy C-22 with 22% Cr, 13% Mo and 3% W lies within the range identified for the lowest corrosion rates in oxidizing and reducing environments. In addition, the composition of 22Cr-13Mo-3W in Ni-base alloys shows much improved thermal stability over that of 16Cr-16Mo-4W in alloy C-276. The corrosion resistance of as-welded alloy C-22 is enhanced over that of alloy C-276 (Figure 4). Also, resistance to pitting (Figure 5) and to crevice corrosion attack is the highest of presently available nickel-base alloys⁵

Figure 5—Corrosion behavior of welded samples showing the improved performance of alloy C-22 over that of alloy C-276.

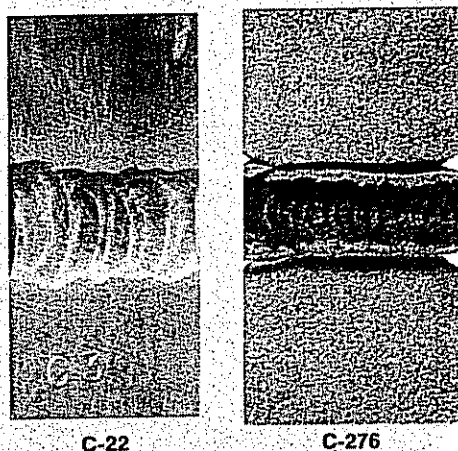
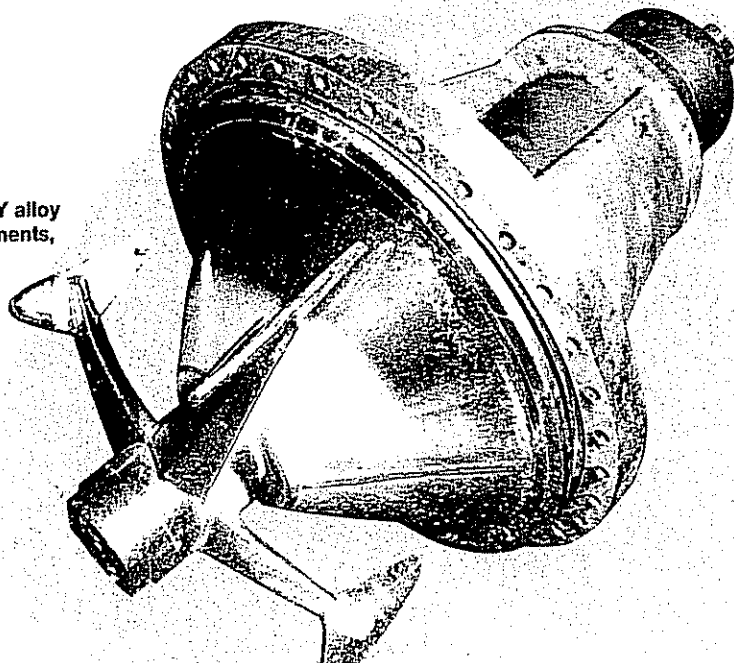


Figure 6—Weld overlays of HASTELLOY alloy C-22, used to protect alloy C-276 weldments, can be seen on bleach plant mixer.



A Wide Range of Industrial Applications

Because of its vastly improved corrosion resistance, HASTELLOY alloy C-22 has very rapidly demonstrated its ability to solve difficult industrial corrosion problems where other corrosion resistant alloys have failed. Details of a few of these applications follow.

- **Pulp and Paper**—HASTELLOY alloy C-22 is being used in a number of applications in pulp bleaching systems in perhaps the most severe environ-

New Advances in Molybdenum-containing Corrosion Resistant Alloys

HE 00649

ments where pulp, water and chlorine exist. This superior performance is clearly evident in the bleach plant mixer at the Crown Zellerbach plant in Camas, Washington (Figure 6). The trouble spot was a mixer for a 685 ADMI/D unit installed in early 1984. The C-276 weldments had experienced corrosion problems. In order to improve service life, the builder, Kamyr, Inc., ground off 3 mm (0.11 in.) of the welds of alloy C-276 and overlaid them with HASTELLOY alloy C-22. At last inspection, the alloy C-22 weld overlay unit which has been operating for over a year and a half had experienced no problems. At this time, six similar chlorine mixers, made entirely

from HASTELLOY alloy C-22, have been put in service and continue to perform well.

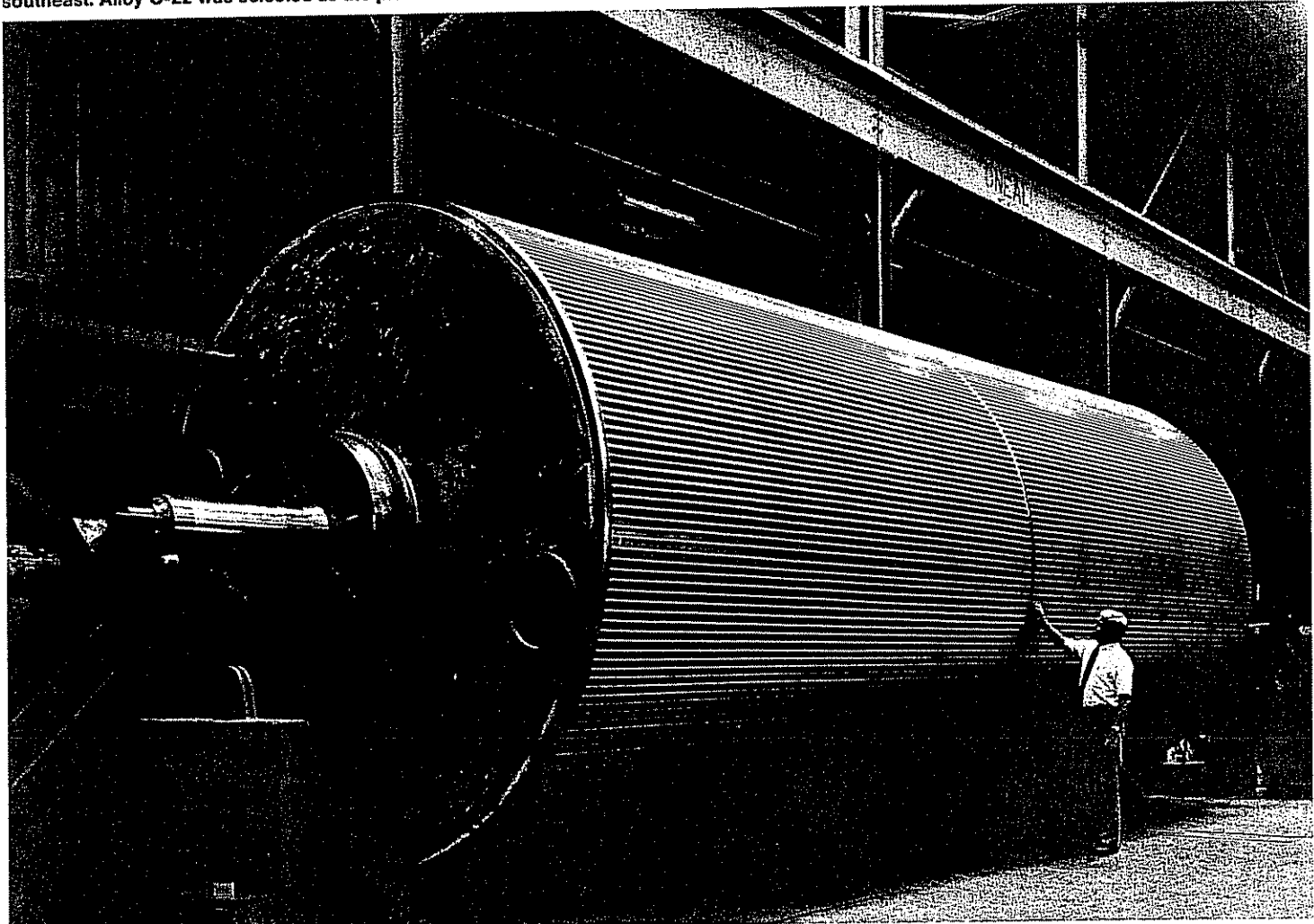
Another application is the large "C" stage bleach washer drum being constructed out of HASTELLOY alloy C-22 at Goslin-Birmingham for a paper mill in the Southeast (Figure 7). The new alloy was selected over titanium because of its excellent corrosion resistance in the residual chlorine, high temperature environment in the bleach washer drum along with its ease of fabrication and repairability.

- **Galvanizing Bath**—Fans used to ventilate zinc galvanizing effluents from a scrubber system were once a source of constant problems at a leading steel company. The effluent [consisting of aluminum, ammonium and zinc chlo-

rides + hydrochloric acid at 26 to 52 C (80 to 125 F)] was eating up 316L stainless steel fans every three to four months. Recently, a fan made of HASTELLOY alloy C-22 was inspected after completing 21 months service (Figure 8) and only slight attack was evident in the form of abrasion/corrosion. Because of the good service provided by the alloy C-22, parts of the housing and shaft that were badly corroded were also replaced with alloy C-22.

Another application involves using HASTELLOY alloy C-22 for electrogalvanizing rolls at several steel mills. Alloy C-276 and C-4 have proven inadequate for this service because of preferential weld and/or HAZ attack.

Figure 7—This bleach washer, made entirely of HASTELLOY alloy C-22 is being constructed at Goslin-Birmingham for a large papermill in the southeast. Alloy C-22 was selected as the prime construction material after extensive corrosion testing.



The corrosive media contains zinc chloride, hydrochloric acid and ferric chloride.

● **Synthetic Fibers**—A European chemical plant is using alloy C-22 in equipment to produce viscose in a gelatinous fiber. The environment consists of an aqueous solution of sulfuric acid containing parts of dissolved and undissolved hydrogen sulfide and carbon disulfide. There is also some dissolved sodium sulfate in this process environment. During the reaction which forms viscose at 40 to 50 C (104 to 122 F), nascent hydrogen sulfide is released which attacks and destroys the passive layer on stainless steels. Even HASTELLOY alloy C-4 proved to be inadequate in terms of corrosion resistance. The weld HAZs of alloy C-4 were also rapidly attacked. Equivalent components made of alloy C-22 show no visible corrosion, even after about two years of service.

● **Pesticides**—A manufacturer of herbicides had severe corrosion problems in a sulfuric acid concentrator made of Type 316L stainless steel which failed in seven months. Test specimens showed alloy C-22 to be ten times more resistant to corrosion than alloy 316L (alloy C-276 was second best with a corrosion rate three times higher than that of alloy C-22). A HASTELLOY alloy C-22 heat exchanger went into service in April 1984 and continues to operate without problems. Several other heat exchangers have been replaced with alloy C-22 at this plant.

An alloy C-276 heat exchanger used in the manufacture of a carbamate insecticide intermediate failed after two years of service. It was replaced by a zirconium heat exchanger which failed in six months. Prior to this failure, the process chemists were not aware of the presence of trace wet chlorine in the system. This caused the rapid failure of zirconium. HASTELLOY alloy C-22 was specified for the replacement heat exchanger at this plant. The



Figure 8—Ventilation fan in a steel strip galvanizing bath. Twenty-one months later, the fan was still in service in galvanizing bath fumes.

unit was fabricated in the spring of 1985 and is now in service without showing any signs of corrosion problems.

These examples highlight some of the successful commercial applications of HASTELLOY alloy C-22. Its outstanding corrosion properties and ease of fabrication will ensure an ever expanding usage. The new alloy will surely make its mark in the outstanding HASTELLOY alloy C family.

References

1. Hodge, F. G., *Corrosion*, 29, 375, (1973)
2. Kirchner, R. W. and Hodge, F. G., *Werkstoffe und Korrosion*, 24, 1042, (1973).
3. Streicher, M. A., *Corrosion*, 32, 79, (1976)
4. Asphahani, A. I., U.S. Patent 4,533,414, (1985).
5. Hibner, E. L., *Materials Performance*, 37, March (1987)

Molybdenum Carburizing Steel Provides Performance Edge

by Michael Antosiewicz, Gary Wiskow and Thomas Oakwood*

The Falk Corporation of Milwaukee, Wisconsin has been manufacturing gear drives, large open gearing, and related equipment to heavy industry for nearly 100 years. During that time they have become the largest and most diversified manufacturer of this type of equipment in the United States. Products include a wide variety of gear drive units, shaft couplings, and precision gears. Both standard and custom-designed products are available. Falk serves many industries including

steelmaking, pulp and paper, chemical, cement, plastics, petroleum refining, and mineral processing, and the marine industry.

Speed Reducers Work Very Hard

One of the items produced by Falk which has been the object of continuing design development is the speed reducer. Basically, a speed reducer is a high power industrial transmission. It is designed to reduce the fixed speed of an electric motor to levels usable for process equipment. Speed reducers

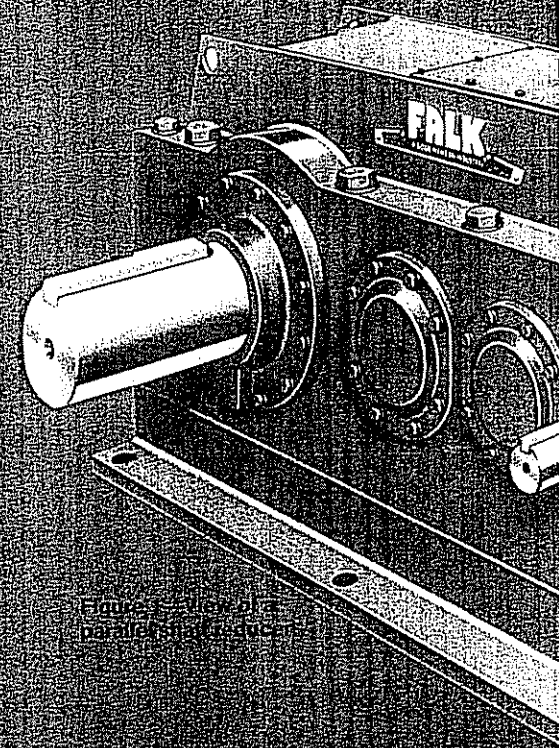
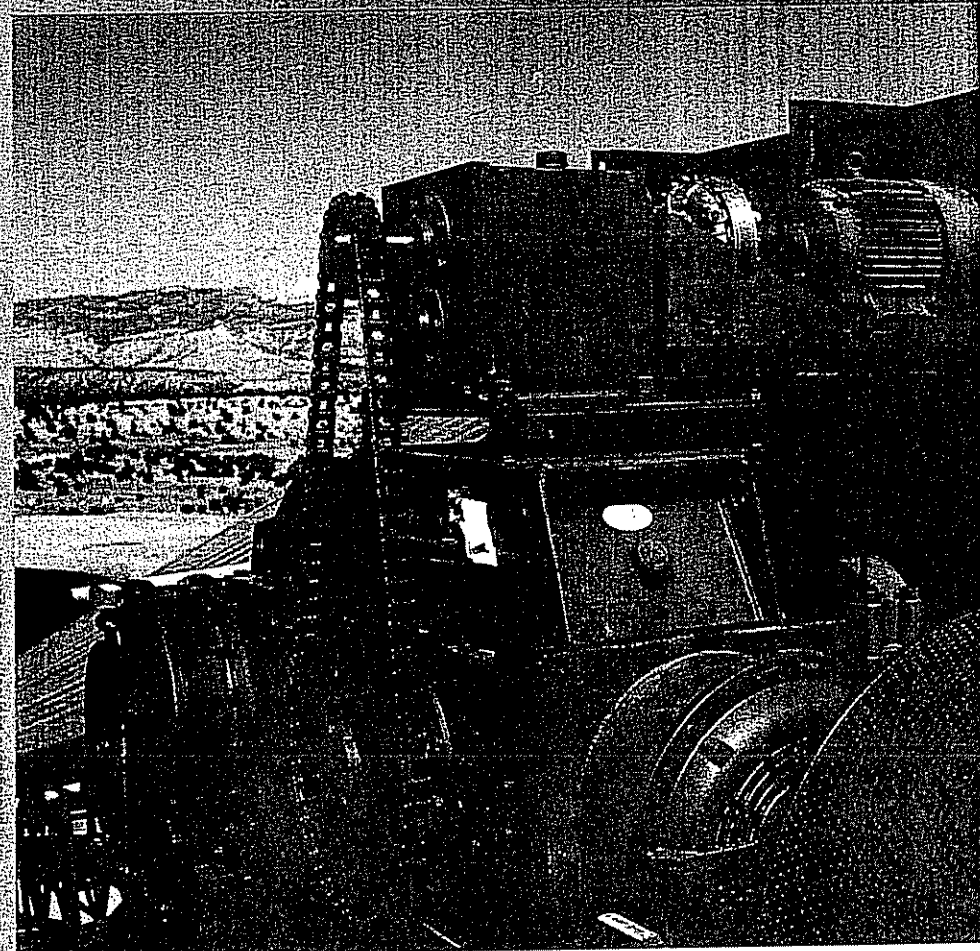


Figure 1—A Falk speed reducer.

* Mr. Antosiewicz is Manager of Research and Technology and Mr. Wiskow is Supervisor of Materials Technology. Both are at Falk Corporation in Milwaukee, Wisconsin. For further information call them at (414) 342-3131. At the time of writing Mr. Oakwood was Manager of Sales Development. Low Alloy Steels, AMAX Metal Products.

Figure 2—Two speed reducers in a coal conveyor application.



All photographs courtesy Falk Corporation

HE 00651

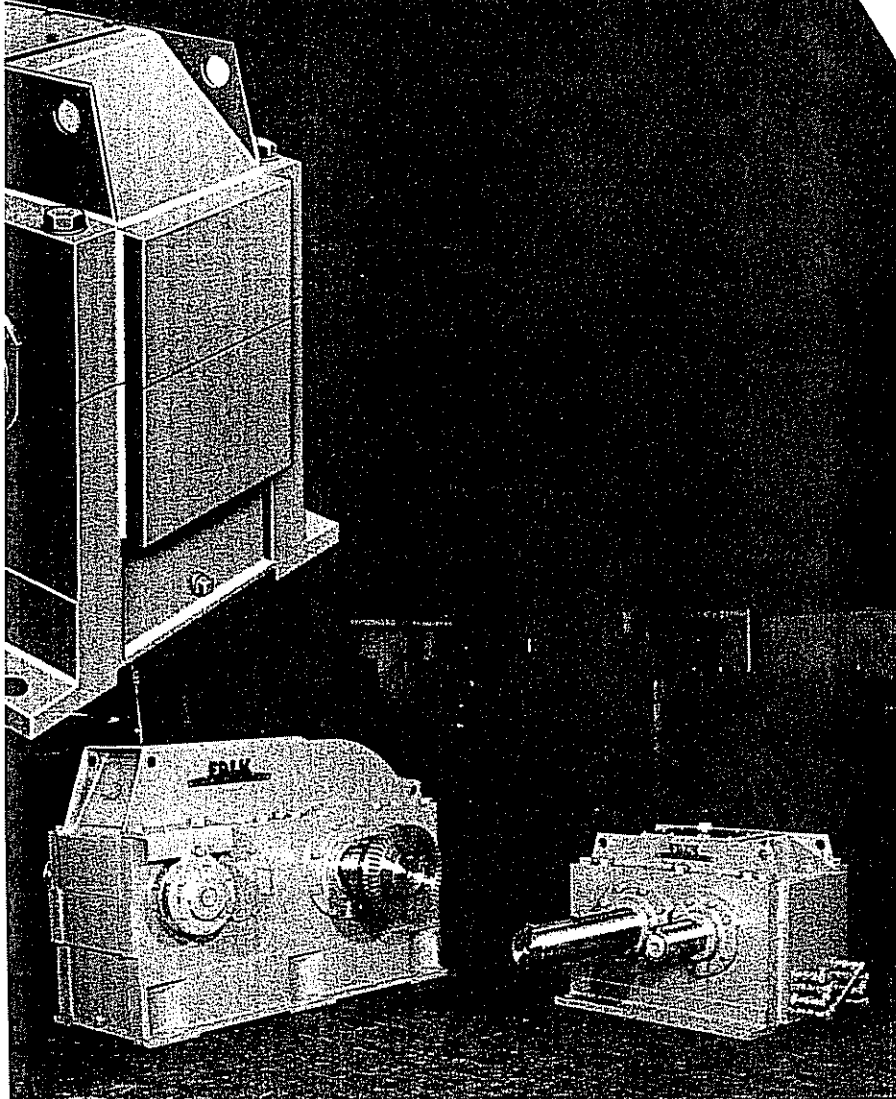


Figure 3—Comparison of a Type A speed reducer with its considerably larger counterpart.

range from 1.5:1 for single reduction units to 1,500:1 for multiple reduction units resulting in tremendous increases in torque output. Standard speed reducers for example offer torque outputs up to 4.0×10^6 lb-in. (4.5×10^5 N·m). The company also provides larger specially designed units with torque outputs up to 100×10^6 lb-in. (113×10^5 N·m). Configurations include concentric shaft, parallel shaft, and right angle outputs. In the right angle configuration the output can be either horizontal or vertical. Figure 1 shows a parallel shaft speed reducer. Figure 2 shows two speed reducers in a coal conveyor application. The 72 in. (1.83 m) wide coal conveyor, designed to deliver 5,000 tons/hr (4,540,000 kg/hr) at a speed of 750 ft/min (13.7 km/h), is driven through the lower right angle speed reducer by a 600 hp (448 kW) electric motor. The upper chain connected reducer is part of the inching drive system for the conveyor.

In order to meet the increasing demands of industry for high reliability speed reducers with low cost per unit

Molybdenum Carburizing Steel Provides Performance Edge

torque output, Falk's design engineers undertook the task of designing a smaller, more compact unit which would be capable of the torque output of much larger units. Through the use of advanced technology, computer aided design and finite element analysis, Falk developed their 'A' unit model. This unit develops maximum torque output in the minimum size package while maintaining high reliability. Figure 3 shows a comparison of the 'A' unit with its larger counterpart. The size reduction illustrated required a complete re-engineering of the gearing, bearings, fittings, and cooling system in order to provide maximum load carrying capacity. As a result of this work, 'A' units are now available with single speed reductions from 1.8:1 to multiple speed reductions of 438:1, and torque ratings from 130,000 to 4 million lb-in. (17×10^3 to 4.5×10^5 N·m)

Carburizing Steel Achieves Design Goals

During the early stages of design of the 'A' unit, it became apparent that the use of carburized and ground gearing would provide a means of accomplishing their design goals. Also, solid-on-shaft pinions were selected along with gearing which was to be shrink-fitted to shafts.

It was also evident that if a carburizing steel with insufficient hardenability were to be used in the new unit, the core strength of the shafts and gearing would be considerably lower than that of the through hardened components in the large predecessor. The selection of an alloy steel, which would achieve the hardenability needed to withstand the stresses anticipated on the shafts and gears, was a critical part of the design of the 'A' unit.

Four Carburizing Grades Considered

Four alloy steels were considered: SAE 8620H, SAE 4320H, SAE 9310H, and EX 55. The compositions of these steels are shown in the accompanying table. Figure 4 shows the Jominy hardenability band for EX 55 along with that of SAE 9310H. The hardenability bands for SAE 8620H and SAE 4320H are lower than either of the grades described in Figure 4. Using minimum hardenability data, Falk's engineers established the minimum hardness expected beneath a carburized case for each of the four alloy steels. By then applying American Gear Manufacturing Association (AGMA) standards for allowable shaft stresses, they were able to establish the maximum bending and torsional design stresses which carburized shafts could withstand using each of the four grades. It became readily apparent that EX 55 could be used at significantly higher stress levels than the other steel grades being considered. Furthermore, Falk's engineers were also able to establish that EX 55 develops much higher tensile strengths at the center of various sections than the other steel grades. Thus EX 55 was found to be the

Figure 4—Hardenability bands for EX 55 and AISI 9310H steels.

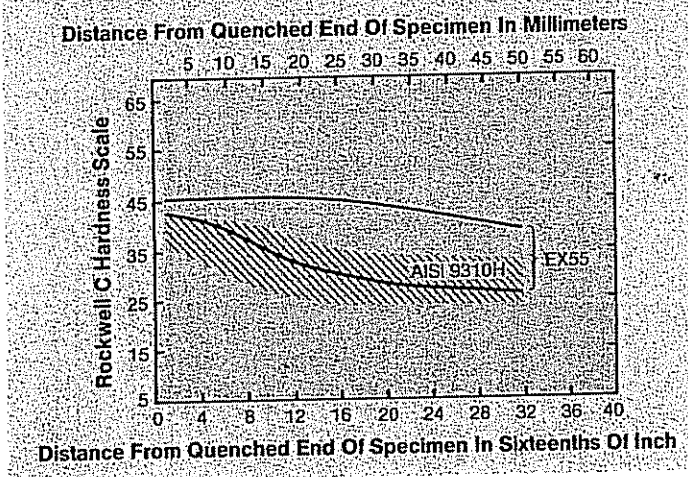
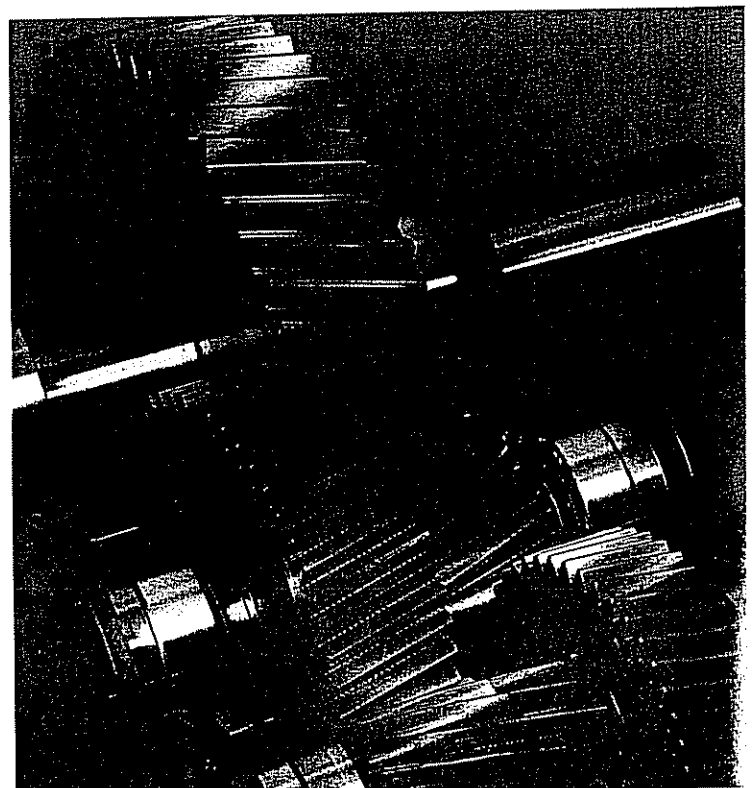


Figure 5—Close-up view of the components in the new 'A' unit where EX 55 is used.



optimum steel grade for withstanding the interference fit stresses anticipated for the shrink fit gearing. As a result of these design considerations, EX 55 was selected as the primary alloy carburizing steel to be used for the shafts and gearing in Falk's 'A' unit. Falk refined the steel composition and developed heat treating practices which optimized both machinability and performance. Figure 5 shows a close-up view of the components on the new 'A' unit where EX 55 is used.

The high hardenability of EX 55 was a key factor in Falk's selection of this grade for the 'A' unit. EX 55 offers additional advantages over other carburizing steels where high performance is required.

The fracture toughness of EX 55 is superior to that of many other alloy carburizing steels. Figure 6 shows the fracture toughness gradient for carburized EX 55 compared with SAE 8620. These results, developed at the AMAX Materials Research Center, were obtained from Charpy-sized bend specimens. A fatigue crack was grown to a controlled depth from a notch electrically discharge machined at each specimen surface. The specimens were then broken in three-point slow bend. Fracture toughness is lowest at the surface of the carburized case and increases as the core is approached. It is evident that the fracture toughness of EX 55 increases much more rapidly than SAE 8620.

EX 55 Especially Suitable

The high toughness of EX 55 makes it especially suitable to withstanding random peak overloads often experienced by carburized gears. Figure 7 illustrates a test specimen developed at AMAX which permits measuring the resistance of a carburized steel to the bending stresses applied to gear teeth during service. Figure 8 shows a laboratory loading cycle whereby incrementally increasing overloads are applied to this specimen over and above a base high cycle fatigue load. By carefully monitoring the deflection obtained with each overload, curves such as

those shown in Figure 9 can be developed. The load at which permanent damage to the carburized case occurs can be easily defined. This so-called "critical overload" value is a measure of the capability of a carburized alloy gear steel to withstand not only the nominal fatigue stresses encountered during service, but random overloads as well. It is evident from Figure 9 that the high hardenability EX 55 significantly outperforms EX 24 which has a hardenability equivalent to SAE 8620. AMAX research has shown that, in general, higher hardenability carburized gearing steels have better tough-

Figure 6—The fracture toughness gradient for carburized EX 55 compared with SAE 8620.

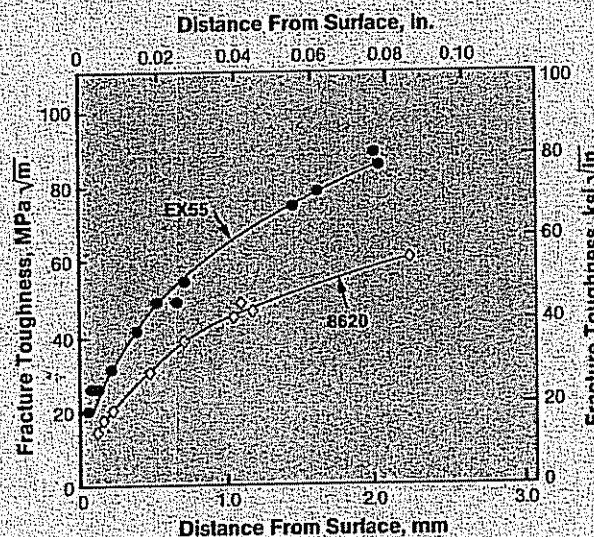
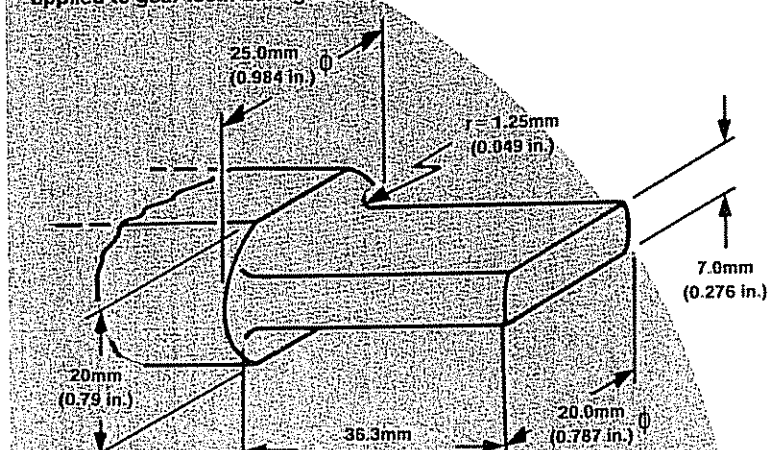


Figure 7—A simulated gear tooth test specimen developed by AMAX which permits measuring resistance of a carburized steel to the bending stresses applied to gear teeth during service.



Molybdenum Carburizing Steel Provides Performance Edge



ness and resistance to overload failures than lower hardenability grades. Thus EX 55 not only meets the gear and shaft design requirements established by Falk, but also provides the capability of withstanding the peak overloads which can occur during speed reducer operation.

The development of Falk's new speed reducer is an excellent example of how careful engineering design coupled with appropriate materials selection can result in cost efficient industrial equipment. The 'A' unit with carburized ground gearing offers Falk's customers a smaller unit with reduced floor space requirements along with performance and reliability comparable to its larger predecessor.

References

Y. E. Smith and D. E. Diesburg, "Fracture Resistance in Carburizing Steels" Reprinted from *Metal Progress*, May, June and July 1979. Request M-388.

"Molybdenum in Carburizing Steels," 20 page AMAX brochure. Request M-615.

Both publications can be obtained from AMAX Metal Products, Technical Information, P.O. Box 1568, Ann Arbor, Michigan 48106.

SAE No.	C	Mn	Cr	Ni	Mo
8620H	0.20	0.80	0.50	0.60	0.20
4320H	0.20	0.55	0.50	1.80	0.25
9310H	0.10	0.55	1.20	3.00	0.10
EX 55	0.17	0.85	0.55	1.80	0.75

Figure 8—Laboratory loading cycle. Periodic overloading is imposed during cyclic loading, as shown by the peaks.

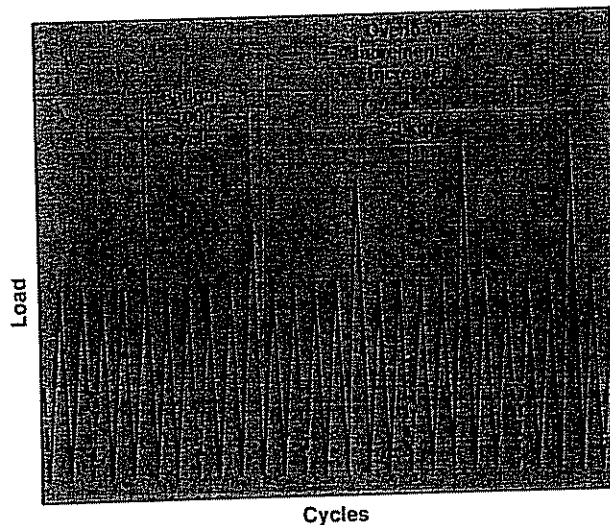
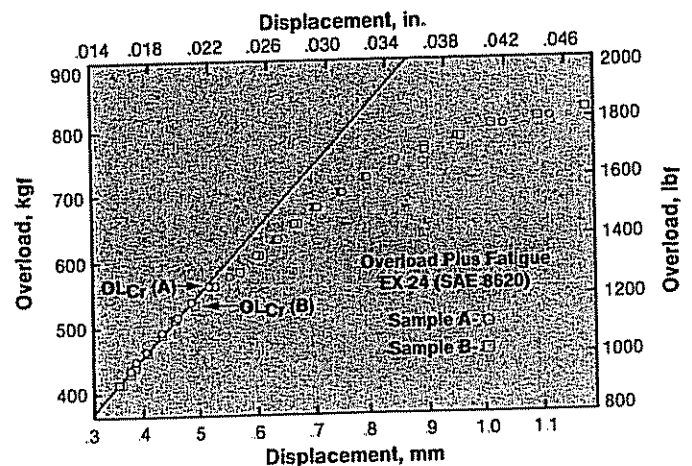
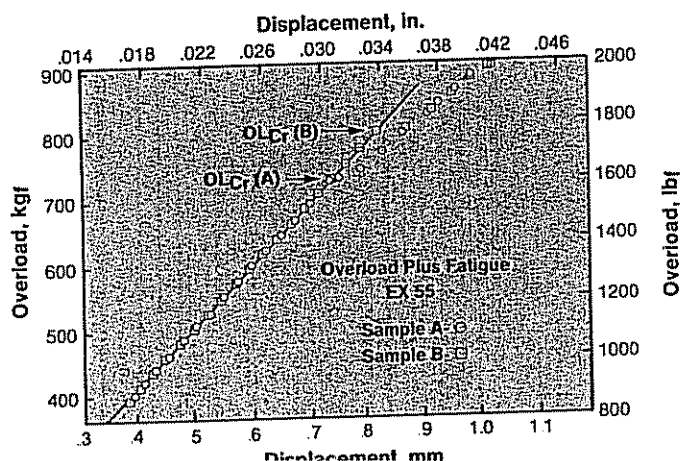


Figure 9—The high hardenability of EX 55 significantly outperforms EX 24, which has hardenability equivalent to SAE 8620.



New CCT Diagrams for Carburizing Steels

In recent years the AMAX Materials Research Center generated several new continuous-cooling transformation (CCT) diagrams to aid the development of new, more effective carburizing steels, and to better define heat treating characteristics of existing and new steels. The principal advantage of

CCT diagrams is their ability to show the relationship of microstructure and hardness to the conditions of cooling from the austenitizing or carburizing temperature for a particular composition. Because of the wide range of cooling rates available in the experimental technique, one can predict the micro-

Continuous-Cooling Transformation Data Sheets for Carburizing Steels

PS (EX) 30	0.16	0.25	0.79	0.005	0.019	0.56	0.86	0.47	I-255
PS (EX) 31	0.17	0.27	0.80	0.013	0.022	0.54	0.85	0.51	I-49
PS 31 + case	0.18	0.27	0.82	0.016	0.023	0.40	0.84	0.54	I-260
PS (EX) 55	0.17	0.24	0.85	0.015	0.007	0.59	1.75	0.73	I-256
PS (EX) 55	0.17	0.28	0.87	0.015	0.023	0.49	1.84	0.74	I-254
"8816"	0.16	0.30	0.86	0.023	0.015	0.50	0.53	0.36	I-51
"54Mo8816"	0.16	0.31	0.85	0.023	0.014	0.49	0.54	0.54	I-52
"74Mo8817"	0.17	0.27	0.86	0.021	0.022	0.51	0.56	0.74	I-53
4620 + case	0.20	0.23	0.49	0.016	0.022	—	1.78	0.25	I-262
"49Mo4620+case"	0.20	0.23	0.49	0.016	0.022	—	1.78	0.49	I-263
"0.2C-Mn-B"	0.20	0.19	1.25	—	—	0.04	0.05	0.03	0.0009 I-59
SAE 8822	0.24	0.28	0.95	0.019	0.025	0.44	0.56	0.31	I-60
SAE 4027	0.28	0.25	0.86	0.010	0.028	0.06	0.03	0.23	I-91

New CCT Diagrams for Carburizing Steels



structure and hardness in quenched light and heavy sections, or after normalizing or annealing treatments. AMAX Metal Products wishes to share this valuable information with those who specify materials and design components, as well as those who carburize and heat treat steels.

The accompanying table lists the compositions of carburizing steels for which CCT data sheets are available, both data sheets recently developed and those that have been available since 1978 (Reference 1). Also shown is a new data sheet for SAE 4815 steel, to indicate the nature of the data available. Please note in the list the availability of data sheets (designated "+ case")

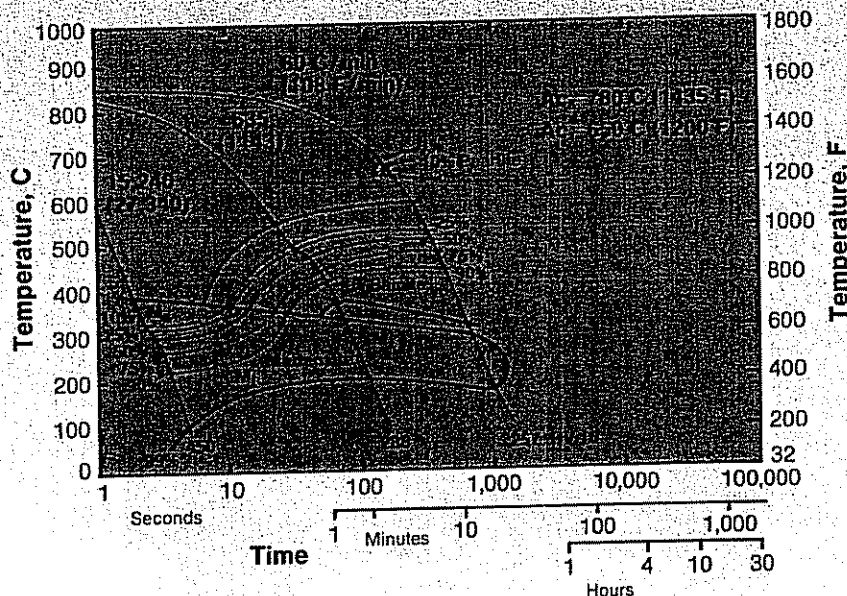
which include CCT data for several carbon levels in the carburized case of certain steels. Also included are diagrams for a few widely used powder metallurgy (P/M) steels.

A description of CCT diagrams and their use is included in the AMAX brochure *Molybdenum in Carburized Steels* (M-615). This brochure can be ordered, along with specific CCT data sheets. A more detailed description of the methods used to generate the CCT diagrams is given in Reference 2, available from The Metallurgical Society of AIME.

References

1. Enclosure with W. W. Cias, "Austenite Transformation Kinetics of Ferrous Alloys," Climax Molybdenum Company brochure M-291, 1978.
2. G. T. Eldis, "A Critical Review of Data Sources for Isothermal and Continuous Cooling Transformation Diagrams," in Proceedings of a Symposium *Hardenability Concepts with Applications to Steel*, edited by D. V. Doane and J. S. Kirkaldy, a 1978 publication of TMS/AIME, Warrendale, PA 15086.

Data sheets and the brochure M-615 are available without charge and may be ordered from AMAX using the attached Business Reply Card.



Alloy: Commercial SAE 4815H carburizing steel.

Chemical Composition: 0.16% C, 0.24% Si, 0.63% Mn, 0.010% P, 0.012% S, 0.21% Cr, 3.35% Ni, 0.24% Mo, 0.19% Cu.

Preparation and Processing: Slabs from commercial billet 76 mm (3 in.) square normalized at 925 C (1700 F) for one hour.

Austenitizing: 870 C (1600 F) for 20 minutes.

Research Objectives: To characterize a standard grade of carburizing steel for comparison with recently developed grades.

New Literature

HE 00658

The following publications and reprints have either become available since the last issue of Molybdenum Mosaic or have not been previously announced. They are free of charge. Please fill out the coupon below and mail to:

Technical Information
AMAX Metal Products
P.O. Box 1568
Ann Arbor, Michigan 48106, USA

STRUCTURE AND MECHANICAL PROPERTIES OF AUSTEMPERED DUCTILE IRON Written by D. J. Moore, T. N. Rouns and K. B. Rundman of Michigan Technological University, this paper is a progress report on the AFS-sponsored research on austempered ductile iron at MTU. Several alloys of ductile iron with various amounts of Mn and Mo were subjected to austempering heat treatments
(Request Code M-631)

CASTING MORE LIGHT ON GRAY IRON MACHINABILITY. Reprinted from *Tooling & Production* magazine, this article attempts to resolve the question of whether the better machinability of high strength gray iron is worth the increased foundry costs.
(Request Code M-632)

MOLYSULFIDE NEWSLETTER INDEX. This four-page index lists all articles published to date in the *Molysulfide Newsletter* since 1970. Listing is by subject and application. Supersedes all previous editions.
(Request Code L-89)

MOLYSULFIDE—THE UNIQUE SOLID LUBRICANT. A new 12-page brochure covering the basics of molybdenum disulfide as a lubricant, its applications in a wide range of lubricants and applicable government specifications. The brochure also provides information on the use of MoS₂ as filler for plastics and elastomers
(Request Code L-92)

EVALUATION OF MoS₂ IN NEWER GREASE THICKENER SYSTEMS Written by T. R. Risdon. This technical paper describes six laboratory procedures used to evaluate a range of greases and presents the results.
(Request Code L-93)

PARTICLE SIZE ANALYSIS OF MOLYSULFIDE. This brochure will cover the various techniques used to analyze particle size distribution curves for the three grades of MoS₂ offered by AMAX. Copies may be reserved in advance
(Request Code L-94)

BONDED LUBRICANT COATINGS—AN UPDATE. A technology frequently overlooked by engineers designing machinery that requires lubrication to reduce friction between sliding and rolling parts is the use of bonded lubricant coatings. Such coatings can often be used under conditions that would cause failure in conventional fluid lubricants
(Request Code L-95)

MOLYSULFIDE—PRODUCT DATA SHEET. Two-page bulletin provides product description, packaging and typical analysis and chemical specification of lubricant grade MoS₂.
(Request Code L-96)

PROPERTIES OF MOLYBDENUM DISULFIDE. The six-page bulletin contains comprehensive data on the crystal structure, physical, thermodynamic, electrical, optical and magnetic properties of MoS₂. In addition, the uses of molybdenum disulfide are given. There are 77 literature references
(Request Code C-5c)

MOLYSULFIDE LITERATURE. The four-page literature list contains currently available literature on molybdenum disulfide in lubricants. Supersedes all previous editions.
(Request Code L-0)

Please send me the following literature:

☐ M-631 ☐ L-89 ☐ L-93 ☐ L-95 ☐ C-5c
☐ M-632 ☐ L-92 ☐ L-94 ☐ L-96 ☐ L-0

Name _____

Title _____

Company _____

Address _____

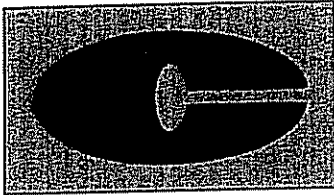
Return to: Technical Information, Dept. MM 10/1, AMAX Metal Products.
P.O. Box 1568, Ann Arbor, Michigan 48106



AMAX
Minerals + Energy

AMAX Metal Products Offices:

AMAX Metal Products, P.O. Box 1700, Greenwich, CT 06837	(203) 629-6400
AMAX Metal Products, P.O. Box 397, Arlington Heights, IL 60006	(312) 392-7100
AMAX Metal Products, 3411 Office Park Drive, Dayton, OH 45439	(513) 298-3611
AMAX Metal Products, 1370 Washington Pike, Bridgeville, PA 15017	(412) 257-1560
AMAX Metal Products, 301 East Florence Avenue, Downey, CA 90240	(213) 861-7144
AMAX Specialty Businesses, 900 Victors Way, Ann Arbor, MI 48108	(313) 662-0100
AMAX Asia, Ltd, Fuji Building Room 311, 2-3 Marunouchi 3-chome, Chiyoda-ku, Tokyo 100, Japan	(03) 201-2911
AMAX Italia SRL, via Larga 16, I-20122 Milano, Italy	(02) 805-8826
AMAX Mineral Sales Corp. SARL, 96, rue de la Victoire, 75009 Paris, France	(33) 1-42-81-91-05
AMAX Minerals & Metals, Ltd, 55 Macquarie Street, Sydney, N.S.W. 2000, Australia	61-2-222-3675
AMAX Scandinavia AB, Stora Gatan 38, S-722 12 Västerås, Sweden	(021) 114090
Climax Molybdenum GmbH, Cecilienallee 79, D-4000 Düsseldorf 30, West Germany	(0211) 45590
Minworth Metals Ltd, Needham Road, Stowmarket, Suffolk IP14 2AE, England	Stowmarket 4431-7



limax is the first name in moly—the one people know, trust and recommend. It's the brand name for moly products from AMAX

Minerals, the largest supplier of molybdenum in the world. With two mines and four conversion plants producing consistent high quality in a wide range of product forms.

Perhaps most important, AMAX is your most reliable source for molybdenum. Year in and year out, we generate the supply to meet our

customers' demands. With superb technical service and meaningful marketing support. You're not just buying molybdenum. You're buying leadership, technology, commitment.


For more information contact your nearest AMAX Metal Products Office. Or call Pittsburgh (412) 257-1560, Chicago (312) 392-7100, Dayton (513) 298-3611, Los Angeles (213) 540-6612 or Greenwich (203) 629-6437.



AMAX METAL PRODUCTS

AMAX
Minerals+Energy

THE MOLY SOURCE THAT'S SOLID AS A ROCK.



HE 00659

SHIPMENTS OF HASTELLOY C-22 PRODUCT US OPERATIONS

	1984	1985	1986	1987	1988	1989	1990	1991	1992	1993	1994	1995	1996	1997	1998	1999	2000	2001	2002	2003	2004
POUNDS																					
BAR																					
BAR FROM PLATE																					
EXTR. BILLET																					
FITTING																					
OTHER																					
PLATE																					
RCS																					
RCS BILLET																					
REDRAW																					
ROUND BILLET																					
SEAMLESS																					
SHEET																					
SLAB/INGOT																					
WELDED																					
WIRE																					
Grand Total																					


	1984	1985	1986	1987	1988	1989	1990	1991	1992	1993	1994	1995	1996	1997	1998	1999	2000	2001	2002	2003	2004
REVENUE																					
BAR																					
BAR FROM PLATE																					
EXTR. BILLET																					
FITTING																					
OTHER																					
PLATE																					
RCS																					
RCS BILLET																					
REDRAW																					
ROUND BILLET																					
SEAMLESS																					
SHEET																					
SLAB/INGOT																					
WELDED																					
WIRE																					
Grand Total																					

This copy redacted for Court filing.


Unredacted version produced to Defendant.

CONFIDENTIAL
ATTORNEY EYES
ONLY

HE 00660



Manufacturer of high-pressure forged pipe fittings



PA Sales StaffTexas Sales Staff

Packing List / MTR Proof of Delivery

Product Catalog

MTR RETRIEVAL

List Price Sheets

Material Selection

Canadian CRN Numbers

MSDS

HAZIA Form


Terms and Conditions

Services


News Letter

Directions to Facilities

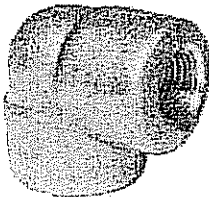
Employment




About Penn Machine



Free customer training Downloads



Information or quote



Product Catalog

Price
Ef
June
Stain
Forged
Un
\$

EDI

Fax
Nu

Free MT

Revised: Wednesday 09/21/05
Web page created by Pennsylvania Machine Works.
© Copyright 2003 by Pennsylvania Machine Works, Inc.
Privacy Policy | Acceptable Use Guide
Any comments? Please send e-mail to John Lafferty.

HE 00826

9/21/2005 2:48 PM



Materials

Carbon steels	A105: Galvanized, Normalized, Plus A694- Y42; Y52; Y60; Y65 A106B, WPB
Low Temp Carbon	LF2, LF3, WPL6, WPL3
Stainless steels	304/304L, 316/316L, 310, 317L, 321/H, 347/H, AL6XN (N08367), F44 (254SMO), F51 (2205), F53 (2207) 405, 410, F6A, A904L (N08904), Alloy 20 (N08020)
Nickel alloys	A400 (N04400), A200 (N02200), A201 (N02201), A800 (N08800), A800H (N08810), A800HT (N08811), A825 (N08825), A600 (N06600), A625 (N06625), C276 (N10276), C-22 * (N06022), B2 (N10665)
Chrome moly alloys	F11, F12, F22, F5, F9, F91, F92
Titanium	Grade 1, Grade 2, Grade 3, Grade 4
Aluminum alloys	6061, 5083, 5086
Copper nickel	70/30, 90/10

Penn Machine home page

C-22 is a registered trademark of Haynes International, Inc.

Web site created by Penn Machine. Send questions or comments to John Lafferty.

HE 00827

Penn Machine

Nickel Alloy Material Grade Composition Chart

NAME	ASTM#	GRADE	UNS #	NOMINAL COMPOSITION
ALLOY 200	FORGING B564	A200	N02200	C-.15max Cr-.01max Ni-99min Cu-.25max Fe-.4max
ALLOY 200	BAR B160	A200	N02200	C-.15max Cr-.01max Ni-99min Cu-.25max Fe-.4max
ALLOY 400*	FORGING B564	A400	N04400	Ni-63min Cu-28-34 Fe-2.5max
ALLOY 400*	BAR B164	A400	N04400	Ni-63min Cu-28-34 Fe-2.5max
* ALLOY 400 can also be furnished to Federal Specifications QQN-281 *				
ALLOY 600	FORGING B564	A600	N06600	Ni-72min Cr-14-17 Fe-6-10 Cu-.5max
ALLOY 600	BAR B166	A600	N06600	Ni-72min Cr-14-17 Fe-6-10 Cu-.5max
ALLOY 625	FORGING B564	A625	N06625	Ni-58min Cr-20-23 Fe-5max Cb+-3.75-4.15 Al-.4max Ti-.4max
ALLOY 625	BAR B564	B446	N06625	Ni-58min Cr-20-23 Fe-5max Cb+-3.75-4.15 Al-.4max Ti-.4max
ALLOY 800	FORGING B564	A800	N08800	Ni-30-35 Cr-19-23 Fe-39.5min Al-.15-.60 Ti-.15-.60 C-.10max
ALLOY 800	BAR B408	B408	N08800	Ni-30-35 Cr-19-23 Fe-39.5min Al-.15-.60 Ti-.15-.60 C-.10max
ALLOY 800H	FORGING B564	A800H	N08810	Ni-30-35 Cr-19-23 Fe-39.5min Al-.15-.60 Ti-.15-.60 C-.05-.10
ALLOY 800H	BAR B408	A800H	N08810	Ni-30-35 Cr-19-23 Fe-39.5min Al-.15-.60 Ti-.15-.60 C-.05-.10
ALLOY 800HT	FORGING B564	A800HT	N08811	Ni-30-35 Cr-19-23 Fe-39.5min Al-.15-.60 Ti-.15-.60 Al+Ti-.85-1.2 C-.06-.10
ALLOY 800HT	BAR B408	A800HT	N08811	Ni-30-35 Cr-19-23 Fe-39.5min Al-.15-.60 Ti-.15-.60 Al+Ti-.85-1.2 C-.06-.10
ALLOY 825	FORGING B564	A825	N08825	Ni-38-46 Cr-19.5-23.5 Mo-2.5-3.5 Fe-22min Cu-1.5-3 Al-.2max Ti-.6-1.2 C-.05
ALLOY 825	BAR B425	A825	N08825	Ni-38-46 Cr-19.5-23.5 Mo-2.5-3.5 Fe-22min Cu-1.5-3 Al-.2max Ti-.6-1.2 C-.05
C276	FORGING B564	A276	N10276	Cr-14.5-16.5 Mo-15-17 Fe-4-7 W-3-4.5 Co-2.5max V-.35max (Nickel remnant)

C276	BAR B574	A276	N10276	Cr-14.5-16.5 Mo-15-17 Fe-4-7 W-3-4.5 Co-2.5max V-.35max (Nickel remnant)
B-2	FORGING B335	ALLOY B-2	N10665	Cr-1max Mo-26-30 Fe-2max Co-1max
B-2	BAR B335	ALLOY B-2	N10665	Cr-1max Mo-26-30 Fe-2max Co-1max
C-22 *	FORGING B564	AC22	N06022	Cr-20-22.5 Mo-12.5-14.5 Fe-2-6 W-2.5-3.5 Co-2.5max V-.35max (Nickel remnant)
C-22 *	BAR B574	AC22	N06022	Cr-20-22.5 Mo-12.5-14.5 Fe-2-6 W-2.5-3.5 Co-2.5max V-.35max (nickel remnant)

[Carbon steel](#) | [Stainless steel](#) | [Chrome moly](#) | [Titanium](#) | [Aluminum](#) | [Copper nickel](#)
[Materials](#) | [Request quote/information](#) | [Home](#)

C-22 is a registered trademark of Haynes International, Inc.
Web site created by Penn Machine. Send questions or comments to [John Lafferty](#).

HE 00829